Numerical and Experimental Investigation of the Performance of an Improved Conical Spouted Bed Coffee Roaster

Obsinan Birri Neda

A Thesis Submitted to

The Department of Mechanical Engineering

School of Mechanical, Chemical, and Materials Science Engineering

Office of Graduate Studies

Adama Science and Technology University

February 2021

Adama, Ethiopia

Numerical and Experimental Investigation of the Performance of an Improved Conical Spouted Bed Coffee Roaster

By: Obsinan Birri Neda
Advisor: Dr. Addisu Bekele

A Thesis Submitted to
The Department of Mechanical Engineering
School of Mechanical, Chemical, and Materials Engineering

Presented in Partial Fulfillment of the Requirement for Master of Science in Thermal Engineering

Office of Graduate Studies
Adama Science and Technology University

February 2021

Adama, Ethiopia

DECLARATION

I hereby declare that this Master Thesis entitled "Numerical and Experimental Investigation of the Performance of an Improved Conical Spouted Bed Coffee Roaster" is my original work. That is, it has not been submitted for the award of any academic degree, diploma, or certificate in any other university. All sources of materials that are used for this thesis have been duly acknowledged through citation.

Obsinan Birri Neda		
Name of the Student	Signature	Date

RECOMMENDATION

We, the advisors of this thesis, hereby certify that we have read the revised version of the thesis entitled “Numerical and Experimental Investigation of the Performance an Improved Conical Spouted Bed Coffee Roaster” prepared under guidance by Obsinan Birri submitted in partial fulfillment of the requirements for Master of Science in Thermal Engineering. Therefore, we recommend the submission of a revised version of the thesis to the department following the applicable procedures.

Dr. Addisu Bekele	______________________	______________________
Advisor	Signature	Date

APPROVAL PAGE

We, the advisors of the thesis entitled "Numerical and Experimental Investigation of the Performance an of Improved Conical Spouted Bed Coffee Roaster" and developed by Obsinan Birri, hereby certify that the recommendation and suggestions made by the board of examiners are appropriately incorporated into the final version of the thesis.

Major Advisor	Signature	Date
Co-advisor	Signature	Date

We, the undersigned, members of the Board of Examiners of the thesis by Obsinan Birri have read and evaluated the thesis entitled **"**Performance Investigation of Improved Conical Spouted Bed Coffee Roaster Using CFD-DEM" and examined the candidate during the open defense. This is, therefore, to certify that the thesis is accepted for partial fulfillment of the requirement of a Master of Science in Thermal Engineering.

Chairperson	Signature	Date
Internal Examiner	Signature	Date

External Examiner Signature Date

Finally, approval and acceptance of the thesis is contingent upon submission of its final copy to the Office of Postgraduate Studies (OPGS) through the Department Graduate Council (DGC) and School Graduate Committee (SGC).

Department Head	Signature	Date
School Dean	Signature	Date
Office of Postgraduate Studies, Dean	Signature	Date

ACKNOWLEDGEMENT

First, I would like to thank the Almighty Creator for giving me the strength and patience to complete this research. I would like to show my sincere gratitude to my teacher and supervisor Dr. Addisu Bekele for giving me valuable advice, innovative ideas, constructive comments, encouragement, motivation, and guidance throughout the Thesis work. Without his encouragement, and guidance this project would not have materialized and finished.

I am especially grateful of my parents and friends, who have continuously supported me throughout my career and have been willing to give everything so that I may pursue my educational and personal goals. I would not be where I am without the drive that they have always instilled in me.

CONTENTS **PAGES**

LISTS OF TABLES

LIST OF FIGURES

ACRONYMS

ANSYS	Analysis of Systems
CFD-DEM	Computational Fluid Dynamics- Discrete Element Method Coupling
CAD	Computer-Aided Design
CFD	Computational Fluid Dynamics
DEM	Discrete Element Method
CSBWID	Conical Spouted Bed with Internal Device
SBCR	Spouted Bed Coffee Roaster
SBR	Spouted Bed Roaster
CSB	Conical Spouted Bed
HTST	High temperature/short time
HTLT	High temperature/long time
SB	Spouted Bed
KW	Wattage Requirements
FPM	Feet per minute
CFM	Cubic per minute
CHT	Convective heat transfer
GPU	Graphical processing Unit
Multi- GPU	Multi- Graphical processing Unit
ETA	Estimated Amount of Time (Duration)
GHG	Greenhouse Gas
mN	Milli Newtons

NOMENCLATURES

Di	Diameter of the Inlet Air Pipe (m)
Dc	Diameter of the Column (m)
Do	Inlet/Bottom Diameter of the Cone (m)
Hc	Conical Bed Height (m)
Ho	Stagnated Bed Height (m)
Dp	Particle Diameter (m)
u_{ms}	Minimum Spouting Velocity (m/s)
Re_{ms}	Reynolds number at Minimum Spouting Velocity (m/s)
Nu	Nusselt Number
Pr	Prandtl Number
Re_p	Reynolds Number
V_t	Terminal Velocity (m/s)
H	Convection Heat Transfer Coefficient (W/m^2K)
ρ_B	Bulk Density (kgm^3)
γ	Included Cone Angle (°)
ρ_f	Density of Fluid (kgm^3)
φ	Sphericity
ϵ_f	Void Fraction (%)
Ut	Maximum Fluidization Flow Rate (m/s)
Umf	Minimum Fluidization Flow Rate (m/s)
ρ_p	Density of solid particles, (kg/m^3)
μ	Viscosity of air, Kg/m/s
V_{gc}	The absolute volume of green coffee (m^3)
LF	Length of Draft Tube (m)
W_H	width of the face of the open-sided draft tube(m)
L_T	Length of the draft tube (m)
D_T	Diameter of the draft tube
DF	Diameter of fountain confiner (m)
LT	Length of the fountain confiner (m)

ABSTRACT

Obtaining high-quality coffee depends on the roasting process. The quality parameter like bean temperature is one of the most important and difficult physical changes in roasting. This implies controlling the roasting time, temperature, and geometry of the contactor such that achieving a uniform and efficient heat transfer rate, without affecting the aroma and flavor of coffee beans could be adapted. Hence, this paper is aimed to improve the performance of conventional spouted beds based on the combined approach of computational fluid dynamics (CFD) and the discrete element method (DEM), and also the full-scale and operating prototype is fabricated for an experimental investigation to validate the numerical results. Based on the analysis results obtained from the existing model, a device useful as batch type conical spouted bed with an internal device (CSBWID) like fountain confiner and open-sided draft tube for roasting one kilogram of coffee beans estimated to 6030 number of particles with a static bed height of 0.20m is designed, developed and analyzed using the same approach to study and improving the thermo-hydrodynamic parameter. Engineering software like that of Ansys Space Claim was used for 3D modeling, CFD Fluent, and Rocky DEM for simulation and DEM analysis. The result of the simulation indicates that the coffee bean temperature T_b increases with the increment of air inlet temperature and time. Therefore, the variation in the particle temperature with a conical spouted bed with an internal device for the operating air temperature of 250℃ specifies that coffee beans increase to a very high level (more than "500K"), while in a conventional spouted bed, particle temperatures are found to be lower (around "470K"). The convective heat transfer coefficient instantaneously increases with coffee beans temperature distribution, which is the most important factor that enhances the heat transfer rate during coffee bean roasting. The estimated heat transfer coefficients for coffee bean using a conventional spouted bed (existing) which was found to be 31 W/m^2K, whereas it is increased to about 77.5 W/m^2K for an improved conical spouted bed with an internal device. To achieve the spouting phenomenon for the required capacity of a conical spouted bed, the blower was selected as capable of handling 250 *CFM of the mass flow rate of air, and an air heater for maintaining the required temperature of coffee roasting from 190-250℃ is selected with the power consumption of an 18kW wattage requirement. The analysis of variance reveals that the air speed accounts for the largest % contribution of about 60.90% which is a most significant factor, while the mass of coffee beans is about 36.45% which is the next significant factor in the performance of the roasting machine. Generally, the results are predicted by the numerical method are approximately near to the result that is experimentally obtained.*

Keywords*: - CFD-DEM, Coffee beans, Hydrodynamics, Heat transfer coefficient, Minimum spouting velocity, Conical spouted bed, Temperature*

CHAPTER ONE

INTRODUCTION

1.1 Background of the Study

Coffee is one of the most appreciated beverages worldwide and its annual trade volume accounts for around 7 million tons of green coffee. The popularity of coffee is not based on nutritional value or potential health benefits, but, besides the slight stimulating effect, simply on its characteristic flavor properties.

Roasting is a crucial stage in coffee processing, that is aimed to change markedly the chemical, physical, structural, and sensorial properties of the green beans by heat-induced reactions. In this way, the roasting process makes coffee beans suitable for brewing. Despite the long-time experience, roasting is still an empirical standard technology. There are different ways to roast coffee, starting from grandmother's roasting pan to industrial batch roasters of different designs and continuous roasting systems with large product throughput. Numerous studies have investigated the influence of roasting conditions, including how beans are agitated (Cristo et al. 2006) and water-cooled (Baggenstoss et al., 2007), on the aroma and flavor of the roasted beans.

Several patents have been reported for high temperature/short time (HTST) roasting. Among these, the fluidized bed roaster is used for large-scale roasting that is suitable for both medium and large-scale operations and they allow continuous processing of coffee beans for making instant coffee. However, it bears a problem when the particles to be roasted are large (about 5 mm) like coffee beans and tend to develop unstable fluidization, higher pressure drop, and residence time.

Among different kinds of batch roaster, the asymmetric conventional spouted bed is one. The volume, where coffee beans are loaded and hot gas is addressed, has a geometrical configuration optimized to ensure good mixing and enough bean-air contact surfaces for very rapid roasting. More in detail, hot gas passes through the chamber and the fluid-dynamic conditions of the flow cause turbulences that mix beans and achieve well agitation. Nevertheless, conventional spouted beds agitate the particles well, and realizing effective gas-particle contact, requires high flow rates and causes random motion of particles which reduces the tendance of gas-particle contact.

Different modifications of the original spouted bed (cylindrical with conical base) are proposed in the literature to improve its performance. These modifications concern mainly the geometry of the contactor and/or gas inlet to the bed and the insertion of an internal device (Altizibar et al., 2009).

Up to yet, there is no reported study on the thermo-hydrodynamic behavior of a conical spouted bed with an internal device like a fountain confiner and draft tube for the roasting of food grains especially coffee beans in the literature. The main objective of this present research is to study conventional spouted bed (existing) and as well as to design, develop and analyze the fountain confined conical spouted bed with an open-sided draft tube and as well as to investigate the thermo-hydrodynamic characteristics of heat-sensitive particulate solids such as coffee beans during roasting which is a time-temperature dependent process, plays a major role in determining the flavor characteristics of the brewed coffee. The thermos-hydrodynamic parameters obtained at elevated temperatures such as minimum spouting velocity, static bed height, processing time, and the heat transfer coefficient were analyzed by numerical modeling using CFD Fluent and Rocky DEM to verify the simulation modified model results by the existing data.

1.2 Statement of the Problem

Traditional coffee bean roasting machines require a high temperature/long time (HTLT) which is about 260℃ at a roasting time of 600sec to roast the beans (Schenker et al., 2002). These HTLT is scorching of some beans, oil, and char deposits on the cylinder walls and, invariably, fire when doing a dark roast. Further, the machines are difficult to clean after processing, resulting in roasted beans with an acrid, smoky taste. Hence these traditional coffee roasting machines are unhygienic.

Although heat transfers during roasting can involve conduction, convection, and radiation, convection by far is the most important mode of heat transfer that determines the rate and uniformity of roasting. Coffees roasted in a drum roaster that involves mainly conductive heat transfer from roasting hardware to processed bean surfaces have less soluble solids, more degradation of chlorogenic acids, more burnt flavor, and higher loss of volatiles which is inefficient to achieve high-quality roasting with desired flavor and aroma.

Although fluidized bed roasters could achieve proper uniformity of product and better control of process parameters, it poses problems when the particles to be roasted are large (about 5 mm) and tends to develop unstable fluidization (slugging), higher pressure drop, and residence time. The conventional spouted bed roaster (cylindrical with conical base) is an alternative to fluid bed roasting, for achieving a very good mixing of solids and effective gas-particle contact which facilitates HTST processing i.e., at about 220℃ to roast the beans for 160sec and provides clean and uniformly roasted products. However, conventional spouted beds require higher flow rates due to spouting media being located at a pre-determined height in the column. And also heat-carrying fluid transfers heat to particles, with instant heat exchange which leads to poor gas-solid contact and affects the heat transfer rate. There is very little information in the literature on the thermo-hydrodynamics of spouted beds at high temperatures for coffee bean roasting, which needs further investigation.

Therefore, to fill these gaps; this study is done to design develop and analyze a conical Spouted Bed with Internal Device for Coffee Roasting using CFD Fluent- Rocky DEM coupling methods.

1.3 Objectives

1. 3.1 General Objective

The general objective of this study is to investigate the Performance of an Improved Conical Spouted Bed Coffee Roaster both numerically (CFD-DEM) and experimentally.

1. 3.2 Specific objectives

The specific objectives of this study are:

- Model and study the performance of conventional spouted beds.
- Model, design and develop an improved conical spouted bed with an internal device like a fountain confiner and draft tube.
- Analyze the thermo-hydrodynamic performance of existing conventional spouted bed and modified conical spouted bed using the CFD-DEM Coupling method.
- Development of an experimental prototype.
- To verify and validate the performance of the improved model with that of the existing model, data, and as well as to the experimental result.

1.4 Scope of the study

The scope of this study includes modeling the spouted bed using Ansys Space Claim software and analyzing it using Ansys CFD Fluent and Rocky DEM Coupling Approach and valid by experimental test for its thermo-dynamic performance.

1.5 Significance of the Study

This work is expected to:

- Reduce labor and time
- Controlling of roasting parameters.
- Improve and achieves the best coffee quality for brew

Beneficiaries: All Coffee Consumers, Companies, Society, and the Country as a whole.

1.6 Limitation

In this study, Rocky DEM was fully coupled with Ansys Fluent to study the roasting process of coffee bean particles in both conventional and modified conical spouted bed with an internal device.

The coupling between Ansys Fluent (CFD) and Rocky DEM emerges as one additional option amongst the comprehensive set of capabilities for solving fluid particulate systems available in Ansys tools, enlarging the range of granular-fluid systems that can be modeled. With the advancement in computational techniques, CFD-DEM coupling has been applied to processes involving multiphase flow, including those using spouted beds.

The numerical simulation multiphase flow needs a high-performance computer, especially when using custom polyhedron particles of coffee beans modeled in CAD. This kind of problem is accomplished with ANSYS Fluent to work with Rocky in parallel using CPU and GPU and/or Multi-GPU capabilities, which leads to very fast DEM-CFD simulation results. Since it was very challenging to get such versatile machines, thus, With HP Intel (R) Core (TM) i7, processor 3.2 GHz 8RAM simulation of custom polyhedron particles of coffee beans takes more than a month and about a week with modified particles in Rocky.

1.7 Thesis Structure

The thesis work was organized into the following chapters.

Chapter one: Introduction

The basic introduction to roasting technology, the problem of the statement, and the objective of the study i.e. improved conical spouted bed have been detailed and the more specific topics may be addressed.

Chapter two: Literature review

Chapter 2 is all about the literature review for describing roasting technology and the fundamentals of spouting. Unstable spouting will also be discussed as it should be taken into account when designing the CSB. And also in this chapter existing empirical correlations that can be found in the literature and related work on CSB and with their respective summary and gap is a discussed.

Chapter three: Materials and Methods

Different materials used for manufacturing, modeling, and analysis were mentioned and listed in this chapter, and also the procedures used to achieve the objective of the project are mentioned under the methods.

Chapter four: Systems Design and Specifications

In this chapter, a detailed design of the modified system and previously studied specifications data of the system and required and design factors would be included.

Chapter five: Numerical Modeling

This chapter presented the detail of the modeling and analysis procedures used for analyzing the existing and modified spouted bed using the CFD-DEM coupling method.

Chapter six: Results and Discussions

In this chapter, the result of different CFD-DEM computational simulations was imported and discussed. It details the result and discussion of the, existing conventional spouted bed model and modified conical spouted bed with internal devices.

Chapter seven: Conclusions and recommendations

The key conclusions of the work conducted, findings are highlighted and recommendations for further work were indorsed.

CHAPTER TWO
LITERATURE REVIEW

2. 1 Chapter Overview

This chapter describes the overview of the coffee roasting process, spouted bed technology, the characteristics of spouting phenomena, and a short review of the extensive literature so far published on the spouted bed and related work.

2.2 Coffee Roasting Process Technology

2.2.1 Coffee Roasting Process

Roasting is the most important unit operation in converting green coffee beans into flavorfull roast coffee. The primary objective of the process is to produce the desired taste and aroma. The aroma of green coffee beans is very weak and it is only through roasting that the seeds gain the characteristic aroma and flavor of coffee (Nicolas, 2004).

During roasting, heat energy is induced from the roaster into the green bean through hot gases or hot metallic surfaces to raise their temperature in the range of 170-230°C for 10-20 min (Sinnott, 2010) and thereby start complex chemical and physical changes (Kelly, 2018). Generally, the coffee roasting process can be divided into three stages: a drying phase, during which moisture is eliminated at around 100°C, and several complex pyrolytic reactions take place (Yeretzian*et al.*, 2002); during the second stage, the actual roasting process starts once the beans' moisture content reaches about 6%. Hence, the temperature of the coffee beans rises again and reaches around 170°C, where exothermic and pyrolytic reactions begin generating heat, building high pressure inside closed voids within the porous coffee bean microstructure (Ivon, 2002) and releasing large quantities of gas (5-12 l/kg of mainly Co_2) (Marilisa & Anese, 2018) as shown in figure 2.1. During the roast phase, over two hundred different reactions occur causing various volatiles to be produced and released from the coffee beans. The release of water vapor and Co_2 accounts for the majority of the mass loss of the bean during roasting (Bustos-Vanegas *et al.*, 2017). As the roast continues into its final stage, charring and burning cause the coffee beans to gradually lose their positive acidity, and rich aroma and develop a pronounced burnt taste (Yeretzian*et al.*, 2002). The coffee beans go from dark brown to black (Kelly, 2018). When the desired degree of roast is reached, the beans must be discharged from the roaster and cooled rapidly by water quenching or air cooling to avoid over-roasting due to subsequent exothermic reactions. Air cooling is preferred to water quenching because further water increases the risk of microbial growth (Nicolas, 2004). However, the cooling process must be fast, so it is better to do it using a fan or forced air convection. The efficiency of this process depends on the properties of the coffee bean (Vanegas *et al.*, 2017).

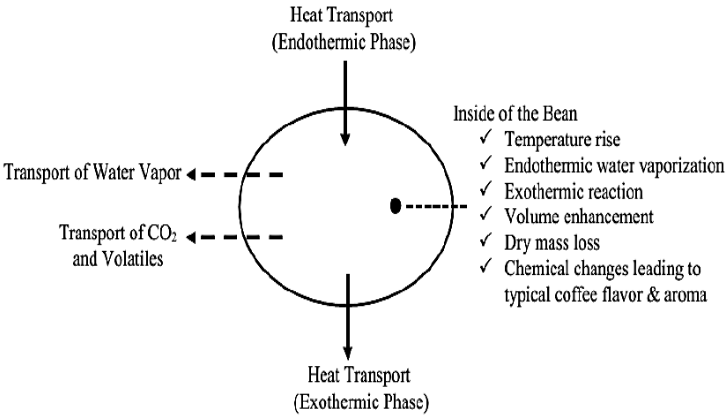

Figure 2.1: Main Aspects of Roasting Coffee Beans (Geiger et al., 2001)

2.2.2. Types of Coffee Roasting Technologies

Different types of roasters are designed with different mechanical principles so that beans and hot gas come into contact in different ways to get properly roasted coffee beans (Kelly, 2018). The mode of heat transfer during roasting can involve conduction, convection, and radiation (Baggenstoss *et al.*, 2008). In all types of roasting machines, coffee is usually agitated to ensure that it is evenly roasted (Kelly, 2018).

I. Traditional Roasters

Coffee beans are traditionally roasted in a saucepan or a tin can with a handle that is slowly and continually stirred over a fire to provide a more even heat as indicated in Figure 2.2 (UCDA, 2007).

Figure 2.2: Traditional Ethiopian Oven Top Coffee Roaster (UCDA, 2007).

II. Drum Roasters

The most common roasters available for home and industrial use are traditional drum roasters or rotating cylinders which involve placing the coffee in a rotating drum that tumbles the beans above a powerful gas burner, heating the coffee by hot air pumped through either the center of the cylinder or through its perforated sides and ensuring an even roast as shown in Figure 2.3 (Nicolas, 2004). Usually, the roasting process takes 8 to 12 minutes. This roasting system is used in both batch and continuous roasting systems. And the process is ended by rapid cooling of the coffee (Marilisa & Anese, 2018). The mass-loss rate of the beans required to achieve a commercial degree of roast is constant for cylindrical types of roasters (Guillermo *et al.*, 2016). A typical drum roaster involves three forms of heat transfer to roast coffee (convection, conduction & radiation) (Diallo, 2019).

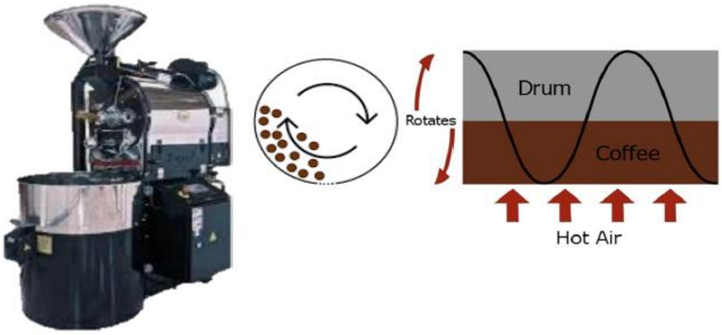

Figure 2.3: Drum Roaster with Low-Speed Hot Air (Diallo, 2019)

Drum roasters require an operator with sensory expertise who must react to the audible, visual, and aromatic changes that occur during the roasting process by adjusting the heat and airflow settings (Diallo, 2019).

III. Fluidized Bed Roasters

One of the recent developments in coffee roasting technology is fluidized bed roasting in which high-velocity hot gas is directed towards the beans, usually from the bottom of the roasting machine, so that the gases heat and move the floating beans simultaneously (Clarke and Vitzthum, 2001). The maximum temperatures used in industrial fluidized bed roasters generally vary from 210 to 240^{o}C (Nicolas, 2004). Fluidized bed roasters, which are shown in Figure 2.4 preferred for industrial use because they are faster with typical roasting times of 1 to 4 minutes (Kelly, 2018), allow better control of air temperature and speed inside the roasting chamber, and produce a more homogeneous color than other roasters. Fast roasted coffee beans are different from traditionally roasted beans: they are larger, have a reduced density, and have greater porosity. Because of these structural differences, the fast roasted beans allow for better water penetration and extraction of the soluble compounds (Kelly, 2018). According to Eggers and Pietsch (2001) and Diallo (2019), coffees roasted in a fluidized bed roaster are almost exclusively based on convective heat transfer that results in low density and high yield coffee. Whereas, Nagaraju *et al.,* (1997) stated that drum roasters mainly involve convective heat transfer producing roasted coffees with less soluble solids, more degradation of chlorogenic acids, more burnt flavor, and higher loss of volatiles than those roasted using fluidized bed roasters.

Figure 2.4: Fluidized Bed Roasting of Coffee (Kelly, 2018)

2.3 Spouted Bed Technology

The words spouted bed and spouting were first coined by Mathur and Gishler, (1955) at the National Research Council of Canada during the development of a technique for drying wheat. The first extensive assimilation of the literature came from the publication of Spouted Beds by Mather and Epstein, (1974). A more recent review can be found in Epstein and Grace, (1997).

Spouted beds were originally developed as an alternative method of drying moist seeds that need prompt and effective processing. Sooner the interest in spouted beds grew and their application included coal gasification and combustion, pyrolysis of coal and oil shale, solid blending, nuclear particle coating, cooling, and granulation as well as polymer crystallization and solid-state polymerization processes.

Stable operation in conventional conical-cylindrical spouted bed is only attained when the ratio between the gas inlet diameter and particle diameter, D_O/d_P, is smaller than 20-30 times the particle diameter and is a crucial parameter that limits the scaling-up of spouted beds (Olazar et al., 2011). Higher values of this ratio lead to slugging and highly unstable beds, with these phenomena occurring with either fine or coarse particles.

Spouted beds with fully conical geometry combine the features of the cylindrical spouted beds (such as the capacity for handling coarse particles, small pressure drop, cyclic movement of the particles, and so on) with those inherent to their geometry, such as stable operation in a wide range of gas flow-rates Mastellone and Arena, (2002). This versatility in the gas flow rate allows for handling particles of irregular texture, fine particles, and those with wide size distribution and sticky solids, whose treatment is difficult using other gas-solid contact regimes Sharma et al, (2011). Moreover, the operation can be carried out with short gas residence times (as low as milliseconds) in the dilute spouted bed Sharma et al, (2011).

The D_O/d_P, is the ratio may be increased to 2 to 60 in fully conical spouted beds (Olazar et al., 2009), and thereby, the limits are not for stability but only for operativeness. This means that very small inlet diameters (a few millimeters) are required for the treatment of fine particles, which leads to very high-pressure drops at the inlet and poor solid circulation. Thus, the use of draft tubes is the common solution to overcome this problem. For instance, a comparison of the hydrodynamics of plain and draft tube conical spouted beds shows that draft tube systems require lower minimum spouting velocities, with higher stability on a larger scale spouted bed. Whereas, plain spouted beds are adequate for bench scale. Different draft tube configurations have been developed: porous, nonporous, and open-sided. The open-sided draft tube is the most efficient due to its higher solids circulation rate and better gas-solid contact (Altzibar et al., 2008, Altzibar et al., 2009, Olazar et al., 2012, Altzibar et al., 2013).

The conical spouted bed, as shown in Figure 2.5 is a vessel that has a small inlet that diverges through a conical section towards a larger fixed-diameter column which is filled with static spouting media. By injecting fluid with enough momentum, a small hollowed channel, that has similar dimensions to the inlet diameter, can form. Once the fluid exists in the channel formed by spouting media, it will diffuse rapidly into the larger column region. As spouting media fall from the annular region into the core, they are carried by the fluid to the top of the bed where they will fall back into the column or annular region creating a circulatory pattern.

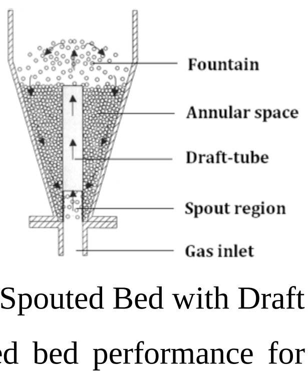

Figure 2.5: Zones in the Conical Spouted Bed with Draft Tube (Altzibar et al., 2013)

To improve the conventional spouted bed performance for many applications, different modifications have been carried out. Among these, the fountain confiner is used to reduce the operating bed pressure drop and the maximum cycle time of the particles in the contactor but does not affect the minimum spouting velocity. Nevertheless, the greatest advantage of the fountain confiner lies in the stabilization of the fountain and the homogenization of the solid circulation in the bed, which leads to a significant increase in the gas-solid contact in the fountain. This device was originally designed for the drying of fine materials to avoid particle entrainment and stabilize the spouting regime Altzibar et al., (2017).

The use of fountain confiner and draft tube in conical spouted bed increases the applicability range of the conventional systems, because the confiner allows operating with Geldart A, B, and D particles, or even with a small fraction of C particles. Another study has determined that the fountain confiner increases the conventional Do/dp ratio from 20-30 (olazar et al., 1992) to 800 without the need for any draft tube Pablos et al., (2017), Tellabide et al., (2020).

2.3.1 Fluidized and Spouted Bed Characteristics

Fluidized beds have been in use in the industry since 1879 with applications such as roasting, drying of grains, and pneumatic conveying in which particles can be circulated into a system where the fluid momentum pushes particles through to a collection port at the top. In the process of particle transport, the particles may be dried or heated by the fluid based on its physical properties, Gegenheimer, (2017).

The idea of the spouted bed, a subset of the fluidized bed, was first introduced to the research community by Gishler and Mathur in 1954 at the National Research Council of Canada (NRCC) as a denser solid-phase alternative Epstein and Grace, (2010).

The fluidized bed was insufficient for drying wheat particles as the wheat was less characterized in shape and had a mean particle size too large for fluidization, whereas slugging, an unwanted phase of fluidized beds, would often occur Epstein and Grace, (2010). It was at this point that the NRCC initiated further research and found that the spouted bed “appears to achieve the same purpose for coarse particles as fluidization does for fine materials” Gegenheimer, (2017).

Spouted beds gained much more popularity in 1959 with the book titled Fluidization in which the spouted bed was introduced as its chapter Epstein and Grace, (2010).

Since then, over 1300 works have been published with a variety of applications, such as coal combustion, solid blending, cooling, granulation and coating, electrolysis in liquid spouted beds, and drying of grains and evaporative solutions Gegenheimer, (2017). In more recent years, there has been a major shift from using spouted beds for industrial purposes towards laboratory experiments where the effectiveness of various purposes can be accurately studied.

The fluidized bed and spouted bed have similar features and have been used to achieve similar results until only recently (1954-present) with findings showing each variation excelling at separate tasks Gegenheimer, (2017). The fluidized bed is a very general term that characterizes a multitude of sub-systems where it utilizes multi-phase mixing in which a gas is sent through a solid spouting media similarly to the spouted bed. The most classic fluidized beds use finer spouting media (20-600μm), larger gas inlet offices, and smaller particle densities (1.4-4g/cm^3) in which the goal is not to not create a spout, but to entrain the particles in a fluidized state, Arabiourrutia et al., (2007)

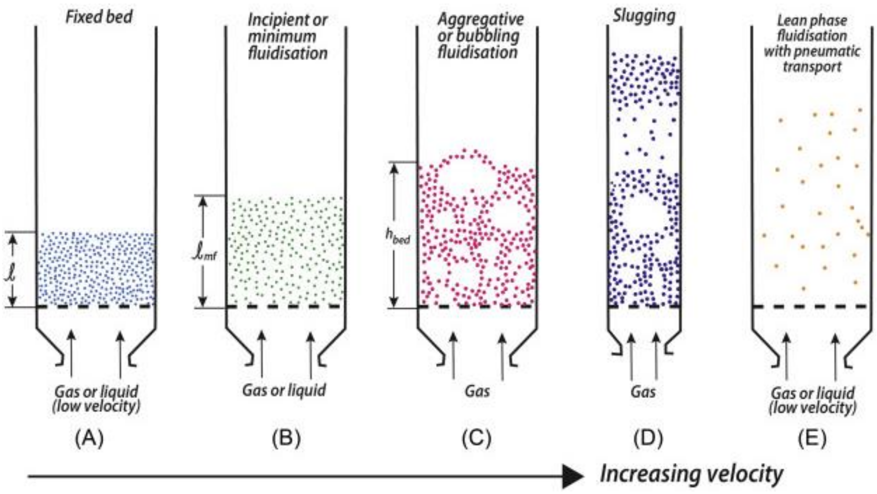

Figure 2.6: Regimes of Fluidization in Fluidized bed (Arabiourrutia et al.,2007)

Depending on the momentum of the fluid, the bed can have multiple phases of solid-fluid interaction as shown in Figure 2.6 These phases generally include incipient fluidization, a fluid bed, a floating bed, and pneumatic transportation. As discussed previously, when larger, coarser, and less characterized particles were placed into fluidized beds the fluid momentum was not sufficient in creating a fluidized state giving birth to the conventional spouted bed.

The conventional spouted bed is based on a cylindrical cone that diffuses to a fixed diameter column as shown in Figure 2.7. Conventional spouted beds require higher flow rates due to spouting media being located at a pre-determined height in the column. The conical spouted bed (CSB), a variation of the conventional bed is a newer field of study that has been developed as the research needs of spouted beds have evolved, Gegenheimer, (2017) CSBs, as seen in Figure 2.8, have spouting media located only in the conical region of the bed allowing for larger, courser and less uniform spouting media to be used compared to the conventional spouted bed, Gegenheimer, (2017).

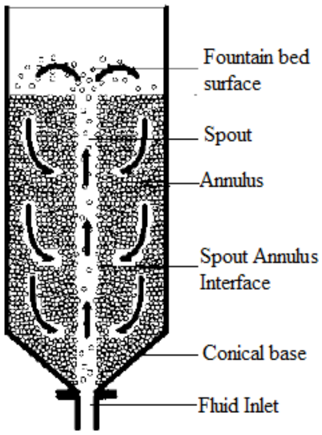

Figure 2.7:Typical Spout Produced in a CSB (Gegenheimer, 2017)

Though these coarser, larger particles create a more chaotic and random motion, it also increases the circulation of the particles which can allow for shorter gas-solid contact, or residence time, useful in certain applications, Gegenheimer, (2017). Due to these modifications of the CSB, it is more useful in applications such as particulate drying, coal gasification, pyrolysis, and catalytic polymerization, Bacelos and Freire, (2008).

Additional features of CSBs include less particle segregation compared to a fluidized bed. However, particle segregation is a positive feature that could reduce the residence time of the gas.

2.3.2 Flow Regimes

As the gas inlet velocity is increased, evolution will occur in the spouting media as shown in Figure 2.8 This evolution is described as happening in four dominant flow phases.

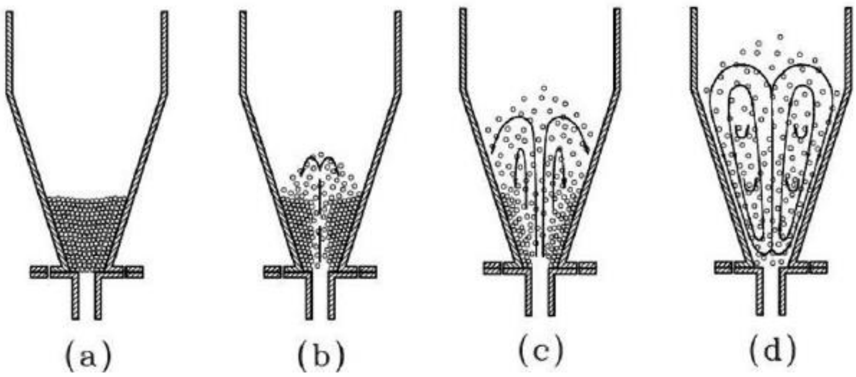

Figure 2.8: Spouting Regimes for Different Inlet Velocity: fixed bed (a), Stable Spouting Operation (b), Transition Regime (c), and Jet Spouting (d) Tube (Altzibar et al., 2013).

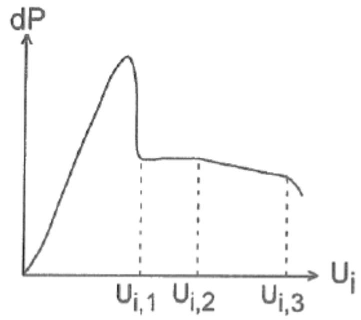

Figure 2.9: Theoretical Pressure-Velocity Curve for CSB (Gegenheimer, 2017)

I. Static or Fixed Bed

A static or fixed bed is the first phase, which would be found at low flow rates where the fluid momentum is insufficient to break through the spouting media.

II. Stable Spout

A stable spout is created when fluid momentum is sufficient to break through from the base of the CSB to the top of the bed of particles. The spout will create a circulatory pattern in the spouting media where the particles agglomerate on the walls where diffuse to the hollowed core and are then carried to the top of the channel by the fluid momentum, Epstein and Grace, (2011)

III. Transition, Phase

The third, or transition, phase is not as well characterized compared to the first two phases. This phase is the intermediate process between the formation of the spout and the fourth phase, jet or dilutes spouting.

IV. Jet or Dilute Spouting

The last phase is characterized when there is no agglomeration of particles on the conical walls of the CSB. While jet spouting is similar to a fluidized state, significant differences still exist between a CSB and a fluidized bed. A fluidized bed is characterized by the solid particles acting in a state of disorder while the jet spouting phase still has a circulatory pattern as seen in (d) of Figure 2.8. It should also be noted that additional bubbling and slugging phases can exist at higher bed heights in the conventional spouted bed. These phases are undesirable for most applications as they are non-uniform and non-axisymmetric giving the conical spouted bed an advantage over the conventional spouted bed. In short, the general characteristics of the jet spouted bed are high gas velocity, high bed voidage (over 0.75 depending on the operating conditions), cyclic movement of the particles, hydrodynamic behavior different from that of the conventional spouted bed, and fewer instability problems than the spouted bed regime

It is often found that the transition region is even less noticeable than seen in Figure 2.8. making it difficult to decipher. Visual determination can even be more reliable in some cases depending on instrument sensitivity. Also, notice the pressure drop across at the formation of spouting or pressure needed to break through the bed of particles represented as the breaking.

The theoretical performance curve is shown in Figure 2.8. above does not portray a perfect representation of the phase diagram. The individual geometry of each apparatus, different operating particle contactor conditions, and static bed height can cause deviations in the pressure-velocity curves; however, it is accepted as a theoretical curve one would expect to obtain.

2.3.3 Geldart Particles Classifications

As shown in Figure 2.10, Geldart classifies the particles according to particle density and diameter. The particles are divided into Group A, Group B, Group C, and Group D Yehuda and Kalman, (2020). Group A density lower than 1.4 g/cm^3. These solids fluidize easily with low gas inlet velocity; thus, they are called aeratable. Catalysts used for the fluidized catalytic cracking process can be categorized into this group

Due to the larger diameter, the physical properties of biomass materials and oxygen carrier particles generally belong to Geldart Group D. However, in the past decades, the research for dense gas-solid flow mainly focuses on small-scale fine particles, which belong to Geldart group A, B.

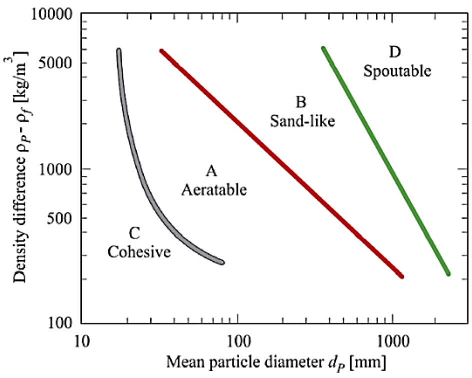

Figure 2.10: Geldart Particles Classifications (Kalman, 2020)

2.4 Geometric Configuration of Conical Spouted Bed

A range of parameters exists that characterize the CSB and can be grouped into three categories: geometric, fluid, and spouting media properties. Figure 2.11 shows the standard nomenclature used to represent the geometric parameters.

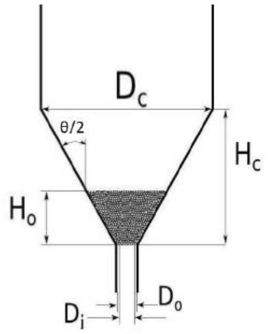

Figure 2.11: CSB Geometry (Sharma et al., 201)

Di represents the diameter of the inlet air pipe while D_O represents the inlet diameter of the cone which may be separate values. Ho represents the stagnated bed height of the particles. If $H_o > H_C$, then the system is described as a conventional spouted bed, whereas for this study, $H_o < H_{Cs}$ the system remains defined as a conical spouted bed (CSB). D_C is the diameter of the column.

2.4 Unstable Spouting

The phenomenon of unstable spouting is also a condition to be considered in spouted beds and commonly happens for two reasons. The first is due to the periphery of the external spout continuously opening and closing while the second is due to spouting media sinusoidally collapsing into the core of the spout, Olazar et al., 2011. Though these features are separate and unique, a combination of the two is most common as they are near indistinguishable without the assistance of an optical study.

Unstable spouting is undesirable as it interrupts the normal circulation of the spouted bed and is more difficult to determine from the pressure due to high fluctuations from the continuously opening and closing spout. Certain factors have been shown to affect the spouting velocity in which the main focus is the geometric conditions of the CSB, Wang, et al 2004. These factors include the ratio of Di/dp, Di/Do, θ, and a maximum spout-able bed height, which will be discussed below.

2.4.1 Inlet Diameter/Particle Diameter Ratio (Di/dp)

Mathur found strong differences between conventional and conical spouted beds in the inlet diameter/particle diameter ratio (Di/dp), Gegenheimer, (2017). For conventional beds, this ratio was said to be less than 30 for stable spouting while 2-60 for conical beds. This hints that this non-dimensional zed factor may be a weak function of stability in CSBs as compared to conventional beds. This also supports the idea that CSBs can use a larger variety of particle sizes.

2.4.2 Inlet Diameter/Cone Bottom Diameter (Di/Do)

It was found by Olazar that a minimum and maximum value exists for the inlet diameter/cone diameter (Di/Do). A minimum intuitively exists due to flow separation a dead space for the fluid created from the sudden expansion. Seemingly, this can create circulatory issues at the base of the spout causing instabilities. The minimum ratio was found to be 0.5 while the maximum was found to be 0.83. However, an upper limit is not as intuitive as a lower limit. Olazar stated that this limit may be exceeded but will be less likely in producing a stable spout, Olazar et al., 2011. This effect is due to non-agglomerating particles at the base of the discontinuity of the inlet diameter.

2.4.3 Cone Angle

Insight can once again lead to a minimum cone angle to produce spouting. A cone angle of 0° would result in a straight column which would hinder the circulation of any particles and defeat the purpose of the spouted bed by creating a fluidized bed. Instability, however, is a factor in the CSB due to larger, coarser particles. The lower limit is 28° by Olazar and was confirmed by Sharma at 30° in the previous study. Sharma et al., 2011. It should be noted that while an upper limit does not exist, higher angles (approaching 180°) provide little to no circulation also defeating the purpose of the spouted bed Olazar et al., 2011.

2.4 Existing Correlations for Minimum Spouting Velocity

Minimum spouting velocity (ums) is defined as the minimum air velocity required to maintain a spouting regime. A multitude of correlations can be found to determine the minimum spouting velocity for conical spouted beds. A non-dimensionalized Reynolds number (Rems), is generally used with a power-law curve fit with non-dimensionalized parameters. table 2.1 shows the correlations that will be used as a reference in this study. A parameter occasionally used, but not specified to this point is Db, or the diameter of the spouting media at the bed height of Ho. This can easily be determined from the geometry of the system.

Table 2.1: Existing Spouting Velocity Correlations

Source	Correlation
Bi et al. (1997)	$(Re_o)_{ms} = [0.30 - 0.27/(D_b/D_o)^2]\sqrt{Ar\,(D_b/D_o)[(D_b/D_o)^2 + (D_b/D_o) + 1]/3}$
Choi (1992)	$(u_o)_{ms} = \sqrt{2gH_o}\,0.147((\rho_p - \rho)/\rho)^{0.477}(d_p/D_c)^{0.61}(H_o/D_c)^{0.508}(D_o/D_c)^{0.243}$
Gorshtein (1964)	$(Re_o)_{ms} = 0.174\,Ar^{0.5}[1 + 2\tan(\gamma/2)\,(H_o/D_o)]^{0.25}\tan(\gamma/2)^{-1.25}$
Markowski (1983)	$(Re_o)_{ms} = 0.028\,Ar^{0.57}(H_o/D_o)^{0.48}(D_c/D_o)^{1.27}$
Mukhlenov (1965)	$(Re_o)_{ms} = 3.32\,Ar^{0.33}(H_o/D_o)^{1.25}\tan(\gamma/2)^{0.55}$
Sharma (2011)	$(Re_o)_{ms} = 717.26\,(Ar)^{0.08}(H_o/D_o)^{0.85}(d_p/D_o)^{1.23}$
Tsvik et al. (1967)	$(Re_o)_{ms} = 0.4\,Ar^{0.52}(H_o/D_o)^{1.24}\tan(\gamma/2)^{0.42}$
Olazar et al. (1992)	$(Re_o)_{ms} = 0.126\,Ar^{0.5}(D_b/D_o)^{1.68}\tan(\gamma/2)^{-0.57}$ $d_p > 1$ mm
Olazar et al. (1996)	$(Re_o)_{ms} = 0.126\,Ar^{0.39}(D_b/D_o)^{1.68}\tan(\gamma/2)^{-0.57}$, $d_p \leq 1$ mm

The characteristic length used for the Reynolds number is dp leading too:

$$(Re_{ms})_0 = \frac{(u_{ms})_0 d_p \times \rho}{\mu}$$

The Archimedes number is a parameter classically used to characterize systems of different fluid densities and has been modified to be used in gas-solid mixed systems with the following correlation:

$$Ar = \frac{g d_{p^3} (\rho_p - \rho)}{\mu^2}$$

2.5 Related Works

A fluidized bed (Nutting et al., 1971, Bannar 1978, Clarke and Macrae 1987) consists in maintaining the coffee beans in suspension thanks to a strong air flux fed below the coffee beans. The advantage of using a fluidized bed is that the bean heating is more homogeneous and has better control of process parameters. However, these units pose problems when handling medium and small batches.

Vanessa (2019) designed and evaluate Fluidized Bed Coffee Roaster with a chamber made of stainless steel with a capacity of one kilogram mainly to contain the green coffee beans as shown in Figure 2.12 Accordingly, with the optimal airflow rate of 9.2m/s, the machine was able to roast coffee beans in medium roast for 13.68 min at 234.33°C and duration of 17.98 min at 261.67°C for a dark roast.

The amount of hot air used in a roasting process about the batch size of coffee beans is defined by Mahlmann (1986) as an air-to-bean ratio (kg air per kg green coffee). This ratio is a characteristic parameter in a roasting process but only applies to a given degree of roast. According to Mahlmann, figures can range from 1 in a typical conventional process up to 150 in fully fluidized-bed systems.

A spouted bed roaster is a variant of the fluidized bed roaster (Mujumdar, 1987). This has special advantages relative to the fluidized bed roaster when the particles to be roasted are large (about 5 mm) and tend to develop unstable fluidization (slugging). Very good solids mixing and effective gas-particle contact make it possible to use higher temperature heating air for short periods (HTST) and to provide a clean, uniform roasted product.

Nagaraju et al., (1997) have been conducted an experiment on a spouted bed roaster for coffee beans (peaberry) using hot air as the heating medium with a glass column of 150 mm diameter and 350 mm long and evaluate conditions for optimum roasting as represented in Figure 2.13. Roasting times for various inlet air temperatures for bed heights of 100 mm (1

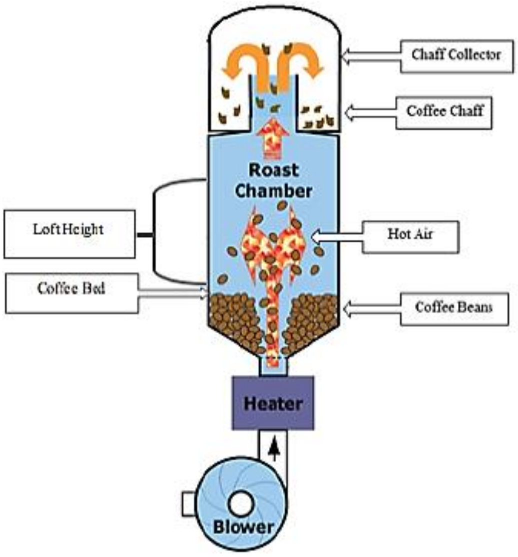

Figure 2.12: Schematic Diagram of Fluidized-Bed Roaster (Vanessa et al., 2019)

kg) and 75 mm (0.75 kg) were studied. It was found that the best quality product was obtained at an air temperature of 250°C for a roasting time of 5 min. Nagaraju and Suvendu (2010) study the roasting of pea-berry grade green coffee (Coffea arabica) beans using a spouted bed roaster at a laboratory model and optimized combinations of temperature and time of roasting are about 237-250 C and 180-240 s. The roasted samples were analyzed for instrumental color (hue, chroma, and brightness) and texture. The brightness of the roasted samples varied between 5.2 and 20.4%, and the time of roasting markedly decreased the brightness values.

A process for roasting coffee beans involving spouted bed roasting (SBR) as indicated in Figure 2.14, followed by cryogenic cooling and grinding was developed. Roasting experiments were carried out with an indigenously designed spouted-bed roaster in batches of 500 g beans. The temperature and time of roasting were 210°C and 22 minutes. It was found that coffee subjected to SBR roasting followed by cryogenic cooling had a greater impact on the retention of volatile Stable operation in a conventional conical-cylindrical spouted bed is only attained when the ratio between the gas inlet diameter and particle diameter D_O/d_P, is smaller than 20-30 times the particle diameter (Mathur and Epstein, 1974; Olazar et al., 1992)**.** Higher values of this ratio lead to slugging and highly unstable beds, with these phenomena occurring with either fine or coarse particles.

Several authors managed to attain stable operation with fine particles (Du et al., 2015; Estiati et al., 2017; Mostou et al., 2015; Nagashima et al., 2013; Zhu et al., 2005; Wu et al., 2015), but in all cases, they used low values of the mentioned ratio or stabilized the system with internal tubes.

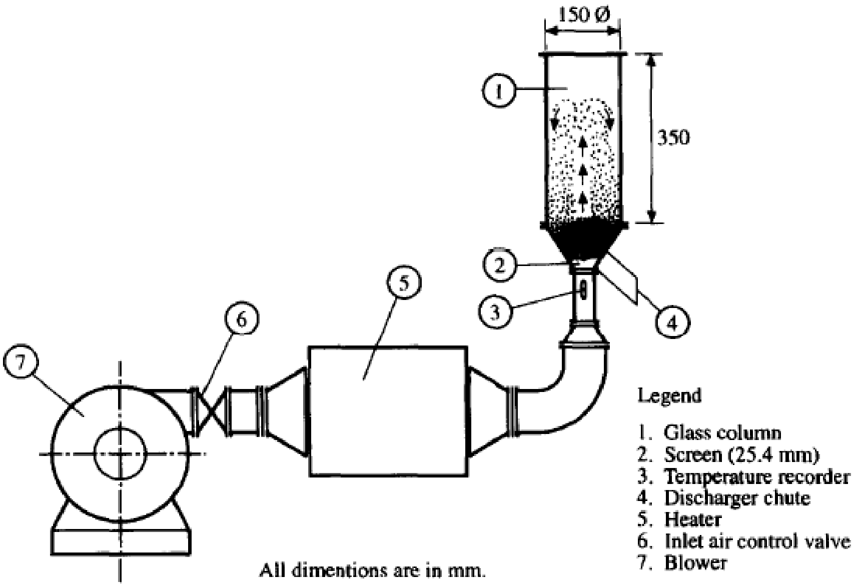

Figure 2.13: Schematic Diagram of a Spouted Bed Roaster (Nagaraju et al.,1997)

compounds especially the furans and thiols than the conventional drum roasting (CDR) Nagaraju et al., (2016)

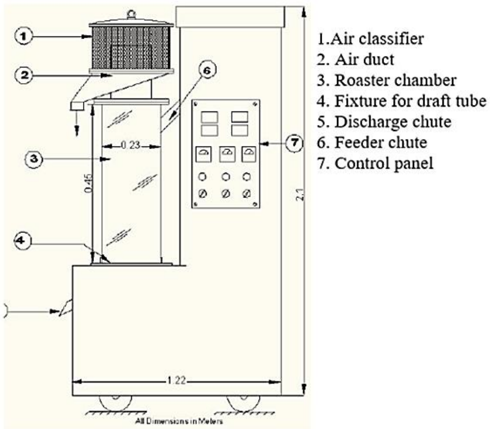

Figure 2.14: The Apparatus for the Spouted-Bed Roasting (Nagaraju et al.,2016)

There are different variants of conventional spouted beds (conical, cylindrical, mechanical, two-dimensional, slot-rectangular) (Saldarriaga et al., 2015; Shao et al., 2014; Rudolph, 2006; Golshan et al., 2017; Taylor et al., 2012), with each one having advantages and disadvantages, but none have solved the problem of scaling up.

One of the most promising configurations is the slot-rectangular spouted bed, whose hydrodynamics, stability, and scale-up have been experimentally investigated (John, 2004; Taylor et al., 2000; Shirvanian and Calo, 2004; Freitas et al., 2000). However, the problem of scaling up has not been solved, which limits their application in large-scale industrial processes.

The usual solution to stabilize the bed is the insertion of a draft tube (Estiati et al., 2017; Berghel and Renström, 2014; Altzibar et al., 2011; Caussat et al., 2006; Altzibar et al., 2008; Shuyan et al., 2010). Buchanan and Wilson (1965) use the draft tube as an internal device for the first time, and nowadays different draft tube configurations have been reported in the literature, as are: conventional nonporous draft tube, porous draft tube, and open-sided draft tube.

Nonetheless, draft tubes modify the hydrodynamics and solid circulation flow rate of the system (Epstein and Grace, 2011; Ishikura et al., 2003), changing the minimum spouting velocity, operating pressure drop, solid circulation patterns, gas distribution, and particle cycle times (time required for a solid to complete a full cycle, crossing all the zones in the spouted bed).

The performance of the lower conical section of the contactor is different when a draft tube is used, and largely depends on the bed geometry, draft tube diameter, the height of the entrainment zone, and operating conditions (Nagashima et al., 2009; Kmiec et al., 2009;).

Conical spouted beds have proven to perform well in many applications, such as drying of sand, biomass, or milk (Olazar et al., 2012; Perazzini et al., 2017); pyrolysis of citrus wastes, biomass, or plastics (Amutio et al., 2012; Alvarez et al., 2017); fine sawdust combustion (Saldarriaga et al., 2018) and steam gasification (Lopez et al., 2016). Many of these operations involve the treatment of fine particles with draft tubes as the only way to attain stable spouting, but the treatment of course particles needs further work.

The D_o/d_p the ratio may be increased to 2 to 60 in fully conical spouted beds (Olazar et al., 2009) and whereby, the limits are not for stability but only for operativeness. This means that very small inlet diameters (a few millimeters) are required for the treatment of fine particles, which leads to very high-pressure drops at the inlet and poor solid circulation. The use of draft tubes is the common solution to overcome this problem.

Saldarriaga et al., 2015 study on the influence the draft-tube configuration have on the solid circulation in conical spouted beds made up of sawdust. In the experimental units portrayed in Figure 2.15, the main component is the conical contactor. The unit was operated with contactors of polymethyl methacrylate of different cone angles, γ = 28, 33, 36, and 45°, and at two inlet diameters of textures. The results obtained based on runs carried out according to an experimental design show that particle cycle times are influenced by both the draft tube configuration and contactor geometry. On average, cycles times are twice to triple longer when nonporous tubes are used. Therefore, the open-sided internal device provides stability and ensures high turbulence to beds made up of fine and irregular particles, with their behavior being similar to stable beds made up of coarse particles in which no draft tube is required.

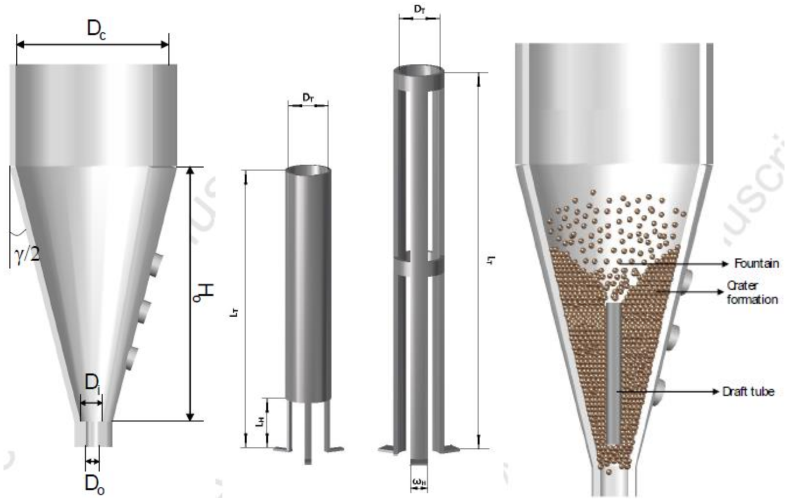

Figure 2.15: Saldarriaga Bed Geometry (Saldarriaga et al.,2015)

Altzibar et al., 2013 have carried out an experimental design on the minimum spouting velocity of conical spouted beds equipped with draft tubes of different configurations to show that the hydrodynamics is different from plain spouted beds. The results show that the minimum spouting velocity is influenced by the type of draft tube used and its geometry, the contactor/particle factors, and operating conditions. A statistical analysis of the results shows that the factors of greater influence on the minimum spouting velocity for all systems (with and without tubes) and materials (coarse and fine) are particle diameter (d_p) and gas inlet diameter (D_o), followed by the factors of each type of tube (W_H, L_H) and bed height (H_o). In the case of open-sided tubes and sand with a particle size distribution, contactor angle (γ) is the factor of greater influence. In addition, the minimum spouting velocity has lower values for an angle of 36°, and a wider one (45°) and a narrower one (28°) give way to higher values of this velocity.

Olazar et al., (2009) study on spouting performance in conical spouted beds at high temperatures and under vacuum by using materials of different textures, densities, and particle diameters. The correlations on the hydrodynamic parameters in the literature for conical spouted beds have been obtained under atmospheric conditions and most of them are empirical ones. The experiments have been carried out using the contactor unit's main component, being a spouted bed of conical geometry with a cylindrical upper section. The total height of the reactor is 34 cm, the height of the conical section 20.5 cm, and the angle of the conical section 28°. The nitrogen gas is used as a fluidization agent and heated to the desired temperature in a preheater provided with an electric cartridge. Both temperature and pressure cause a decrease in the minimum spouting velocity, which is mainly due to the increase in viscosity and density, respectively, and therefore to the increase in the momentum transfer from the gas to the solid. A new equation for predicting the minimum spouting velocity from ambient conditions to high temperatures and vacuum conditions has been obtained by modifying a previous one obtained for ambient conditions.

Modifying the conventional conical spouted bed by inserting a fountain confiner in the contactor, an experiment has been carried out on the efficiency of the confinement device to avoid fine particle entrainment which is publicized in Figure 2.17. The influence of the geometry of the device on the hydrodynamics of conical spouted beds has been studied. The results show that the fountain confined largely avoids fine particle entrainment, i.e., 60-70% (80-90% entrainment without confinement versus 20% with the fountain confiner) reduction depending on the type of draft tube used. The fountain confiner reduces the operating bed pressure drop and the maximum cycle time of the particles in the contactor but does not affect the minimum spouting velocity. Nevertheless, the greatest advantage of the fountain confiner lies in the stabilization of the fountain and the homogenization of the solid circulation in the bed, which leads to a significant increase in the gas-solid contact in the fountain. Furthermore, nonporous draft tube systems lead to higher fine retention than open-sided tube systems, with entrainment reduction being 69.4% in the former and 61.2% in the latter, (Altzibar et al., 2017)

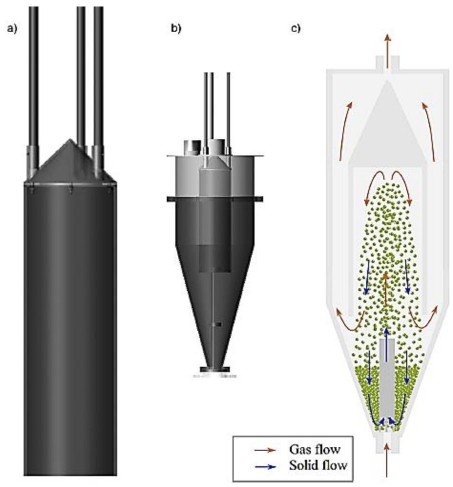

Figure 2.16:The fountain Confiner (a), Location (b), and its Trajectories (c) (Olazare et al., 2009)

Olazar et al., (2019) study on new operation regimes in fountain confined conical spouted beds using an experiment at a pilot scale as indicated in Figure 2.18. Nevertheless, the most important limitation of a conical spouted bed lies in its scaling up, since the inlet diameter/particle diameter ratio must be below 20-30 to avoid bed instability. To overcome this limitation, a new internal device called a fountain confiner has been developed, which stabilizes the system and allows operating with fine particles even without any type of draft tube. The use of this new device allows for attaining highly stable operation regimes, widening the operational range to 4 times that of plain spouted beds, and increasing the inlet diameter/particle diameter ratio from 20-30 to 1000. Moreover, the optimum distance between the bed surface and the lower end of the confiner is in the 0:06 -0:08 m range (between 1/2 and 1/3 the confiner diameter) for the operation conditions studied without a draft tube or with open-sided draft tubes, whereas it is irrelevant when nonporous tubes are used.

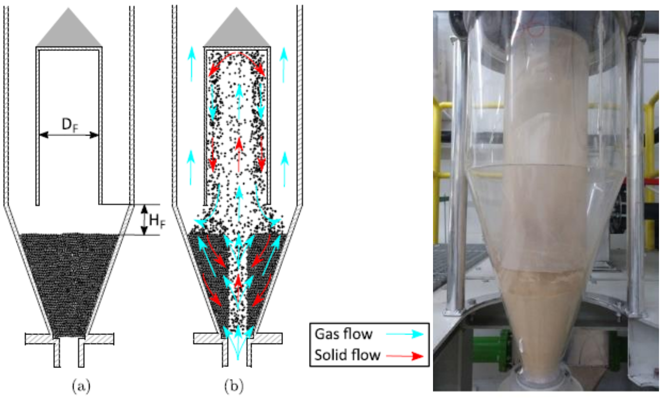

Figure 2.17: Fountain Confiner and its Geometry (a) CSB using Sawdust (b) (Olazar et al., 2019)

Subsequently, the conical spouted bed reactor provided with a draft tube and a fountain confiner has been used for biomass gasification (Lopez et al., 2017). They are worth mentioning the flexibility and stability of the spouting regime and the capability of increasing the fountain height in a controlled way to improve the contact between the reacting gases and the catalyst. Moreover, owing to the fountain confinement, the gas is forced to flow down to leave the confiner through its bottom, which increases the biomass-derived volatile residence time in contact with the catalyst.

The roasting process is largely a function of fluid dynamics associated with the air flowing through the roaster and the transfer of heat and mass between coffee beans and the surrounding gaseous molecules. FEM is used for the simulation of the fluid dynamics and transfer of heat within a coffee bean roaster (Chao et al., 2016). The coffee roaster modeled in this study was based on a commercial device, the FUJI Royal R-101 1KG where constructed in the form of three concentric cylinders as shown in Figure 2.19. The results demonstrate that the power output of the heat source has a direct effect on temperature in the roasters; i.e., increasing the output from 3,000 to 4,000 W (30%) increased the average temperature in the roaster chamber from 100 to 1308℃ (30%).

Duarte (2005) studied the fluid dynamics of the spouted bed using an Eulerian multiphase model. The calculation was made for the same geometry as that used in the experimental work of, He et al. (1994) including a glass sphere and for a two-dimensional spouted bed using soybean seeds operated in the laboratory. The results obtained show good agreement between the simulated and the experimental results.

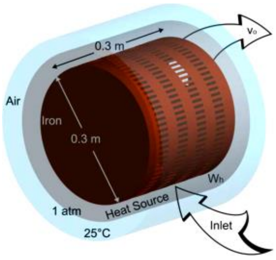

Figure 2.18: Illustration of the Model used in the Simulation of Heat (Duarte, 2005)

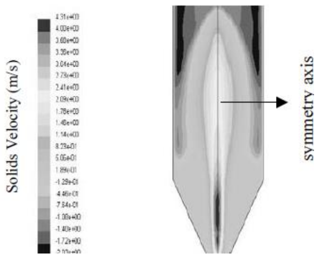

Figure 2.19: Solids Velocity Profile (Duarte, 2005)

Hosseini et al., (2015) simulate the hydrodynamics of a pseudo-2D rectangular spouted bed as displayed in Figure 2.21, by CFD using the Eulerian-Eulerian two-fluid model in conjunction with the kinetic theory of granular flows (KTGF) with different values of the specularity and particle wall restitution coefficients, for wall boundary conditions.

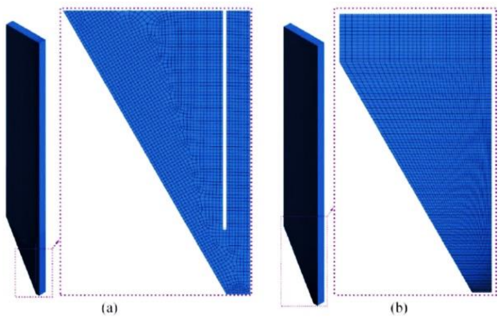

Figure 2.20: Mesh of (a) 2DSB with, (b) 2DSB without draft plates (Hosseini et al., 2015)

As the simulation results are indicated in Figure 2.22 showed that the 3D (CFD) model is more sensitive to the specularity coefficient and the particle-wall restitution coefficient compared to the 2D model. In addition, the 3D model was more significantly affected by the variation of the specularity coefficient when compared with changes in the particle-wall restitution coefficient.

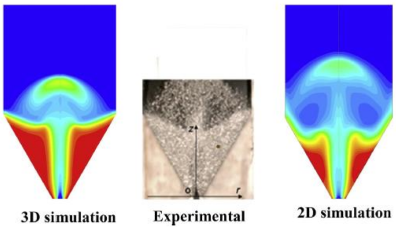

Figure 2.21: 2D and 3D CFD, Experiment Results of Solid Particles (Hosseini et al., 2017)

Ahmadabadi et al., (2020) investigate the hydrodynamic parameters of micro/nanoparticles in a conical spouted bed using experimental and computational fluid dynamics (CFD) techniques which are shown in Figure 2.23. The Eulerian-Eulerian approach, in conjunction with the kinetic theory of granular flow (KTGF), has been used, and the effects of solid wall boundary condition parameters such as specularity coefficient (φ), and particle-wall restitution coefficient (*e*w), on the hydrodynamics of the bed were studied. The CFD predictions were in good agreement with the experimental data in terms of pressure drop and particle distribution.

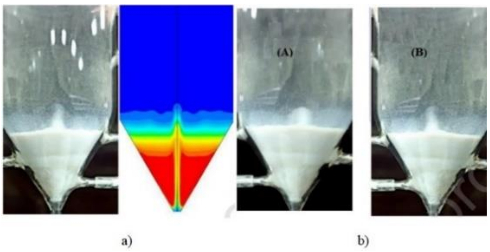

Figure 2.22: The Nanoparticles (a) and their Fluidization (b) (Ahmadabadi et al., 2020)

2.6 Conclusions of Literature Review

Roasting coffee beans is experienced to impart specific organoleptic characteristics to the brew and also for ease of grinding and extraction. It is a time-temperature-dependent process involving physical and chemical changes. The degree of roasting plays a major role in determining the flavor and aroma characteristics of the brew. Although heat transfers during roasting can involve conduction, convection, and radiation, convection by far is the most important mode of heat transfer that determines the rate and uniformity of roasting. Accordingly, the advancement of coffee roasting early from grandmother's roasting pan to industrial batch roasters of different designs and continuous roasting systems with large product output.

Among existing commercial roasters, drum roasters mainly involve convective heat transfer producing roasted coffees with less soluble solids, more degradation of chlorogenic acids, more burnt flavor, and higher loss of volatiles than those roasted using fluidized bed roasters.

A fluidized bed is one of the recent developments in coffee roasting technology in which high-velocity hot gas is directed towards the beans so that the gases heat and move the floating beans simultaneously. A fluidized bed roaster is almost exclusively based on convective heat transfer, allows better control of air temperature and speed inside the roasting chamber, produces a more homogeneous color than other roasters and the fast roasted beans allow better water penetration and extraction of the soluble compounds.

The spouted bed roaster, an alternate to fluid bed roasting, is also suitable for particulate solids like green coffee beans and similar materials. Although the areas of application of a spouted bed overlap with a fluid bed system, the functional mechanism in the two cases are different. A steady axial jet causes agitation of particles in a spouted bed technique, while it is regular and cyclic in a fluid bed system. There is a very good mixing of solids and effective gas-particle contact in SBR which facilitates HTST processing provides clean uniformly roasted products and maintains the quality of flavoring materials such as coffee beans.

The conventional spouted bed is not fully satisfactory to achieve good gas-solid contact due to the instability of the bed, especially at a large scale. The crucial parameter that limits the scaling up and stability of spouted beds are the geometry of the contactor and the ratio between the inlet diameter of the contactor and particle diameter. Thus, the insertion of a draft tube and fountain confiner is the usual solution to this problem, specifically to improve fluidization and the efficiency of the spouted bed and as well as to stabilize and scale up the spouted bed. The numerical simulation of coffee bean roaster by using commercial and recent technology, like that spouted bed in case of studying the fluid dynamics and heat transfer using FEM mainly Eulerian and Lagrangian Approach.

2.7 Research Gap

A review of the literature reveals conventional spouted beds ensure good solids mixing and effective gas-particle contact however; it has a certain drawback that requires different modifications to improve its performance for different applications. Conventional spouted beds require higher flow rates due to spouting media being located at a pre-determined height in the column.

In a conventional spouted bed, the solid trajectory i.e., the fountain created at the top of the bed when spouting gas is high enough to open spouting thereby, the solid particle rain back on the bed but the hot fluid leaving the bed which is a direct pass heat exchange within the particle in the bed. This, kind of phenomenon leads to poor gas-solid contact and reduces the cycle time of gas past solid trajectories which lead to a low heat transfer coefficient. The estimated heat transfer coefficients for coffee beans using conventional spouted bed and other existing commercial coffee roasting technology is less than 31 W/m^2K for an air temperature not exceeding 250°C.

From the review, the FEA analysis, like CFD Fluent is used to seek numerical simulation, which is based on a continuum approach, in case both the fluids and particles are treated as interpenetrating continua. However, the phenomenon of inter-particle collision among particles that is raised from the dynamics of a particle in the real situation, cannot be studied due to the limitation of CFD as a numerical method that mostly works with the Eulerian and Lagrangian Approach.

Therefore, to overcome the problem of poor gas-solid contact in the bed and enhance the heat transfer rate and as well as to improve the performance of conventional spouted bed, the conical spouted bed with an internal device like a fountain confiner and the draft tube would be designed and developed for coffee bean roasting. Thus, in this thesis, Performance Investigation of Improved Conical Spouted Bed with the internal device is designed and developed for the coffee Roasting Application using the CFD Fluent-Rocky DEM Coupling method.

CHAPTER THREE
MATERIALS AND METHODS

This chapter introduces the materials and method used for the proposed Thesis. The developed spouted bed coffee roasting machine entailed a general description of the roasting machine, design, sizing of the bed components, and selection of component materials. In addition, before the design stage, an assessment of the physical properties of the green coffee bean was conducted.

3.1 Materials of Conical Spouted Bed with Internal Device

3.1.1 Material Constructing Spouted Bed

Selection of materials for roaster was based on hygiene, strength, availability, machinability, and malleability for components to be machined and cold work, rigidity, durability, corrosiveness, and maintainability to guarantee longer machine life span and affordability of the machine.

This thesis used material for roaster construction, material to be roasted, and other auxiliary apparatus as listed in Table 3.1. The construction material included a plate of stainless steel, a perforated plate of stainless steel, mild steel for the frame, a blower and corresponding driver mechanism, air heating resistor; while the material to be roasted is coffee bean, using ambient air to elevated temperature. Stainless steel 316 material was used to construct the components of spouted that have direct contact with a coffee bean which includes; a roasting bed, fountain confiner, draft tube coffee, cooling bin, and others.

Table 3.1: Materials

Materials Lists	Remarks
Stainless Steel 316	Good heat Resistance
Mild Steel	Low cost
Fiberglass	For insulating materials
Coffee beans	To be roasted
Electrical Air Heater	With variable resistor
Blower	With adjustable speed control

The other components such as air heater housing, hot air inlet pipe, chaff collector, frames, and others were made of mild steel, material for side covers and outlet air duct. In addition to this, as shown in Table 3.2 the following tool and equipment are used to achieve the respective objects of the research.

Table 3.2: Tools and Equipment

Equipment	Remarks
Computer	HP Intel (R) Core (TM) i7, processor 3.2 GHz 8 RAM
GPU	NVIDIA GeForce 940MX with total global memory of 2.0 GB
CFD Fluent	Flow Field Simulations
Rocky DEM	Particle Simulator

3.1.2 Spouted Bed Material

According to the general objective of this thesis, the spouted bed material is necessarily coffee beans. Therefore, the engineering properties of coffee beans must be considered. Three Ethiopian coffee bean varieties were selected from the local market Adama namely Jimma, Wallaga, and Sidama for dimension physical properties analysis.

3.1.3 Dimensions Coffee Bean

The three linear dimensions as shown in Figure 3.1; length=9.38mm (major), width=6.3mm (intermediate), and thickness t=4.18mm of 30 green beans from each variety were measured using a digital caliper.

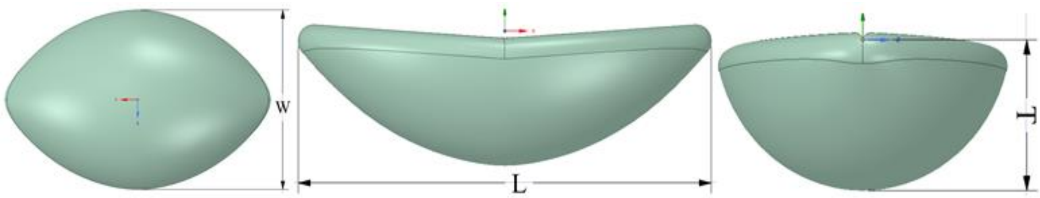

Figure 3.1: Dimension of Coffee Beans

The mean diameter of geometric (Dg), arithmetic (Da), square (Ds), and equivalent (De) were calculated from Equations (3.1), (3.2), (3.3), and (3.4), respectively.

The mean geometric D_g

$$D_g = (WLT)^{1/3} \tag{3.1}$$

D_g=6.24mm

The mean arithmetic (Da),

$$D_a = \frac{W+L+T}{3} \tag{3.2}$$

D_a=6.6mm

The mean square (Ds)

$$D_s = \left[\frac{LW+WT+TL}{3}\right]^{1/2} \quad (3.3)$$

D_s=6.42mm

The mean equivalent (De)

$$D_e = \frac{D_g + D_a + D_s}{3} \quad (3.4)$$

D_e=6.42mm

3.1.4 Physical Properties of the Green and Roasted Bean

I. Moisture Content of Washed Coffee Beans

The moisture content of coffee beans was determined by drying 14-18g of the sample at 105°C in an oven for 24 hours. The well-dried of Wallaga, Jimma, and Sidama, with moisture contents of 11, 16, and 20% w.b. were also obtained from the estate for use in the experiments.

II. Bulk Density

The green coffee bean's bulk density was measured using a 500 mL measuring cylinder. The ratio between the weight and volume was used to evaluate the bulk density according to the method described by Pittia et al., (2007). The results of bulk density as given in equation 3.5 are expressed as the mean value of three measurements.

$$\text{Bulk density } (\rho_B) = \frac{\text{weight of green coffee beans}}{\text{bulk volume of green coffee beans}} \quad (3.5)$$

III. True Density

The true density of the samples of coffee beans was determined by the water displacement method. The three variants of coffee beans i.e, Jimma, Wallaga, and Sidama samples of about 14, 18, and 19 g were weighed and dropped into a 100 ml measuring cylinder filled with water up to 50 ml. The rise in water indicated the true volume of the beans. From the mass and the true volume of the beans, the true density was calculated. For each case, the determination was replicated three times and the mean was about 1.2, 1.1, and 1.02 g/cm^3 respectively.

Physical properties of green and roasted coffee beans are required to calculate the capacity of a roaster, primarily to determine the dimension of the roasting column, cooling tray, wattage requirement for heating element, and blower for ambient air supplier. Table 3.3 shows the physical properties of Arabica and Robusta green and roasted coffee beans because of the preliminary study. Bolay et al., (2010); Dadang et al., (2020)

Table 3.3: Physical Properties of Arabica and Robusta Coffee Bean

Physical properties	Arabica			Robusta		
	Green Bean	Light to Medium	Medium to Dark	Green Bean	Light to Medium	Medium to Dark
Moisture content (%)	13.08	6.54	6.24	11.22	7.56	6.12
Weight (g)	0.22	0.17	0.17	0.16	0.14	0.13
Bulk density (g/cm^3)	0.69	0.35	0.31	0.72	0.40	0.32
Mass decrease (%)	-	19.80	20.30	-	10.87	14.90
Volume increase (%)	-	49.97	54.85	-	44.93	56.20

3.2 Research Methods and Methodology

The methods and methodology used to achieve the objectives of this thesis are discussed here below and the detail of workflow shown in Figure 3.2.

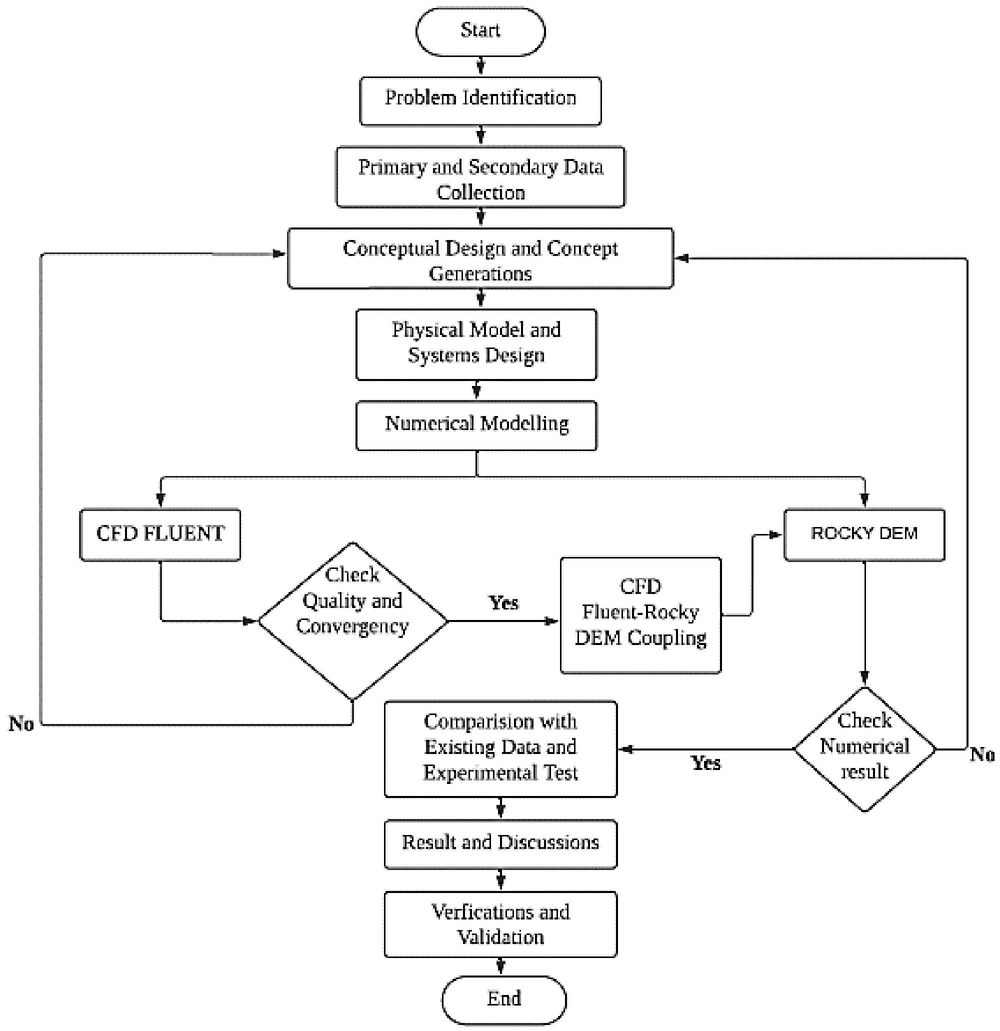

Figure 3.2: Methodology

3.2.1 Problem Identification

As stated in chapter one above, both the drying and roasting processes are achieved by conduction, convection, and radiation mode heat transfers. However, convection by far is the most important mode of heat transfer that determines the rate and uniformity of roasting. Although much commercial coffee roasting developed that accompanied by convection mode of heat transfer, commencing from the rotating drum, Fluidized bed to conventional spouted bed (i.e cylindrical with conical base), it poses problems and drawbacks to achieving proper uniformity of product and better control of process parameters due to the limitation of their thermo-hydrodynamic gas-solid contact and particle dynamics. Therefore, to overcome this problem further investigation was carried out to improve the performance spouted bed for coffee roasting application.

3.2.2 Data Collection

Primary Data

The researcher has tried to collect the primary data by direct contacting the customer. The necessary data collected are like that of the number of coffee beans processed per day by the coffee seller of cafes in our country and exporter.

Secondary Data

Secondary data is collected from published articles, Reports, Theses works, journals, the internet, etc.

3.2.3 Conceptual Design

The conventional spouted bed is based on a cylindrical cone that diffuses to a fixed diameter column as shown in chapter one. Conventional spouted beds require higher flow rates due to spouting media being located at a pre-determined height in the column, while Conical Spouted beds, as discussed in chapter two have spouting media located only in the conical region of the bed allowing for larger, courser, and less uniform spouting media to be used compared to the conventional spouted bed.

Spouted beds with fully conical geometry combine the features of the cylindrical spouted beds and are highly versatile in the gas flow rate, allowing operation with particles of irregular texture, coarse and fine particles, and those with wide size distribution and sticky solids, whose treatment is difficult using other gas-solid contact regimes. And also, have capable to achieve dynamic cyclic movement, small pressure drops, and less residence time. These features of the conical spouted beds make them attractive for different applications. Thus, a conical spouted bed with the different internal devices was selected to investigate and developed for coffee roasting application as mentioned next.

The first design criteria to design and develop a conical spouted bed is the stability operational conditions. According to Olazar et al., 1992; the ratio of Do/dp may be increased to 2 to 60 in fully conical spouted beds, and thereby, the limits are not for stability but only for operativeness. This means that very small inlet diameters (a few millimeters) are required for the treatment of available particles, which leads to very high-pressure drops at the inlet and poor solid circulation. Thus, the use of draft tubes is the common solution to overcome this problem.

The other design criteria to consider is the maximum cycle time of the particles inside the bed to lengthen residence time. The device intended for this problem is the insertion of a fountain confiner used to reduce the operating bed pressure drop and maximize the cycle time of the particles in the contactor. Nevertheless, to review the literature, there was no reported study on the hydrodynamic behavior of conical Spouted Bed with an internal device like a fountain confiner and draft tube for applications to the roasting of coffee beans. The objective of the present study is to design and develop the fountain confined conical spouted bed with an open-sided draft tube and investigate the thermo-hydrodynamic characteristics of heat-sensitive particulate solids such as coffee during roasting.

The hydrodynamic parameters obtained elevated temperatures such as minimum spouting velocity, particle trajectories, and processing time, and the heat transfer coefficient was analyzed numerically and verified the simulation results by the existing data and as well as to experimental test is conducted for validation.

3.3 Preliminary Design and Concept Generation

The CSB had to be designed based on the guiding principles to avoid hydrodynamic instability discussed in Chapter 2 which includes the ratios of Di/Do, Di/dp, and θ. The evolution of pressure drops with air velocity from the fixed to the spouted bed has been analyzed to determine the performance of the bed and minimum spouting velocity, the peak pressure drop, and the operating pressure.

3.4 Performance curve

The most common method used to determine the spouting phases is not by visual means, but by measuring the pressure concerning fluid velocity which yields Figure 3.3.

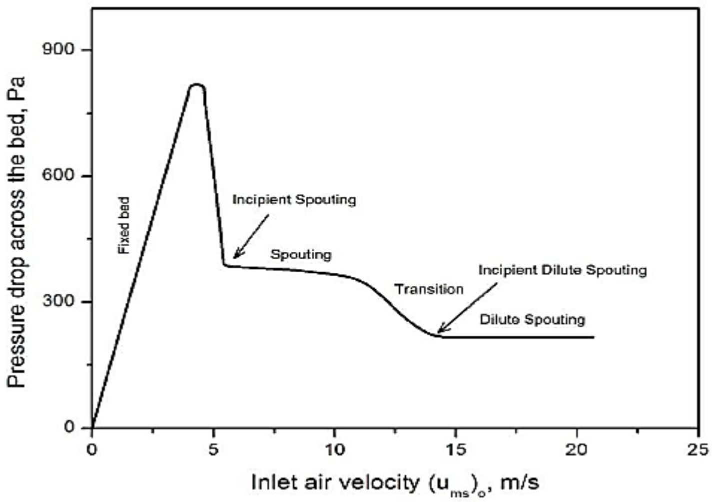

Figure 3.3: Gorshtein Pressure-Velocity Curve Gorshtein et al, 2017

The spouting phase is characterized at the end of the peak pressure drop, or approximately 5m/s in this example. The transition region is much less defined as it happens over a range of inlet velocities eventually leading to jet or dilute spouting.

3.5 Spouting Velocity

3.5.1 Minimum Spouting Velocity of Cold Flow

The minimum spouting velocity (U_{ms}) is an important parameter for the design and operation of spouted beds. Minimum spouting velocity (ums) is defined as the minimum air velocity required to maintain spouting regime. Olazar et al., 1992; Olazar et al., 2006; Olazar et al., 2004.

For $d_p > 1mm$

$$Re_{ms} = 0.126Ar^{0.50}(D_b/D_o)^{1.68}[\tan(\gamma/2)]^{-0.57} \quad 3.6$$

The characteristic length used for the Reynolds number is d_p leading too:

$$(Re_{ms})_0 = \frac{(u_{ms})_0 d_p \rho}{\mu} \quad 3.7$$

The Archimedes number is a parameter classically used to characterize systems of different fluid densities and has been modified to be used in gas-solid mixed systems with the following correlation:

$$Ar = \frac{g d_p^3 \rho\left(\rho_p - \rho\right)}{\mu^2} \quad 3.8$$

The top diameter of the stagnated bed, m

$$D_b = D_o + 2H_o tan(\gamma/2) \quad 3.9$$

3.5.2 Minimum Spouting Velocity of Hot Flow

For any given bed height, U_{ms}**,** increases with increasing temperature according to the empirical equation of Mathur and Gishler ***(1955):***

$$U_{ms} = \left[\frac{d_p}{D_c}\right]\left[\frac{D_i}{D_c}\right]^{1/3} \sqrt{\frac{2gH(\rho_p - \rho_f)}{\rho_f}} \qquad 3.10$$

The Reynolds number;

Where; Ar =Archimedes number; Db, Dc, Di, Do =Top diameter of the stagnant bed, of the column (or upper diameter needed for the cone), of the bed bottom, and the bed inlet, respectively (m); Hc= Height of the cone, m; Ho=H= Height of stagnated bed of particles, m; $(Re_{ms})_0$ =Reynolds number of minimum spouting referred to Do; $(u_{ms})_0$ = Minimum spouting velocity referred to Do, m/s; γ =included cone angle, degrees; ρ = density of air, respectively (kgm^3); ρ_p = Density of solid particles, (kgm^3); μ =Viscosity of air, Kg/m/s; ρ_f = density of Fluid

The top diameter of the stagnated bed, m

$$D_b = 0.068 + 2 * H_o * tan(30)$$

3.6 Flow Rate fluidization

According to Gegenheimer, (2017) and from various sources, the minimum and maximum fluidizing flow velocity can be calculated from the empirical equations 3.13 and 3.19 as shown below.

3.6.1 Minimum Flow Rate Fluidization

In the conical spouted bed system, the flow rate must be greater than the minimum fluidization velocity in the inlet but should be less than the maximum flow velocity in the cylinder section fluidization so that the grain is not carried by the gas stream. The minimum velocity of fluidization is derived from the Ergun equation, and can be estimated using the equation:

$$U_{mf} = \frac{(\varphi d_p)^2}{150\mu}\left[g(\rho_s - \rho_g)\right]\frac{\epsilon_f^3}{1 - \epsilon_f} \qquad (3.13)$$

Where:

φ = The sphericity value is a measure that states the state of the grain shape seen from the roughness and is compared with perfectly rounded grains. Merely, it is defined as the ratio of the surface area of an equal-volume sphere to the actual surface area of the particle. The volume of spherical particles is expressed by Sukarsono et al., 2014.

$$V_p = \pi \frac{d_p^3}{6} \tag{3.14}$$

$V_p = 1.27 * 10^{-7}$

And its surface area is

$$A_s = \pi d_p^2 = \pi \left[\left[\frac{6V_p}{\pi} \right]^{1/3} \right]^2 \tag{3.15}$$

$A_s = 1.22 * 10^{-4}$

$$\varphi = \frac{A_s}{A_p} = \frac{\pi \left(6V_p/\pi\right)^{2/3}}{A_p} \tag{3.16}$$

These parameter values φ range from 1-1.2, and values of 1.1 are commonly used values for solid granularity.

The second parameter is the void fraction at the minimum point of fluidization, ϵ_f. There is a correlation that seems to provide an accurate prediction of the ϵ_f values for the particles in the small fluidized bed:

$$\epsilon_f = 0.586\varphi^{-0.23} \left[\frac{\mu^2}{\rho_s g(\rho_s - \rho_g) d_p^3} \right]^{0.029} \left[\frac{\rho_g}{\rho_s} \right]^{0.031} \tag{3.17}$$

Another commonly used relationship is Wend and Yu, 2012

$$\epsilon_f = \left[\frac{0.071}{\varphi} \right]^{1/3} \tag{3.18}$$

For $\epsilon_f = 0.4$; the minimum flow rate U_{mf} =8.4m/s

3.6.2 Maximum Fluidization Flow Rate

If the gas velocity increases with a sufficiently high value, the resistance on the individual particles will go beyond the gravitational force on the particles, and the particles will rise in the gas and carry out of the bed. The point at which the resistance on individual particles will exceed the force of gravity is called the maximum flow rate of fluidization. When the upward velocity of the gas exceeds the particle terminal velocity, U_t. the particle will be carried upward by the gas stream. Reynolds number for small particles will be small. The maximum flow rate of fluidization can be calculated using equation 3.19 presented by Kunii and Levenspiel:-

$$U_t = \frac{\eta d_p^2}{18\mu} \qquad for\ Re < 0.4 \tag{3.19}$$

$$U_t = \left(\frac{1.78x10^{-2}\eta^2}{\rho_g \mu} \right)^{\frac{1}{3}} (d_p) \qquad for\ 0.4\ Re < 500 \tag{3.20}$$

With $\eta = g(\rho_s - \rho_g) = 6{,}860.4$

$U_t = 22.22 m/s$

3.7 Numerical Methods

3.7.1 Computational Fluid Dynamics (CFD) Fluent

CFD, a branch of fluid mechanics, is a powerful numerical tool that has been widely used to simulate various kinds of food processing in food industries (Norton & Sun, 2006). CFD was developed around the early 1900s by the pioneering efforts of some researchers (Courant et al., 1928; Lax, 1954; Richardson, 1911; Von Neumann & Richtmyer, 1950), who have addressed the fundamental issues in numerical analyses for CFD (Shang, 2004). The governing equations of CFD for fluid flow and heat transfer can be considered mathematical formulations of the conservation laws of fluid mechanics. The Navier-Stokes equations have been involved in the equations of CFD. The conservation laws can be considered as:

a) Mass is conserved (the mass flows entering a fluid element must balance exactly with those leaving)
b) $F = ma$ (Newton's second law states that momentum is conserved)
c) Energy is conserved (the first law of thermodynamics states that the rate of energy change of a fluid particle is equal to the added heat and the work done on the particle).

3.7.2 Rocky DEM (Discrete Element Method)

Simulation and modeling based on DEM have increasingly been applied in particulate research in the past two decades or so (Zhu et al., 2008). DEM is a popular approach to investigating the flow of particles in the drying sector. DEM was originally developed in 1979 (Cundall & Strack, 1979). Every particle has two types of motion in a considered system namely translational and rotational which can be described by Newton's second law of motion. This method considers a finite number of discrete particles interacting employing contact and noncontact forces with neighboring particles or walls and with the surrounding fluid. DEM simulations can provide dynamic information, such as the trajectories of and transient forces acting on individual particles, which is extremely difficult to obtain by physical experimentation, (Zhu et al., 2008). Commercial DEM codes are now available that can simulate complex industrial applications including industrial food drying (Tatemoto & Sawada, 2012).

Rocky DEM is a powerful, 3D Discrete Element Modeling (DEM) program that quickly and accurately simulates the granular flow behavior of different shaped and sized particles within a conveyor chute, mill, or other materials handling equipment. Several capabilities set Rocky DEM apart from other DEM codes, including its multi-GPU processing capabilities, truly non-round particle shapes, its ability to simulate particle breakage without loss of mass or volume, and its deep integration with ANSYS FEA and CFD tools.

3.7.3 CFD-DEM Approach

The combined CFD-DEM approach was first proposed in 1992 (Tsuji et al., 1993; Tsuji et al., 1992). The combined approach of CFD and DEM is an effective method to model particle fluid flow simultaneously which provides a better insight into the system being modeled. The numerical method behind the combined CFD-DEM model is well established (Feng et al., 2004; Xu & Yu, 1997; Zhou et al., 2010) and can account for the particle-particle and particle-fluid interactions (Chu et al., 2009; Yu & Xu, 2003; Zhou et al., 2010).

A powerful tool for simulating granular-fluid systems:

- ✓ The coupled DEM-CFD approach is a promising alternative for modeling granular-fluid systems, enlarging the range of coupled particle-fluid processes that can be managed with numerical simulations.
- ✓ Complex phenomena such as pneumatic conveying, granular drying, slurry flow inside grinding mills, or even chemical reactions between particles and fluids can be simulated and analyzed with these powerful tools.
- ✓ Considering the industry necessities for both single-phase and multiphase simulations, both 1-way and 2-way coupling between Rocky and ANSYS Fluent are provided.
- ✓ The coupling of the terms of the Navier-Stokes equation of fluid-to-particle interactions, which by taking into account drag, lift, buoyancy, virtual mass, angular momentum, and other forces, provide physically consistent and very trustworthy results.
- ✓ The work that Rocky DEM and ANSYS accomplished also allows ANSYS Fluent to work with Rocky in parallel CPU and GPU capabilities, which leads to very fast DEM-CFD simulation results.
- ✓ A plugin designed for ANSYS Fluent makes the combined DEM-CFD setup task easy, less error-prone, and guarantees consistency between both physics.

The numerical approach could be the alternative to experimental studies for this purpose with lower cost and higher feasibility. There are some numerical methods to simulate the roasting in the spouted bed. Since in a spouted bed roasting, the roasting particles have existed as a solid phase with the fluid phase (roasting air), two types of numerical methods could be used to describe the motion of the solid phase.

3.7.4 Minitab Statistical Software

Minitab is a powerful statistical software package used in the areas of mathematics, statistics, economics, sports, and engineering. It is highly interactive software that makes entering data, conducting regression analysis, ANOVA analysis, designing experiments using DOE and performing Taguchi analysis. It is the best tool for data-driven quality improvement programs.

Although there are a few studies in the literature are available on experiments and numerical investigation roasting of coffee bean in conical spouted bed, CFD-DEM coupling has not been employed yet as alternative means of the numerical approach

3.8 Working Principle Conical Spouted Bed Coffee Roaster with Internal Devices

The unit consists of a stainless-steel cylindrical column of 36 cm diameter and 60 cm long and also has a conical base frustum at the bottom with an included cone angle of 45^o, cone bottom diameter, and height of about 68 and 55 cm respectively. The upper base of the cylindrical column is tied to a flat-like plate at the head in between gasket material with bolt and nut as depicted in Figure 3.4. At the conical bottom of the unit, a spouting nozzle of 12.5 mm diameter and perforated screen were installed from the upper pipe and also, the stand of draft tube, and the hot air inlet pipe from the upper pipe was tied together with gasket material in between using bolt and nut.

The fountain confiner as indicated in Figure 3.5, is a cylindrical tube made of stainless steel with the upper end closed to avoid air and solid leaving the device through its top section. A stainless-steel cone is welded to the top of the confiner to avoid the deposition of the particles on the top section outside the device, i.e., to force the particles deposited on the cone to slip and fall onto the bed. It makes the shape of the fountain to be that of the confiner and forces the air to make a longer trajectory. Thus, an operation is possible at high values of the gas flow rate without direct loss of spouting gas in the bed and ensuring high solid circulation flow rates. Thus, it enhances the gas-solid contact, which significantly improves efficiency in the physical and chemical processes of roasting.

The draft tube is stainless steel tube of cylindrical shape, which is located along the axis of the contactor and provided with a flat base in whose center there is a hole of the same diameter as the tube diameter. The benefits of an open-sided draft tube of conical spouted beds with draft tubes are greater flexibility, lower gas flow rate, lower pressure drop, higher bed stability, narrower residence time distribution, solids of any size or nature may be treated, and better control of solid circulation and maximum spouted bed height can be avoided. Consequently, the draft tube is an interesting option for optimizing the hydrodynamic performance of spouted beds, especially when scaling up, given that it is simple, of low cost and greatly increases flexibility as well as saving energy

The material to be roasted is charged from the top of the spouted bed column through the feed hopper inlet. After initial adjustments of the velocity of air required for spout-able height and temperature, a weighed quantity of coffee beans (bean characteristics: ellipsoid shape with an average size of 6.24 x 3. 44 mm, bulk density of 700 Kg/m^3) was fed to the column.

Hot air is supplied from a blower through an electrical heater. The temperature and volume of air are controlled through a control system. From the values reported in different literature, it is observed that the color of the roasted beans is very sensitive to the roasting temperature. The inlet air temperature is measured by a thermocouple sensor. At temperatures above 250°C, the color of the beans is much darker. Depending upon the temperature, any desired shade of color from light to dark can be obtained by controlling the inlet temperature. When the material had attained the required degree of roasting, which was directly visualized via a Plexiglas window the airflow was stopped and the material can be withdrawn through a spout arrangement called a discharge chute at the bottom and charged to the coffee cooling bin. The cooling air was bypassed through the cold air inlet pipe as soon as the electrical resistor stopped and feed into the coffee cooling bin mounted with a screen from the bottom. Hot coffee bean agitated for cooling purposes using bevel gear mechanism, manually and/or using the motor.

The selected blower has capable of handling the required amount of air mass flow rate of air at a certain temperature and standard density. Depending on the requirement the airflow rate is controlled by adjustable speed control and enters into the air heater housing. The pressure drop inside the bed is measured by manometer devices for the seeking of system adjustment to achieve stable operations. Hot air is generally heated up employing an electrical heater with a variable resistor by which heat is mostly transferred to the roasting beans from the hot gas by convection. The gas leaving the roaster passes through a chuff collector and is dumped into the atmosphere.

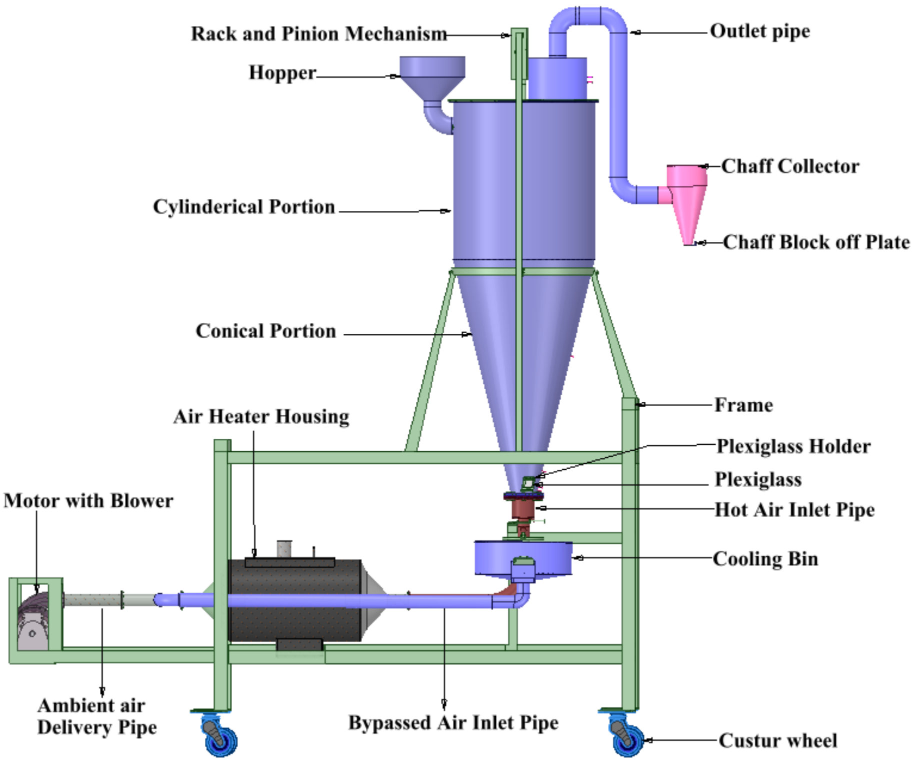

Figure 3.4: CSB coffee Roaster with Different Internal device (Front View)

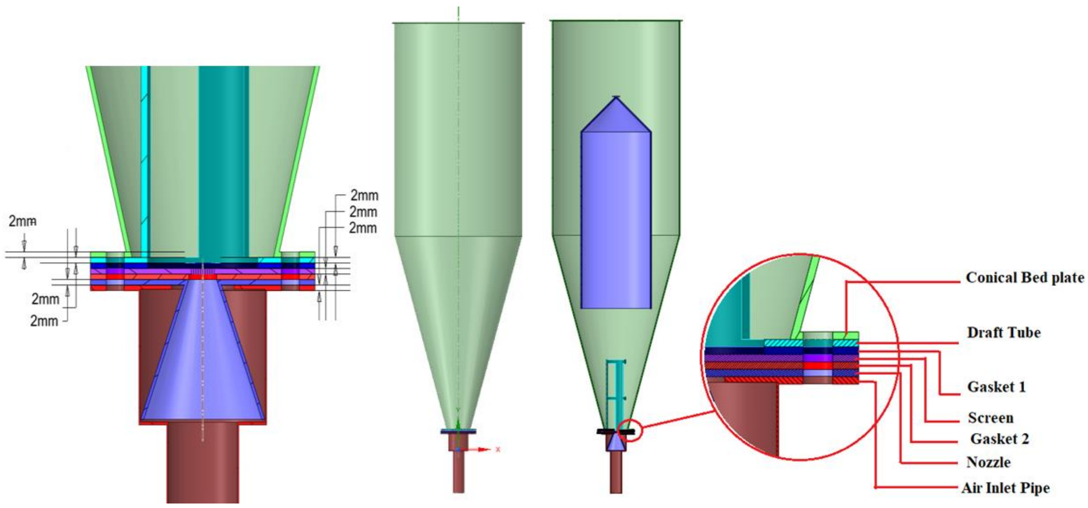

Figure 3.5: Sectioned of CSB Around its Flange

CHAPTER FOUR

SYSTEMS DESIGN AND SPECIFICATIONS

4.1 Design and Development of Conical Spouted Bed (CSB) Geometry

The CSB had to be designed based on the guiding principles to avoid hydrodynamic instability discussed in Chapter 2 which includes the ratios of Di/Do, Di/dp, and θ. Considering the physical apparatus used for the CSB, only two parameters would be changed regularly Di and θ.

4.2 Design Specifications of Conical Spouted Bed (CSB)

CSB is characterized by the three ranges of parameters such as bed geometry, working fluid, and spouting media properties. The standard nomenclature used to represent the geometric parameters of CSB is shown in Figure 2.8 of chapter two.

The fluid properties used include thermal conductivity (k), specific heat (cp), viscosity (μ), and density (ρ) while the spouting media of coffee beans is characterized by the particle density (ρp) and mean particle diameter (dp). Combined, these properties characterize the CSB with a well-followed nomenclature in the literature and its geometry is designed and developed based on the previous study and especially by Altzibar et al., (2017). The specification design of the parameters CSB, fountain confiner, and draft tube chosen and expanded to the current study and will be tabled in Tabless 4.1 and 4.2.

Table 4.1: Shows Parameters of the Design Specification of the Current Study

Variable	Values	Explanation
	30	Mathur et al., 2010 for CSB
(Di/dp)	2-60	Olazar et al., for conical spouted bed
Di/Do	0.5-0.83	Olazar et al., 1992
Di/Do	> 0.83 with stability considerations	Olazar et al., 1992; Sharma et al., 2011
Cone Angle	28°-180°	Olazar et al., 1992; Sharma et al., 2011
Height of bed		Depending on the diameter of particles, cone angle and ratio Di/Do

4.2.1 Design and 3D Modelling of Conical Spouted Bed

Therefore, the CSB was subdivided into two portions consisting of a base with a conical section and a cylindrical column that was left as a free board where the fountain of spouting mechanism circulated well. These three pieces should be built in one continuous design for numerical analysis but, separating them allows for more efficient manufacturing as Di and θ could be matched independently as discussed in the section below.

The design dimension of the conical bed spouted roaster i.e. the geometry and size of the CSB cannot be separated from the planned capacity of the roaster to be made along with hydrodynamic stability criteria. Hence, for small capacity i.e at laboratory scale, the size of the geometry bed was designed. The design capacity of about 1 Kg beans/batch was considered. For CSB the upper diameter was taken as about Dc= 36 cm, and the conical bed height Hc=55 cm. Selecting conical spouted bed roaster, of 36 cm diameter is chosen and roasting capacity of approximately one-kilogram, the equivalent diameter of coffee beans, do = 6.24 mm, the ratio of inlet diameter to particle diameter (D_i/d_p) taken to be 10 from Table 4.2 below, then

$$D_i/d_p = 10 \tag{4.1}$$

Table 4.2: The Geometric Comparison of Conical Spouted Bed

Source	**dp (mm)**	**Do (mm)**	**Dc (mm)**	**Di (mm)**	**ϒ (deg)**	**Ho (mm)**	**Hc (mm)**
Markows-ki (1983)	3.41~10.35	5.6~300	300-1100	5.6 ~300	37	3.36~690	
Choi (1992)	2.1~2.8	21~35	240-450	38	60	240~400	
Olazar et al., (1993)	1~9.6	30~60	360	60	28~45		360~600
Jose et al., (1996)	1~8	20~60	150	60	30~150	up to 350	12~168
Bi et al., (1997)	1.16	12.7-25.4	65~95.8	38.1	30~60	80 ~ 335	
Sharma et al., (2011)	0.483~1.092	3.3~9.525	63.5~70	3.3~9.5	30~60	10 ~ 65	50.8~115.6
Saldarriaga et al.,(2015)	0.76	40~50	360		28~45	3000	
Altzibar et al., (2013)	2 and 4	30~40	360		28~45	110~300	360~600
Altzibar et al., (2017)	0.41~4	30~50	360	68	28~45	270	360~600

The inlet diameter of the bed is about 62.4 mm from the above equations and approximated to D_i =68 mm from existing literature.

Although, minimum spouting velocities were found to be lower for the 30° cone, spouting operation was found to be unstable. Hence, the optimum CSB cone angles are between 40° and 60°. All results reported in the present study were obtained for a 45° cone angle. (Wang et al., 2004, Sharma et al., 2011)

Spouted bed design for coffee roasting depends on the following criteria:

i. Spouted bed design

Factors taken into consideration for the design of a roasting bed are the edibility of the end product, volumetric capacity, thermal properties of the bed materials, and also durability. Since coffee beans will be in direct contact with the roasting chamber, all contact materials used were stainless steel. The drum is expected to process 1 kg of coffee beans per batch operation.

ii. Design requirements and/or assumptions

- Process 1kg of green coffee bean at approximately dry based
- Green coffee volume V_{gc} to the cylinder volume V_c is in the range of 24 % to 32 %.
- Thermal expansion is not accounted
- The initial moisture content of the coffee bean was neglected.
- Allow for a 30% volume clearance of open space in the drum after the coffee beans have been roasted

Sizing the drum for a maximum of 1 kg of coffee is done accordingly to existing commercial roasters. On the roasters observed,

- The ratio V_{gc}/V_c of green coffee volume V_{gc} to the cylinder volume V_c is in the range of 24 % to 32 %.
- The beans close to double volume during roasting reaching a roasted coffee volume V_{rc}. This leads to a volume ratio V_{rc}/V_c of 48-64 %. Hadzich et al., 2014

iii. Drum dimension calculation

The volume of the green coffee to process per batch was determined using equation 4.2.

$$V_{gc} = \frac{m_{gc}}{\rho_{gc}} \tag{4.2}$$

Where; V_{gc} = is the absolute volume of green coffee at the dry base; m_{gc} = is the mass of green coffee at approximately at dry base; ρ_{gc} = is the bulk density of green coffee at dry based and given is about 700 Kg/m^3.

The bulk density of coffee beans is about 700 Kg/m^3 and the weight of coffee/batch in the conical space taken to be 1 kg.

From equation 4.2 above, the volume of green coffee is about $1.43\text{x}10^{-3}$ m ^{3} $= 1.43\ litre$

The equation 4.3 below was used to determine the volumetric capacity of the roasting cylinder, 28% was used being the average of the green coffee to drum volume ratio range.

$$\frac{V_{gc}}{V_c} = 28\% \tag{4.3}$$

Where, V_c is the volume of the roasting cylinder:

$$V_c = \frac{1.43\text{x}10^{-3}}{0.28} = 5.1\text{x}10^{-3}\ \text{m}^3$$

Considering, the volume of roasted coffee beans volume V_{rc}, the volumetric capacity of the roasting cylinder was calculated based on dark roasted coffee beans. The average mass decrease of arabica green bean after roasting was 20.05% i.e about 0.201 kg lost due to moisture removal or other factors. The density of dark roasted coffee beans is about 310 Kg/m^3. Hidayat et al., 2014

$$V_{rc} = \frac{m_{gc}}{\rho_{rc}} \tag{4.4}$$

$$V_{rc} = \frac{0.8}{310}$$

Hence, the volumetric capacity V_{rc}, is $2.58\text{x}10^{-3}$ m ^{3} $= 2.58\ litre$

The average volume ratio of roasted coffee volume V_{rc} to cylinder volume is taken as 56.2%,

$$\frac{V_{rc}}{V_c} = 56.2\% \tag{4.5}$$

$$\frac{2.58\text{x}10^{-3}}{0.562} = \text{V}_\text{c} = 4.59 \times 10^{-3} = 4.59\ \text{liter}$$

Therefore, the volumetric capacity of the cylinder that should be occupied by roasted coffee beans due to thermal expansions of volume increment was obtained to be $5.74\text{x}10^{-3}$ m^3.

And also, the lower portion of the conical spouted bed coffee roaster is frustum as shown in Figure 4.1. Hence, the height and top diameter of the cone where green coffee beans settled in are calculated using the following formula.

$$V = \frac{\pi h}{3}(R^2 + Rr + r^2) = V_{gc} \tag{4.6}$$

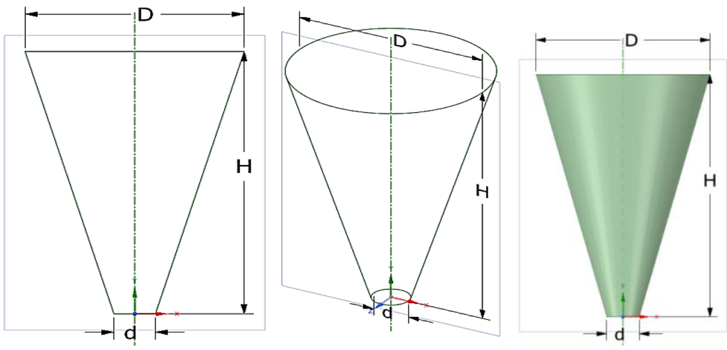

Figure 4.1:Geometry of Cone

In addition to this the top diameter of the stagnated bed, i.e. the upper diameter of the cone calculated using the equation stability equation stated in chapter two. Therefore, for 1 Kg of coffee beans, the upper diameter of the cone and height was about 0.1275 and 0.21 m respectively.

Hence, the dimension of conical sections considered in this study is chosen from previous experimental data and determined as the following;

- A cone angel, θ= 45° and
- Bottom of the cone, Di=68 mm.
- The diameter of the cylindrical section, Dc, was determined to be 360 mm.

The total height of the cone or maximum height particles that can be placed in the system is the addition of H_{C1} and H_{C2} that accounted for the thickness of perforated screen gasket material and air inlet nozzle as publicized in Figure 4.2. Because Dc was held constant, the maximum height of the particles is dependent on Di and θ. The CSB was designed such that a maximum height of 360~600 mm can be reached for Di and θ. Hence, the total height of the cone Hc=550 mm.

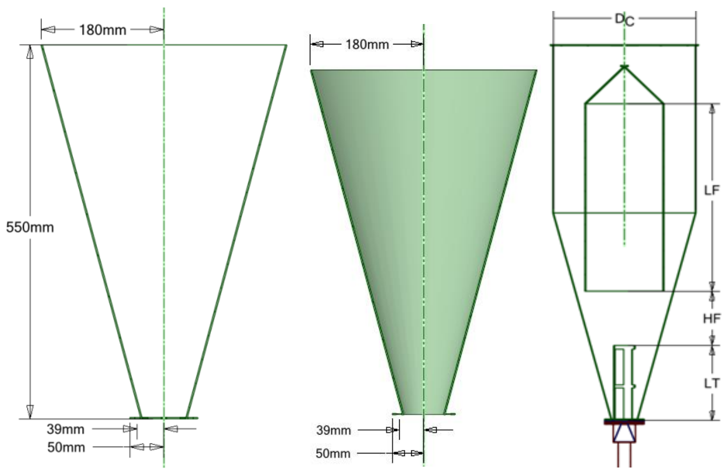

Figure 4.2: Conical Section of the Designed CSB

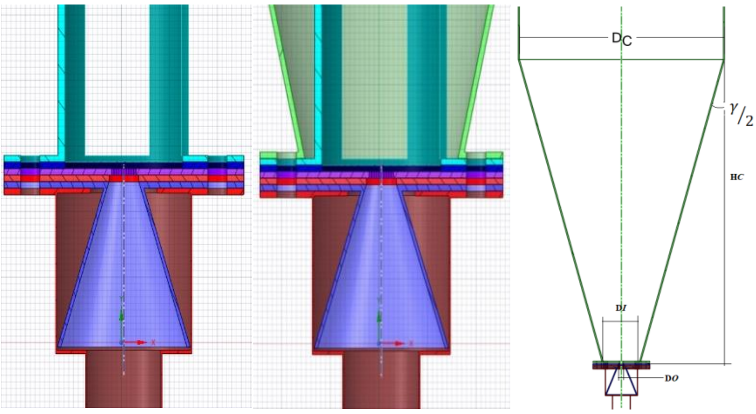

Figure 4.3: Bottom Section of the CSB Figure Conical Spouted Bed Geometry

The bottom section of the CSB is used to mount the flow inlet pipe, house the pressure monitor port, and establish the inlet diameter as seen in Figure 4.3.

4.3 D Modeling of Conventional Spouted Bed (Existing)

The geometry of conventional spouted bed roaster for coffee beans (peaberry) was developed by Nagaraju, et al.,1997; which consists of a glass column of 150 mm diameter and 350 mm long, and at the conical bottom of the unit is a spouting nozzle of 25 mm diameter. However, the length of the Nagaraju bed was increased by 850 mm for the seek of numerical study as displayed in Figure 4.4.

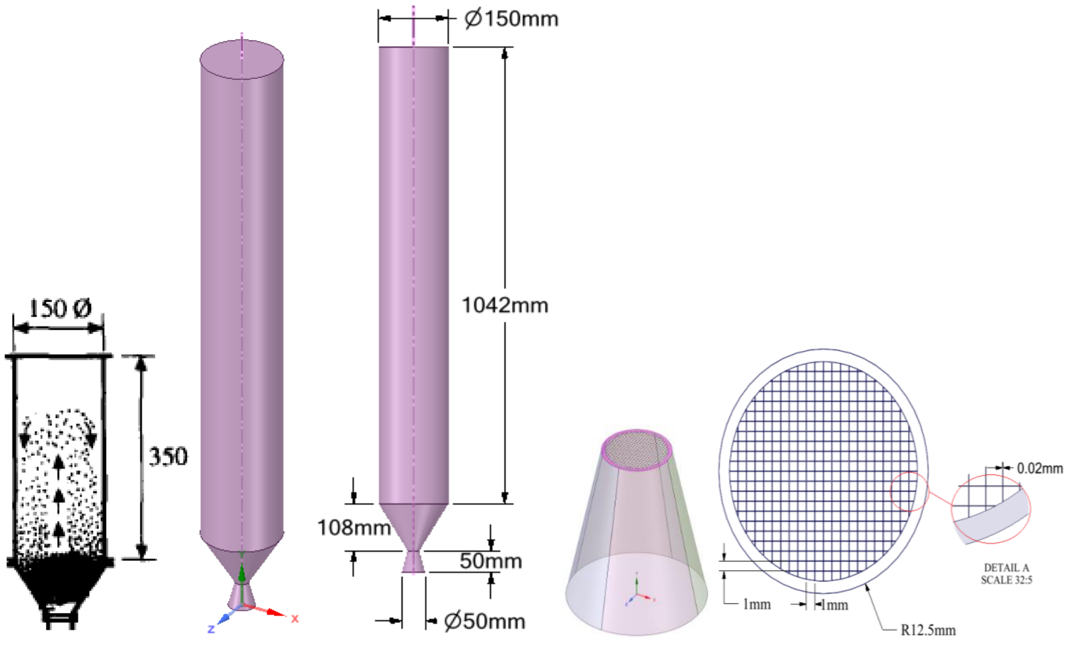

Figure 4.4: Nagaraju Bed a) and Developed as 3D Model for Analysis b)

4.3.1 Stagnated Bed Height

The stagnated height of the spouting media was varied in 30mm increments between 0.2 m for most numerical analyses in the 45° cone due to 360 mm being equal to the height of the cone. If a higher height was used, the system would become a conventional spouted bed, which is not in the scope of this study.

4.3.2 Inlet Diameter

The three designs factors are the ratio, the Di/Do ratio, the contactor angle, and solid density. For high values of Di/dp, and low values of Di/Do (near to 1, big bubbles rise through the bed without spout formation, especially for the smaller particles (0,001 and 0.002 m) and for the smaller angles. On the other hand, the influence of the angle is not as sharp as that of the other two design factors. For solids of density lower than 1500 kg/m^3 (beans, rice, chickpeas, peas, lentils, and polystyrene) the bed does not have any instability. For higher densities, instability phenomena are depending on the value of the design factors previously pointed out in chapter two.

$$\frac{D_i}{D_o} = 5 \tag{4.7}$$

Hence, the inlet diameter was calculated to be 13.6 mm but, 12.50 mm.

4.4 Specifications of Cylindrical Bed

The cylindrical column in this design is used as the enclosure and housing of the fountain with a fountain confiner, a stainless-steel cone that is welded to the top of the confiner and mount/hold the other auxiliary device like hopper and outlet pipe. Therefore, the total distance is the sum of the length of confiner L_T, the length of draft tube L_H, the distance between the lower end of the fountain confiner and the bed surface H_F, and the remaining steel cone with joining material. Hence, the diameter of the column, Dc is equal to the diameter of the

Table 4.3: Changing Parameters for Current Study

Parameters	Symbol	Range	Units
Diameter of particle	dp	6.42	mm
Diameter of an inlet air pipe	Do	12.5	mm
Diameter of the upper part of the cone	Dc	360	mm
Diameter of column	Dc	360	mm
Height of the cone	Hc	550	mm
Stagnated height of the bed	Ho	270-360	mm
Density of particles	ρp	700	kg/m3
Fluid Density	ρ	vary	kg/m3
Cone angle	θ	45	deg

Table 4.4: Parameter Comparison between the Previous and Present Study Altzibar et al., (2017)

Source	**Material of bed**	**dp (mm)**	**Do (mm)**	**Dc (mm)**	**ϒ (deg)**	**Ho (mm)**	**Hc(mm)**	**Gas**
Altzibar et al (2017)	glass beads, black peas, bread crumbs	0.41-4	30,40, 50	360	28, 36, 45	270	360,450 600	Cold air
Present Study	Coffee beans	6.42	50	360	45	270 ~350	360,450 600	Hot air

Dc =360 mm and the height of cylindrical column H_{Cy}=0.4 m as observed in figure 4.5. The total height of the contactor (conical plus cylindrical section) is 1.2 m.

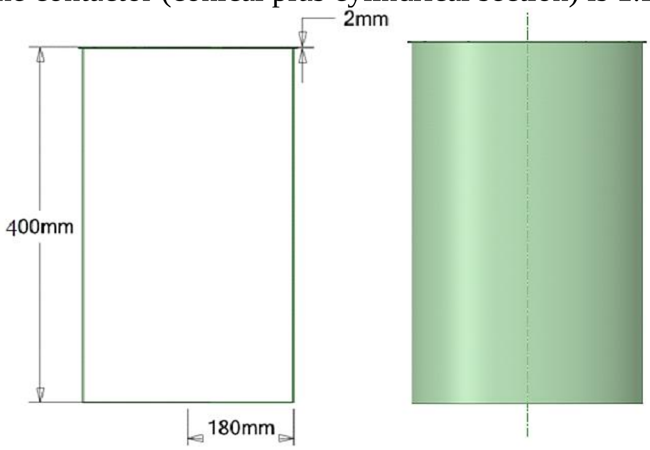

Figure 4.5: Cylindrical Column

Design Specifications of Fountain Confiner and Daft Tube

Design specifications of the fountain confiner and the daft tube are given in Table 4.5 below.

4.5 Design and 3D Modeling of Conical Spouted Bed with Fountain Confiner

The fountain confiner is a cylindrical tube made of stainless steel with the upper end closed to avoid air and solid leaving the device through its top section. A stainless-steel cone is welded to the top of the confiner to avoid the deposition of the particles on the top section outside the device, i.e., to force the particles deposited on the cone to slip and fall onto the bed.

As shown in Figure 4.6, this device is located in the contactor above the bed surface and avoids the solids in the fountain leaving the contactor. It makes the shape of the fountain to be that of the confiner and forces the air to make a longer trajectory. Thus, the operation is possible at high values of the gas flow rate without direct loss of spouting gas in the bed and ensuring high solid circulation flow rates. Thus, it enhances the gas-solid contact, which significantly improves efficiency in the contactor.

Table 4.5: Summary of Range of Parameters Used in the Literature and the Present Study.

Name of Author	Open Sided Draft Tube					Fountain Confiner		
	D_T(m)	L_T(m)	L_H (m)	W_H (m)	Apertu -re ratio %	D_F(m)	H_F(m)	$L_F(m)$
Altzibar et al (2017)	0.042	0.50	---	0.018	%57	0.15 &0.19	0-0.020	
Estiati et al., (2020)	0.04 and 0.05		0.0 7		20, 42, 57&79	0.2	0.08	0.25, 0.5 & 0.75
Tellabide et al., (2019)	0.04		0.0 7		57	0:15 & 0:20	0.02-0.1	
Tellabide et al., (2020)	0.04& 0.05	0.20 &0.27	0.0 7		78 57 &42	0.15 &0.20	0.02-0.1	
Pablos et al., (2017)	0.042-0.054	0.22&0 .50			20			
Lopez et al., (2017)	Non porous draft tubes					0.054		0.33
Present study	Open Sided Draft Tube							
	0.054	0.5	0.2	0.025	57	0.15	0.06	0.5

Figure 4.6 shows the gas and solid trajectories in the fountain confined conical spouted bed equipped with an open-sided draft tube. The solid trajectory is similar to that in conventional systems, but the trajectory of the gas is different. Thus, when the gas reaches the top of the fountain (upper end of the confiner), it is forced to descend and pass through the slot between the lower end of the device and the bed surface. This fact causes an additional gas-solid contact in the fountain. The slot between the lower end of the confiner and the bed surface is enough to allow the passage of chaff of coffee beans to escape the bed. According to Altzibar et al., (2017), the distance between the bed surface and the lower end of this device, H_F, is a key geometric factor for stable operation and system performance. They observed that low H_F values (of around 2 cm) allowed for operating with coarse particles, but the operating pressure drop is too high and the blower cannot supply the airflow rate required to open the spout and operate under stable conditions. Furthermore, a higher distance of

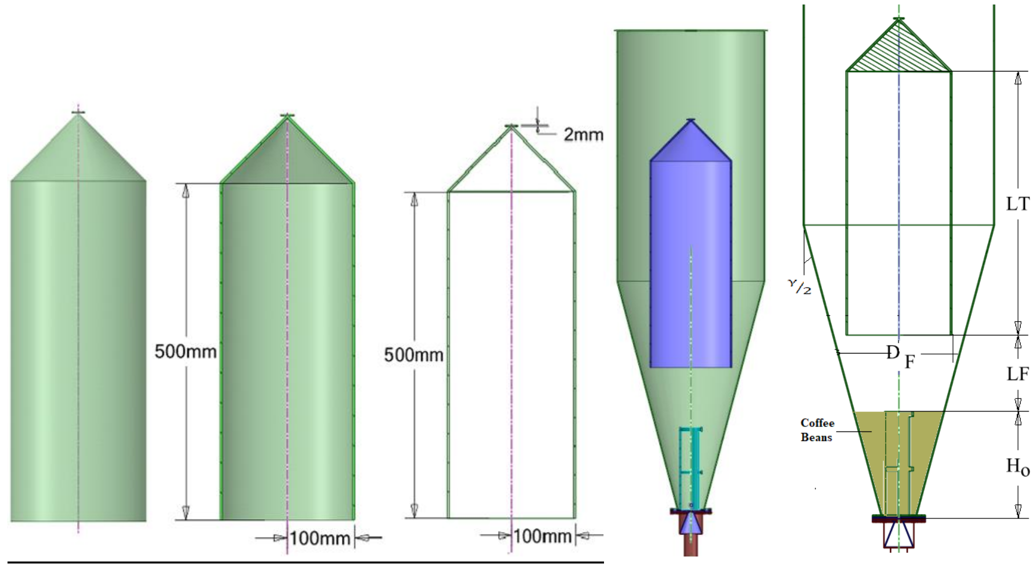

Figure 4.6: Geometric Factors of the Confiner

(HF) may not fully confine the fountain or may lead to instability. Hence, the dimensions of the fountain confiner for this study as shown in Figure 4.6 determined to be:

- The length of the device LF=0.5 m.
- The diameter of the fountain confiner DF=0.20 m.
- The distance between the lower end of the fountain confiner and the bed surface is adjusted by rack and pinion gear that is fitted with a system for moving up and down. Therefore, the distance between the lower end confiner and the bed surface is based on the number of coffee beans introduced into the bed for processing.

The upper cover is of conical shape to avoid solid deposition, i.e. enhance solid sliding from the cover onto the annular bed surface.

4.6 Design and 3D Modeling of Conical Spouted Bed of Open Sided Draft Tube

The draft tube is stainless steel tube of cylindrical shape, which is located along the axis of the contactor and provided with a flat base in whose center there is a hole of a different diameter from the tube diameter which is shown in Figure 4.7. This design of the base allows an accurate fit of the tube along the axis of the bed. Design criteria: -

- The height above the bed of the open-sided draft tube must be at least 1/2-1/4 of the stagnant bed height or else, it must be at least 2/3 of the stagnant bed height.
- Different open-sided tubes could be designed by varying the width of the faces (WH) and the diameter of the tube (DT).
- However, in this study, the static bed height is equal to the length of the draft tube (LT) in all the runs and /or (simulations) to attain the optimum experimental conditions.

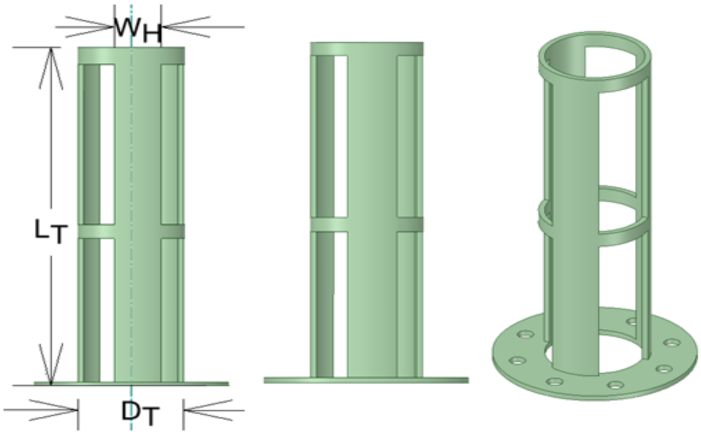

Figure 4.7: Geometric Factors of the Open-Sided Draft Tubes

Where W_H is the width of the face of the open-sided draft tube (m)

L_H is the height of the entrainment zone (distance between the gas inlet nozzle and the lower end of the draft tube),

L_T Length of the draft tube and D_T Diameter of the draft tube

- The widths of the face Wh=0.025 m lead to an aperture ratio of (AR=55%). This value of aperture ratio is an intermediate one between a nonporous draft tube (0% aperture ratio) and no draft tube (100% aperture ratio) and has been chosen as optimum based on previous studies (Altzibar et al., 2013).
- The diameter of the open-sided tube, DT= 0.054 m. This is chosen because the coffee bean is courser than glass bead i.e., the reference material.
- Aperture ratio (AR) has been defined as the open area of the tube lateral surface, according to the following expression:

$$AR = \frac{A_o}{A_T} = \frac{\pi D_T - 3W_H}{\pi D_T} \tag{4.8}$$

AR=55%

- Moreover, the total length of the open-sided tubes LT= 0.20 m, which means they stand 0.20m above the bottom bed surface. This length has been chosen according to previous experimentation in which the total length of the open-sided tubes is equal to static bed height (Altzibar et al., 2008, 2009, 2017)

4.7 The Loading Hopper

The dimension of the loading hopper, as shown in Figure 4.8, was determined using the following equations (Zegarelli, 2007).

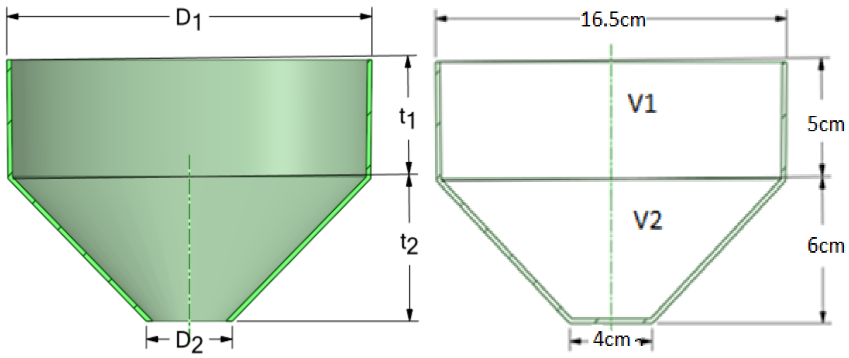

Figure 4.8: Cross-Section of the Loading Hopper

$$V_1 = \frac{\pi \times D_1^2 \times t_1}{4} \tag{4.9}$$

$$V_2 = \frac{\pi \times t_2}{3}\left[\left(\frac{D_1}{2}\right)^2 + \left(\frac{D_2}{2}\right)^2 + \left(\frac{D_1}{2}\right) \times \left(\frac{D_2}{2}\right)\right] \tag{4.10}$$

$$\sum V = V_1 + V_2 \tag{4.11}$$

The results of the calculation show that the volume of one kilogram (1 Kg) of coffee beans is about 1.43×10^{-3} m ^{3} $= 1.43\ litre$, while the volume of the loading hopper (ΣV) was 1625 cm^3 or 1.63 liters. This means that the hopper capacity exceeded the volume target of the coffee to be roasted so that the coffee bean could be entirely placed in the hopper.

It was simply installed on top of the drum assembly by placement with a fastener from three sides and one side left for a manual sliding of the cover plate at the coupling point to the drum to prevent the chaff from being thrown out during the roasting operation.

4.8 Cooling Bin

The average mass decrease and volume increase of arabica green bean after roasting was 20.05 % and 52.41 % respectively. The dimension of cooling bin parameters calculated based on the volume of 1.43 $litres$ of green arabica bean after roasting would become 2.58 liters. And as well as considering sufficient space for agitation during cooling of roasted coffee beans. The results of the calculation found that the diameter and height of the cooling tray were 24 and 8 cm, respectively as shown in Figure 4.9. The volume of the cooling plate was determined as follows (Mohsenin, 1986; Zegarelli, 2007; *Dadang et al., 2020*).

$$V_1 = \frac{\pi \times D^2 \times}{4} h_1 \tag{4.12}$$

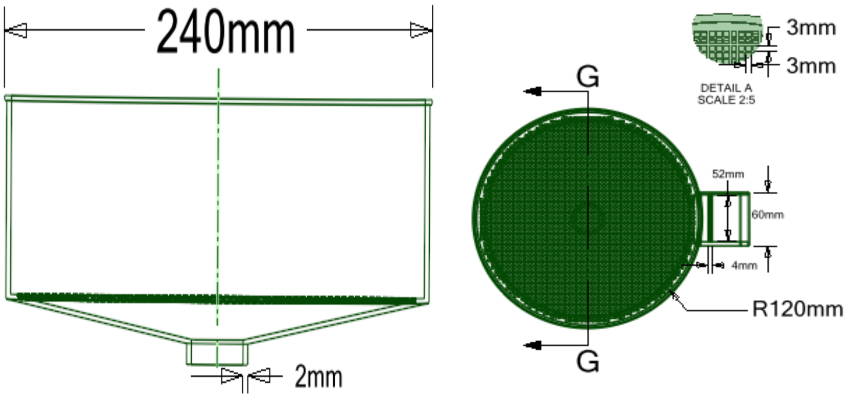

Figure 4.9: Cooling Bin

The cooling drum was made of a 2 mm mild steel sheet with a cover base and open top with an air duct also made from the same material. The cooling bin should have the capacity to hold the smallest possible roasted coffee bean through which the air bypassed at ambient from the blower is forced through the just roasted coffee beans thereby creating a forced convection cooling effect. Also, an agitator made of mild steel rod and plate, whose stirring motion was taped from the main shaft with the use of a slider-crank mechanism converting horizontal motion to vertical motion, was provided to increase the even and fast cooling effect.

4.9 Chaff Collector

The chaff (also known as silver skins or husk) is the epidermis of coffee beans that falls off during roasting due to the application of heat. when chaff breaks down in landfills it emits methane which is a powerful greenhouse gas (GHG) thought to be 80 times more damaging to the environment than carbon dioxide over 20 years. In addition, chaff does not taste pleasant when brewed, it must be thoroughly sifted from the coffee before being packaged and should remove to eliminate the risk of fire. The amount of chaff produced by each bean depends on several factors, including the coffee variety and processing methods. Silver coffee represents about 4.2% dry-weight of the green coffee bean, Muzaifa et al., 2021; Bliova et al., 2017. Accordingly, for one kilogram of coffee beans about 42 grams of chaff were extracted during roasting. As a result, to separate the chaff dragged by the air, a chaff collector with a screen mounted on the top is used to retain the chaff particles inside the collector, and the air is purged through the screen. Hence, it is indicated in Figure 4.10, that the dimension of the chuff collector that used to hold 42 grams of chaff and certain free space that much enough to hold it.

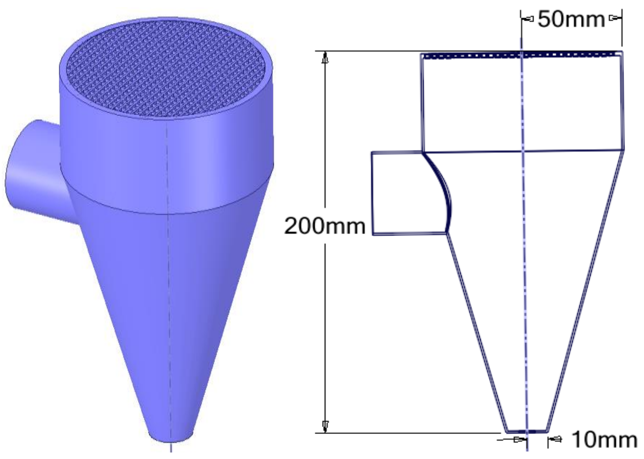

Figure 4.10: Chaff Collector

The chaff from the beans becomes separated during the roasting process and then is entrained in the exhaust gases which pass upward from the hot air blowing base for roasting the beans and through the open bottom. The chaff is collected on the electrostatically charged screen and is easily removed after the roasting process.

4.10 Perforated Screen

A stainless-steel screen mesh, supplied by NIRO Inc, (1 mm) sized, was placed at the bottom of the distributor plate to prevent the materials from falling into the plenum chamber. A screen will be placed at the location between the upper cone and air inlet pipe so that the spouting media does not travel into the flow inlet pipe. The perforated plate screen consisted of 100 holes of 1 mm in length which is shown in Figure 4.11. The 316 Stainless steel wire mesh is selected due to its low-pressure loss, constant mesh opening, good dimensional stability high open surface area, and good fireproof property.

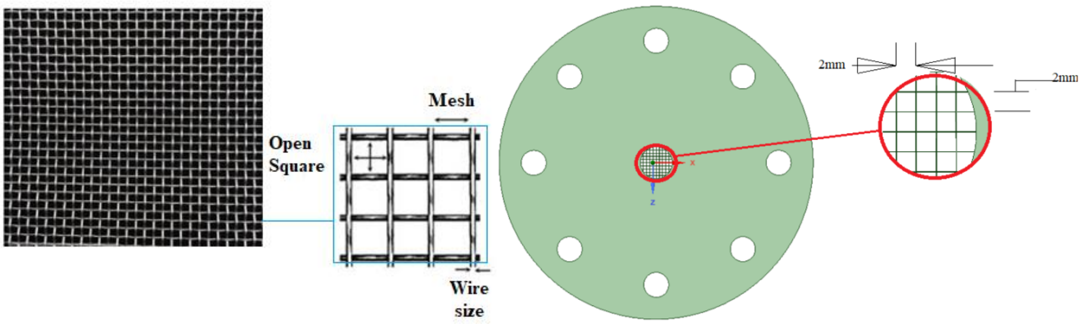

Figure 4.11: Perforated Screen

4.11 Air inlet Nozzle

The air inlet nozzle shown in Figure 4.12, draws hot air from the air heater housing and injects it with existing air screens and from the bottom of the spouted bed. It is designed based on the design guideline given in equation 4.1 above.

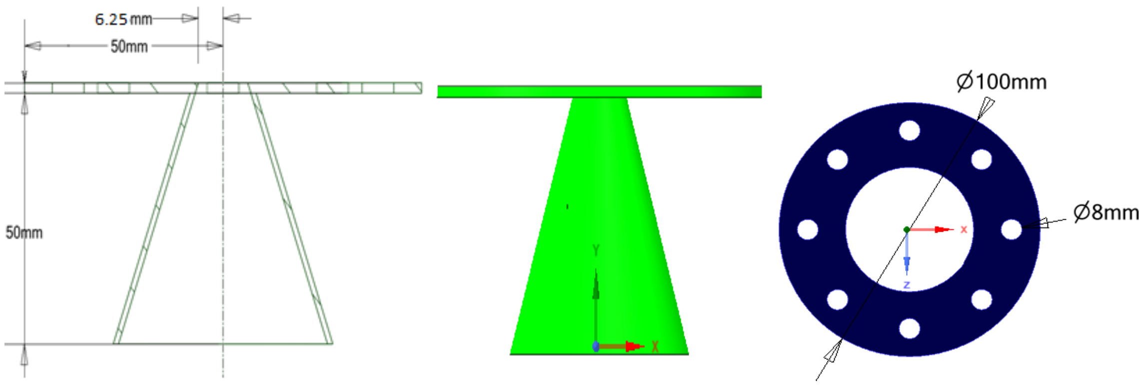

a b

Figure 4.12: Air Inlet Nozzle

4.12 Gasket

A gasket is a mechanical seal that fills the space between two or more mating surfaces, generally to prevent leakage from or into the joined objects while under compression. It is indicated in Figure 4.12 b that a gasket is used to seal the hot air inlet pipe and the bottom end of the spouted bed that assemble by the bolt and nut method of mechanical.

4.13 Frame

A frame is a load-carrying unit majorly made of 50 mm mild steel angle bar to provide rigidity and stability of the roasting column unit and other components support/attachments including air heater and its housing, control unit, blower and its motor and speed and cooling bin unit. This supporting unit is shown in Figure 4.13.

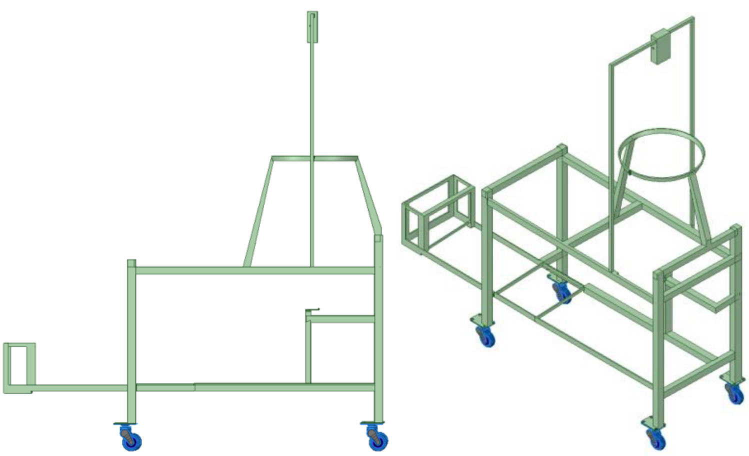

Figure 4.13: Frame a) Front and b) 3D View

4.14 Insulating Materials

Thermal insulation is an important way to reduce heat losses and improve roaster efficiency. A textile is chosen for its neutrality with food processing. Although the temperatures the insulation faces are at the limits of the material resistance. Cotton has low thermal conductivity *cotton = is 0.06W/m/K* providing very good insulation. A layer of about 5 cm keeps the outer surface of the insulated spouted bed at a certain surface temperature. Alternative material would be mineral or glass wool. If such a material is chosen, it is recommended to carefully enclose the insulation to ensure no fiber can be mixed with the coffee. This would lower the quality, possibly putting in danger the consumer's health.

4.15 Working Fluid

The working fluid is hot air at temperature ranges of 190-250 ℃ as the gas density and viscosity vary with temperature and time. This flow can simulate a flow under elevated temperature which is the main goal of the study.

4.16 Heat Demand for Coffee Beans

I. Nusselt Number

The heat transfer from hot air to each coffee bean was analyzed to calculate the overall heat transfer rate for a roasting capacity of certain grams of green bean coffee. The coffee bean was assumed as a spherical shape, thus the heat transfer from the hot air to each coffee bean occurred by force convection for external flow over a sphere. Nusselt number calculation follows the formula recommended by Whitaker (1972) with an expression as 4.13.

$$Nu = 2 + \left(0.4Re_p^{1/2} + 0.06Re_p^{2/3}\right)Pr^{0.4}\left(\frac{\mu}{\mu_s}\right)^{1/4} \tag{4.13}$$

Where Re_p is Reynolds number, Pr is Prandtl number, μ is dynamic viscosity, Ns/m^2, evaluated at T_∞ (hot air temperature) and μ_s is dynamic viscosity evaluated at an average temperature of coffee bean and hot air.

II. Prandtl number (Pr)

$$\mathrm{P_r} = \frac{\mathrm{c_f \mu_f}}{\mathrm{k_f}} \tag{4.14}$$

II. Reynolds number Re_p

Reynolds number is a dimensionless number (i.e., it has no units) that is a measure of the type of flow through a fluid. In the case of falling particles, this describes the way that air flows around the particle. The atmosphere's density and viscosity are the two properties used to calculate the Reynolds number (Re) of a particle moving through the atmosphere.

$$Re_p = \frac{d_p V_t\, \rho_f}{\mu} \tag{4.15}$$

III. Terminal velocity

The maximum velocity (V_t) is (speed) attainable by an object as it falls through a fluid (air is the most common example) where the drag force equals the driving force and calculated as below. The larger particles, those > 2 mm in diameter, fall in a turbulent flow regime (Re > 500) through the atmosphere Mohsenin, (1986).

$$V_t = \left(\frac{3.1 g d_p\, \rho_p}{\rho_f}\right)^{1/2} \tag{4.16}$$

$Re_p > 500$

$V_t = 17.98\, m/s$

Hence, $Re_p = 2750.88$ and $Pr = 0.69$

Where:

$V_t =$ Terminal velocity of a particle, $d_p =$ Particle diameter, $\rho_f =$ Air density, (fluid) and $g =$ gravitational acceleration. The calculation of the convection heat transfer coefficient is defined in equation 4.17 Incorporeal et al.,2007

$$h = \frac{k_f N\mathrm{u}}{d_p} \tag{4.17}$$

$h = 199.2$

Where k_f is hot air thermal conductivity (W/mK). The heat transfer from hot air to coffee bean, q_{hc} (W), was calculated using the convection heat transfer equation as 4.18.

$$q_{hc} = hA_{scb}(T_a - T_{cb}) \tag{4.18}$$

Where A_{scb} the surface area of coffee bean (m2) is, T_a is hot air temperature (K) and T_{cb} is coffee bean temperature (K).

$$A_s = 4\pi\left(\frac{(ab)^{1.6} + (ac)^{1.6} + (bc)^{1.6}}{3}\right)^{1/1.6} \tag{4.19}$$

$A_s = 4.9242 * 10^{-4}\, m^2$

With the assumption the green bean shape is half of the ellipsoid:

$$A_{scb} = \frac{1}{2} A_s$$

$A_{scb} = 2.5 * 10^{-4}\, m^2$

For N=7000 coffee beans particles

$A_{scb} = N * a_s = 1.75$

Hence, $q_{hc} = 3486\, W$

Thermal energy rate equation 4.20 was used to calculate the temperature of the hot air supply to the roasting chamber, T_{sa} (K).

$$T_{sa} = \left(\frac{q_{hc}}{\dot{m}_a C_{p,a}}\right) + T_a \tag{4.20}$$

Where $\dot{m}_a$ *airflow is* rate (kg/s) and $C_{p,a}$ is the specific heat of the air (J/kgK).

$$\dot{m}_a = \rho A_{duct} U_{av\ ms} \tag{4.21}$$

$A_{duct} = \pi r^2$

For $r = 0.05m$

$A_{duct} = 7.85 * 10^{-3}\ m^2$

$\dot{m}_a = 0.08\ kg/s$

$T_{sa} = 565\ K$

While the thermal energy rate of the heater, the energy rate to heat the air supply, *qh* (W), was calculated using the thermal energy rate equation 4.22,

$$q_h = \dot{m} C_{p,a}\left(T_{a,i} - T_{a,o}\right) \tag{4.22}$$

$q_h = 21{,}900\ W$

Where $T_{a,i}$ the input-air temperature at the heating chamber is equal to the temperature of air from the blower (K) and $T_{a,o}$ is the output-air temperature at the heating chamber (K). The thermal energy rate was calculated with the assumption the wall of the heating chamber and roasting chamber are well insulated, $T_{a,0} = T_{s,a}$.

Energy consumption calculation was calculated using thermal energy rate and the time of coffee roasting takes about 10min, the energy consumption, *Ec* (kWh), can be calculated using equation (10).

$$E_c = q_h t_{cr} \tag{23}$$

Where $t_{cr} = 10/60$ is the time coffee roasting (h).

$E_c = 3.65\ kW$

4.17 Design and Selections of Heating Element

Air heater used for heating collected ambient air before entry into conical spouting bed-chamber controlled by predetermined coffee bean processing temperature. The heat is transferred into the beans by convection via heated air updraft and by thermal conduction from bean to bean throughout the packed coffee bean in the spouted bed and provides (leads) thermal equilibrium and a uniform roast.

The heater includes a heating coil providing the heated air via a pipe with a temperature range from about 190-250°C. The spouting gas is generated in the heater, which should be adequately sized to fulfill heat balance, at the same time, and the mass flow rate should be capable to maintain spouting. This step was carried out by estimating thermal power and desired temperature.

I. Open Coil Duct Heaters

Open coil elements are the most efficient type of electric heating element while also the most economically feasible for most heating applications. Used predominantly in the duct heating industry, open coil elements have open circuits that heat air directly from the suspended resistive coils. These industrial heating elements have fast heat-up times that improve efficiency and have been designed for low maintenance and easy, inexpensive replacement parts which are illustrated in Figure 4.14.

II. Design and Selection Guidelines of Air Heater

The major factor that is required to be considered, when selecting open coil air heaters are as follows:

- Minimum feet per minute (FMP), airflow velocity at heater inlet assumed to be continuous.
- Inlet air temperature should be known as which ambient air in this study.
- Outlet air temperature and temperature rise through the heating element
- Selection of element watt density to keep sheath material within its temperature limits and mounting and airflow around the restriction of the elements and kW sizing

III. Material for Heating Elements

The selection of a material for heating elements is depending upon the service conditions such as maximum operating temperature and the amount of charge to be heated, but no single element will not satisfy all the requirements of the heating elements. The materials normally used for heating elements is nickel-chromium-iron which is cheaper when compared to simple nickel-chromium alloy. At its most basic level, an air heater works by passing air across a heated element to elevate the temperature of the air. That hot air can then be used for roasting coffee beans applications. Every air heater is comprised of two main components:

- Once the desired type of heating element is selected, the next step is to calculate the air velocity and estimate sheath temperatures to verify that maximum operating temperatures are not exceeded.
- Calculate the air velocity over the elements and refer to allowable watt density graphs for estimated operating temperature.

Material and Properties of Nichrome Iron heating element

- Good corrosion resistance and oxidation properties.
- Good corrosion stability and typically used in round elements and other properties as shown in Table 4.6.

Figure 4.14:Air Heater

Table 4.6: General physical and Mechanical Properties of Alloy (i.e., Ni Cr-Fe)

Max. operating Temperature °C	950
Nominal Composition	
% Cr	16
Ni	60
Fe	24
Density g/cm3	8.20
Resistivity $\mu\Omega$-m	1.06
Specific gravity	8.27

4.17.1 Wattage Requirement (kW)

For most air heating processes and if forced air incoming at ambient temperature, it is fairly simple to find the wattage required by using the equation 4.24:

$$\mathrm{kW} = \frac{\mathrm{CFM\ x\ \Delta T}}{3160} \tag{4.24}$$

$\mathrm{kW} = 17.6$

Where;

- kW is the required heater power, in kilowatts;
- CFM is the rate of airflow in CFM
- $\Delta T = T_2 - T_1$ is the rise in temperature (the temperature difference between the inlet and the desired outlet temperature) in °C; and
- T_2=Desired outlet air temperature °C and T_1 =Inlet air temperature °C

3.17.2 Duct Heater Temperature Rise

The following formula may be used to determine the approximate temperature rise of a duct heater when the kW and CFM are known:

Table 4.7: KWH to Heat Air at Selected Flow Rate

ATM of air CFM	Temperature Rise in °F										
	50	100	150	200	250	300	350	400	450	500	600
	Kilowatt Hours to Heat Air										
100	1.7	3.3	5	6.7	8.3	10	11.7	13.3	15	16.7	20
200	3.3	6.7	10	13.3	16.7	20	23.3	26.7	30	33.3	40
300	5.0	10.0	15	20.0	25.0	30	35.0	40.0	45	50.0	60
400	6.7	13.3	20	26.7	33.3	40	46.7	53.3	60	66.7	80

$$\Delta T = \frac{KW \times 3160}{CFM} \qquad (4.25)$$

ΔT=222.5 K

3.17.3 Minimum Air Velocities

The minimum uniform airflow in a duct heater is directly related to the inlet air temperature. Consideration must be given to both airflows across the heater and inlet air temperature. Therefore, sufficient airflow must be provided to prevent overheating and nuisance tripping of the thermal cutouts.

Air velocity can be calculated from the following formula:

$$\text{Velocity(fpm)}=\frac{\text{Flow (CFM)}}{\text{Area of Duct } (ft^2)} \qquad (4.26)$$

$$A_s = \pi D L \qquad (4.27)$$

Where; A_s =Surface area in square feet; D = Diameter (D) of the heating area in feet, 0.2 ft; L = Total heating length in feet, 16ft; $A_s = 10.048 ft^2 = 1445\ in^2$

FPM=25

If the air handler equipment is expressed in FPM, then a direct cross-reference can be made by comparing the temperature of the air (as it enters the Duct Heater) to the KW rating on the chart of rated velocity given in Table 4.7. The velocity should never be lower than the velocity as determined from the chart. In cases where this is not true, the velocity must be increased or the KW required must be reduced.

4.17.4-Watt Density (Kw/sq. Ft)

Watt density is the rated wattage of the heater divided by the overall area being heated for a given application it depends on how well the material being heated distributes its heat throughout its volume and depends on the process's airflow rate, the wattage requirements, the maximum air temperature, and other specification heaters might be considered.

$$\frac{\mathrm{KW}}{\mathrm{ft}^2} = \frac{\mathrm{KW}}{\mathrm{A_s}} \tag{4.28}$$

$kW/\mathrm{ft}^2 = 1760$

$kW/\mathrm{in}^2 = 12.2$

When high operating temperatures are needed, watt density must be limited in order not to exceed the maximum sheath temperature. Watt density is given in the specifications for each tubular heater and the graph and formulas are used to ensure that the maximum allowable watt density for the heater is not exceeded in the application.

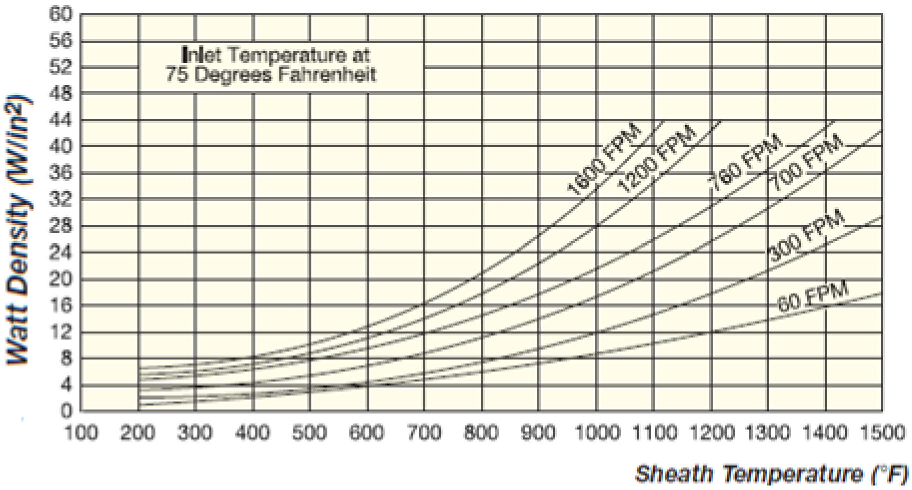

Figure 4.15: Element Watt Density Sheath Temperature and Air Velocity

4.18 Selection of Blower

4.17.1 Type of Blower

Blowers can achieve much higher pressures than fans, as high as 0.1177 mpa. They are also used to produce negative pressures for industrial vacuum systems. Major types are centrifugal blower and positive-displacement blower. Centrifugal blowers use one of seven types of wheels that are enclosed in scroll-shaped housing and look more like centrifugal pumps than fans. The impeller is typically gear-driven and rotates as fast as 15,000 rpm. In a single-stage blower, air does not take many turns, and hence it is more efficient. Centrifugal blowers typically operate against pressures of 0.034 to 0.0686 mpa but can achieve higher pressures. Generally, a centrifugal blower with backward-curved is chosen for open element heaters. Proper selection of blower depends on four key data: -

- ✓ Volumetric flow rate (CFM)
- ✓ Fan static pressure (SP),
- ✓ Inlet air/ gas density and intended fan duty

4.18.2 Volumetric Flow Rate (CFM)

The most basic parameter used for blower selection is the rate of airflow through the blower. The volumetric flow rate measures the volume of air at the fan inlet over a while and in units of Cubic Feet per Minute (CFM) or the metric equivalent, cubic meters per hour (m^3/hr). The volumetric flow rate calculated using the average minimum fluidizing velocity is about 250 CFM (424.75 m^3/hr).

4.18.3 Static Pressure (SP)

Static Pressure is the resistance to airflow (friction) caused by the air moving through a pipe, duct, hose, filter, hood slots, air control dampers, or louvers. Hence, it is the potential energy put into the system by the blower and rated in inches water gauge (in WG).

- The volumetric flow rate CFM=250
- There are 0.91 m of 4 in (0.102m) diameter pipes with three (1) 90-degree elbows.
- Static pressure loss as given by the manufacturer is 3.8-inch (0.0965m) WG.

The pipe static pressure is figured as friction loss per 100 feet at a certain CFM as shown in the figure below. Use a duct calculator or the chart provided in Appendix B to figure the static pressure of 100 feet of a given diameter of the duct at a given CFM. The flow velocity, FPM

$$\text{FMP}=\frac{\text{CFM}\times 144}{\text{A}_{\text{pipe}}} \quad (4.29)$$

For pipe diameter $d_{pipe} = 4\ in$, the area of the pipe is $A_{pipe} = 12.56\ in^2$. Hence, the airflow velocity is 2866 ft/min equivalent to 14 m/s.

- Using a duct calculator or the charts Appendix B, the resistance for (250), CFM moving through 100 ft (30.5 m) of 4-in. diameter pipe is 3.7 in. SP per 100 ft.

Each elbow is figured as equivalent to a certain number of feet of straight duct. Add total elbow equivalents to the length of the straight duct to arrive at the total system duct length. The resistance per elbow on the back of the pipe calculator or on the charts Appendix C (one 4 in. diameter elbow is equivalent to 8 ft of the straight duct) 1 elbow at 8 equivalent feet each=8 equivalent feet.

- Add 3 ft (0.9 m) for the straight duct to the 8 equivalent feet for the elbows equals 11 ft (3.35 m).
- 11 ft. is 11 percent of 100 feet. Multiply 0.11 times the resistance for 100 feet (3.7-inch WG) = 0.41-inch WG.
- Now, the Total Static Pressure is the summation of static pressure loss (the resistance) and static pressure due to any dampers, valves, etc. i.e add 0.41-inch SP

WG for the pipe to 3.5-inch SP WG for the pipe = 3.91≅ 4-inch (0.102 m) WG is total static pressure for the system.

4.18.4 Inlet Air Density

The third piece of parameter needed for fan selection is inlet air density. The inlet air density was calculated using three key factors such as air temperature altitude of the installation fan inlet and pressure. Standard conditions are considered to be 70 °F, with an elevation of zero feet (sea level) and an inlet pressure of zero inches of the water column, giving a density of 0.075 pounds per feet cube. Standard air has a density of 0.075 lb/ft^3 and is based on a temperature of 70°F and 29.92 in Hg barometric pressure (sea level). Fan performance tables are based on using standard air. Corrections for density changes resulting from temperature and/or barometric pressure variations, such as higher altitudes, must be made to the static pressure before selecting a fan or blower based on standard performance data.

I. Operating Temperature

The temperature of the air going through the fan or blower will affect the density and performance of the fan or blower. The temperature should be shown in degrees Fahrenheit (°F). The metric equivalent is degrees Centigrade (°C). The annual temperature of Adama is about 20.7°C and /or °F = 70.

II. Operating Pressure (Altitude)

The altitude the fan or blower will be operating at will also affect the density and performance of the fan or blower. The altitude should be given in feet above sea level. The metric equivalent is metered (m). Hence, the altitude of Adama is about 780ft.

To select a blower for 250 CFM at 4 in WG at 70°F and 780 feet elevation at Adama. From the table in Appendix D, the conversion factor for 70° and 780 ft. altitudes is 1.031 m. The corrected static pressure is 4 in WG x 1.0312= 4.1 in WG at standard conditions. Approximately, round off to 4.2 in WG. Hence, using fan performance tables, 250 CFM at to 4.2 in WG/22 Psf/ 1046.17 Pa per 100 mm WG blower is selected.

4.18.5 Horse Power Centrifugal Blower

The Horsepower centrifugal blower is

$$\text{HP}=\frac{\text{CFM}+\text{PSF}}{33000\times \text{ efficiency of the fan}} \tag{4.30}$$

For CFM=250; PSF = 4 and the average recommended efficiency of a centrifugal blower with backward-curved as given in Figure 4.16 is about 81%, 0.21 HP which is equivalent to 0.2 kW/200 W.

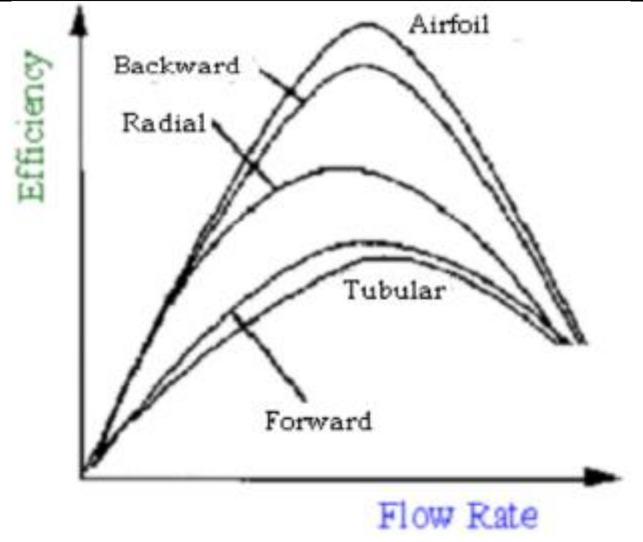

Type of fan	Peak efficiency Range
Centrifugal fan	
Airfoil, backward curved/Inclined	79-83
Modified radial	72-79
Radial	69-75
Pressure blower	58-68
Forward curved	60-65
Axial Fan	
Vane axial	78-85
Tube axial	67-72
Propeller	45-50

Figure 4.16: Efficiency Versus Flow Rate of Fan (BEE India, 2004)

CHAPTER FIVE
NUMERICAL MODELING

5.1 DEM versus Continuum Approaches of Granular Flows

Granular media flow can be quite complex, as these flows are known to exhibit solid-like, fluid-like, or a combination of both behaviors. For example, sand in an hourglass behaves like a fluid while a stockpile of sand can have a solid-like stress-strain response. Traditionally, continuum-based methods like Computational Fluid Dynamics (CFD) have been used to simulate granular flows, which were achieved by ignoring the individual particles and treating the granular phase as a continuous phase.

In continuum approaches, the entire domain has meshed into discrete cells, and conservation laws for mass, energy, momentum, and constitutive stress-strain relationships are solved in each. However, these constitutive relationships are often empirical and hard to derive, and the application is restricted to specific cases. Furthermore, discretization of the flow field places an additional constraint on these approaches, especially when the particles are much larger relative to the characteristic length scale of the flow. And, also these models show a serious over-prediction of the local heat transfer coefficient compared to experimental data and difficult formulation of constitutive equations (e.g. particle-particle drag) which may affect the simulation accuracy.

In contrast, DEM is essentially a mesh-free method that solves Newton's equations of motion for each particle. The most important consideration for ensuring a high-fidelity simulation is to account for all the relevant forces acting on each particle. This in turn depends upon several factors including the accuracy of the inputs and the implementation of physics models, and the validity of assumptions made to simplify the simulation to generate meaningful results in a practical time frame.

5.2 Coupled DEM-CFD Simulation

Granular-fluid systems design and scale-up, as well as optimization, require a deep understanding of the thermo-hydrodynamics, which is determined by the particle-level interactions between the fluids, particles, and boundaries.

Modeling the fluid-solid flow present in granular-fluid systems is **a** complex and challenging task. The primary source of difficulties is due to differences in the order of magnitudes amongst the characteristic scales existing in the problem.

First of all, there is the device scale, which is naturally respected. Secondly, the typical fluid flow scales are captured in a CFD solution by solving the flow at the mesh scale, which is generally much bigger than the particle but yet quite small when compared to the device scale.

Finally, there is the scale of the fluid-particle interactions, which has the magnitude of the smaller particles, therefore making it computationally prohibitive to solve the flow in a sub-particle resolution for most industrial applications. These difficulties are what make the coupled DEM-CFD approach so promising: it provides an intermediate level between using the sub-particle resolution for the fluid and the mesh resolution for both fluids and particles. Combining Computational Fluid Dynamics (CFD) and Discrete Element Model (DEM) makes it possible to simulate fluidic-granular systems. In DEM, the motion of discrete particles is tracked by solving Newton's second law of motion and in CFD, the flow of a continuum fluid is simulated by solving the Navier-Stokes equations, based on the concept to flow local averaging.

Over the past 50 years, the Discrete Element Method (DEM) has emerged as a powerful first principal simulation tool for a wide range of industries dealing with bulk particulate solids or granular media. DEM's power is derived from the underlying simplicity of the concept each particle in the granular assembly is treated as an individual entity for which Newtonian equations of motions are solved.

5.3 Why are couple DEM and CFD together?

The coupled DEM-CFD approach is a promising alternative for modeling granular-fluid systems since it can capture the discrete nature of the particle phase while maintaining computational tractability. This is accomplished by solving the fluid field at the cell level instead of at the detailed particle level. Due to the reduced fluid calculations required, this technique enlarges the range of equipment and processes that can be studied with numerical simulations.

The coupling of DEM with a finite volume method for the solution of fluid phase at a computational cell level was first reported by Tsuji et al., 1993. and Hoomans et al.,1996, using the soft-sphere model and hard-sphere model for the interaction force between particles, respectively. Since then, numerous authors have published their work using the Euler-Lagrange type of model to study granular flow (Hoomans et al., 2000, Xu et al., 2000, Feng and Yu 2004, Ye et al., 2005, Goldschmidt et al., 2002), proving this approach as a very promising method. In the DEM-CFD method, the fluid flow is obtained by the conventional continuum approach, providing information to calculate the fluid forces acting on individual particles while the motion of the particle is obtained by using a discrete particle method. Some specific benefits to using the DEM-CFD coupled method vs. using CFD alone are listed below.

- Unlike continuum methods, the motion of every particle is simulated, so particle-particle interactions are taken into account. Therefore, there is no need to provide equations of state-motion of granular systems, which are quite difficult to derive.
- By the same token, there is no limitation of low particle size concentration, and particle size distribution is easily prescribed without increasing CFD solver computational cost.
- It is possible to deal with non-spherical particles.
- It is possible to model adhesive-cohesive materials by modeling the attractive force between a pair of particles and between particles and walls.
- Additionally, particle-particle and particle-walls heat transfer as well as the convective heat transfer with the fluid can be included.

5.4 Governing Equations

In the Rocky-Fluent coupling, the fluid flow is obtained by the conventional continuum approach using ANSYS Fluent, in which the conservation equations for mass, momentum, and energy are solved by the finite volume method. The solid phase flow is modeled using the discrete approach within Rocky. The coupling between solid and fluid is accomplished by interphase momentum and heat transfer terms due to the interaction between phases.

5.4.1 Particle Phase Modeling

I. Translational and rotational motion of a particle

In the frame of the DEM, all particles within the computational domain are tracked in a Lagrangian way, by solving explicitly Euler's first and second laws, which govern translational and rotational particle motion, respectively; Ye et al, 2005.

$$m_p \frac{dV_p}{dt} = F_c + F_{f\rightarrow P} + m_p g \tag{5.1}$$

$$J_p \frac{d\omega_p}{dt} = M_c + M_{f\rightarrow P} \tag{5.2}$$

Where: -

mp is the particle mass; g is the gravitational acceleration vector; Fc is the contact force that accounts for particle-particle and particle wall interactions; *w*p is the angular velocity vector; Jp is its moment of inertia tensor and Mc is the net torque generated by tangential forces that causes the rotation of the particle.

5.4.2 Energy Balance in a Particle

If the thermal model is considered, an additional equation for the energy balance is solved along with the equations governing the motion of the particle. The temperature variation of a particle can be obtained over time according to the differential equation:

$$m_p C_P \frac{dT_P}{dt} = \dot{q} \tag{5.3}$$

Where: -cp is the specific heat of the particle material and $\dot{q}$ is the total particle heat transfer rate. The total heat transfer rate accounts for the heat transfer that occurs during contact with other particles or walls, $\dot{q}_c$, and the convective heat transfer between particle and fluid phase, $q_{\mathrm{f}\to\mathrm{P}}$, according to the expression:

$$\mathrm{q} = \dot{q}_c + q_{\mathrm{f}\to\mathrm{P}} \tag{5.4}$$

5.4.3 Fluid phase modeling

1. Mass and momentum conservation equations

The fluid phases are described by the classical Navier-Stokes equations averaged in volume. The averaged mass conservation equation is given by:

$$\frac{\partial}{\partial t}\left(\alpha_f \rho_f\right) + \nabla.\left(\alpha_f \rho_f u_f\right) \tag{5.5}$$

whereas the averaged momentum conservation equation is written as:

$$\frac{\partial}{\partial t}\left(\alpha_f \rho_f u_f\right) + \nabla.\left(\alpha_f \rho_f u_f u_f\right) = -\alpha_f \nabla p + \nabla.\left(\alpha_f T_f\right) + \alpha_f \rho_f g + F_{\mathrm{f}\to\mathrm{P}} \tag{5.6}$$

Where αf stands for the fluid volume fraction, p is the shared pressure, ρ_f is the fluid density, **u**f is the fluid phase velocity vector and Tf is the stress tensor of the fluid phase, defined as:

$$T_f = \mu_f\left(\nabla u_f + \nabla u_f^T\right) + \left(\lambda_f - \frac{2}{3}\mu_f\right)\nabla.\mu_f I \tag{5.7}$$

In the equation above, Fp-f represents the source term of momentum from interaction with the particulate phase, calculated according to the expression:

$$F_{f\to P} = -\frac{\sum_{p=1}^{N} F_{f\to P}}{V_c} \tag{5.8}$$

Where; Vc is the computational cell volume, N is the number of particles inside the computational cell volume is and $F_{f\to P}$ accounts for the forces generated by the fluid on the particles, calculated according to the equations in section.

2. Energy conservation equation

To describe energy conservation, a separate enthalpy equation is written for each fluid phase, according to Chunhua et al., 2015.

$$\frac{\partial}{\partial t}(\alpha_f \rho_f h_f) + \nabla.(\alpha_f \rho_f u_f h_f) = \alpha_f \frac{\partial p_f}{\partial t} + \alpha_f T_f : \nabla u_f - \nabla . q_f + Q_{\mathrm{p}\to\mathrm{f}} \tag{5.9}$$

where; hf is the specific enthalpy of the fluid phase, q_f is the heat flux and $Q_{\mathrm{p}\to\mathrm{f}}$ is the heat exchange between the fluid and particulate phases.

The heat exchange with the particulate phase is calculated according to the equation:

$$Q_{P\to f} = -\frac{\sum_{p=1}^{N} q_{f\to P}}{V_c} \tag{5.10}$$

Where; $q_{f\to P}$ is the heat transfer rate between the fluid and particle, the calculation for which is shown in section 4.2.

5.4.4 Particle-Fluid Interaction Forces

The fluid interaction force, $F_{f\to P}$, is commonly split into two terms: the drag force, F_D, and a second term composed of the remaining (non-drag) forces, F_{N-D}, in the following way:

$$F_{f\to P} = F_D + F_{N-D} \tag{5.11}$$

Amongst the most common non-drug forces are the pressure gradient force, $F_{\nabla P}$, the added (virtual) mass force, F_{VM} and the lift force, F_L, so we could write also:

$$F_{f\to P} = F_D + F_{\nabla P} + F_L + F_{VM} + F_{others} \tag{5.12}$$

Depending on the flow conditions, the majority of these forces can be ignored and only the drag and pressure gradient forces need to be considered, such as in cases where the specific mass difference between fluid and particles is high ($\rho_p \gg \rho_f$).

$$F_{f\to P} = F_D + F_{\nabla P} \tag{5.13}$$

$$F_{\nabla P} = \mathrm{F}\nabla\mathrm{p} = -\mathrm{V_p}\nabla\mathrm{p} \tag{5.14}$$

Where:

V_p is the volume of the particle and ∇p is the local pressure gradient.

Drag force

The drag force, F_D, acting on the particles is calculated using the definition of the drag coefficient C_D; Pritchard, (2010).

$$F_d = \frac{1}{2} C_d \rho_f A' |u_f - v_p| (u_f - v_p) \tag{5.15}$$

where u_f and v_p is the relative velocity between particle and fluid and A' is the projected particle area in the flow direction.

All correlations use the relative particle Reynolds number, Rep, defined using the particle diameter and the relative particle-fluid velocity according to Haider and Levenspiel, 2004

$$Re_p = \frac{\rho_f |\mathrm{v} - \mathrm{u}| d_p}{\mu_f} \tag{5.16}$$

Haider and Levenspiel compiled drag coefficient and terminal velocity experimental data for spherical and non-spherical particles. Then, they developed explicit expressions for both spherical and non-spherical particles dependent on their sphericity of particles.

The unified correlation for both types of particles is given by

$$C_D = \frac{24}{Re_p}\left(1 + {Re_p}^B + \frac{C}{1 + \frac{D}{Re_p}}\right) \tag{5.17}$$

On the other hand, non-spherical particles, are given by the expression:

$$A = \exp(2.3288 - 6.4581\phi + 2.4486\phi^2)$$

$$B = 0.0964 + 0.5565\phi$$

$$C = \exp\,(4.905 - 13.8944\phi + 18.4222\phi^2 - 10.2599\phi^3)$$

$$D = \exp\,(1.4681 + 12.2584\phi - 20.7322\phi^2 + 15.8855\phi^3)$$

Where ϕ is the sphericity of the particles, defined as:

$$\phi = \frac{A_{sph}}{A_p} \tag{5.18}$$

5.4.5 Turbulent Dispersion Force and Turbulent Dispersion Model

In Rocky under the CFD coupling settings, the turbulent dispersion acts as a diffusion mechanism in dispersed flows, resulting in the transference of particles from high volume fraction regions to low volume fraction regions due to turbulent fluctuations. The model of turbulent dispersion assumes that the instantaneous velocity of the fluid phase is a combination of a mean and a fluctuating value: Gosman and Ioannides, 1981

$$u_f = \bar{u}_f + u_f' \tag{5.19}$$

Where $\overline{u}$ f is the mean velocity of the fluid phase and u'f is the fluctuation caused by turbulent effects. Rocky takes an approach similar to Gosman and Ioannides, 1981 to model u_f' , where the dispersion of particles due to turbulence in the fluid phase is predicted stochastically. The influence of turbulence over a particle is simulated through the interaction with a succession of discrete fluid phase turbulent eddies. Each eddy is characterized by a fluid velocity fluctuation u_f' and a time scale τe (the eddy lifetime). When a particle is interacting with a turbulent eddy, u_f' influences the particle utilizing an additional drag force during the particle-eddy interaction time τ_{int}.

5.5 Heat Transfer Modes in the DEM-CFD Coupling

According to Zabrodsky et al., (1992) radiation heat transfer can be neglected at low temperatures, typically T < 700 K. Hence, the CFD coupling options in the Rocky 4.3 version do not take into account radiant heat transfer in this study too.

Disregarding the radiant heat transfer, Batchelor and Obrien, (2005) have shown that the conduction through thermal conduction due to particle-particle and particle surface contact dominates the conduction process when, Zabrodsky et al., (1992)

$$\frac{k_s d_c}{k_f \bar{d}_p} \gg 1 \tag{5.20}$$

Where; k_s is the conductivity of the solid phase, k_f is the conductivity of the interstitial media, d_c is the diameter of the contact spot and d_p is the average diameter of the particles.

5.5.1 Heat Transfer between Fluid and Particle

The heat transfer rate between a particle and fluid, $\dot{q}_{f\to P}$, can be calculated using Newton's law of cooling, which states that the rate of heat loss of a body is directly proportional to the difference in the temperature between the surface of the body and its surroundings. Assuming that the heat transfer coefficient is relatively independent of the temperature difference between the body and the surroundings, the heat transfer rate is given by:

$$\dot{q}_{f\to P} = hA_p\left(T_f - T_p\right) \tag{5.21}$$

where T_p is the temperature of the particle's surface, T_f is the local fluid temperature and A_p is the particle surface area.

The heat transfer coefficient h depends upon fluid physical properties, as well as the operating conditions. For instance, for the same fluid and particles, turbulent flows give higher heat transfer coefficients when compared to laminar flows. Therefore, a heat transfer coefficient needs to be provided for the analyzed system. In Rocky, the average convective heat transfer coefficient, h, is calculated based on the Nusselt number, Nu, according to the given expression 4.17. Different correlations can be found in the literature for calculating the Nusselt number, usually in the function of the Reynolds number, Rep, and Prandtl number, Pr, defined as in equation 4.14.

5.5.2 Fluid-Particle Heat Transfer Correlations

The Whitaker (1972) correlation as defined in equation 4.13 the fluid-particle heat transfer depend on both Re and Re $0.71 < Pr < 380$, Reynolds number in the range of $3.5 < Re_p < 7.6.10^4$, and viscosity ratio within $1 < \mu_{f\infty}/\mu_{f\omega} < 380$

5.6 Numerical Design of the System

In this section, the system is designed and developed numerically based on an existing design, correlation, and governing equations as well as considering available data and design requirements. Generally, the workflow for numerical modeling CFD-DEM analysis is accomplished as per Figure 5.1 below.

5.6.1 Finite Element Analysis (FEA)

It is known that finite element analysis is the simulation of any given physical phenomenon using the numerical technique called finite element method (FEM). All boundary and initial conditions are set and the simulations become applied to achieve the goal of the objectives. The problem is solved numerically by the continuum approach in ANSYS CFD Fluent.

5.6.2 Discrete Element Method DEM

DEM is a powerful simulation tool that is derived from the underlying simplicity of the concept; each particle in the granular assembly is treated as an individual entity for which Newtonian equations of motions are solved. The problem is solved numerically by a discrete approach in Rocky DEM.

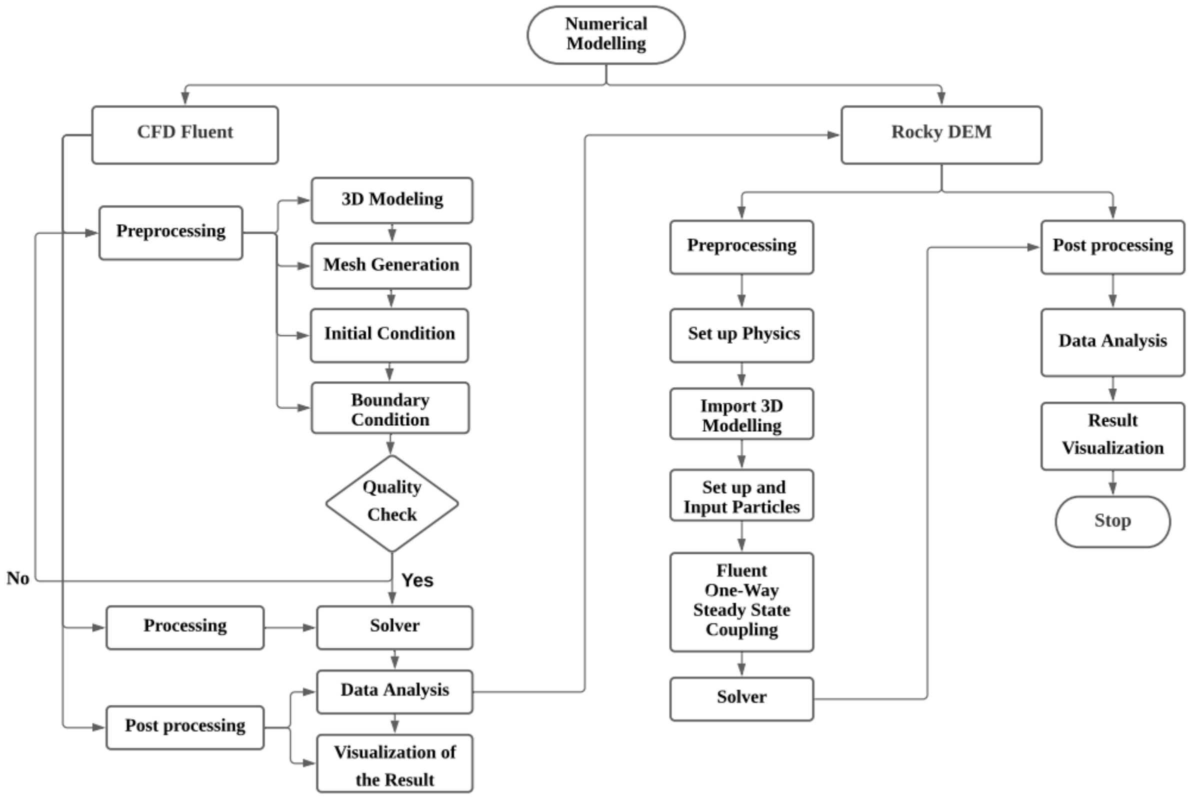

Figure 5.1: Workflow for Numerical Modeling CFD-DEM Analysis

5.7 Pre-processing in CFD Analysis

5.7.1 3D Modeling and Geometry Creation

The geometry used in both CFD Fluent and Rocky DEM simulation was developed in Ansys 19 R3 space Claim and Design Modeler. The domain and boundaries of the problem contain the fluids of interest on which boundary conditions would be assigned to the surfaces outlining the geometry and developed geometry by so-called CAD. Geometric parameters of conventional and conical spouted bed with their internal device are modeled based on the design and specification discussed in chapter three. The geometries in this section are composed of a walled cylindrical with two bottoms conic section i.e. middle is one with coffee bean settled in and other portion of air inlet nozzle volume, and with one inlet and outlet as shown in Figure 5.3. These geometries will save from Computer-Aided Design (CAD) as stereolithography (.STL) and Space Claim Document (. SCDOC) file format for later use in the coming sections.

5.7.2 Mesh Generation

Standard CFD recommendations for mesh generation are also applied to DEM-CFD coupling cases using the one-way coupling approach and 3D Mesh (.MSH) file save for fluent input file. For example, to avoid poor-quality cells and large variations in adjacent cells volumes, apply denser meshes in zones with strong quantity gradients, and so on.

In the one-way coupling approach, it is assumed that the particles do not affect the flow field, as there is no information transfer from Rocky into the CFD solution.

Because of this, there are neither additional recommendations nor limitations imposed in the CFD simulation by the coupling scheme itself. Therefore, the best CFD simulation is necessarily provided for Rocky as possible.

5.7.3 CFD Mesh of Coffee Beans

One coffee bean represented by a semi-elliptical curve with a longitudinal diameter of 0.009m, equatorial diameter of 0.006 m, and depth of 0.004 m was built and meshed in the Hyper mesh. The mesh of one bean was reproduced for one kilogram (1 kg) of beans imported as a .stl file in a form of a volume fill method.

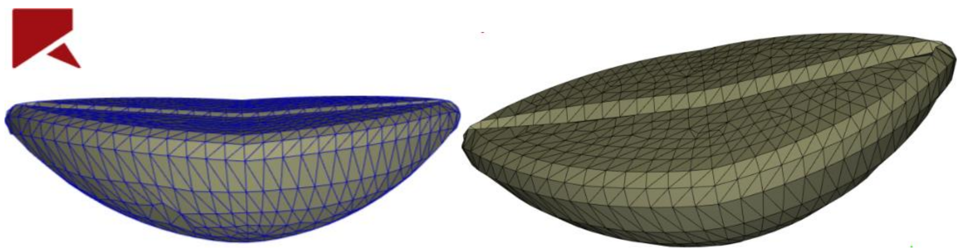

Figure 5.2: Coffee Bean Meshing

One bean´s computational mesh was represented by 1440 triangles and 722 vertices, shown in Figure 5.2.

5.7.4 CFD Mesh Generation of Conventional Spouted Bed (Existing)

The mesh was generated in ANSYS meshing with 20,700 hexahedral elements as depicted in Figure 5.4 and its respective dimension given in Table 5.1. The geometry is developed in the Ansys design modeler and sliced as possible as required for meshing purposes and imported to Ansys Space Claim for share topology with coincidence tolerance of 0.2 mm, to avoid unnecessary contacts and interfaces.

ANSYS Fluent simulations assuming steady-state and isothermal flow. The flow was treated as multiphase with an Euler-Lagrange one-way coupling approach and an SST turbulence model. The meshed geometry is exported as a .msh file for the Fluent input file.

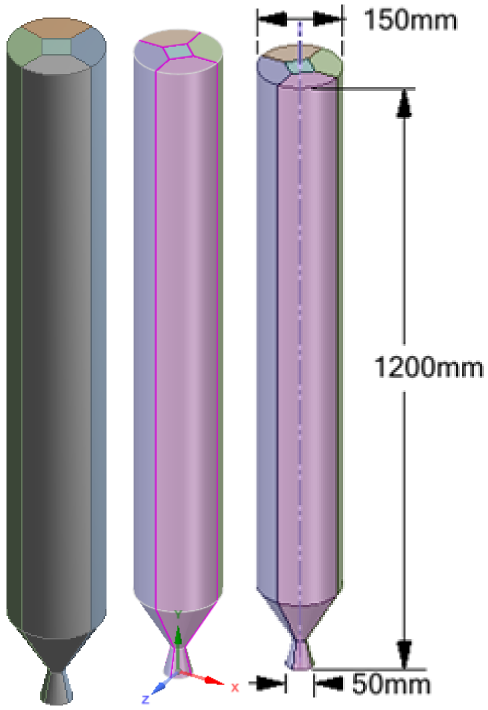

Figure 5.3: Sliced (a), Shared Topology (b), and Full Geometry for Meshing

Table 5.1: Geometry of Conventional Spouted Coffee Roaster

Cone angle, $\gamma/2$	30	Fixed value
Diameter of the upper section, D_c	0.15m	Fixed value
Total height of the column	1.2 m	Fixed value
Gas inlet diameter, D_0	0.025 m	Fixed value
Diameter of the bed bottom, D_i	0.025 m	Fixed value
Geldart particle		Group D

5.7.5 CFD Mesh Generation of Conical Spouted Bed with Internal Device

The meshing of conical spouted with an internal device is commence with geometry arrangement like slicing geometry and share topology, to create hexahedral structured mesh as shown in Figure 5.5 which yields more accurate solutions than their tetrahedral counterparts for the same number of edges and is very simple for computation algorithm. Biswas et al., (1998).

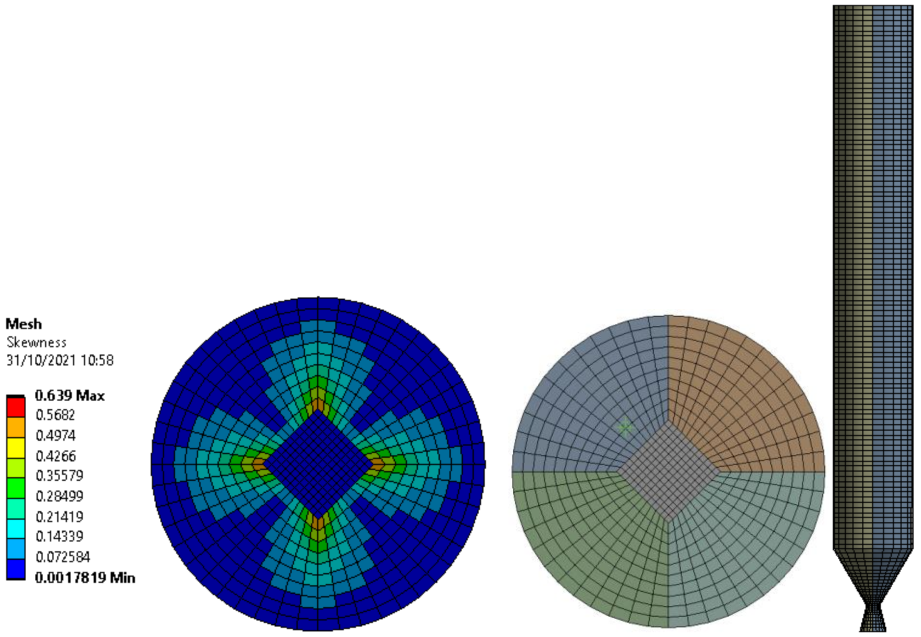

Figure 5.4: Meshing of Conventional Spouted Bed

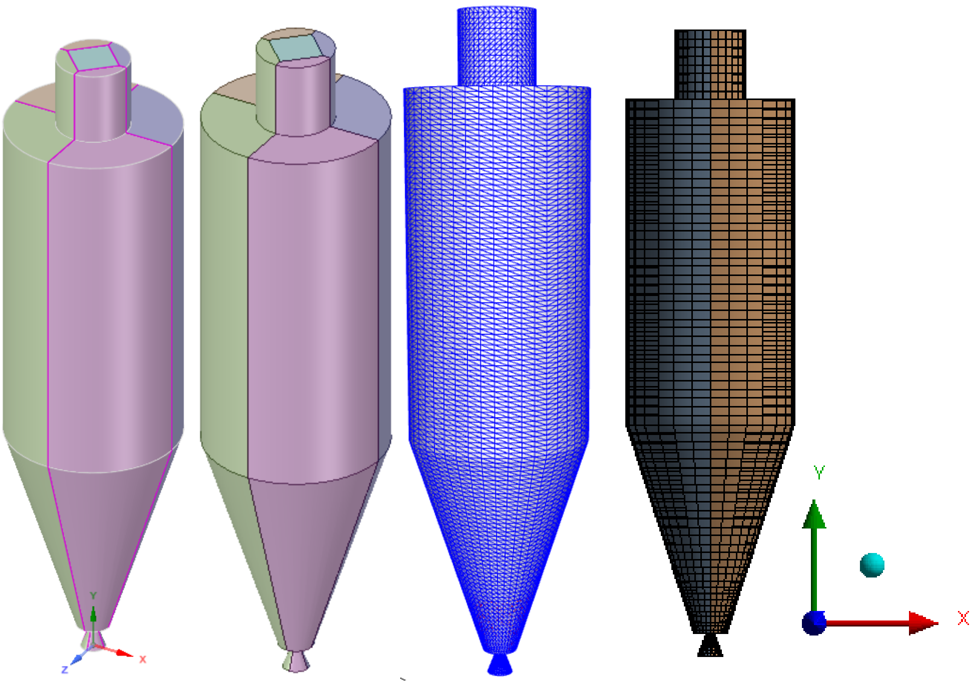

a) b)

Figure 5.5: Sliced a) and Meshing of CSB

The mesh and simulations of 3D conical spouted beds have been carried out with the CFD package FLUENT version 19R3 to investigate the hydrodynamics and heat transfer. The computational domain is shown in Figure 5.6. A quadrilateral type structured mesh with a total grid number of 84,161 has been used. The computational grids and quality of this meshing are very important, because of its thermo-hydrodynamic properties of the fluid domain used through the entire simulation of a conical spouted bed with internal devices.

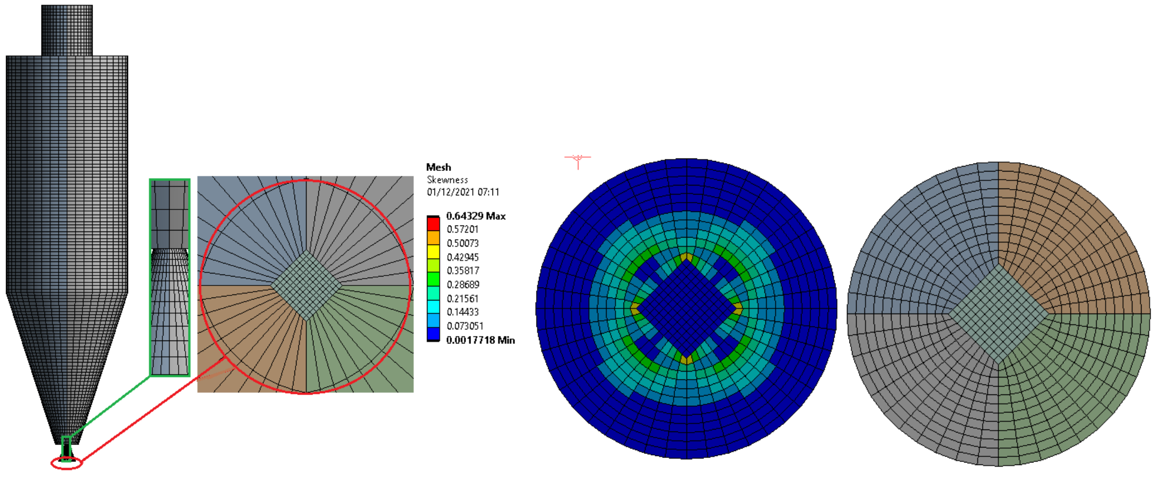

(a) (b

Figure 5.6: Hexahedral mesh of Conical spouted bed

5.7.6 CFD Mesh Generation of Conical Spouted Bed with Fountain Confiner

The computational domain is the same as the actual conical spouted bed. However, grids of a quadrilateral type structured mesh of fountain confiner have been created separately as a single entity in the Ansys Fluent meshing and exported out as a .stl file to rocky for later use.

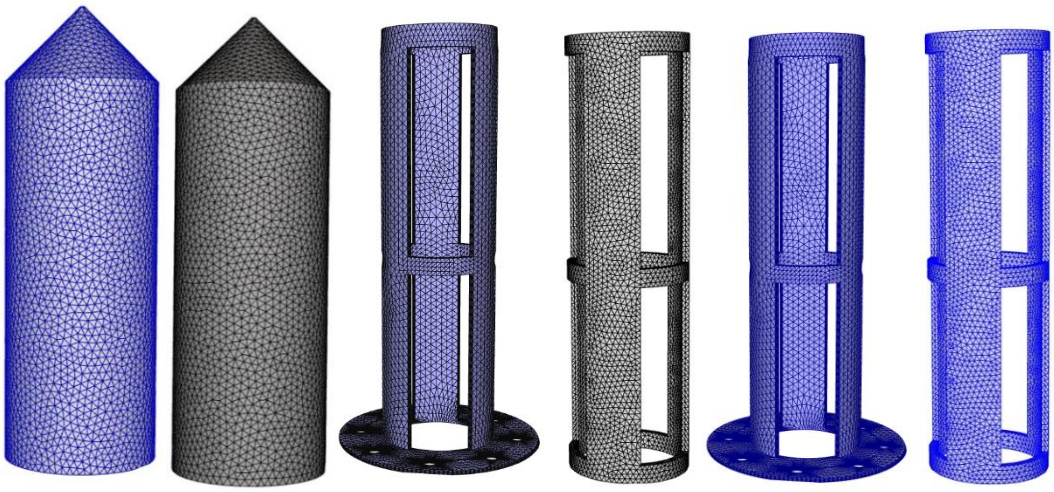

a) b)

Figure 5.7:Tetrahedron Mesh Fountain Confiner a) Draft Tube Grids b)

Accordingly, the fountain confiner has 3466 triangular elements and 1747 vertices as displayed in Figure 5.7.

5.7.7 CFD Mesh Generation of Conical Spouted Bed with Draft Tube

In this case, the mesh draft tube generated and saved as done for fountain confiner and tetrahedron mesh type mesh generated and saved as .stl file for later in Rocky DEM. The Open-sided draft tube has 2104 triangular elements and 1095 vertices. The assembly CFD mesh generation conical spouted bed with draft tube and fountain confiner is shown in Figure 5.8. As seen in the Figures 5.7 for both fountain confiner and draft tube, the polyhedral grid structure for the computational domain was generated and ready for Rocky DEM run.

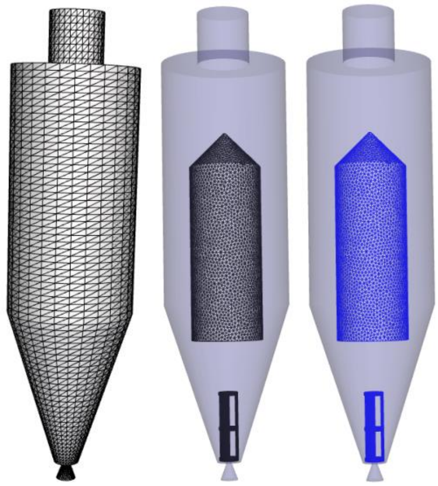

Figure 5.8: Grids of CSB with Draft Tube and Fountain Confiner

5.8 CFD Fluent Simulation setup of Conventional Spouted Bed (Existing)

5.8.1 Numerical Simulation and Setting up Initial Conditions

This section is aimed to design and evaluate the effects of conical spouted bed with different internal devices such as fountain confiner and draft tubes as well as their bed geometry and boundary conditions, on roasting coffee beans on a dry basis using the CFD-DEM model as a tool.

The simulated bed is made of stainless steel and equipped with an open-sided draft tube and fountain confiner. The corresponding physical and geometrical parameters selected for the simulation of batch-wise conical spouted bed contactor are discussed in chapter three.

A Rocky-supported version of Ansys Fluent is installed upon a machine that also contains a Rocky program installation where Workbench was integrated with Rocky through a special add-in.

Assumptions

The following assumptions are made in CFD modeling: -

- The initial temperature of the bean was uniform (300K)

- Bean coffee volume is constant, which means that an ideal condition for coffee beans because the real situation includes beans volume change as a function of time and temperature.
- Coffee beans are roasted under forced convection conditions.
- The physical properties of materials used in the model are constants.
- The interaction between particles is considered
- The walls are assumed to be adiabatic.
- Initially, there is particle concentration in the spouted bed is specified, and gas velocity injected through the spouted bed is considered.
- The particle concentration in the freeboard region is also set to zero.
- The inlet condition was considered as a velocity inlet boundary condition with a uniform velocity profile.
- The pressure boundary condition was considered at the outlet.
- 3D boundary conditions were applied in all phases.

5.8.2 Setting up Boundary Condition

The Fluent One-Way Steady-State Method is a CFD Coupling option that enables Rocky to receive steady-state fluid flow data from ANSYS Fluent, and then calculate how the particles react to that steady-state flow. It is called a one-way coupling simulation because Rocky receives data only once from Fluent and sends nothing to Fluent in return. Because data is only being shared once, and only one way, the fluid portion must be at steady-state before it is sent.

The CFD code uses the Eulerian model for simulation of the gas-solid in the spouted bed. Accordingly, the concept of interpenetrating continua with one phase representing the gas was used. The gas inlet boundary was defined as the velocity inlet such that the gas was injected only in the axial direction as displayed in Table 5.2. For the walls of the bed, a no-slip boundary condition was used and the adiabatic walls were assumed for gas phases. Considering the transfer of turbulent shear stress, the SST turbulence model can predict the onset and amount of flow separation with high accuracy under adverse pressure gradients, Li et al., 2020. Hence, in this study, the SST k-omg turbulence model is employed to calculate the turbulence effects. A convergence criterion of 10^{-5} for each scaled residual component. The Boundary conditions for conventional spouted beds are shown in Figure 5.9.

Table 5.2: Boundary Conditions for Simulations of Conical Spouted Beds

Description	Comment	
Solver	Pressure based, Steady, 3Dimensional, Double precision	
Model Tested	K-ε turbulence model	
Inlet	Absolute velocity normal to the boundary	
	Gas inlet velocity	
	Temperature	
Outlet	Uniform velocity distribution for the fluid phase	
	Pressure outlet	
Wall	Non-slip boundary conditions for fluid phase	
Convergence criterion	10^{-5}, Except continuity 10^{-6}	Default in FLUENT

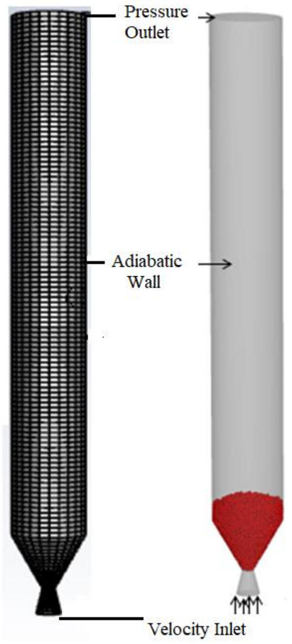

Figure 5.9:Conventional Spouted Bed Boundary Condition (Nagaraju et al., 1997)

5.8.3 Numerical Solution Procedure of Fluid Field using CFD

The CFD simulations were performed with the FLUENT CFD package version 19R3, 3D geometry designed and developed in chapter three for computational grid generation of a spouted bed.

ANSYS Fluent solver set of governing equations of the Eulerian approach solved by the standard finite volume method which is cell-centered and adopts an implicit scheme for a block algebraic multigrid solver used for the solution of the linearized equations.

The momentum and energy equations of the phase that represents the discrete phase are not solved by Fluent, the dispersed phase i.e., particles' velocity and temperature fields are solved by Rocky. A source term is included on the disperse phase continuity equation to impose the disperse volume fraction calculated at the DEM side. The momentum exchange term is not calculated in the CFD solver, but on the DEM side, as explained above, and included through a source term in the continuous phase momentum equation. The PC-SIMPLE algorithm, which is the SIMPLE algorithm extended to multiphase flows, is used for the pressure-velocity coupling.

The convergence criterion of 10^{-5} for each scaled residual component, except the momentum equation was set about 10^{-6} which specified the relative error between two successive iterations. According to Rocky DEM coupling with, CFD Fluent the simulation program setting is done based on Ansys Fluent one-way steady-state coupled simulation.

5.8.4 CFD Fluent Program Set-Up

As ANSYS Fluent 2019 R3 launched, the Double Precision with Parallel (Local Machine), as well as the number of Processors of about 8 CPU for the hardware is selected, and saved in a certain working directory. Following fluent launcher, the.MSH file browsed from the file menu dialog, by navigating the location where the mesh file is stored in the file directory. From the General tab, check to confirm that the mesh was imported correctly using the check button and under time, steady is selected to run a coupled simulation with the direction of the gravitational acceleration definition.

Since ANSYS Fluent solver solves fluid flow data, both energy and viscous model is activated from the fluent models. Hence, the energy equation should enable the calculation of thermal properties on the Rocky side. And from viscous model standard K-Omega model is selected as the Reynolds number ($Re \geq 2000$) to solve the turbulent flow field of the working fluid.

5.8.5 Materials Definition

The working fluid in roasting coffee beans using a conical spouted bed is necessarily ambient air that required elevated roast-able temperature of beans. Therefore, from the materials task pane air is selected with its default properties. For the seek of constant thermal models, the copy of the constant values for both specific heat and thermal conductivity is changed to the polynomial properties, and then paste in their respective constant values as the first polynomial value, and the other required parameter is given in Table 5.3.

This is accomplished by doing all of the following:

i. From the data tree under materials, expand fluid, and then double-click air.

Table 5.3: Parameters Used in the Simulations

Parameters	**Value**	**Comment**
Minimum Spouting velocity, u_{ms}	Vary	Based on D_i
Gas density, ρ_g	Vary	Air
Gas temperature, Tg	250 (°C)	Air
Particle density, ρ_S	700 kg/m^3	Coffee beans
Particle diameter, d_S	6.24 mm	Fixed value
Initial particle temperature, T_{cb}	25 (°C)	Fixed value
Thermal conductivity of gas kg	Polynomial	Fixed value
Thermal conductivity of solids K_s (coffee bean)	0.182 (W/m.K)	Fixed value Danilo et al., 2018
Specific heat capacity of solids $C_{p,s}$ (coffee bean)	Polynomial	Fixed value; Danilo et al., 2018

ii. From the create/edit materials dialog, under properties, click the edit button next to Cp (specific heat).

iii. From the constant profile dialog, copy the constant value, and then paste it to the polynomial one.

iv. From the Cp (specific heat) list, select polynomial, and then click edit again.

v. From the polynomial profile dialog, in the first coefficients box, paste in the constant value, and then click ok, and steps 2-5 are repeated for the thermal conductivity property.

From the solution methods tab, under pressure-velocity coupling scheme, simple was selected and with the following spatial discretization method as given away in Table 5.4.

Table 5.4: Discretization Methods

Characterized Properties	Methods of Discretization
Pressure	Second-order
Momentums	Second order Upwind
Energy	Second order Upwind
Turbulent Kinetic Energy	First order Upwind
Specific Dissipation Rate	First order Upwind

From the save file dialog, the fluent case file is saved as a .cas file format in a known directory required to access it in other steps. Finally, CFD simulation was processed until the fluid flow reaches a steady-state is reached. If CFD simulation converged, both .dat and .cas files were saved for later use and ready for the rocky import file.

5.9 CFD and Rocky DEM Coupling Simulation

The current Rocky formulation calculates buoyancy and additional pressure gradient forces based on pressure derivatives extracted from the CFD solutions, which are exported from ANSYS Fluent.

The heat transfer rate between a particle and fluid is calculated using the average convective heat transfer coefficient, the particle area, and the temperature difference between the particle and the fluid. The average convective heat transfer coefficient, in its turn, is computed based upon the Nusselt number that is calculated using the selected correlation within Rocky. These correlations are a function of the particle Reynolds number and the Prandtl number. In order, to compute these numbers, Rocky needs fluid properties, including fluid-specific heat and thermal conductivity.

These thermal properties are not exported to Fluent when a constant value is prescribed within the Fluent setup. Therefore, when running cases with the Rocky thermal model enabled and constant values set for fluid thermal properties, specific heat and thermal conductivity both need to be changed from constant to polynomial using the constant value as the first polynomial value.

5.9.1 The One-Way Coupling Algorithm Between CFD and DEM

The one-way coupling method is employed for the interactions between particles and airflow. The CFD simulation is performed using ANSYS Fluent to generate steady-state airflow fields. The airflow data as shown in Figures 5.10 a and b were then imported into Rocky DEM to calculate fluid-particle and particle-particle interactions and the resultant particle trajectories in the flow channel of the spouted bed. Setting Rocky DEM Simulation parameters involves setting simulation-wide values as well as parameters specific to particles, geometries, materials, interactions, inputs, and more.

5.9.2 Set up the Rocky DEM Simulation

Simulation-wide parameters are set by first selecting the study, physics, modules, domain settings, and solver sections in the data panel and then editing the results in the data editor's panel. Simulation-wide parameters are settings that can include:

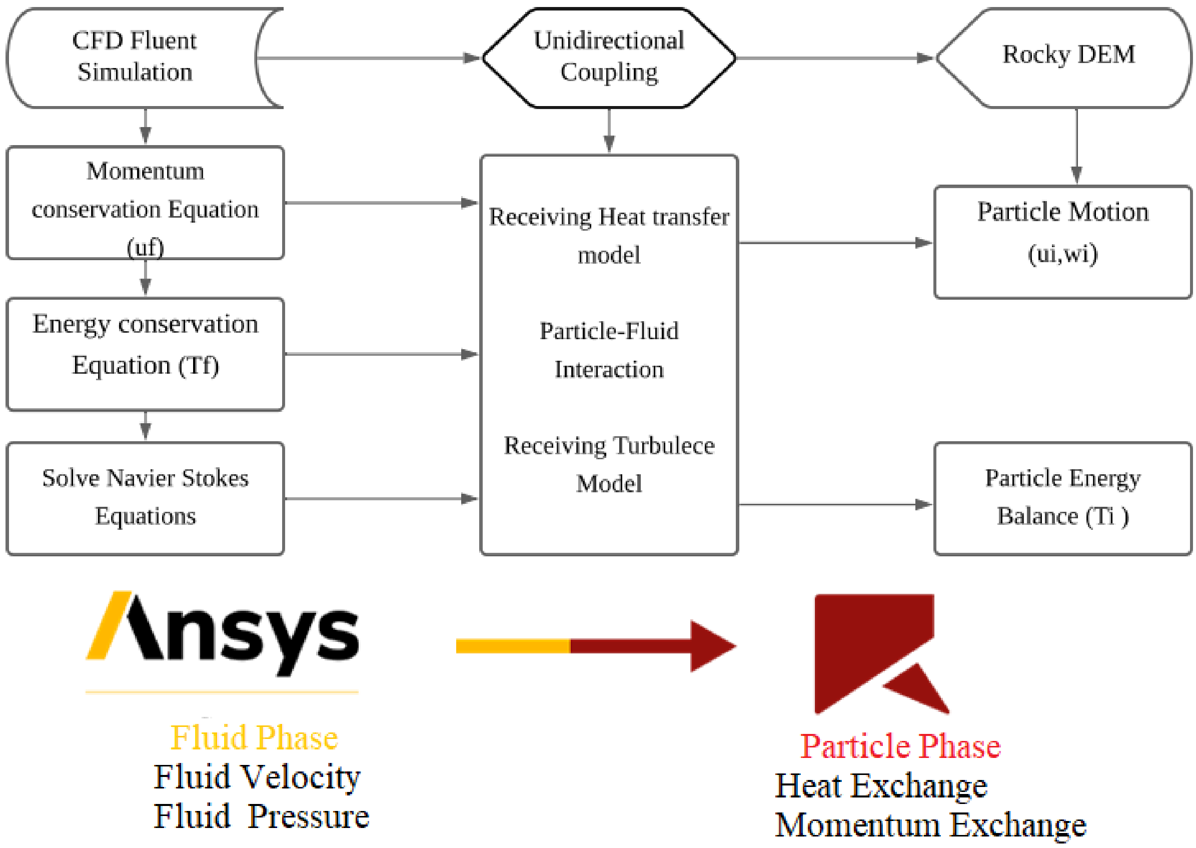

a)

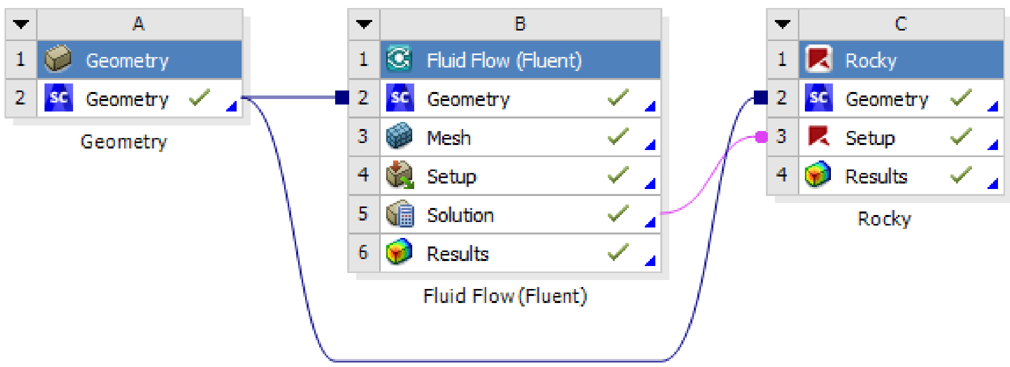

b)

Figure 5.10: CFD Fluent and Rocky DEM Coupling Method

1. In physics items, gravity and heat transfer setups were applied and to be calculated.
2. In domain settings, the simulation domain and necessary boundaries were defined.
3. Solver items, which include setting simulation time length, and certain data collection times
4. Since Energy equations were enabled in the fluent case, thermal modeling settings in rocky were also enabled. Generally, the Rocky DEM Simulation setup is discussed in the following sections.

5.9.3 Rocky-Physics Definition

The Rocky Physics parameters include simulation-wide settings that affect how the components are calculated. These include settings affecting gravity; the rolling resistance and force models used for calculating momentum; and the separate settings that enable thermal modeling and others. The gravity components define the negative Y direction and the time during which it is applied in the model.

5.9.4 Rocky-Geometry Import

Custom geometries created in the Space claim 3D CAD and meshed with certain quality meshing in Ansys fluent and will be exported as.STL files out of fluent as shown in Figure 5.11. In case geometries will be imported to Rocky as the. STL format by selecting it from the file type list and selecting geometry limits (limits in X, Y, and Z direction) with a certain unit from the import unit. When using the .stl file format to import geometries, all named parts will be imported as different named geometries components in Rocky.

Figure 5.11:Imported Geometry into Rocky

5.9.5 Rocky-Material Definition

For this simulation setup, two materials will be used namely particles i.e coffee beans, and boundary materials the stainless steel 316. The boundary material is Stainless Steel 316 whose physical and thermal properties are defined as shown in Table 5.5.

Hence, the following three material interactions are defined:

- Particle x Particle (interactions within coffee beans);
- Particle x Boundary materials (interactions of coffee beans with stainless steel);

For the materials, so-called coffee beans, bulk density, young's modulus, thermal conductivity; specific heat, and poison's ratio should be defined. Characteristics to define static & dynamic friction, coefficient of restitution, and force fraction are discussed in Table 5.6.

Table 5.5:Physical Properties of Stainless Steel 316 Khurmi et al., 2005

Properties	Values
Density (kg/m3)	8000
Tensile Strength (MPa)	530-680
Melting Point (°C)	1400
Modulus of Elasticity (GPa)	193
Electrical Resistivity (Ω.m)	0.74 x 10-6
Thermal Conductivity	16.3 W/mK
Thermal Expansion(/K)	15.9 x 10-6
Specific heat (J/kg.K)	500
Poison's ratio	0.265

Table 5.6: Physical Properties of Coffee Beans

Materials properties	**Values**	**References**
Young's modulus (MPa)	1.95	Mariana et al., 2017
True Density of coffee beans (kg/m^3)	1150	Tested
Poison's ratio of coffee beans	0.24	Boac et al., 2016
Particle-wall restitution coefficient *e*s (-)	0.5	Pieper et al., 2018
Particle-particle restitution coefficient *e*s (-)	0.6	Pieper et al., 2018
Dynamic friction between coffee beans	0.00004	Pieper et al., 2018
Static friction between coffee beans	0.4	Boac et al., 2016
Dynamic friction between coffee beans and boundary	0.00004	Pieper et al., 2018
Static friction between coffee beans and boundary (steel) μ_s on dry basis	0.35	Joseph and Weldon (2019)
The angle of Internal Friction Φ	25-28	
Particles weight kg	1	

5.9.6 Rocky-Particle Group Definition

There are currently three categories of particle shapes that can be used in Rocky v4.3. These are:

- Fiber particles
- Shell particles and solid particles

Among these, solid particles which are closed 3D objects of full interior volume are created. Because these shapes have a non-hollow interior, a solid shape will contain more mass than a similarly shaped shell particle. Seven Solid shapes are provided by default in Rocky v4.3 and import custom polyhedron shape of coffee beans from a .stl file.

Modifying the default shapes particles in Rocky by adjusting the attributes such as the vertical and horizontal aspects, and several corners on the shape sub-tab sphere-polygon (was "Rounded Polygon" in previous versions of Rocky) is created instead of coffee bean imported from CAD as .stl file to reduce computational cost in which both results compared as listed in Table 5.7.

Table 5.7: Comparisons of CAD Developed Coffee Beans and Modified Particle in Rocky

Coffee Beans			Modified particle in Rocky Sphero-Polygon
	Parameters	Values	Values
	Shapes of Particles	Concave	Convex
Attributes of Particles	Vertical aspects ratio	-	1.4
	Horizontal aspects ratio	-	0.50
	Number of corners	-	10
	Equivalent diameters	0.0064 m	0.00642 m
Mesh of particles	Number of particles	6030	5099
	Number of Triangles	1440	1440
	Number of vertices	722	722
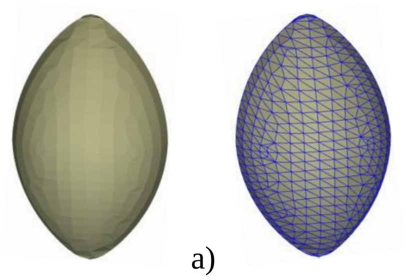 a)			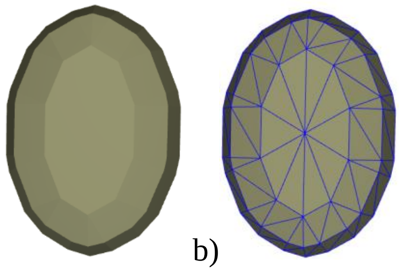 b)

5.9.6 Volume Fill Input Method

In this version of Rocky, there are two different methods by which particles are released or injected into the simulation. These two methods are called continuous injection and volume fill. For the particle inputs step, a volume fill input is enabled to inject closely packed particles into the simulation all at one time as seen in Figure 5.12. When defining a volume fill input, it is important to understand the following components:

- The seed coordinate is the location of a point around which layers of particles are built.

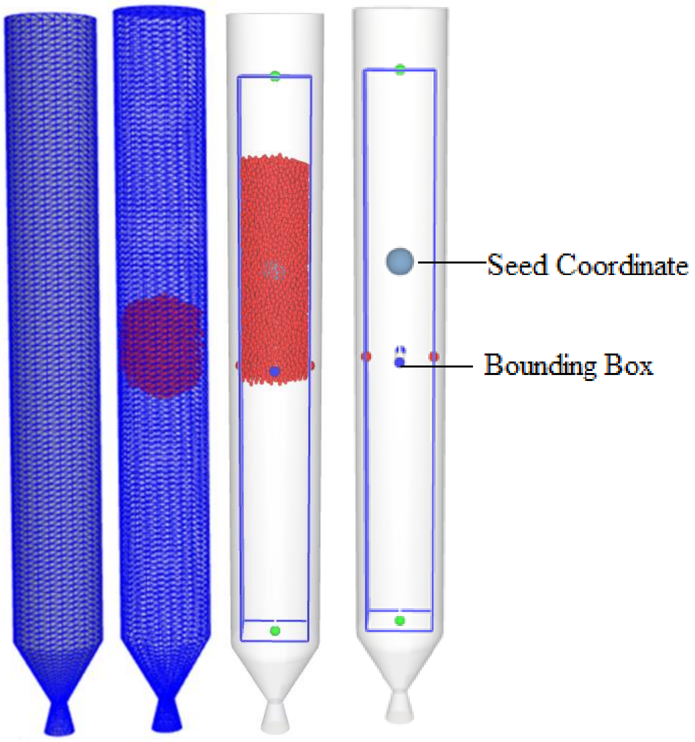

Figure 5.12: Particle Input Using Volume Fill Method

- Mass is the target mass of particles that you want to be built around the seed coordinate.
- Bound is defined as the physical limits by which the particle layers will be constrained. Specifically, the limits must include box bounds, which can be defined manually using coordinates or can be automatically calculated by rocky using the limits of one or more custom geometries selected.

5.9.7 Rocky-Solver Definition

During solver definitions, the simulation duration and output frequency are the two basic parameters that should be defined. The simulation duration is the total amount of real-time that the simulation could run, whereas; the time intervals at which the timestep files are saved. And also from the general settings sub-tab, CPU with 8 target number of processors selected.

5.10 Set up of CFD Fluent and Rocky DEM Coupling Simulation

To make it possible to share the Fluent steady-state fluid flow data with Rocky, Rocky includes a special Ansys fluent coupling support component. Installing this component enables a new export solution to the rocky menu option in Fluent that allows the steady-state fluid data to be packaged into a unique "Fluent to Rocky" or F2R file. This F2R file can then be imported into Rocky as part of the one-way Coupling process.

5.10.1 Exporting the CFD Simulation at Steady State

- After fluid flow data were converged, from the fluent file menu, the export solution to rocky as F2R file and needed to save in the same folder as fluent case file and save fluent case saved ones again and CFD Fluent result saved as shown in Figure 5.13 file format.

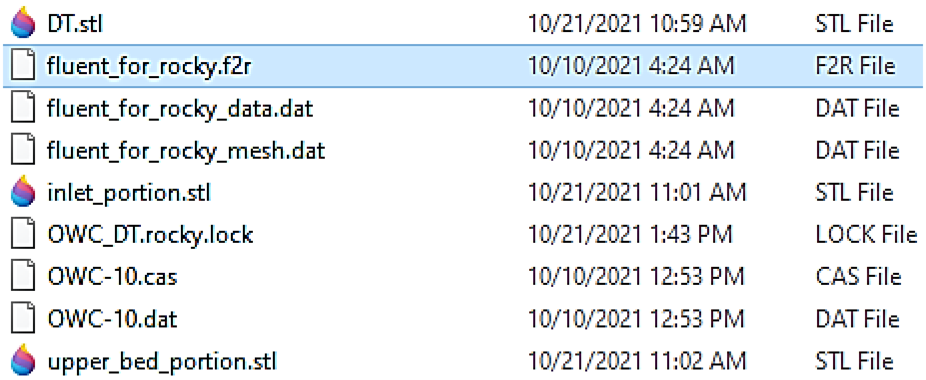

Figure 5.13: CFD Fluent Result File Format

Importing fluent one-way steady-state CFD solutions commenced with importing geometries from where the file directory is available.

1. From the data editors panel, the CFD coupling is activated and a fluent one-way steady-state choose from the coupling mode list.
2. From the select Fluent 2 Rocky export file dialog, the F2R file is located and browsed from the file directory in which a new Fluent One-Way Steady State item appears beneath CFD Coupling in the Data panel.
3. Under CFD coupling and from the data editor’s panel, the laws, and settings set in which the one-way coupling procedure terminates and is ready for processing.

This case is where the laws for drag, turbulent dispersion force, and thermal modeling enabled by convective heat transfer are defined. Then, process the simulation. Initially, the particle concentration in the spouted bed is specified, and gas velocity inside the spouted bed is set to zero. The particle concentration in the freeboard region is also set to zero.

5.11 Challenges in Numerical Modelling

5.11.1 Computational Cost

Computational cost is the execution time per time step during the simulation and is a headache in modeling of Multiphase flow model using CFD Fluent and Rocky DEM coupling method. Numerical analysis of coffee roasting necessarily requires three things i.e one is properties of the coffee bean as particles, the other is working fluid as hot air and the latter one is a digital electronic machine which is a computer. Therefore, the processing speed of the computer on which Rocky is running is very limited for fast processing time.

5.11.2 Measures Taken to Overcome Challenges in Numerical Modelling

I. Reducing Numbers of Particles (Coffee Beans)

The maximum capacity of a conical spouted bed coffee roaster is restricted to one kilogram (1 kg) due to its computational complexity and cost during numerical simulations.

The particle size used in this study is assumed to have the same shape and volume. Sieve Size (formerly "Sieve"), which for especially default Rocky shapes, is defined as the dimension of the smallest square aperture through which the particle can pass through. The **s**ieve size of a coffee bean and a modified sphere-polygon is taken as an equivalent to the equivalent diameter of coffee beans which is about 6.42 mm.

II. Using Graphics Processing Unit (GPU)

GPU is the ability of Rocky to make use of a Graphics Processing Unit (GPU) computer chip to perform rapid calculations and quickly render images and animations on screen. From available resources, NVidia GeForce 940MX with the total amount of 2GB global memory is used parallel to CPU in which GPU information is shown in Figure 5.14 during simulation. However, it does not much fix the difficulty of computing time in which the simulating time is almost the same as to run on HP Desktop i7 8th generation having 8 GB RAM.

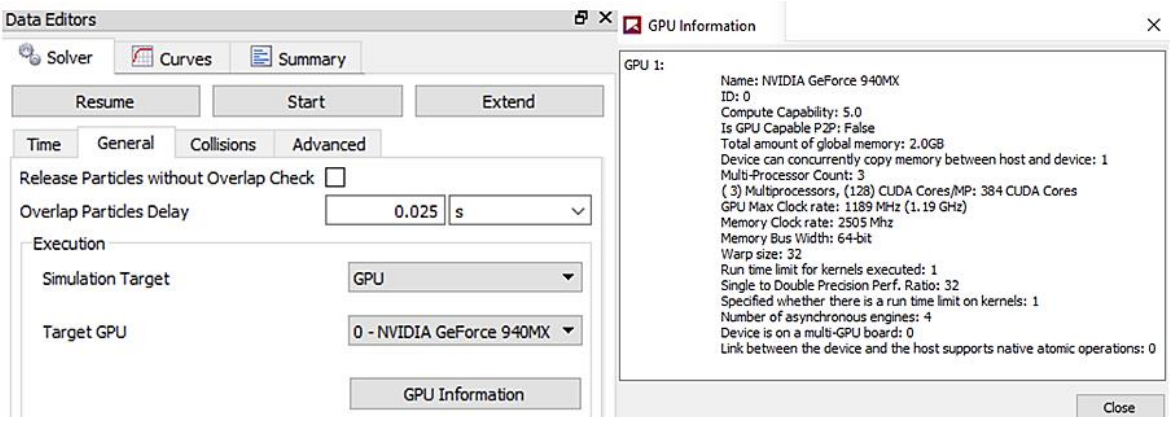

Figure 5.14: Snapshot of available GPU information during simulation

III. Using Modified Default Shapes of Rocky Solid Particles

There are about seven (7) solid 3D particle shapes provided by default in Rocky. If the default shapes aren't enough to meet certain particles, it is possible to import custom particle shapes developed in CAD and modify real particles like Barely, Rice, Pea, Corn, Raisin, Potato, Chocolate, and Navy Bean. Likewise, the coffee bean shape is modified by changing attributes stated in Table 5.7 and creates a sphere-polygon is a closed figure formed by arcs of great circles on a spherical surface in which its shape is near to the coffee bean by redrawing its concavity. This is done because doing the simulation with custom solid polyhedral coffee beans developed in Ansys space Claim takes too much computational time which is very difficult to obtain the required, converged characteristic curve.

For this reason, simulation of custom polyhedral coffee beans is run for about 3 seconds and extrapolates the remaining simulation in a certain way without the need to run the full for extended simulation whereas, modified sphere-polygon run for about 180seconds and finally percentage of error is calculated. Taking this into account, the two determinant phenomena in conical spouted bed coffee roaster are momentum and heat exchange effect, in which the heat transfer coefficient is the most affected parameter to be considered. The heat transfer coefficient depends on the temperature difference between particles (i.e. coffee beans) and fluid which leads to the driving force for the heat flow. As roasting time is elapsed, heat transfer from hot air to the coffee bean via convection and leads to an increase in coffee bean temperature to its roast-able temperature as displayed in Figures 5.15 a and b. To distinguish the differences between the developed coffee bean model in CAD and the modified particle in Rocky the numerical simulation is done for about three (3) seconds. Accordingly, the percentage error between these two particles is about 1.23% which is less than 5% of the acceptable percentage error.

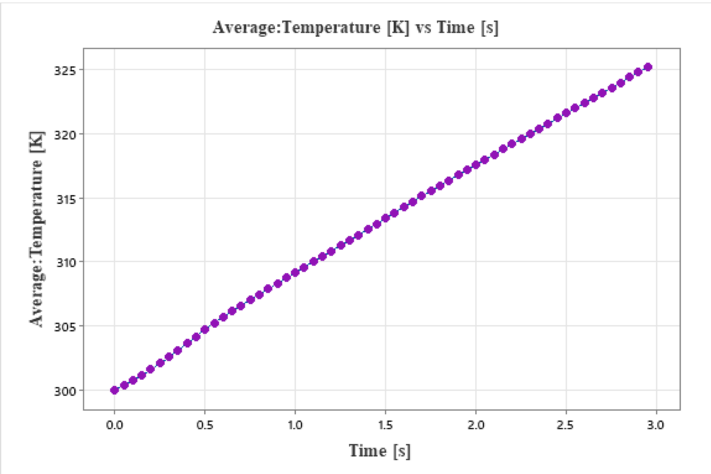

(a)

As observed from Figure 5.15 the trend of the T-S curve guarantee as there is no more deviation in the temperature distribution of particle and as a result heat transfer coefficient will be achieved with very little acceptable deviation.

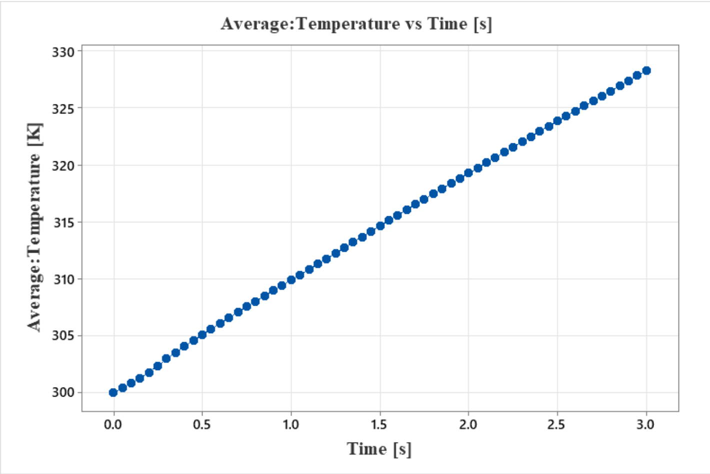

(b)

Figure 5.15: T-S curve of Coffee bean (a) and Modified Rocky Particle (b)

In addition to this, most existing fluid-particle heat transfer correlations assume and are valid for estimating the heat transfer between a spherical particle and its surroundings. Hence, a modified sphere-polygon with the ellipsoidal shape like a coffee bean is an acceptable particle for this analysis and snapshot of particle temperature contour shown in Figure 5.16.

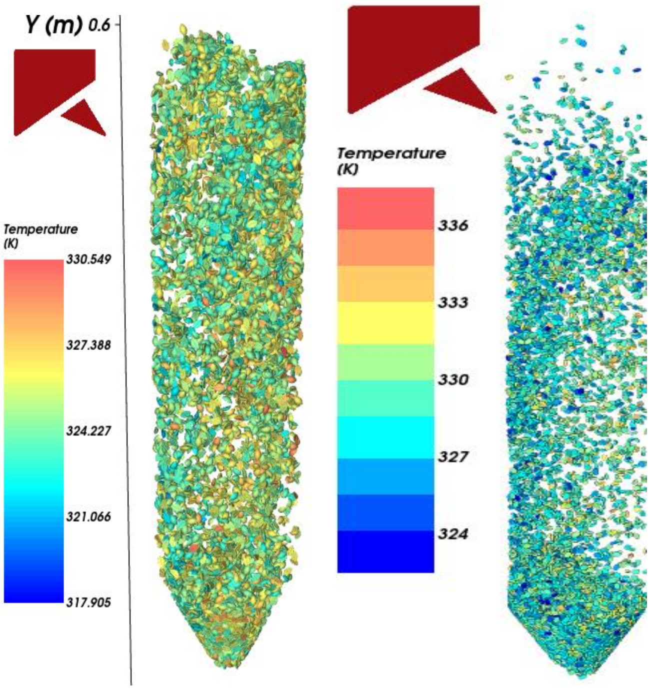

a) **b)**

Figure 5.16: Temperature Contour a) Coffee beans b) modified particles

IV. Reducing the Number of Mesh Elements Used to Define the Geometry

Reducing the Number of mesh elements used to define the geometry like boundary material and particle's shape, will minimize computational without disturbing the accuracy of the result and should be well enough to visualize and concentrate physical characteristic's images and animations. Hence, reducing the number of mesh elements will reduce particle shape and the number of vertices used to define the shape on the other hand it also enables fast computing time. An unstructured mesh with tetrahedral elements of appropriate size was generated in Hyper mesh for coffee beans as shown in Figure 5.17.

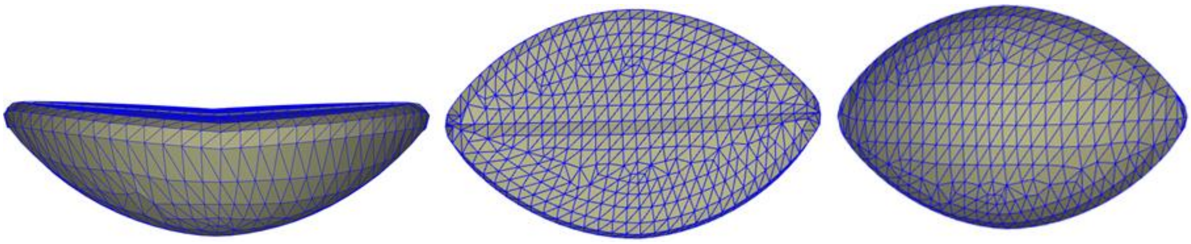

Figure 5.17: Mesh elements of coffee beans

5.12 Modification and Numerical Design of Conical Spouted Bed

5.12.1 Introduction

In recent years, the quest for coffee knowledge is spreading due to the growing appreciation of coffee. Consumers are no longer content with instant coffee and now crave the experience as well as flavors of freshly roasted-high quality coffee. The quality of the coffee beverage is closely related to the chemical composition of the roasted beans, which is affected by the composition of green beans and postharvest processing conditions, i.e. drying, and roasting (Aliah et al., 2015, Franca, et al., 2005; Illy & Viani, 2005).

There are many types of coffee roasting technologies. Taking into account roasting techniques, coffee beans are conventionally roasted in batches or continuous systems. The heat can be transferred to the beans by conduction at direct contact with hot metal surfaces, by free or forced convection due to a streaming media (hot air), or by radiation (Wang & Lim, 2014). The degrees of roasting are controlled by roasting time and temperature and are necessary for the required chemical reactions without burning the beans and compromising the flavor of the beverage (Mendes, 2001). Achieving an ideal roast is a goal that is complicated since coffee beans behave differently and produce distinct results in physical properties, chemical composition, and biological activities when roasted under different conditions (Baggenstoss et al., 2008; Rosa et al., 2016).

Hence, the conical spouted bed is modified by adding a different internal device to achieve uniform heat transfer which is the best control of roasting due to convection heat transfer as well as considering the thermos-hydrodynamic effect of the system.

5.12.2 The Heat Transfer Enhancement

Heat transfer devices have been used for conversion and recovery of heat in many industrial and domestic applications, which can result in a reduction in energy requirements as well as material and other cost-saving. Heat transfer enhancement techniques generally reduce the thermal resistance either by increasing the effective heat transfer surface area or by generating turbulence. Sometimes these changes are accompanied by an increase in the required pumping power which results in higher costs. The effectiveness of a heat transfer enhancement technique is evaluated by the Thermal Performance Factor which is a ratio of the change in the heat transfer rate to the change in friction factor. Various types of inserts are used in many heat transfer enhancement devices. Accordingly, geometrical parameters of conical spouted bed and the insertion of internal devices like fountain confiner are numerically designed within their geometric parameters namely the width, length, and the distance between the bottom end of the confiner and static bed height that affect the heat transfer.

5.12.3 Design of Fountain Confiner

The fountain confiner changes the residence time of the gas, lengthening its trajectory, and thereby increasing the contact between the coffee beans and hot air. The distance between the bed surface and the lower end of this device, H_F, is a key geometric factor to be designed for stable operation and flexible system performance. For this reason, three different devices' geometry, whose dimensions of (H_F) are 0.08, H_F equals to static bed height ($H_F = H_O$) and 0.12m selected for numerical simulations as seen in Figure 5.18. Concerning the other dimensions of the fountain confiner, two different diameters have been used which are 0.154 and 0.2m, and the same length of about 0.5m as shown in Table 5.8.

5.12.4 The Thermo-hydrodynamic Parameters

The dynamic behavior of coffee beans in a conical spouted bed is characterized by the hydrodynamic parameters and must be considered carefully when controlling the dynamic characteristics of the system's operations. The thermo-hydrodynamic characteristics such as minimum spouting velocity, static bed height, processing time, and the heat transfer coefficient of heat-sensitive particles such as coffee beans during the roasting in a conical spouted bed should be analyzed to determine the optimum operating parameters within the designed geometry of the bed. The spouting gas flow rate and the maximum spouted bed height (i.e., particle trajectories) are required to be considered for accounting for the flexibility and stability of the bed. To consider these parameters an open side-draft tube is introduced to the system and designed to improve the performance of the conical spouted bed.

5.12.5 Design of Open Sided Draft Tube

The draft tube is also designed numerically using Rocky DEM by changing its geometric parameters. Among its geometric parameters, the length of the draft tube varied based on the height of the static bed where the coffee bean is temporarily settled as listed in Table 5.8. This will be done, study the thermo-hydrodynamic effect of an open-sided draft tube alongside a fountain confiner when it intrudes inside and protrudes away from the static bed height. The other dimension of the draft tube are the diameters and widths of the face D_T =0.054m W_h =0.025m respectively and are the same through the analysis.

Based on the designed geometric dimension of the bottom cone of conical spouted, the coffee bean's high about 0.2m which is called static bed height as shown in Figure 5.18.

Table 5.8: Geometry design of fountain confiner and draft tube

Number of Simulation Runs	Distance between static bed (H_o) and the Bottom end of the confiner $H_F(m)$	Length of the open-sided draft tube (m)
Static bed height $H_o = 0.20m$		
Bed 1	0.80	L_T=H_o- 1/4 ×H_o=0.150
Bed 2	0.80	$L_T = H_o = 0.20$
Bed 3	0.80	$L_T = H_o + 1/4 \times H_o = 0.150$
Bed 4	0.80	$L_T = H_o + 1/2 \times H_o = 0.30$
Bed 5	$H_F = 0$	$L_T = H_o = 0.20$
Bed 6	0.12	$L_T = H_o - 1/4 \times H_o = 0.150$
Bed 7	0.12	$L_T = H_o = 0.20$
Bed 8	0.12	$L_T = H_o + 1/4 \times H_o = 0.250$
Bed 9	0.12	$L_T = H_o + 1/2 \times H_o = 0.30$
Bed 10	$H_F = 0$	$L_T = H_o + 1/2 \times H_o = 0.30$

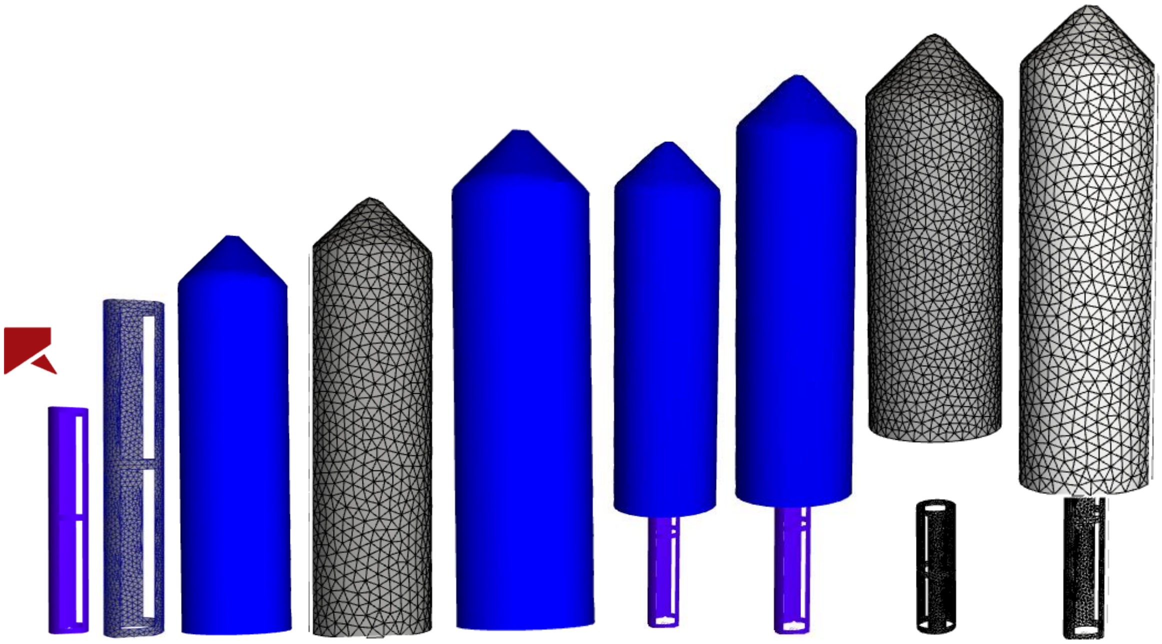

Figure 5.18: Geometries of Fountain Confiner and Draft Tube, and their Assembly

CHAPTER SIX

EXPERIMENTAL PROTOTYPING

6.1 Introduction

This experimental work was carried out in a three-dimensional conical spouted bed to study the roasting quality parameters like bean temperature, the mass of bean, and speed of air during batchwise roasting of coffee beans. The experimental unit's main component is the conical contactor with the draft tube and fountain confiner as shown in Figures 6.1 and 6.2., was made of mild steel and has been used due to its low cost and availability even if it does not recommend for food processing. The outcome results for each experiment were discussed in this chapter in detail. The response results from an experimental investigation carried out by orthogonal array are analyzed using Taguchi methods to identify the optimum roasting parameters and the most influential roasting parameters on the roasting quality.

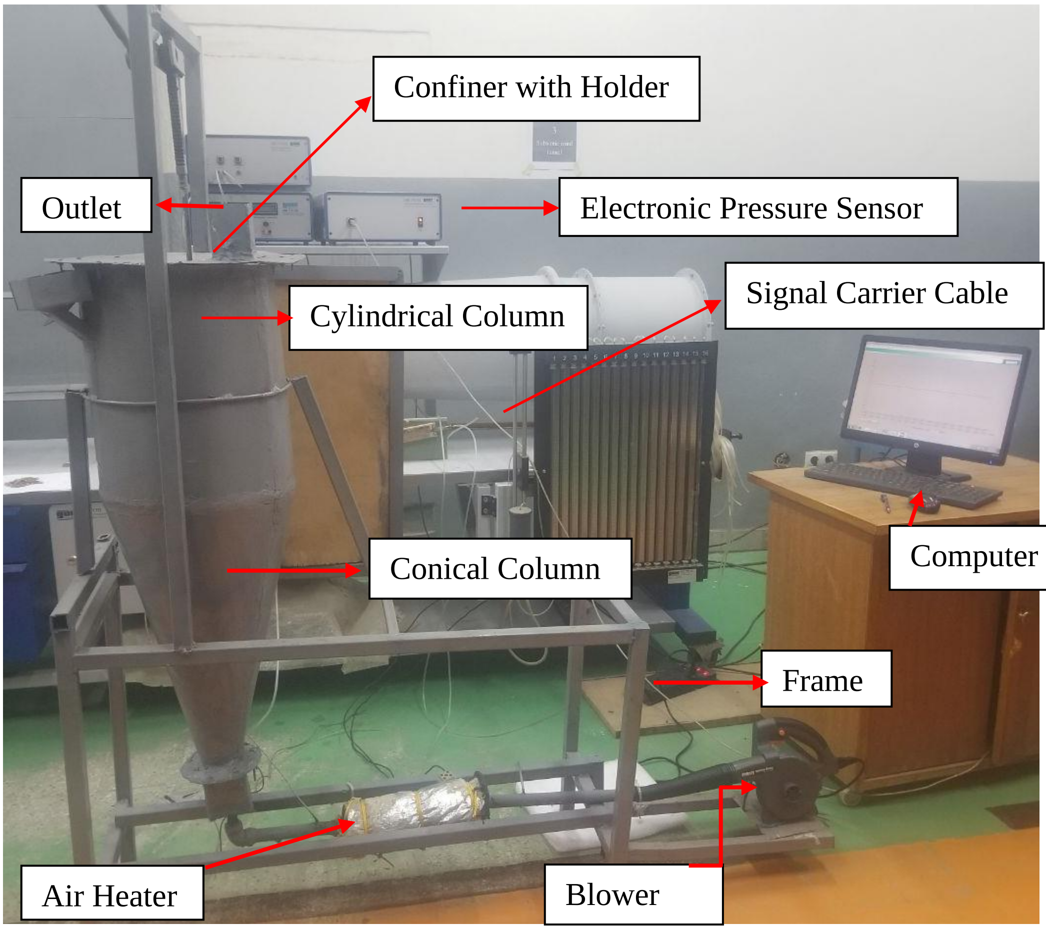

a) (Rear-side views)

b) (Front Side View) c) (Right-Side Views)

Figure 6.1: Main Component of Experimental Units

I. Fountain Confiner

Fountain confiner is made of stainless steel and is a cylindrical pipe of 0.154 m diameter and 0.5 m in length, whose upper outlet is closed with a cone-like shape to avoid gas and solid leaving the contactor through this device and force them to describe a downwards trajectory. It is fitted to the lid of the contactor employing rod mounted on the top as depicted in Figure 6.2 a using bolt and nut, which allow changing the position of the device, i.e., lowering or lifting depending on the operating conditions chosen for the run.

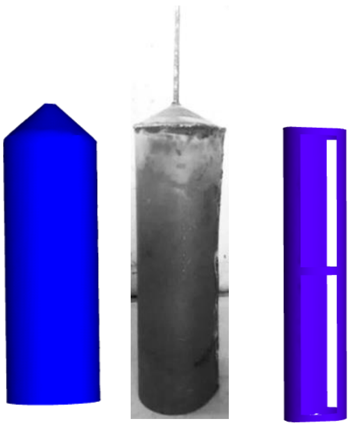

a b

Figure 6.2: Fountain confiner (a) and draft Tube (b)

II. Draft Tube

The draft tube shown in Figure 6.2 b is stainless steel tube of cylindrical shape, which is located along the axis of the contactor and provided with a flat base in whose center there is a hole of the 0.054m diameter as the tube diameter. Moreover, the total length of the open-sided tubes LT= 0.20 m, which means they stand 0.20m above the upper part of the bottom cone surface.

III. Centrifugal Blower

A 600W backward-curved blade centrifugal blower shown in Figure 6.3 supplied the air and a variable speed unit controlled the airspeed passing through the spouted bed. The blower supplies a required airflow rate which is adjusted manually, based amount of coffee to be roasted using an adjustable flow control valve on the blower. The airspeed is calculated using a direct measurement of pressure drop using an electronic pressure sensor throughout the bed.

Figure 6.3: Blower

IV. Air Heater

An electric heater given in Figure 6.4 was manufactured and installed to heat the air to the desired temperature and disconnected manually when the actual roasting time is achieved. The hot runs were carried out at the maximum power supplied by the heater, which heats an air temperature from 27°C. Inlet and outlet air temperatures were monitored throughout the whole run as well as the static bed, annulus bed, draft tube, and fountain confiner temperatures are recorded. The entire air heater system was insulated with layers of mineral wool to minimize heat loss from the system.

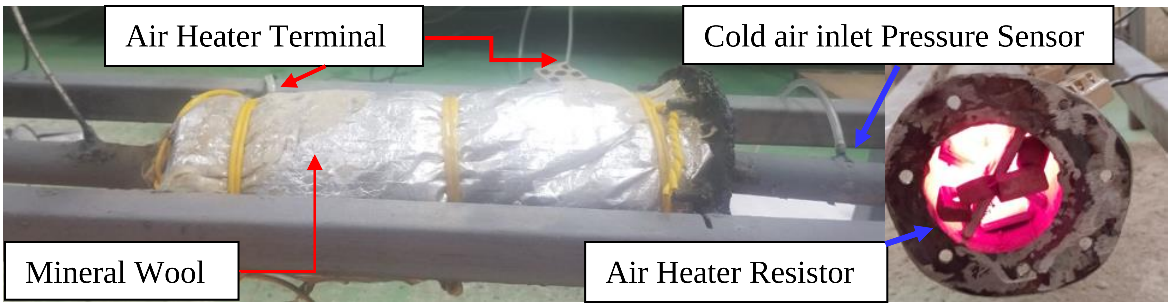

Figure 6.4: Air Heater

6.2 Experimental Procedure

Coffee beans were obtained from local markets in Adama that had the equivalent diameters of 6.42 mm. The initial moisture content of these agricultural materials was in the range of

16-20% dry basis. At this moisture range, the materials did not agglomerate. Different amounts of coffee bean particles (i.e., 6.42mm) have been analyzed in a conical spouted bed. Hydrodynamic studies of these particles have been studied by varying different system parameters precisely the mass of coffee beans and air inlet velocity.

Secondly, the bulk and true density of coffee beans were determined using a graduated cylinder with a diameter equivalent to that of the acrylic tube. In the graduated cylinder, containing a known volume of water, a known mass of coffee bean was added. The volume of water displaced equaled the volume of the particles, and thus, the true density of coffee beans was calculated using the ratio between mass and volume of the particles, and is about 1150kg/m^3.

Coffee beans 0.125, 0.25, and 0.5 kg samples were roasted at inlet air velocities of 1.5,0.25 and 0.5 m/s respectively at different static bed heights. The mass of coffee beans was chosen for experimental runs by considering the current cost available on the market. To minimize the measurement errors, each test has been performed three times (3) under the same conditions, and the average values are reported.

In this study, the unit allows operating with contactors with an angle (γ) of 45° of conical spouted bed with internal devices so-called fountain confiner, and draft tube. The first run of an experiment was carried out with an internal device called a fountain confiner with a so-called kilogram of coffee beans using the above conditions.

The experiments were carried out by changing the different system parameters based on the scope of the experiment (changing velocity and /or flow rate and mass of coffee beans). The bed temperature and pressure readings were noted down at different flow rates of the supplied air.

Three pressure and six temperatures recording as indicated in Figures 6.5 and 6.6 i.e. some at the air inlet pipe, static bed height, and others at the outlet column are provided for noting the bed pressure drop and degree of temperature level. The thermal couple was inserted axially at the 20, 60,100, 360, and 1042mm and from the base for measuring the temperature at the static bed, annulus, draft tube, fountain confiner, and at the top of the outlet respectively. And also, at the bottom and/or top of the air inlet pipe region one temperature sensor is mounted to record hot air temperature inlet pipe. The temperatures at the both fountain confiner and open-sided draft plate were recorded to calculate the heat conducted from the spout to the downcomer region. On the other hand, the pressure recording sensor is mounted axially at a distance of 10 and 1054 mm from the bottom surface of the conical spouted bed and the other at.

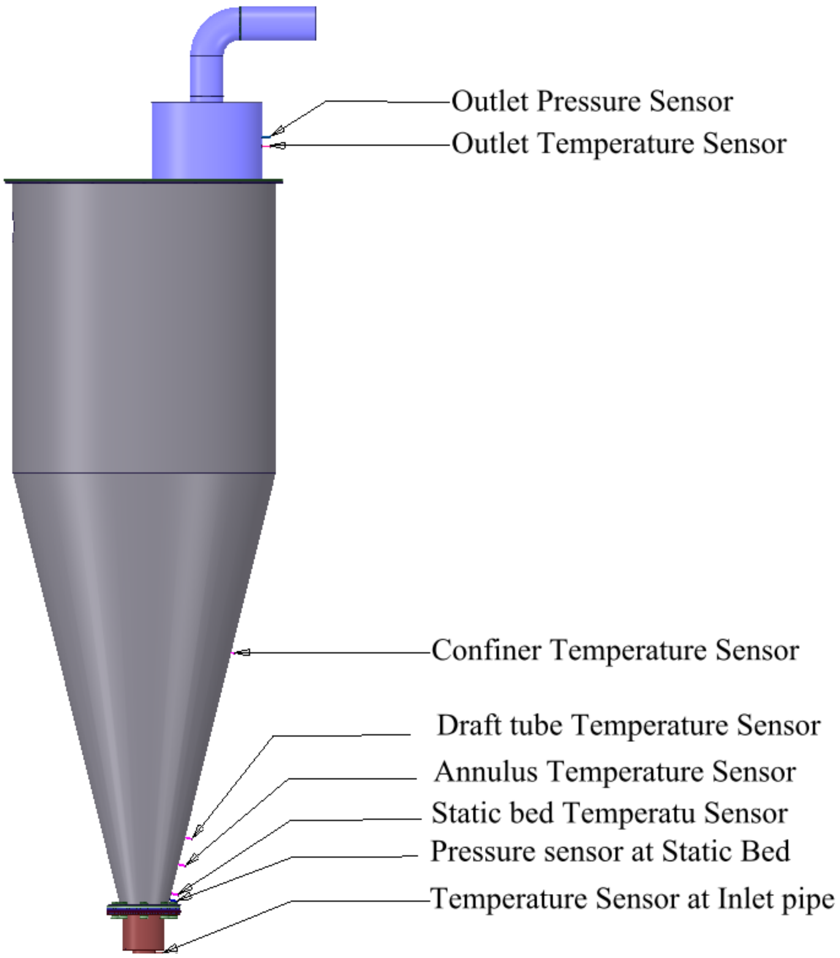

Figure 6.5: Conical Spouted Bed with Internal Devices

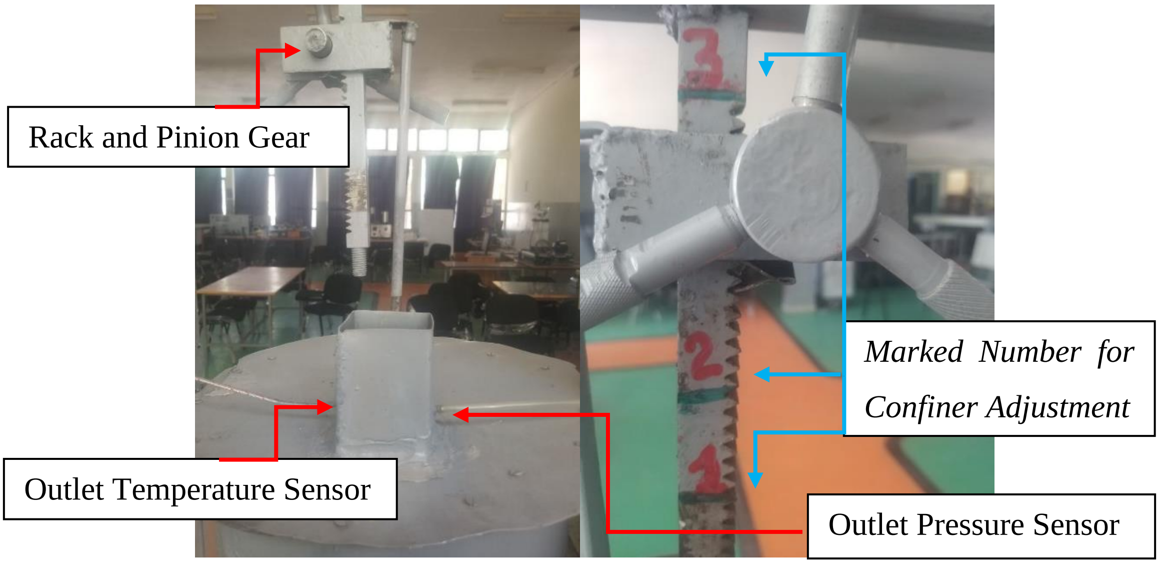

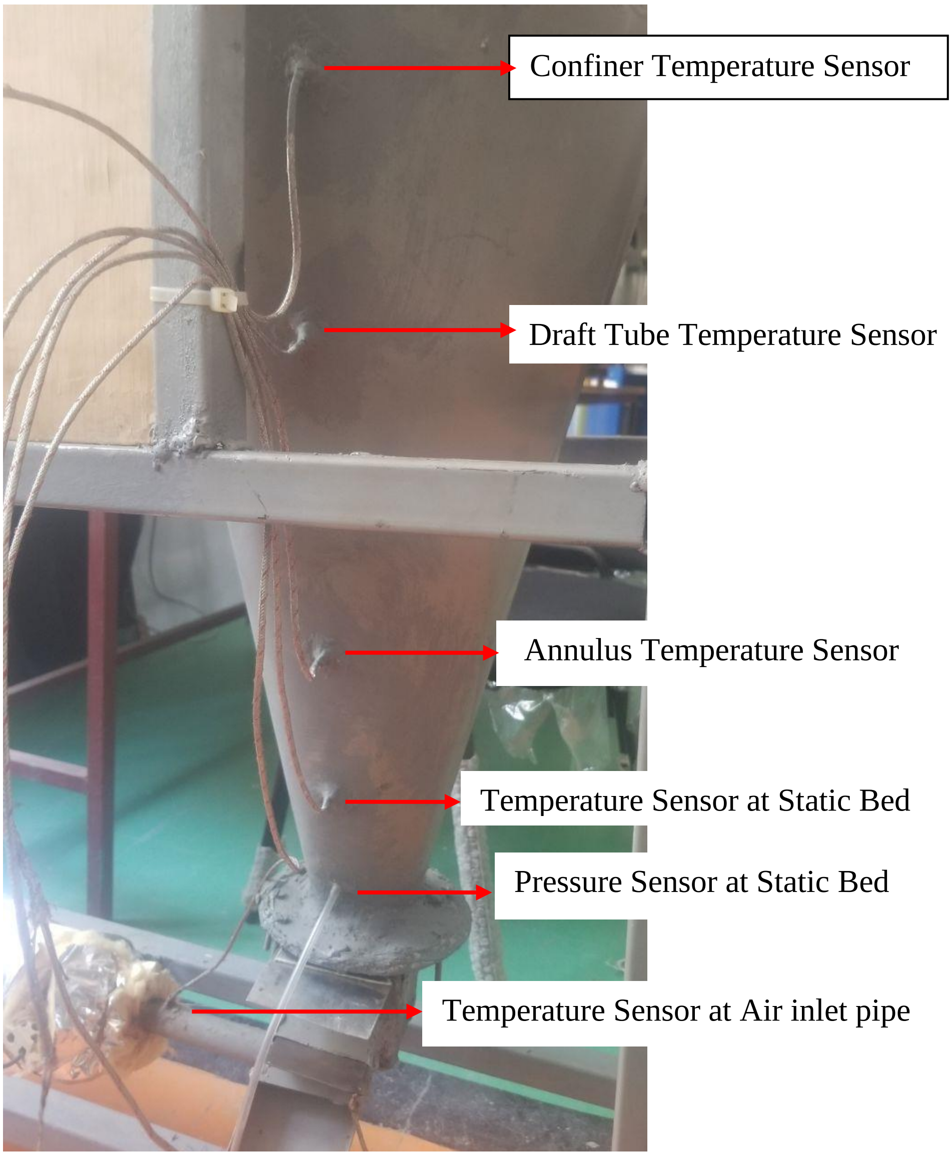

Figure 6.6: Pressure and Temperature Recording Sensors Position

An Electronic pressure sensor as shown in is used to measure the bed pressure drop. In an electronic pressure sensor, a flexible diaphragm separates the process from the actual sensor element. The pressure pushes against this diaphragm, which is designed to deflect consistently across the full pressure range. The sensor then measures the pressure by translating the strain or compression of the diaphragm into a meaningful electronic signal. This is the principle of resistance pressure measurement.

Initially, the conical column was filled with the required amounts of particles. Then the blower was turned on permitting air to be injected into the bed. Airflow was increased until the spouting is established and a continuous particle fountain arose from the bed. In sequence, the air velocity was set in the bed as possible as required. Then, obtaining the bed pressure drop data as a function of air velocity was performed in decreasing order. The relation between pressure and velocity can be given through two independent equations/formulations.

$$P + \frac{1}{2}\rho v^2 + \rho gh = Constant$$

Where:

- P is the pressure of the in-compressible, non-viscous fluid measured using N/m^2.
- ρ is the density of the in-compressible, non-viscous fluid measured using kg/m^3.
- v is the velocity of the in-compressible, non-viscous fluid measured using m/s.
- g is the acceleration due to gravity measured using m/s^2.
- h is the vertical height of the pipe from the reference level measured using m.

Temperature measurements were made with a digital thermometer and a thermocouple wire was inserted axially at the distance stated above from the base.

Figure 6.7: Digital Thermometer

The experimental technique was carried out as the following.

a) With the column empty, the desired airflow rate and temperature were regulated and held until thermal equilibrium was obtained.

b) With the air control valve controlled, the desired mass of coffee beans was charged into the column.

c) A relatively high airflow rate was used to begin the spouting; this flow rate was gradually decreased during the certain durations of operation. Time was counted from the instant the known mass of coffee beans was added.

d) The minimum airflow was maintained utilizing listening the sounds of particle dynamics.

e) Periodically, samples of coffee were taken every few minutes from the column to check the degree of roast.

CHAPTER SEVEN

RESULTS AND DISCUSSION

7.1. Introduction

In this chapter, the results of the simulation of conventional spouted bed and conical Spouted Bed with internal devices are reported and a comparison between the existing and modified methods is made. In addition, a detailed discussion of the results is presented.

7.2. Grid Dependency Test

The grid independence is investigated by comparing the simulation results for five grid sizes. As shown in Table 7.1, the simulation results for particle trajectories in an axial direction were obtained by the very fine, fine, medium, coarse, and very coarse grids of 20,734; 29,664; 84,161; 200,685, and 650,144, and of the hexahedral cells respectively. Mesh 2 and mesh 3, however, lead to little variations in the particle's trajectories along the axial direction. Hence, the medium grid was used in the rest of the simulations for the seeks accuracy and required computational economy.

Table 7.1: Grid Independence Test for Particle Trajectories in CSBWID

Mesh	Elements	Nodes	Elements Size(m)	particle trajectories(m)
1	20,734	22, 376	0.017	0.607
2	29,664	31,737	0.015	0.552
3	84,161	87,992	0.010	0.510
4	200,685	207, 340	0.0075	0.402
5	650,144	663,799	0.005	0.356

7.3. CFD-Fluent Results Conventional Spouted Bed

According to, CFD-Fluent with Rocky DEM Coupling, CFD Fluent the simulation program setting is done based on Ansys Fluent one-way Steady State coupled simulation. The geometry of the computational domain considered in this study was a conical spouted bed with a conical base and cylindrical from the top where particle trajectories freely orbited and the total bed height is good enough to perform. Hence, the ANSYS Fluent solver solves fluid flow, energy, and viscous data, in which both energy and viscous model are activated from the Fluent Models. Hence, the working fluid i.e. ambient air's properties like energy equation should be solved to calculate thermal properties of coffee bean in the Rocky side, and standard K-Omega viscous model is calculated to solve turbulent flow field of working fluid and later for coffee beans in the Rocky side.

The momentum and energy equation are solved by ANSYS Fluent solver and delivers both velocity and pressure flow field and as well as to temperature flow field to Rocky DEM solver. The Pressure coupling, PC-SIMPLE algorithm, which is the SIMPLE algorithm, is used as the method of pressure-velocity coupling solver.

Among existing conventional spouted bed, the bed designed and developed by Nagragu et al.,1997 is selected for this study as the cornerstone, to evaluate its performance using numerical simulation, and, finally, modification is made to maximize and enhance the performance of spouted bed technology for the coffee roasting application.

7.3.1 Velocity Contour of Conventional Spouted Bed

The inlet ambient air velocity is one of the important factors in the roasting of coffee beans. It can significantly affect the spouting of particles as well as the heat transfer in the bed that determines the roasting of bean particles. The exact minimum spouting is determined numerically by using the CFD Fluent and Rocky DEM Coupling approaches, i.e., first simulation data of velocity field is solved in CFD Fluent side and exported to Rocky DEM solver and dynamics effect of coffee beans with applied velocity checked and simulation is continued until certain data is achieved.

The effect of inlet air velocity is investigated here for two particles shape of coffee beans, which are in the range of 10~25m/s. At a low air velocity i.e., at about 10 m/s coffee bean particles remain stationary in the bed and gas could not penetrate through the particles to form spouting.

The motion of bean particles is minor when the gas velocity (~15m/s) is lower than the minimum spouting velocity. At a high gas velocity, coffee bean particles can be transformed into a diluted state. The minimum spouting velocity for the present simulation settings is 20 m/s and the particle flow pattern at selected inlet air velocities is illustrated in Figure 7.1. The results show that the variation of particle flow pattern with the inlet air velocity can be reasonably predicted by the CFD-DEM approach which is discussed in the next section. Since, the air inlet nozzle of about 25mm diameter is used in conventional spouted bed, as shown in Figure 7.1, the CFD fluent Result is (~74m/s) that finally import into Rocky solver as fluent to rocky (f2r) file.

7.3.2 Temperature Contour of Conventional Spouted Bed

Inlet air temperature is one of the dominant factors affecting the roasting rate (Syahrul et al., 2003). The roasting rate increases and the roasting period becomes shorter with the increase in air temperature. The higher inlet air temperature leads to higher air temperature in the bed and higher heat exchange between gas and solids and subsequently resulting in higher particle temperature.

Since the roasting temperature of coffee beans for the dark degree of roasting is achieved at 250℃ of hot air temperature; inlet air temperature is fixed to the stated temperature and used in the entire simulation. Considering constant thermal models, the constant air temperature at 250℃ (523 K) applied from the inlet boundary, with the copy of the constant values for both specific heat and thermal conductivity properties, are changed to their first respective polynomial. The constant temperature and related properties are calculated in fluent and shown in Figure 7.2

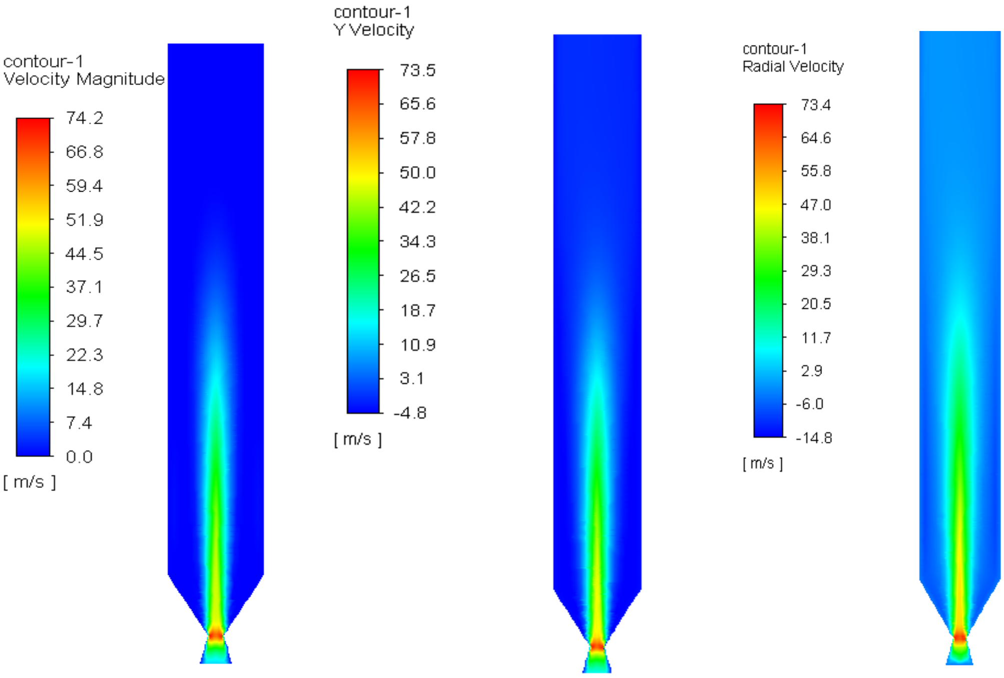

a) b) c)

Figure 7.1: Velocity Contour of Conventional Spouted Bed (20mps Velocity Inlet)

7.3.3 Pressure Contour of Conventional Spouted Bed

As is shown in figure 7.3 the pressure at the bottom of the bed is too high. The high pressure from the inlet port of the bed indicates that the velocity is low at that point. Some of the most common and validated drag correlations for single-particle (dilute flow) are implemented in the Rocky DEM-CFD coupling modules and applied to spherical and non-spherical particles. The pressure-gradient force across a surface should overcome the drag force of particles and achieve a buoyant force, an upward force that is exerted on a particle by a fluid. Archimedes' principle is the fact that buoyant force is equal to the weight of the displaced fluid. The colors on the pressure contour indicate the intensity of the pressure. The red color indicates the maximum pressure and the blue color shows the minimum pressure. The value for each color map is also given on the left of the contour.

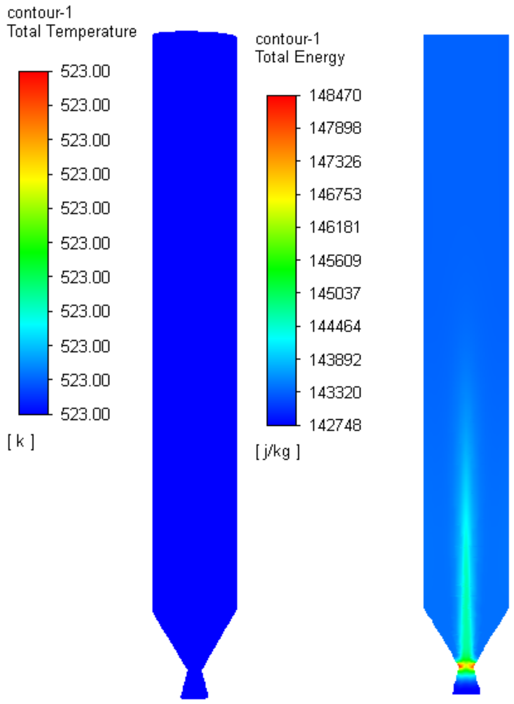

Figure 7.2: Constant Temperature (a) and Energy (b) Contour

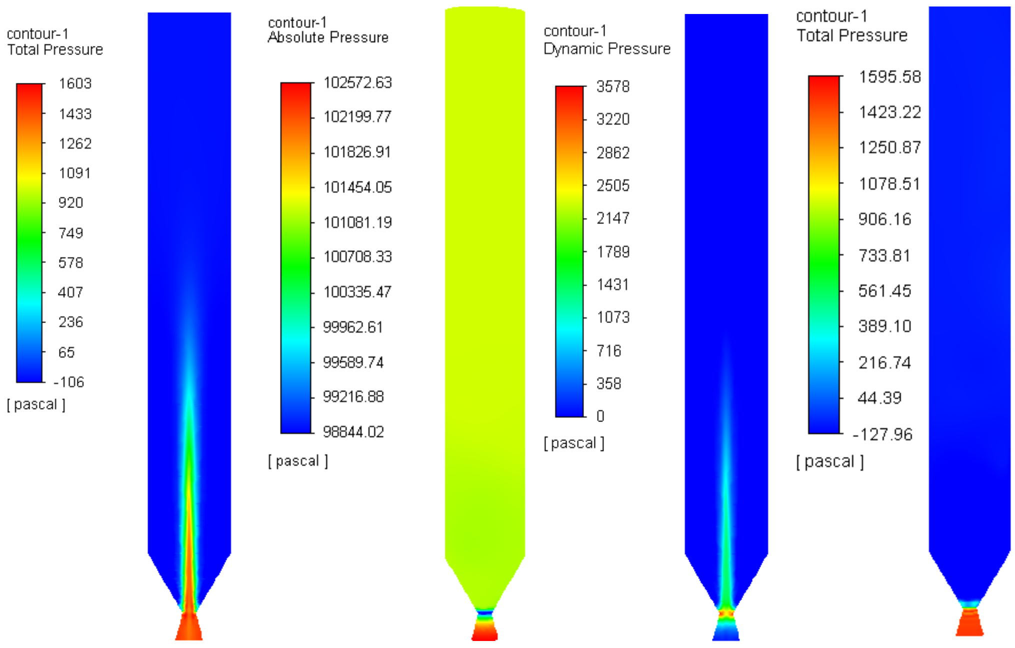

a) b) c) d)

Figure 7.3: Contours of Total a)/d) and Absolute b) and Dynamic Pressure c)

7.3.4 Turbulent Kinetic Energy Contour

The turbulence kinetic energy is the kinetic energy per unit mass of the turbulent fluctuations in a turbulent flow and its average value calculated by CFD is about 24.6 m^2/s^2 as illustrated in the contour of Figure 7.4. The specific turbulence dissipation is the rate at which turbulence kinetic energy is converted into thermal internal energy per unit volume and time which is sometimes called the mean frequency of the turbulence.

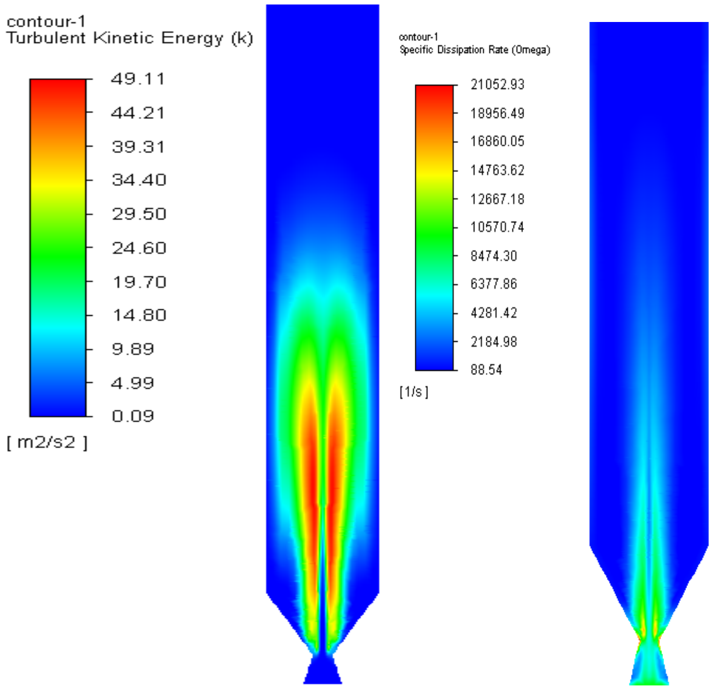

Figure 7.4: Turbulence Kinetic Energy a) and b) Specific Turbulence Dissipation Rate

7.4 CFD-Fluent Results of Conical Spouted Bed

The geometry of the conical spouted bed is designed and developed in chapter three, and the geometric factors of the bed: diameter of the upper cylindrical section, D_c, 0.36 m; included cone angle, γ, 45°; the height of the conical section, H_c, 0.60; 0.7 m of cylindrical portion H_{cy} with a total height of 1.4 m and base diameter of the cone, D_i, 0.068 m. Although a different model is designed numerically, with CFD-DEM coupling, the model with this dimension is used throughout the simulation to calculate all necessary fluid flow data using fluent and later import respective converged data for Rocky to characterize coffee bean particles that behave as granular particulate.

7.4.1 Velocity Contour of Conical Spouted Bed

The simulation result of inlet air velocity for two particles shape of cad developed coffee beans and modified particles for coffee beans is in the range of 3~5 m/s. At a low air velocity, the motion of coffee bean particles is minor when the gas velocity 3 m/s, is lower than the minimum spouting velocity. The minimum spouting velocity for the present simulation settings is within the range of 4 to 5 m/s as demonstrated, however, 5 m/s air inlet velocity is selected due to pressure drop while using fountain confiner and used throughout the entire simulation. Since, the air inlet nozzle of about 12.5 mm diameter is used in conical spouted bed, as depicted in Figure 7.5, the CFD fluent Result is about 95 m/s that is finally imported onto Rocky DEM.

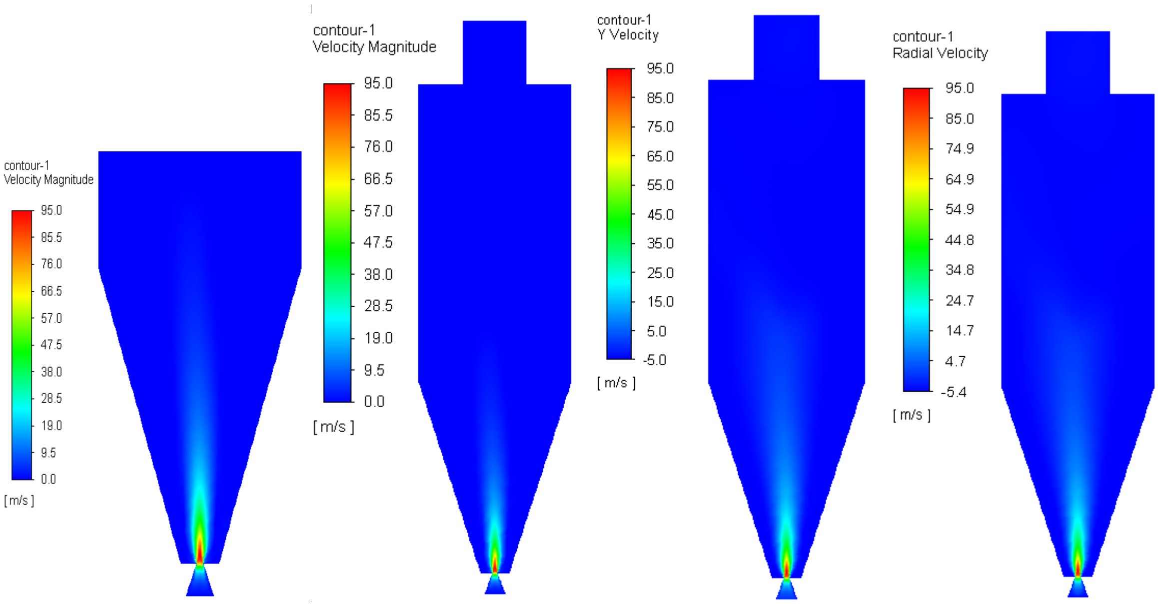

Figure 7.5: Velocity Contour of Conical Spouted Bed with 5m/S Velocity

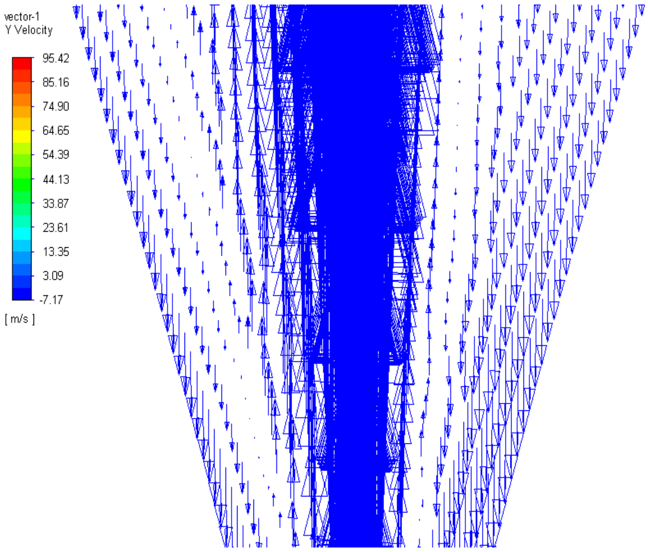

Figure 7.6: Profile Plot of Y-Velocity Vector

7.4.2 Temperature Contour of Conical Spouted Bed

The coupling between Ansys Fluent (CFD) and Rocky DEM has the comprehensive capability for solving fluid particulate systems, enlarging the range of the granular-fluid system's simulation. In the one-way approach, the fluid field affects the particle flow but the particle flow does not, in turn, affect the fluid field. This method is particularly useful for simulating dilute flows in which effective air inlet velocity and temperature data are required for the momentum and energy exchange of granular material called coffee bean particles.

The working fluid is hot air at the temperature of $250°C$ $(523K)$ as the gas density and thermal conductivity vary with temperature and time. This flow is simulated under elevated temperature which is the main goal of the study. Accordingly, constant temperature data is solved on the fluent side and the result of simulated temperature and total energy is shown in Figure 7.7.

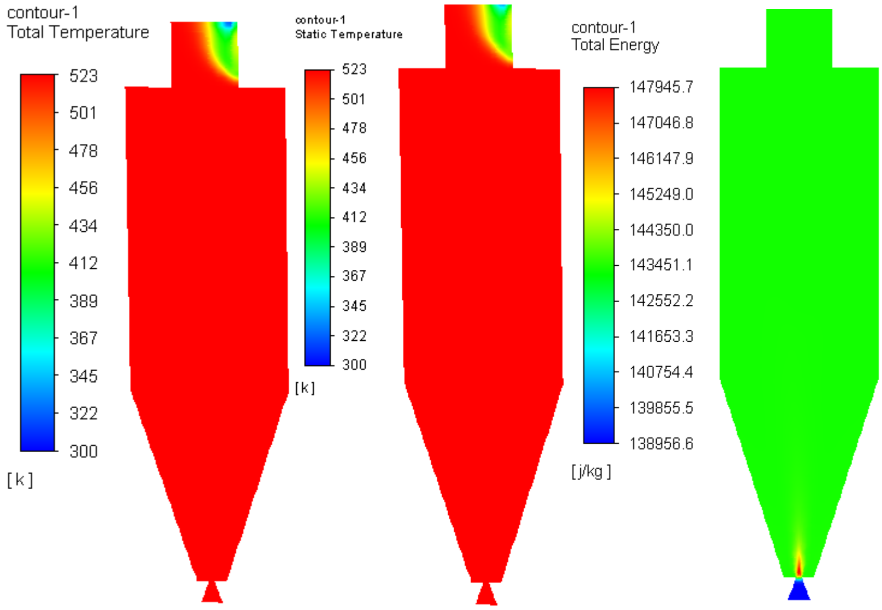

Figure 7.7: The Contour of the Temperature Field and Total Energy

7.4.3 Pressure Contour of Conical Spouted Bed

The static, dynamic, and total pressure contour lines or profiles superimposed on the physical flow domain of the conical spouted bed are calculated in Ansys CFD Fluent as demonstrated in Figure 7.8. As observed from the pressure profile contour, the total pressure calculated in fluent, as result exported to rocky particle solver is about 6102 Pa.

7.4.4 Turbulent Kinetic Energy Contour

The Bed is designed to streamline flow and hence the intensity of turbulence is less inside the nozzle as compared to the flow regime. The maximum turbulence intensity of 644 k (%) is attained at the nozzle exit, beyond which the turbulent intensity steadily decreases. Further downstream, as flow gets agitated and the turbulence intensity increases. While the turbulence of kinetic energy ranges from 2 to $2.068x10^{\ 3}\ m^2/s^2$ as shown in Figure 7.9.

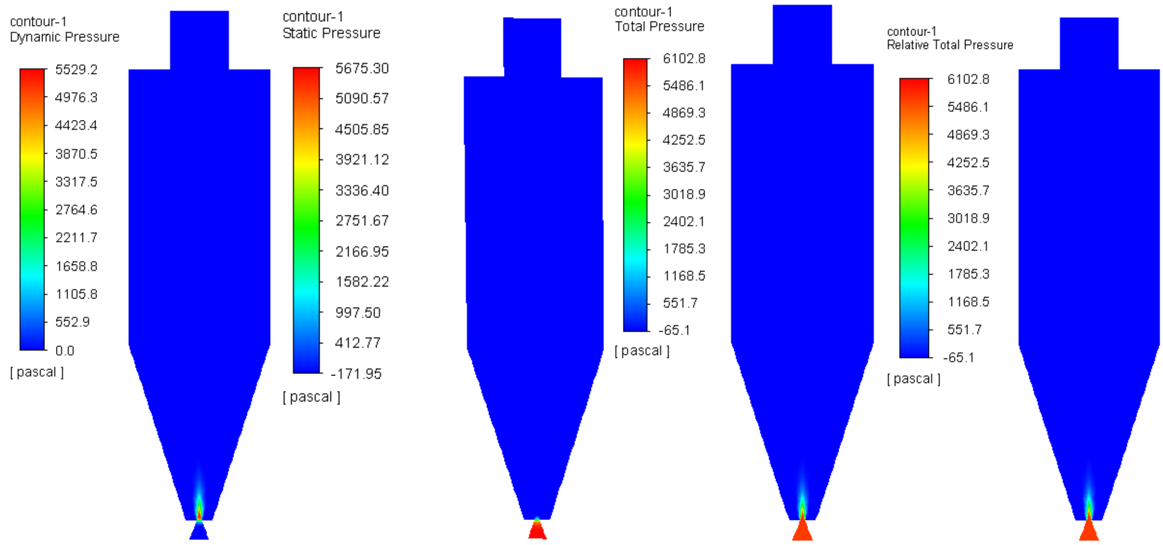

Figure 7.8:Contours of Dynamic a), Static b) And Total Pressure, and Total Pressure c)

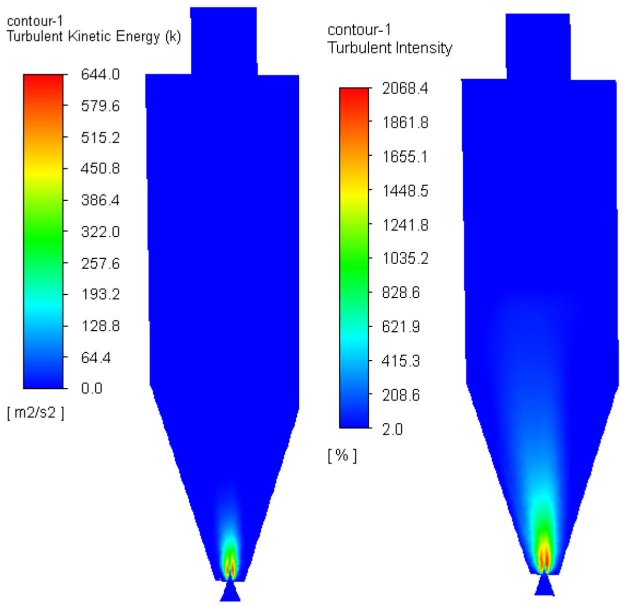

Figure 7.9: The Contour of Turbulence Kinetic Energy and Intensity Distribution

7.5. Computational Fluid Dynamics (CFD) Fluent and Rocky DEM (Discrete Element Method) Coupling Result

Computational Fluid Dynamics (CFD) solves general transport equations using numerical methods such as finite volume method using continuum methods, whereas, DEM simulates the motion of every particle like particle-particle and particle-boundary interactions are solved. DEM is a mesh-free method and does not solve the continuum equations of motion instead of it solves the equations of motion for every individual particle that is numerically integrated with time. The coupling between the simulated airflow at FLUENT and the motion of the particles at ROCKY permits a realistic approach for coffee roasting application. In both approaches of the Rocky-Fluent coupling, all particles are tracked in a

Lagrangian way by the DEM solver, explicitly solving the equations that govern translational and rotational particle motion along with the energy balance on the particle. These equations take into account the forces and torque on particles due to the fluid phase that is imported from the fluent side.

7.6 CFD Fluent and Rocky DEM Coupling Result Conventional Spouted Bed

The coupled use of computational fluid dynamics (CFD) and DEM to model the fluid and solid phases, respectively, is a valuable approach that enables particle-scale information to be obtained. With the advancement in computational techniques, CFD-DEM coupling has been applied to processes involving multiphase flow, including those using spouted beds. The converged fluent fluid data is exported to Rocky where all forces acting on particles are computed by the DEM solver. Accordingly, once the coffee beans particle is generated inside the domain of conventional spouted bed at Rocky side ambient air elevated to high temperature of about 250℃ imported from Fluent side at velocity of 20 m/s which is increased to 74 m/s as pass through an air inlet nozzle 25mm diameter. Figure 7.10 indicates the evolution of coffee bean particles as time elapsed up to 0.5sec where coffee bean preceding be roasted by a strong air flux fed to the bed from the bottom.

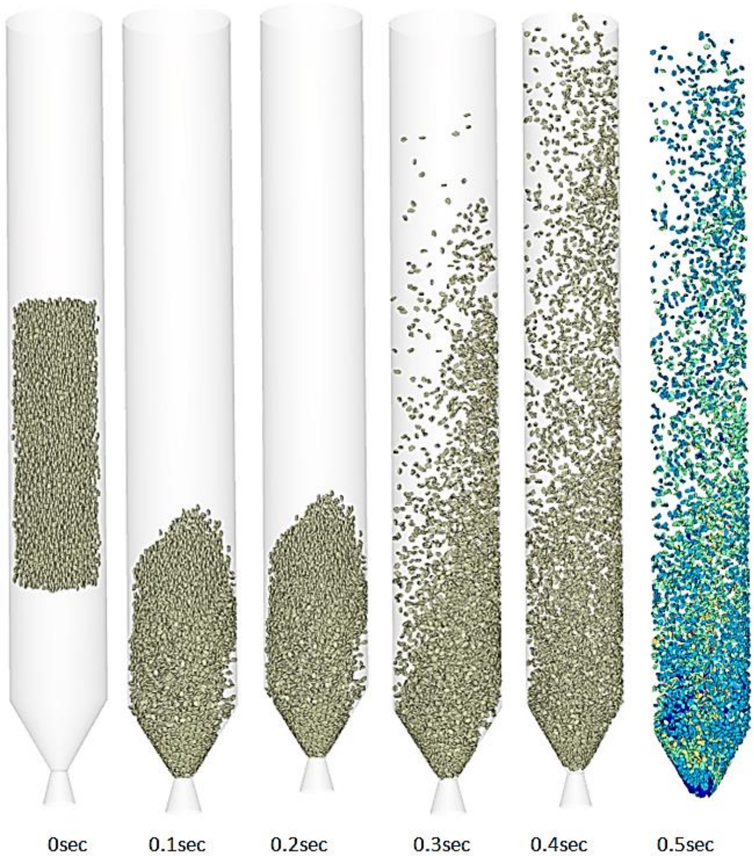

Figure 7.10: Snapshot of the Evolution of Coffee Bean at 20m/S Velocity Injected

7.6.1 Eulerian Statistics

The Eulerian statistics are applied to the cube or cylinder user process to divide the original analysis of the particle's shape into separate blocks for more granular analysis where the information of void and volume fraction is calculated.

i. Void fraction is also known as porosity, it is the ratio between the volume of the block not occupied by particles divided by the volume of the block itself. The average Void fraction of particle is 0.67

ii. Volume fraction is the ratio between the total particle's volumes inside the block divided by the volume of the block itself. The average Void fraction of the particle is 0.33 as shown in Figure 7.11.

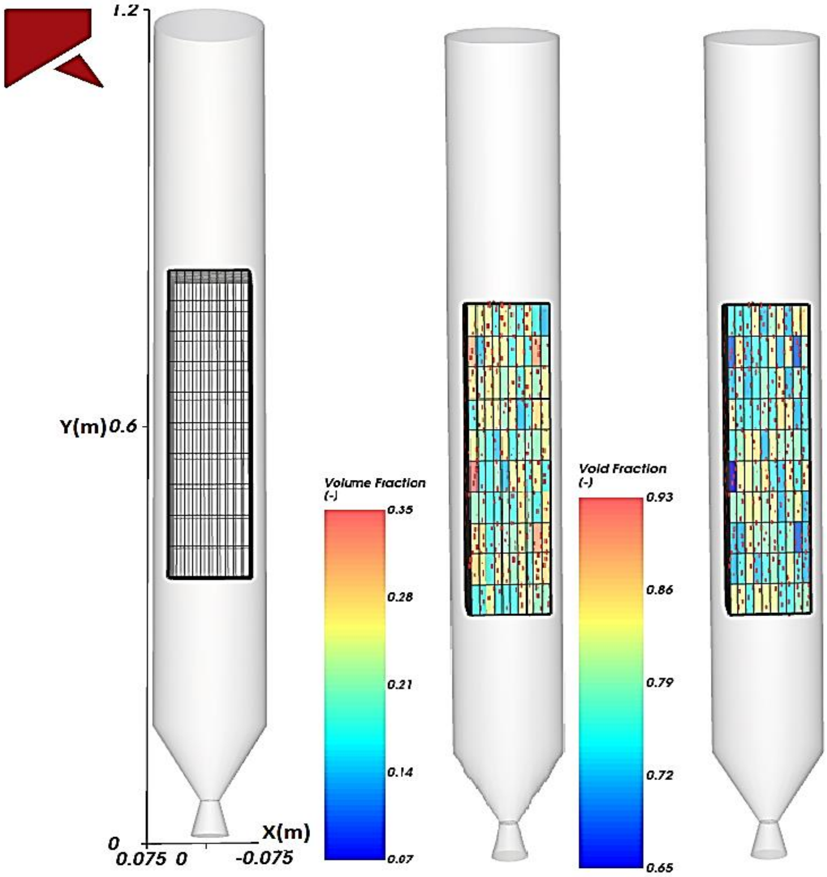

Figure 7.11: Coffee Bean Particles Eulerian Statistics in Cubic Domain

7.6.2 Dynamics of Coffee Bean Particles in Conventional Spouted Bed

In the DEM, all the coffee beans particles within the computational domain are tracked in a Lagrangian way, by solving explicitly Euler's first and second laws that govern translational and rotational particle motion, respectively. The detailed coffee bean dynamics are discussed here below.

I. Absolute Translational Velocity

The magnitude of the translational velocity is the velocity of each whole particle in a certain defined boundary. The maximum, average, and minimum magnitude of absolute

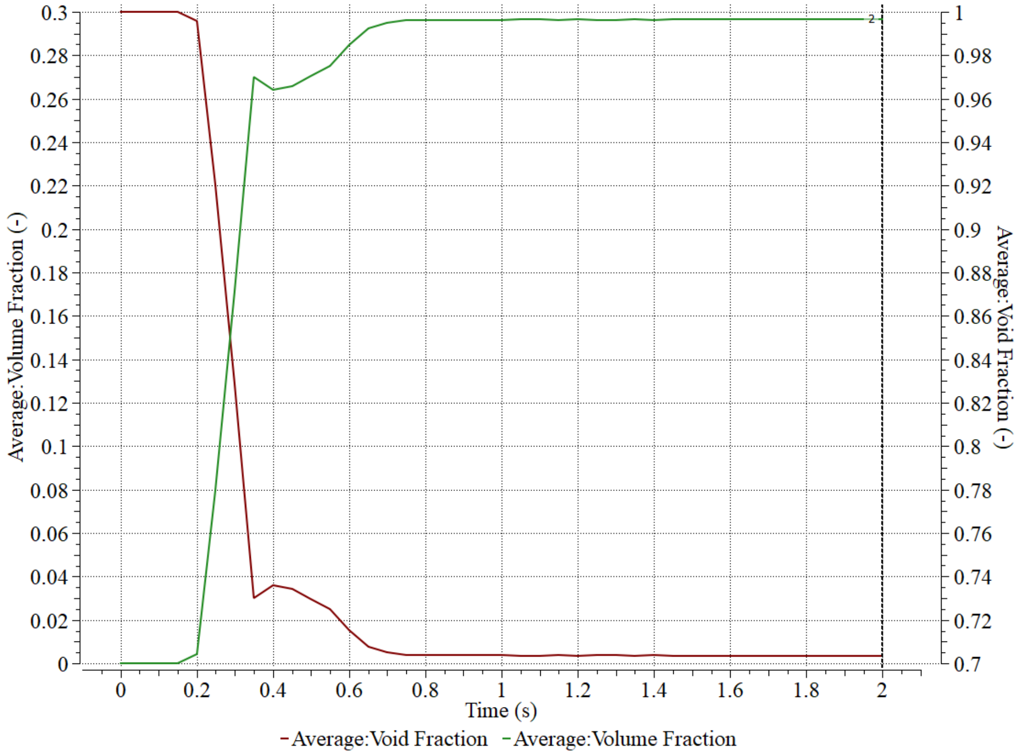

Figure 7.12: Volume and Void Fraction of Coffee Bean over 2sec Particle is Generated

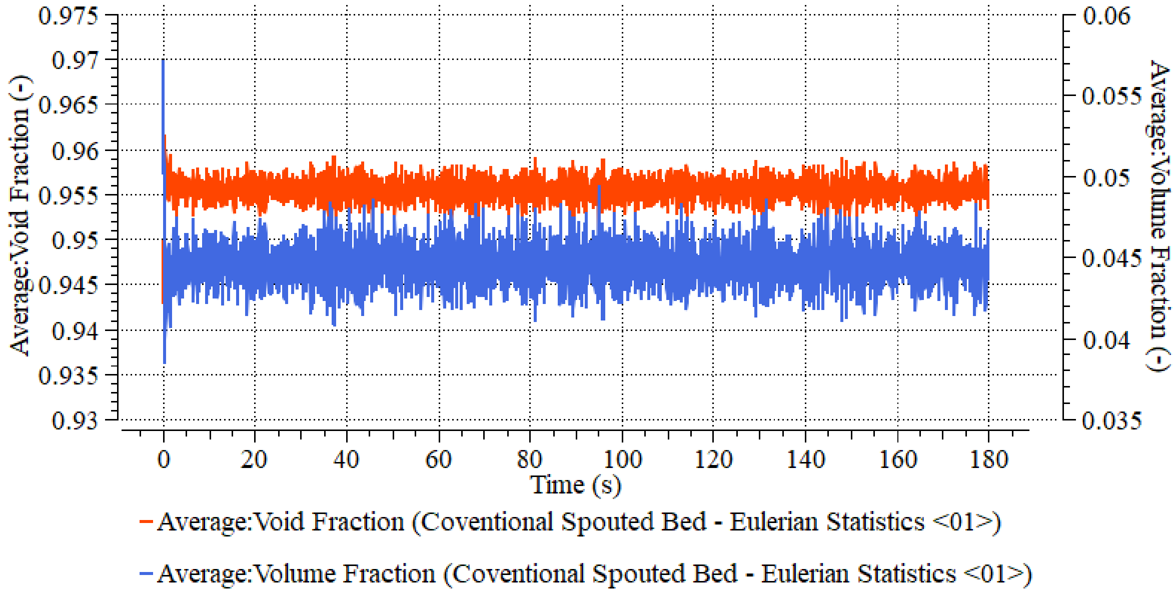

Figure 7.13: Void and Volume Fraction of Coffee Over Time

translational velocity is 7.92, 1.34, and 0.75 m/s as illustrated in Figure 7.15 a, and its velocity contour is shown in Figure 7.14b.

II. Translational Y-Velocity [m/s]

The translational Y-velocity is a velocity vector of each whole particle, and the maximum magnitude of the y component Y velocity is 7.2 m/s as illustrated in Figure 7.14 a and Figure 7.15 b.

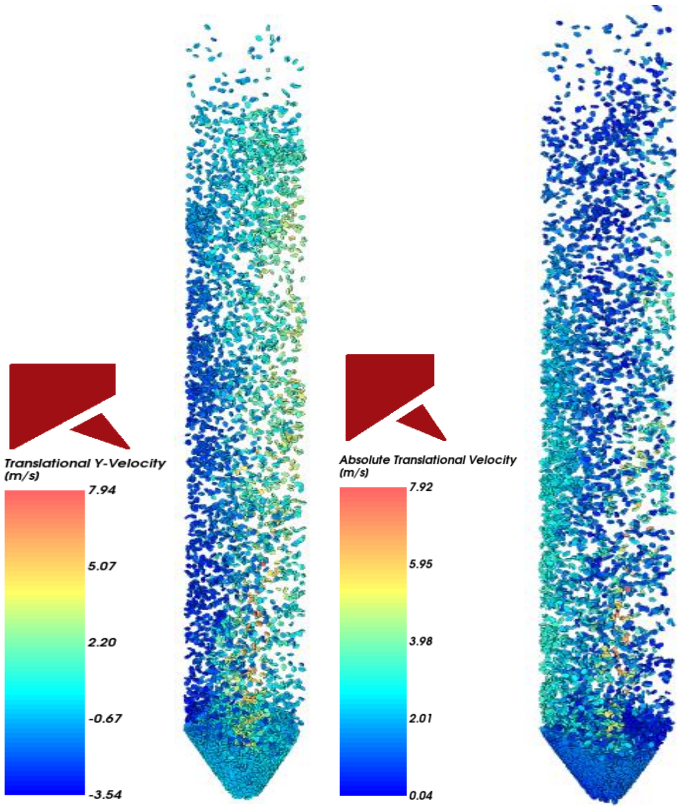

a) b)

Figure 7.14: The Contour of Translational-Y a) and b) Absolute Translational Velocity

III. Absolute Rotational Velocity (Rad/s)

The magnitude of the rotational velocity of each whole particle inside the defined boundary. This is useful for determining the angular momentum of particles, which affects particle rolling. It can be defined as the norm of the rotational velocity vector. As is indicated in Figure 7.16 its average value is about 175 Rad/s and the ve1ocity contour is illustrated in Figure 7.16 a.

IV. Rotational Y-Velocity (Rad/s)

The y-component of the rotational velocity vector of each particle coffee bean. Figure 7.16b.

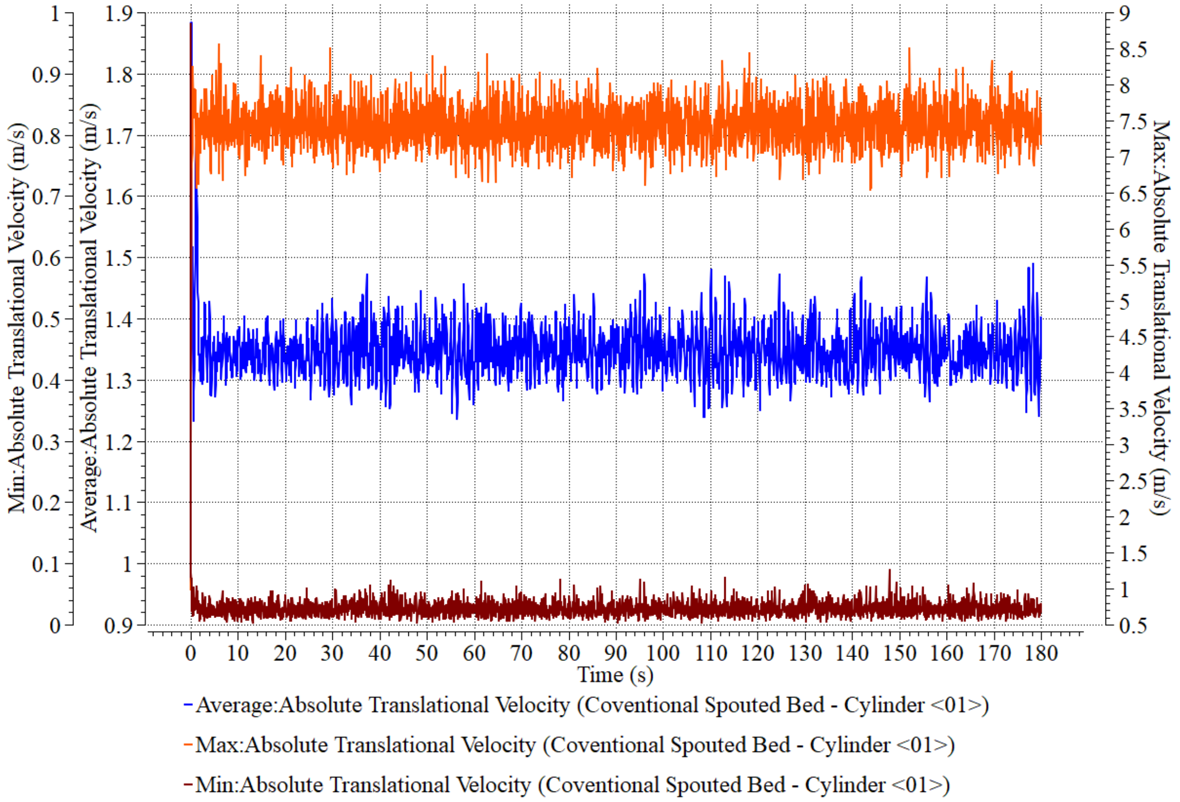

a)

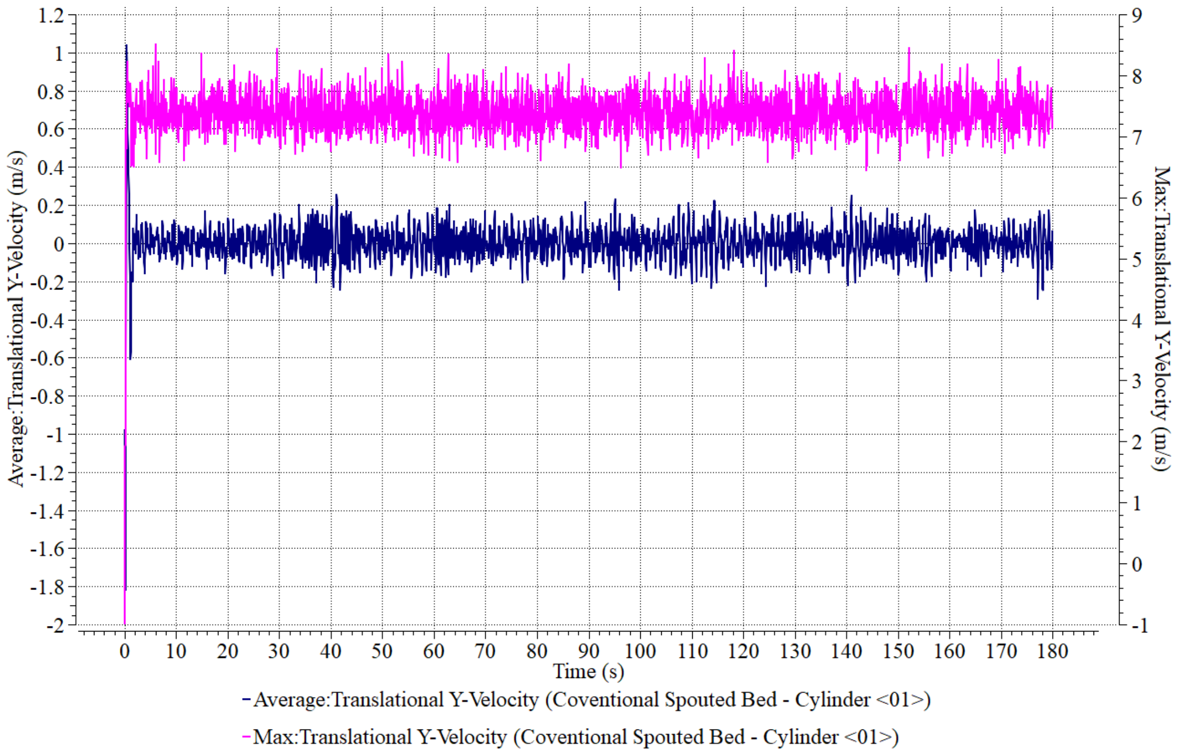

b)

Figure 7.15: Translational-Y a) and b) Absolute Translational Velocity Over Time

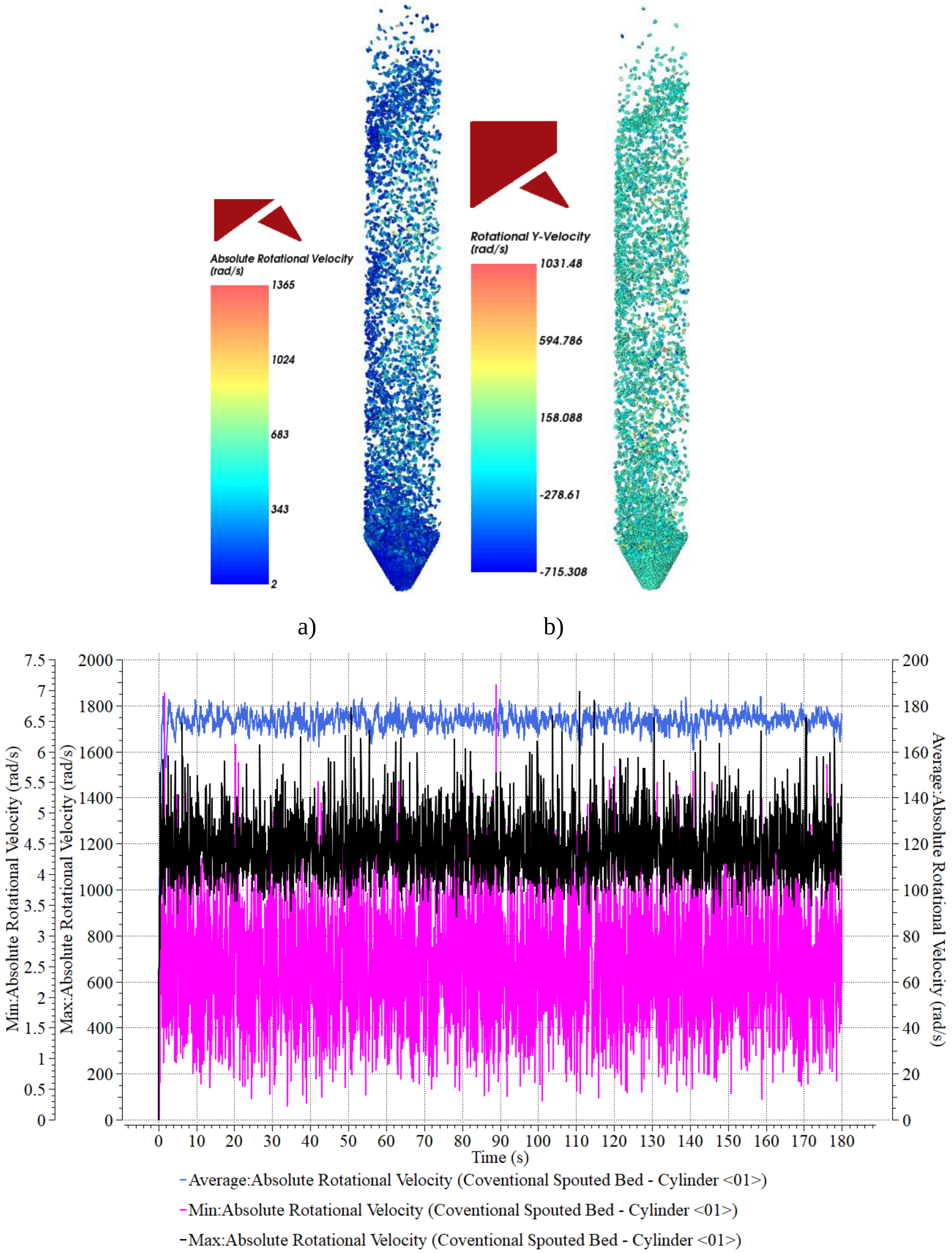

c)

Figure 7.16: The Contour of Absolute Rotational Velocity and Rotational Y-Velocity

V. Particle Y-Coordinate

The maximum height where bean particles can reach axially is called particle trajectories. It depends on the geometry of the bed and inlet air velocity through the nozzle. The space plot of particle trajectories and contour maximum heights of particles y-coordinate is shown in Figures 7.18 and 7.19 respectively. And also, the time plot of particle trajectories during roasting is indicated in Figure 7.20.

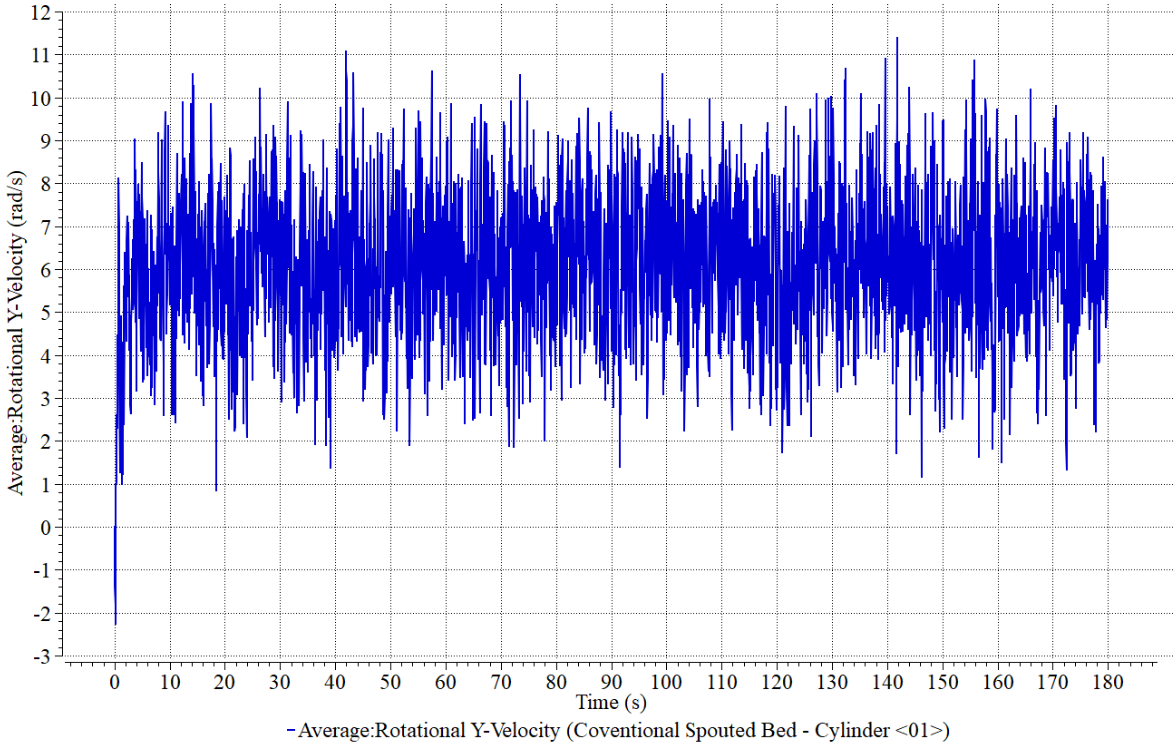

b)

Figure 7.17: Rotational Y-Velocity Over Time

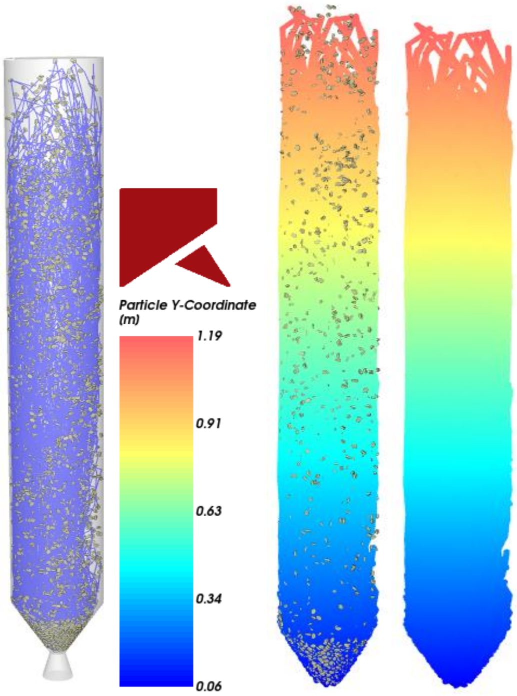

Figure 7.18: Contour Maximum Heights of Particles Y-Coordinate.

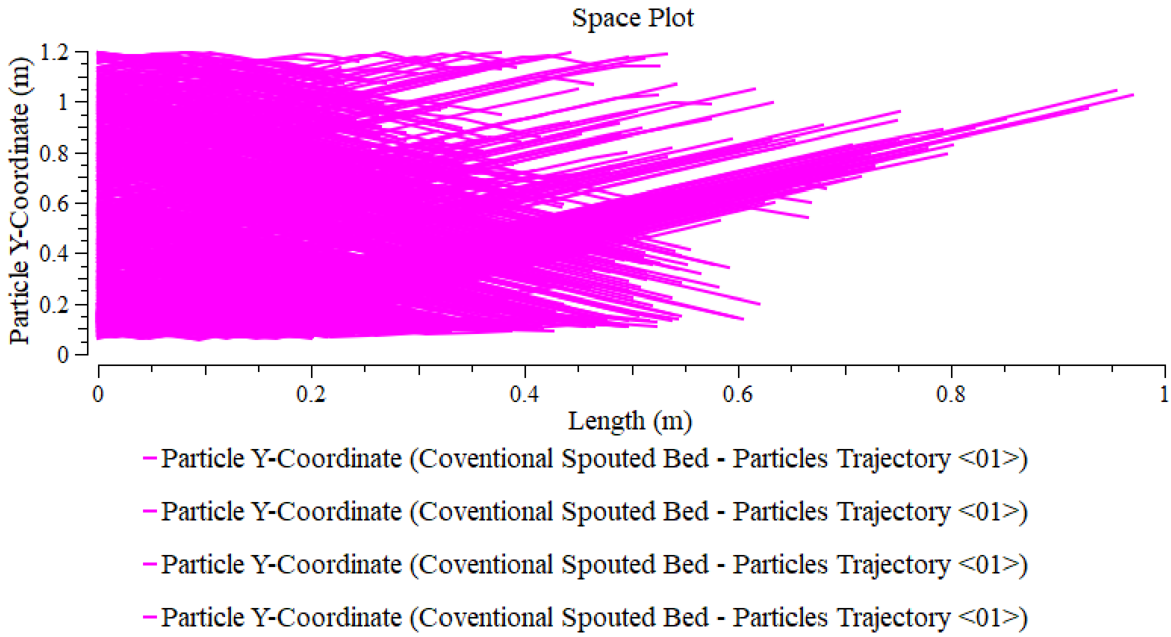

Figure 7.19: Space Plot of Particle Trajectories

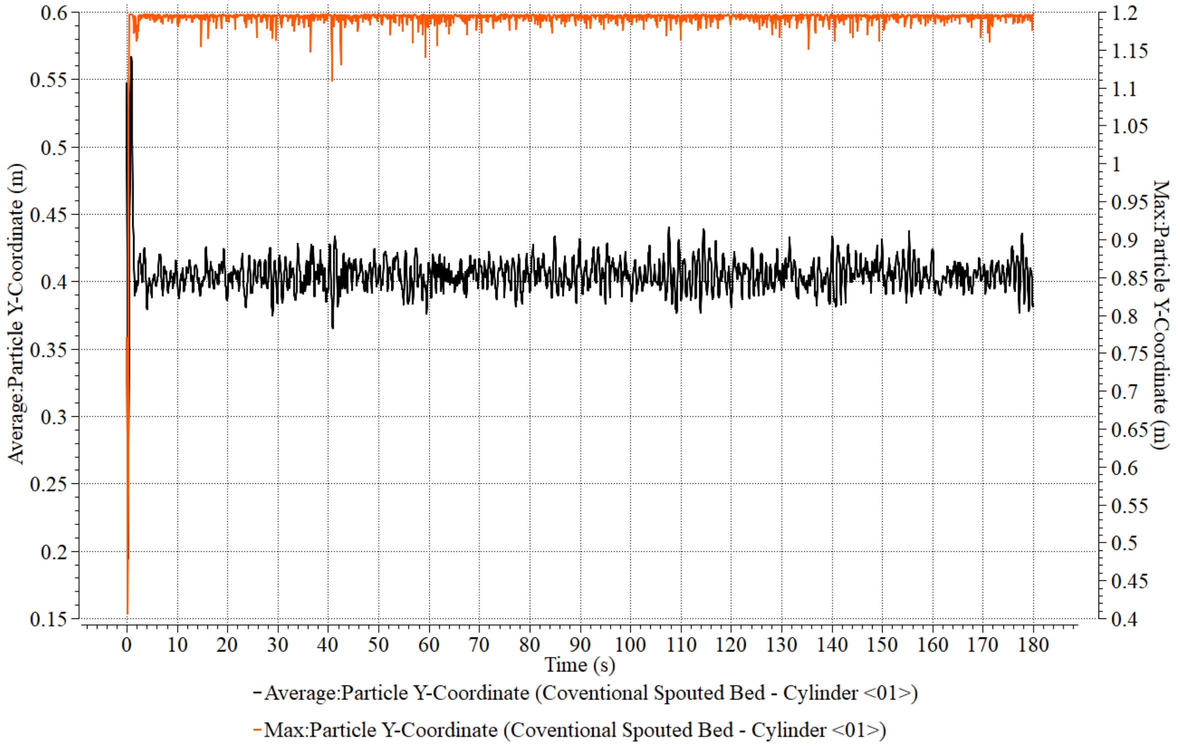

Figure 7.20: The Transient Plot of Particle Trajectories

7.6.3 Temperature of Coffee Bean Particles in Conventional Spouted Bed

The coffee bean temperature is considered to have a significant effect on the roasting rate. Since the higher particle temperature leads to a higher roasting rate. The hot air at the temperature of about 250℃ $(523k)$ is applied to the bed via an air inlet nozzle and the snapshot of the evolution of coffee bean particle temperature is shown in Figure 7.21. In the conventional spouted bed temperature distribution coffee bean particles increase from the upper bed to the lower part of the bed at the entry of the air inlet nozzle which is indicated in Figures 7.22 a and b.

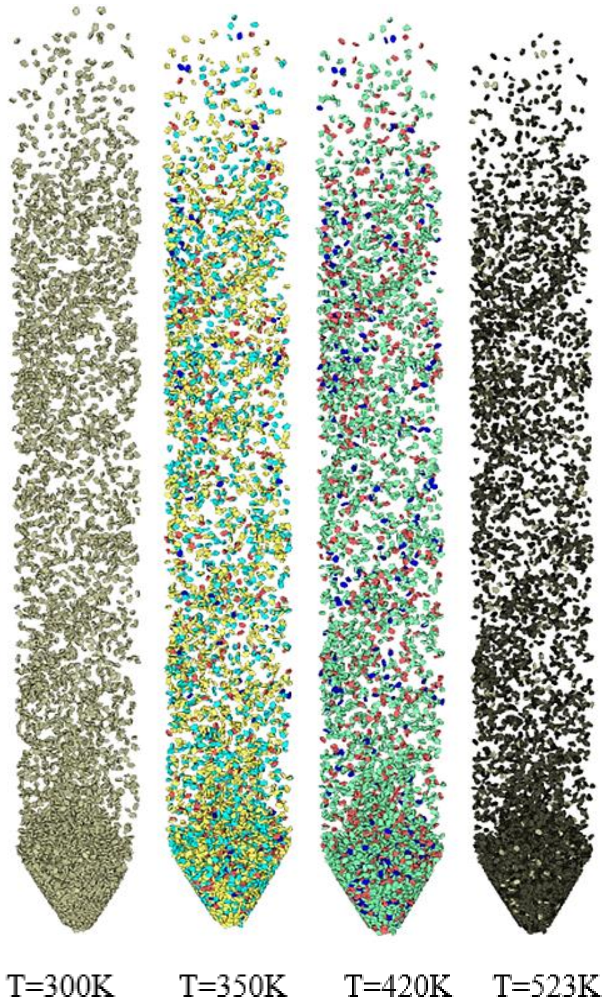

Figure 7.21: The Evolution of Coffee Beans Temperature at Velocity of 20 m/s

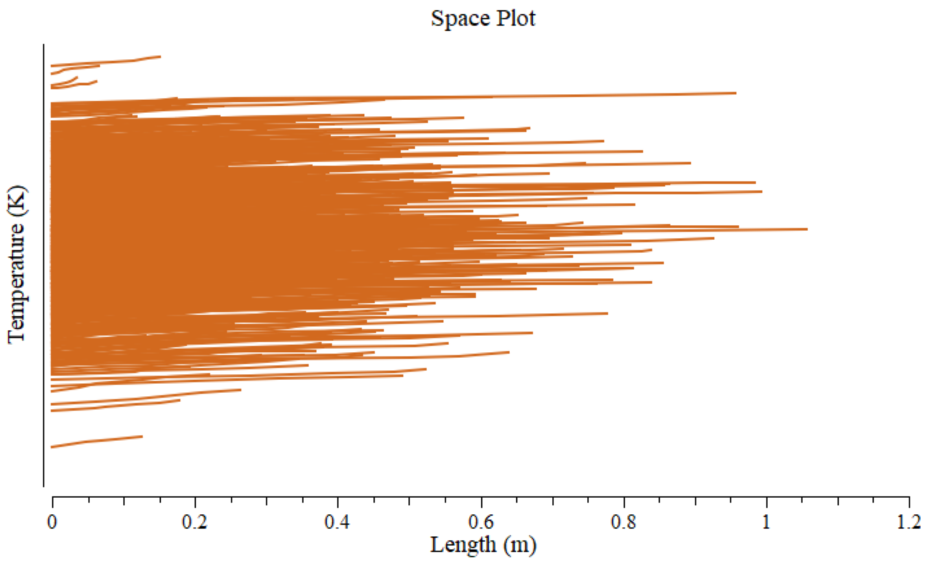

a)

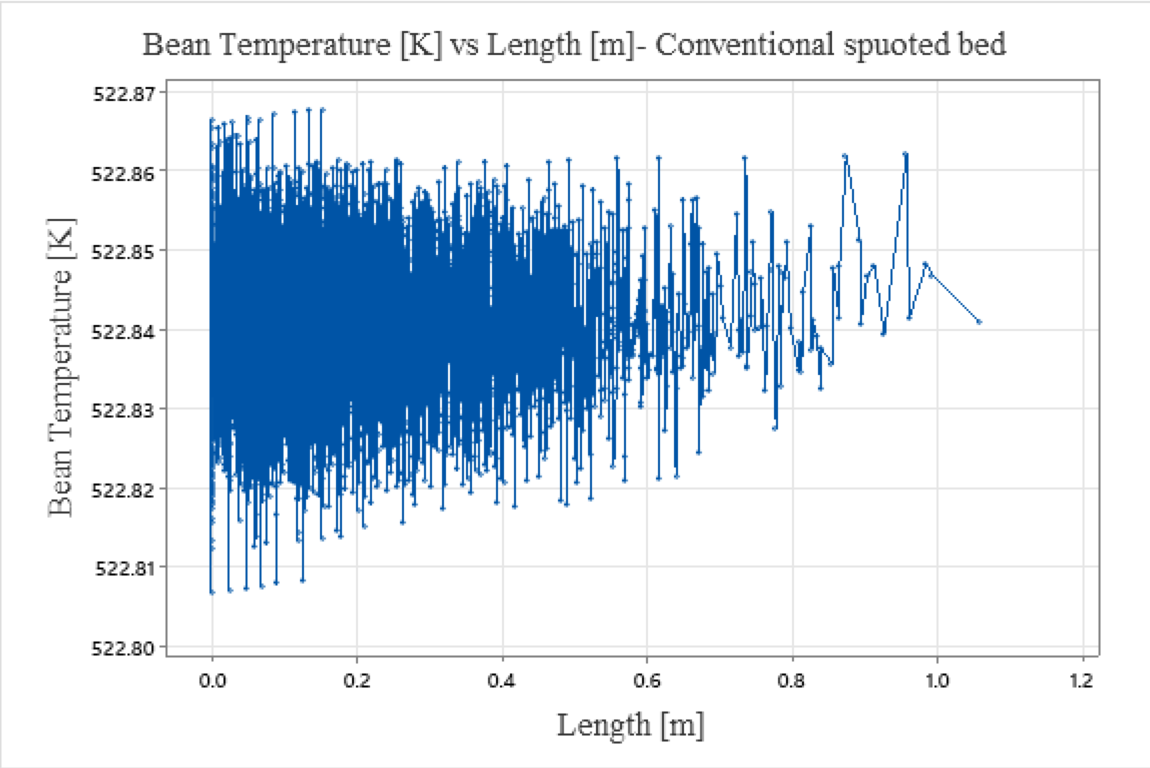

b)

Figure 7.22: Temperature Distribution of Coffee Bean on Space Plot and Axially

As hot air inlet temperature increases and the time elapsed the temperature of coffee bean increases as much as possible as the required degree of roasting. At a temperature up to 250 ℃, the dark roasting is achieved as the simulation in this run is done for this degree of roasting. The result of the simulation indicates that the coffee bean temperature T_b increases with the increment of air inlet temperature and time as illustrated in Figures 7.23 a) and b).

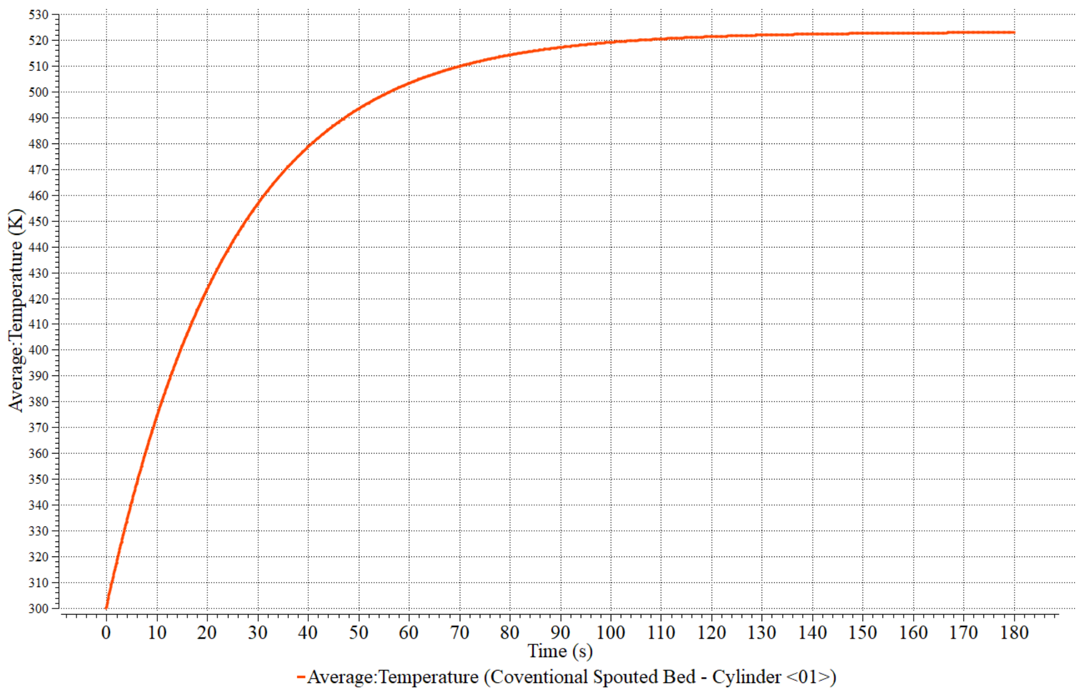

a)

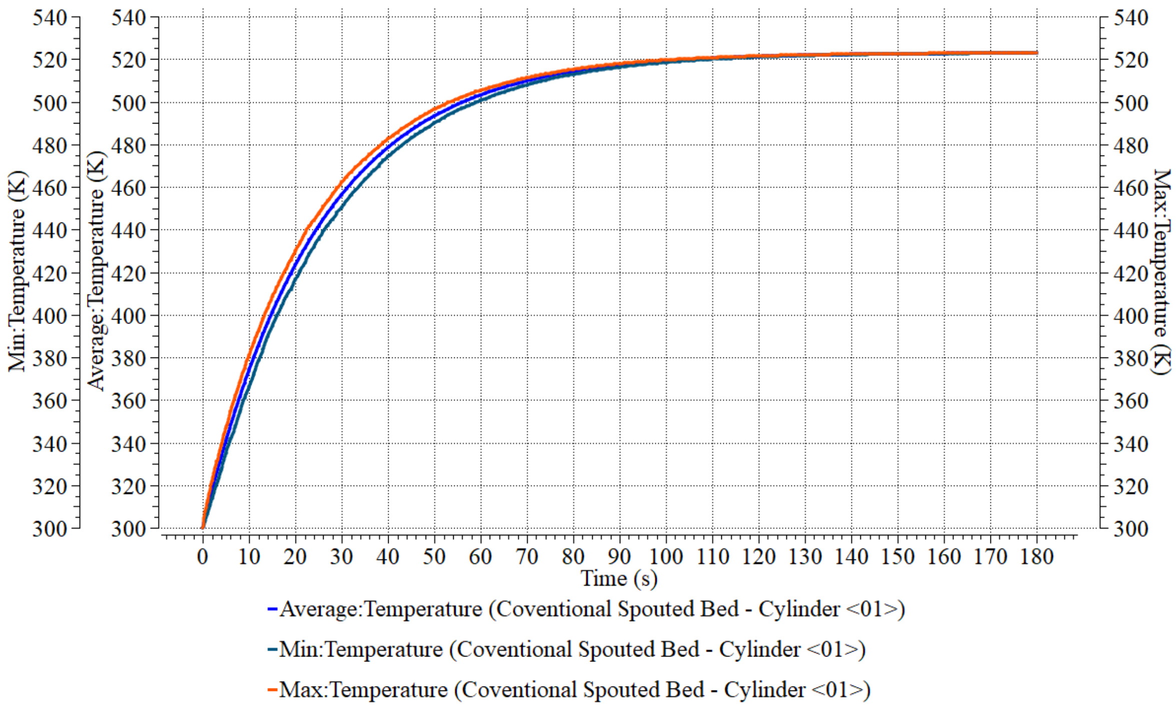

b)

Figure 7.23: Temperature of Coffee Beans Over the Time

7.7 CFD-DEM Ccoupling Result of Conical Spouted Bed with Internal Devices

7.7.1 Simulation Conditions

For all cases, mono-sized particles with a diameter of sieve size 6.42 mm are used at 27ºC as the initial solid phase in the conical spouted bed. A simulation is started with the generation of particles without any overlap in the bed, followed by a gravitational settling process where all the applicable inter-particle forces are considered. One kilogram, about 6030 sets of particle numbers from Rocky particle generation, is assumed to examine the effect and reason behind the effects of bed height on roasting that can be described by analyzing the temperature profile of particles with specified bed heights and geometry of the internal device, i.e. fountain confiner and draft tube which is shown in Figure 7.24.

The elevated temperature of hot air solves in fluent side exported from CFD Fluent to Rocky DEM as Fluent to Rocky (f2r) file. The fluid flow data is then imported through CFD Coupling-Fluent One-Way Steady-State. For instance, coffee bean particles commenced to agitated, as indicated in the snapshot of Figure 7.25 at 5m/s velocity injection.

7.7.2 Eulerian Statistics of Coffee Bean

The Eulerian Statistics of coffee bean, after particle generation in the domain of conical spouted bed, is mostly characterized by volume fraction and void fraction. The average void fraction or porosity of particles over the time of simulation runs is 0.936%, whereas the average volume fraction is about 0.064%, which is publicized in Figures 7.26 and 27.

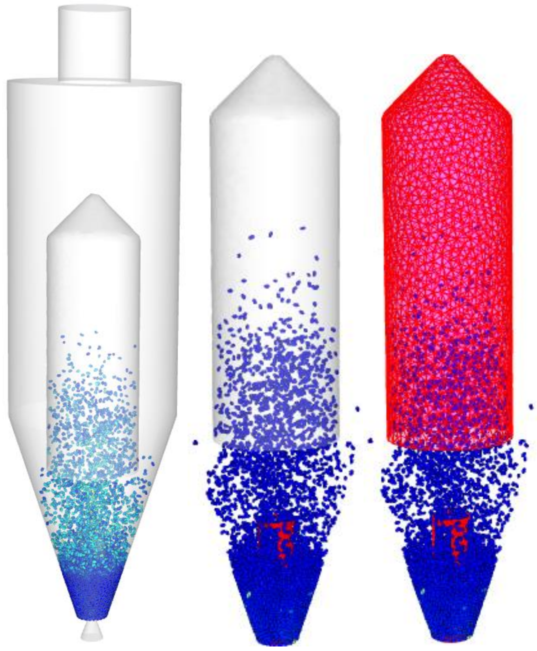

Figure 7.24: The Domain of Coffee Bean in CSB with Fountain Confiner and Draft Tube

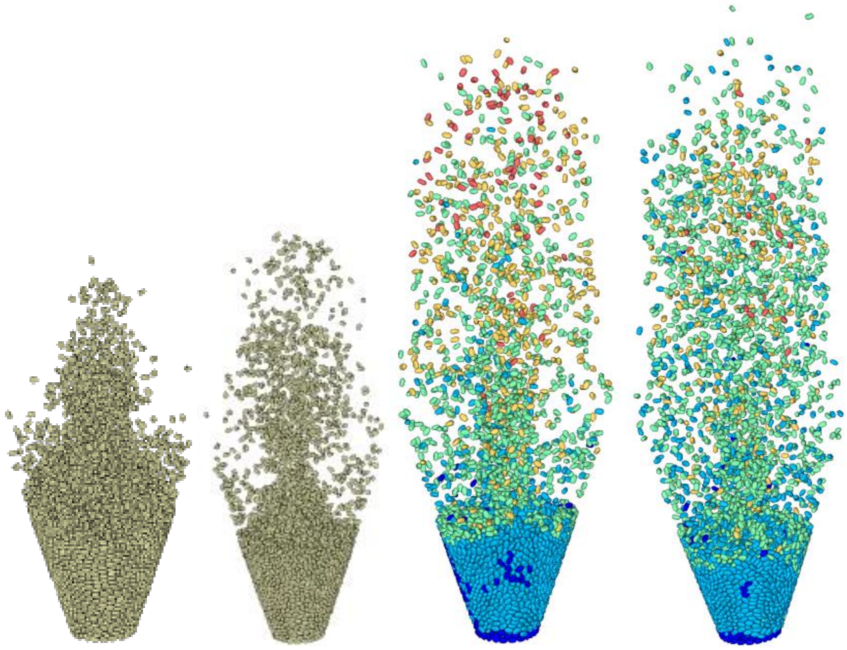

Figure 7.25: Snapshot of the Evolution of Coffee Bean at 5m/s Velocity Injected

7.7.3 Residence Time and Real-Time Simulation

Residence time is the total amount of time that a particle spends inside a defined region. It is really important in this application to guarantee that each particle spends enough time in the roasting region of the conical spouted bed. Hence, the residence time coffee bean roasting simulation takes about 165 sec inside the defined 3D domain as displayed in Figure 7.28.

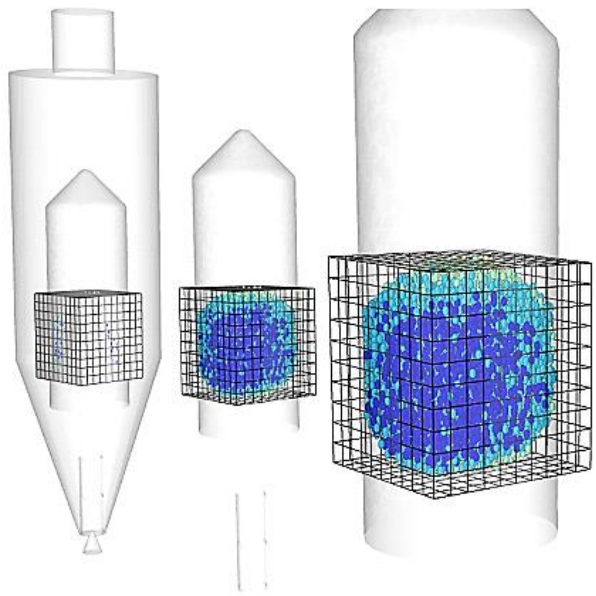

Figure 7.26: Eulerian Statistics of Coffee Bean in Conical Spouted Bed Domains

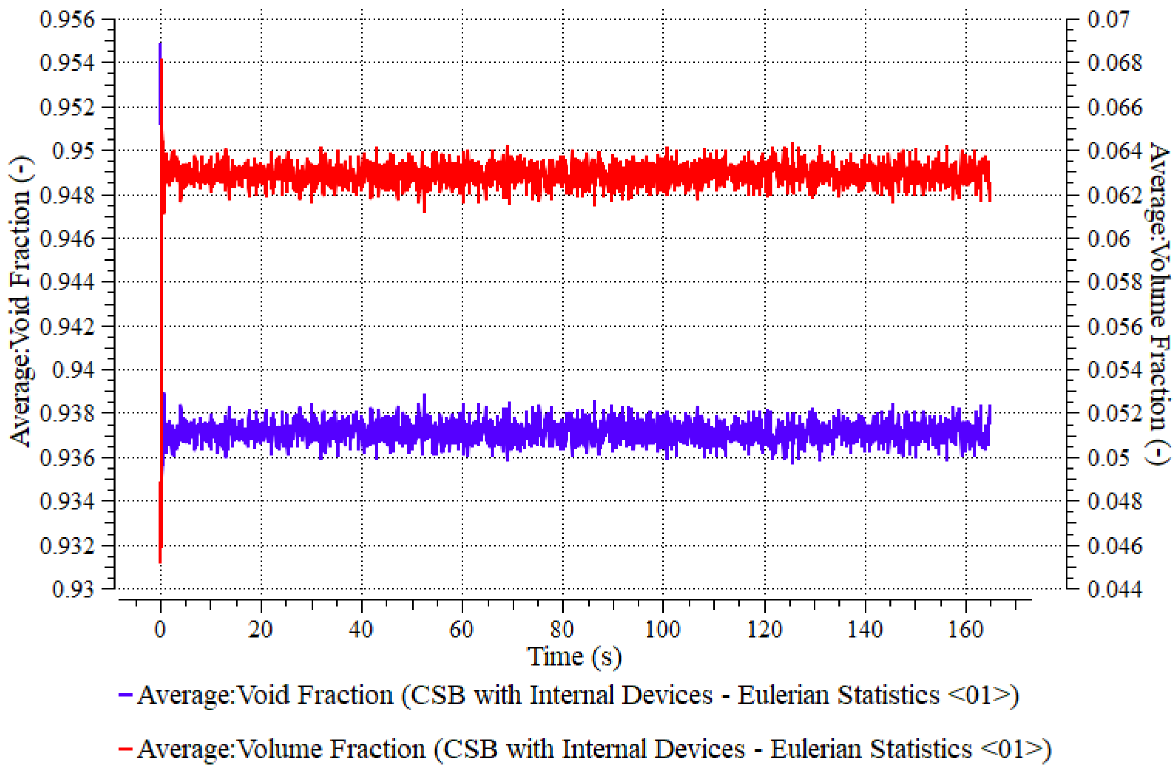

Figure 7.27: Volume and Void Fraction Coffee Beans Over Time

The roasting of coffee beans typically takes place at 200-240°C at different times depending on the desired characteristics of the final product. However, the conditions for optimum roasting of coffee beans for the best quality product were obtained at an air temperature of 250°C for a roasting time of 5 min, Nagaraju et al., 2016. Rocky DEM can run the model at the same rate as the actual physical system of coffee roasting for about 5 min and above. However, simulating the actual coffee roasting time can take several times with an ordinary *central processing unit* (*CPU*), a processor that affects computation time.

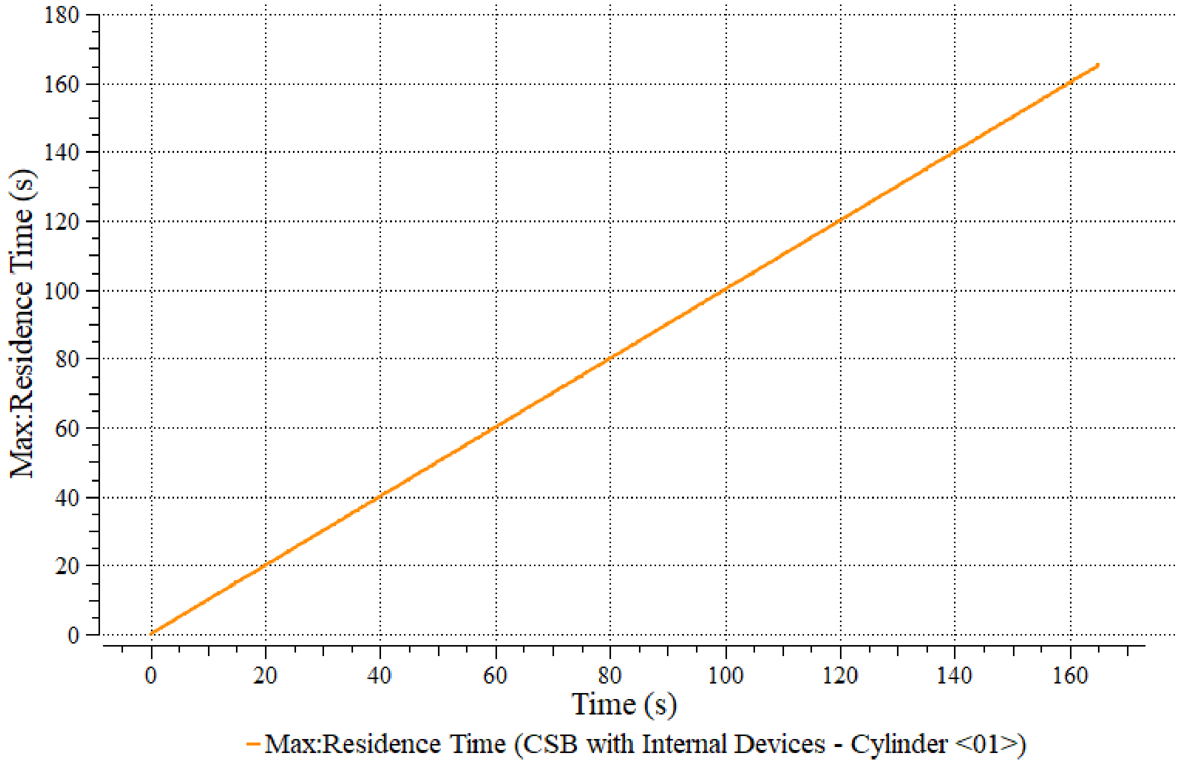

Figure 7.28: The Residence Time of Coffee Roasting

The total elapsed simulation time and simulation ETA are about 320,000 and 350,000 respectively as shown in Figure 7.29.

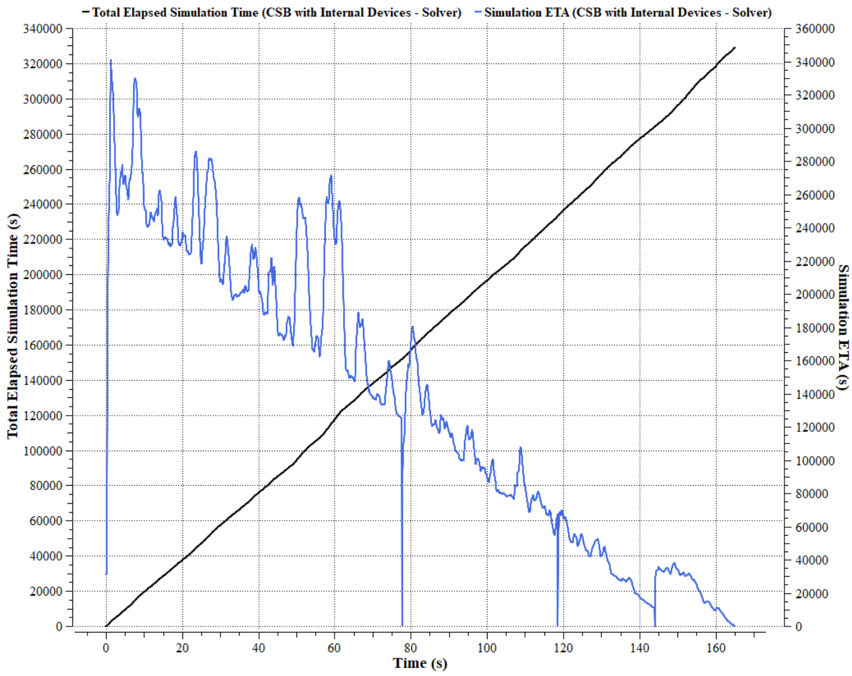

Figure 7.29: Total Elapsed Simulation Time and Simulation ETA

7.7.4 CFD-DEM Study of the Effects of Bed Geometry on the Roasting Coffee Bean

To achieve optimal design and control of a conical spouted bed for the roasting coffee bean, it is important to understand the fundamentals; governing flow, heat, and momentum transfer. On the other hand, roasting is closely related to the heating of the bed and particle temperature. Additionally, the heating of particles is influenced by heat transfer rate where heat transfer in such a bed is related to the gas-solid flow characteristics (Hou et al., 2012). The gas-solid flow characteristics in a conical spouted bed could be controlled by some external factors such as air velocity, inlet temperature material properties, and boundary conditions of the bed.

The design and investigation of the effects of bed geometries on roasting by laboratory or industrial experiment have lower feasibility though such properties should have an impact on roasting rate and quality. Therefore, the alternative numerical approach so-called CFD-DEM coupling could be applied initially, to reduce cost and maximize feasibility. The roasting model and the simulation conditions of coffee beans in a spouted bed based on the combined CFD-DEM has been developed and briefly described in Chapter 3 and 4. Here below, the effects of bed geometries such as bed height, draft tube height, and distance between the static bed and bottom end of confiner in a spouted bed using the developed CFD-DEM model are discussed.

As stated in the design of simulation of chapter four, the following simulation runs are done;

I. Keeping distance between the static bed and bottom end of the confiner to H_F =80mm and vary the height of the draft tube as discussed in chapter four.

II. Keeping distance between the static bed and the bottom end of the confiner to H_F =120mm and vary the height of the draft tube.

III. Keeping distance between the static bed and the bottom end of the confiner to H_F =0mm and vary the height of the draft without changing the height of the draft tube.

The static bed height of one kilogram of coffee bean is 0.20m which is the most significant geometric factor, that affects the stability of the bed similar to another geometric factor of conical spouted bed contactor. It can be observed that the minimum spouting velocity increases with increasing static bed height. The reason for this variation is attributed to increased static bed height due to increased resistance of bed material.

Among simulated runs, the best of all simulations Bed 2 and Bed 5 are selected by using the Temperature versus time (T-S) curve. The minimum spouting velocity required to start spouting for simulation in Bed 2 is greater than that of Bed 2, although, the average deviation of the T-S curve is about 5% as indicated in. Hence, by considering pumping and materials cost the simulation with Bed 2 is selected and used for detailed analysis of a modified conventional spouted bed which is a so-called conical spouted bed with fountain confiner and open-sided draft tube. The values of H_f, 0.12 m do not confine the fountain as much possible as required which leads to the lower residence time of coffee bean inside it and the higher distance higher beyond this, may not fully confine the fountain or may lead to instability when this distance is excessively long.

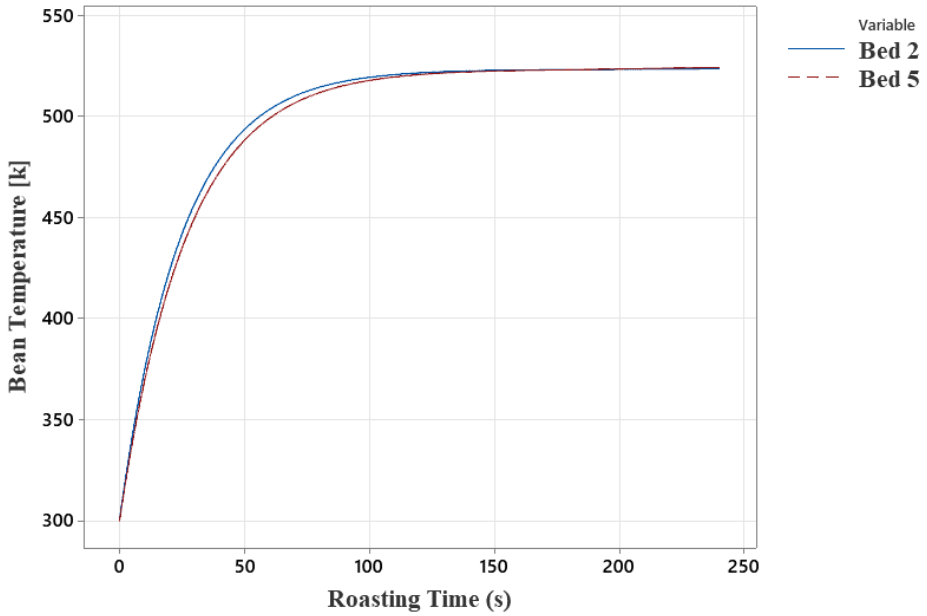

Figure 7.30: T-S Curve of Coffee Bean Particles with Different Bed Geometries

The insertion of a draft tube in a conical spouted bed overcomes the limitations of the spouted for improving gas-solid contact and reducing more resistance to the spout due to the heaviness of the coffee bean particle and for the requirement of higher power to lift the particles in the spouted bed. Since the geometry of open-sided draft tube within bed 2, 0.2 m longs which also selected for afterward analyses.

7.7.5 Dynamics of Coffee Bean Particles in CSB with Internal Devices

A coupled computational fluid dynamics (CFD)-discrete element method (DEM) technique has been adopted to examine the dynamic behavior of coffee bean particles in a conical spouted bed with the internal device and discussed here below in detail.

1. Absolute Translational Velocity

The average absolute translational velocity of coffee beans particle is 0.58 m/s which is indicated in Figures 7.31 a and 7.32 a.

2. Translational Y Velocity [m/s]

The average translational velocity of working particles 0.05 m/s is illustrated in Figures 7.31 b, and 7.32 b.

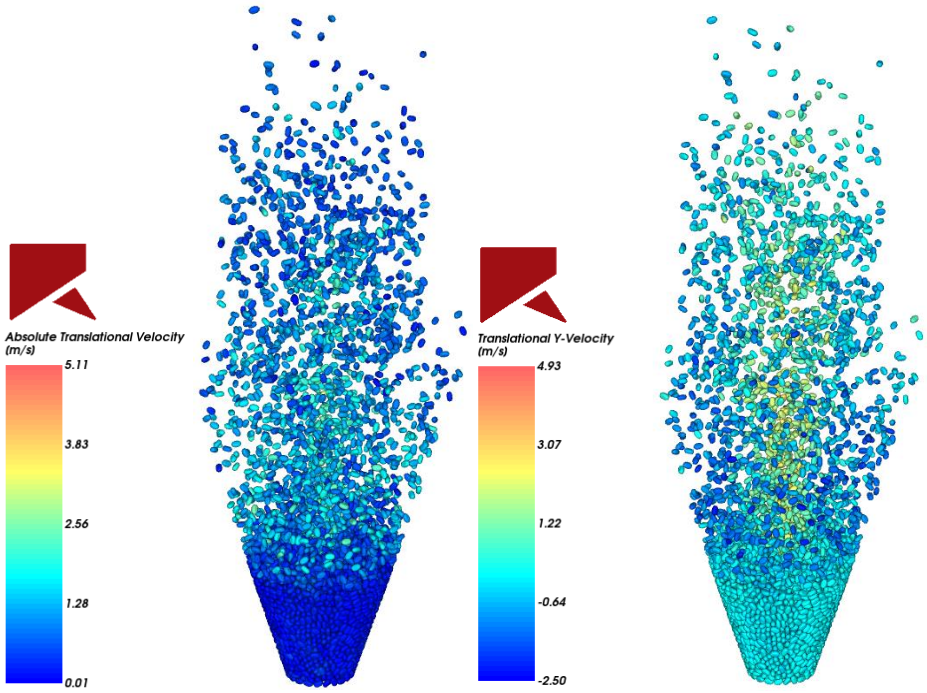

a) b)

Figure 7.31: The contour of Absolute Translational a) Translational Y-Velocity b)

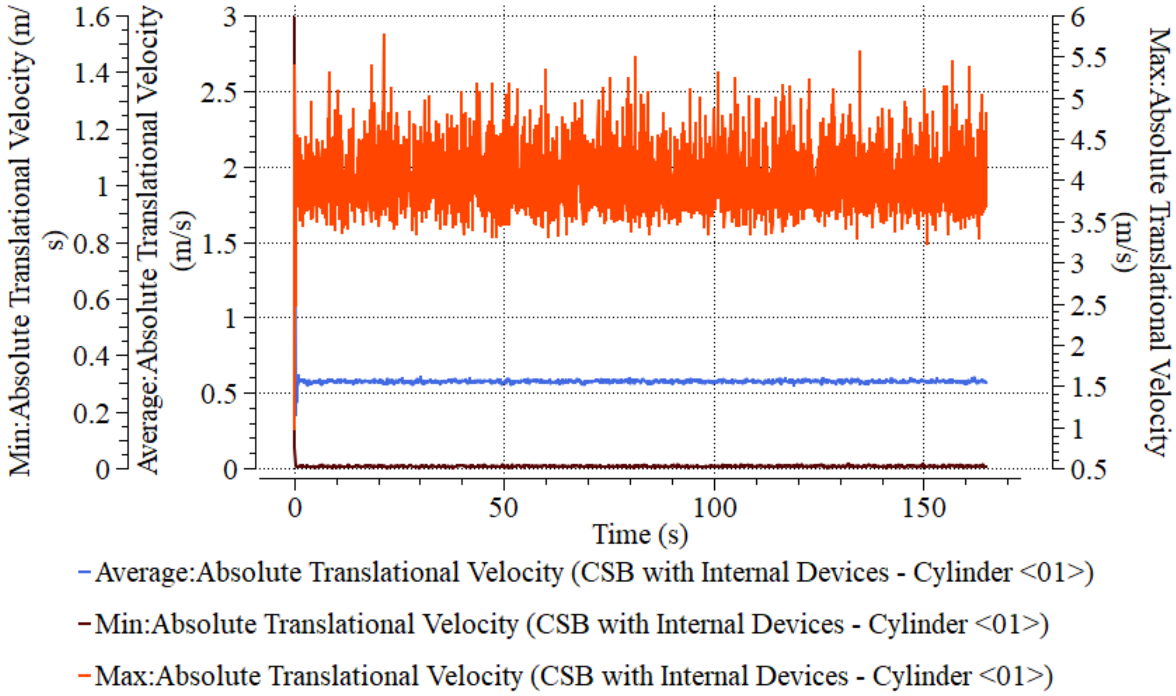

a)

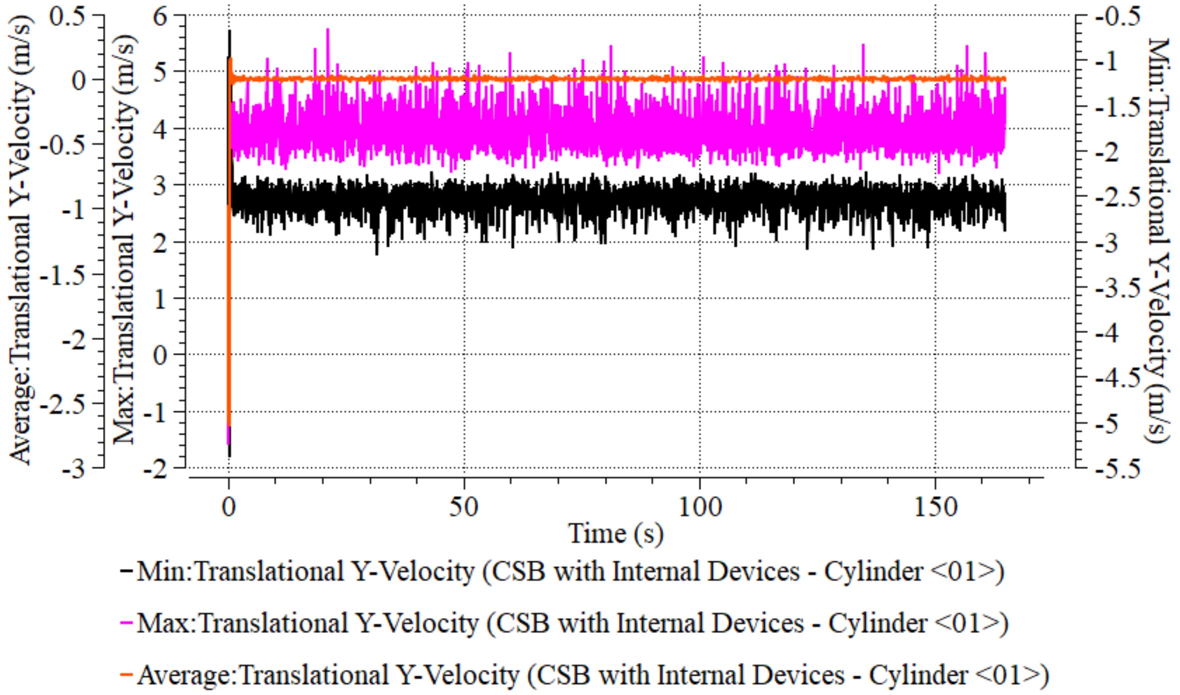

(b)

Figure 7.32: Absolute Translational Velocity a) Translational Y velocity b) Over Time

3. Absolute Rotational Velocity

As is indicated in Figure 7. 33 a is 125 Rad/s the absolute rotational velocity of an individual particle.

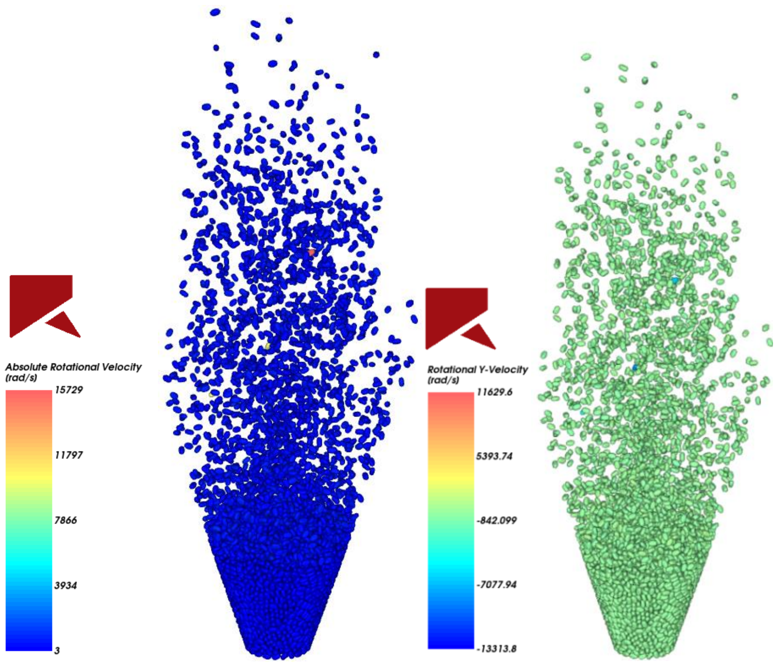

a) b)

Figure 7.33: The Contour of Absolute Rotational Velocity a) Rotational Y-Velocity b)

4. Rotational Y-Velocity

The average Y y-component of the rotational velocity vector of each particle is about 0.5rad/s Figure 7.33 b and 7.34 b.

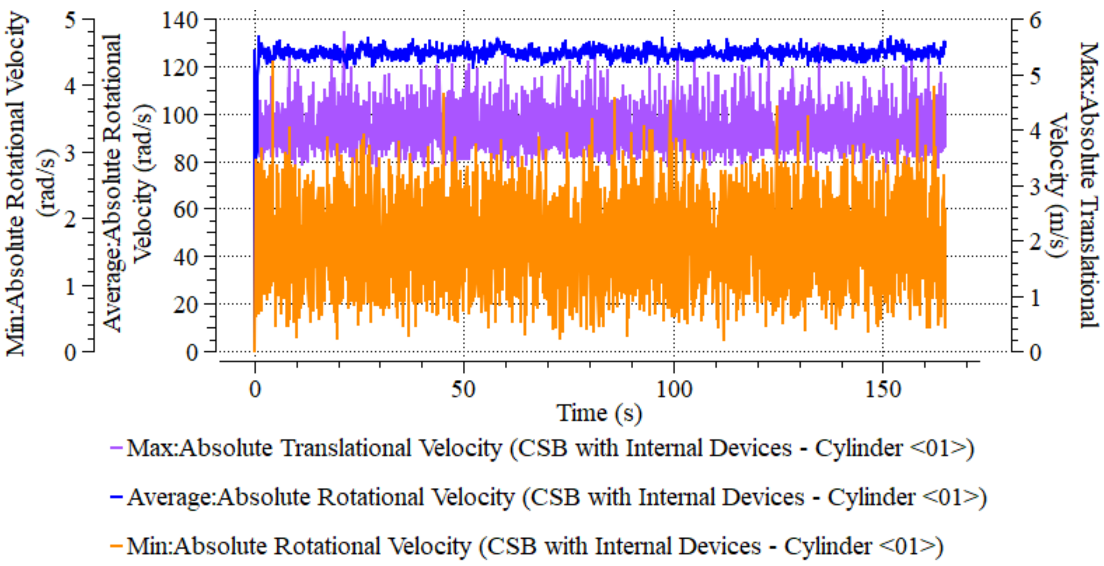

a)

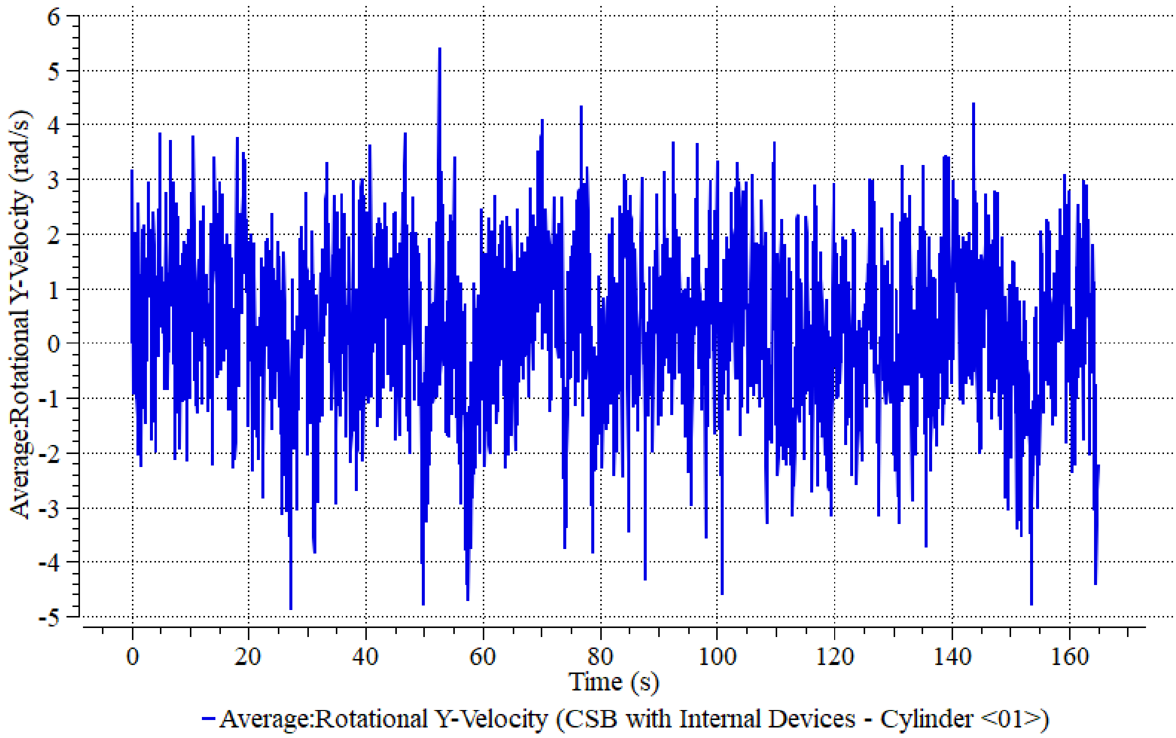

b)

Figure 7.34: The Contour of Absolute Rotational a) Rotational Y-Velocity b) Over Time

5. Particles Y Coordinates

The Rocky DEM is a transient 3D particle simulator in which particle is characterized by both space and time, as a result, the maximum y-coordinate can particle reach is 0.755 m as displayed in Figure 7.35 b.

6. Particles Trajectory

The Particles Trajectory is used to visualize the flow of particles over time by translating their paths into 3D curves. The number of particles picked is used to calculate trajectories out of certain particle strides which are illustrated in Figure 7.35 a at the different number of steps using a 3D curve.

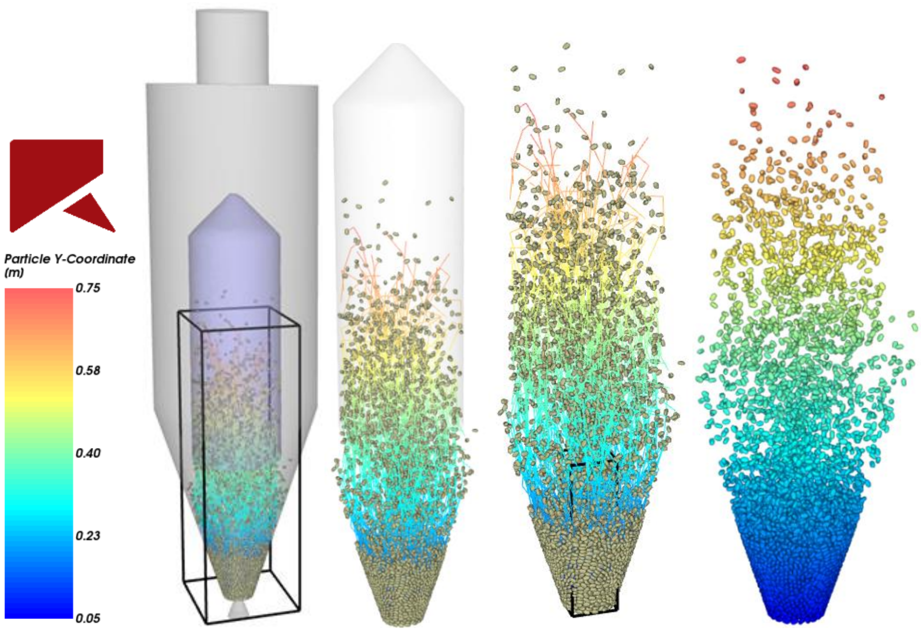

a)

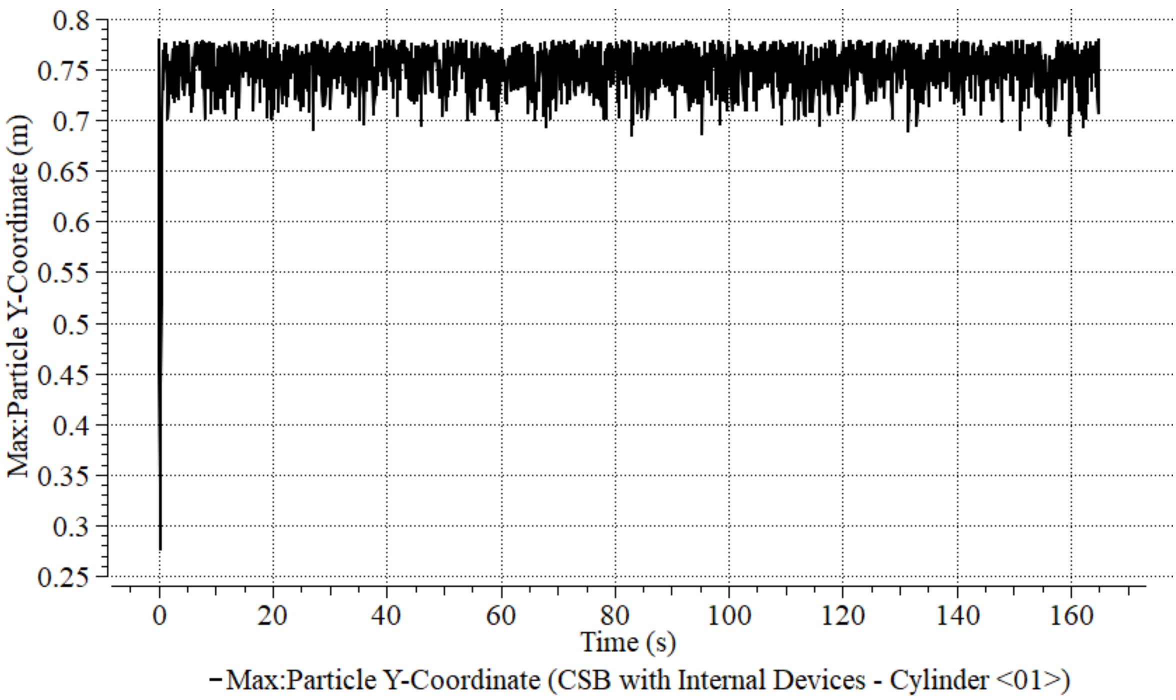

b)

Figure 7.35: Contour Maximum Y-Coordinates (a) and Particles Over Time

7.7.6 Temperature Coffee Bean in Conical Spouted Bed

In a conical spouted bed, the solid trajectory i.e., the fountain created at the top of the bed when spouting gas is high enough to open spouting thereby, the solid particle rained back on the bed as shown in Figures 7.36. a and b, but the hot fluid left the bed which is a direct pass heating. This, kind of phenomenon leads to poor gas-solid contact and reduces the cycle time of gas and through coffee bean particles.

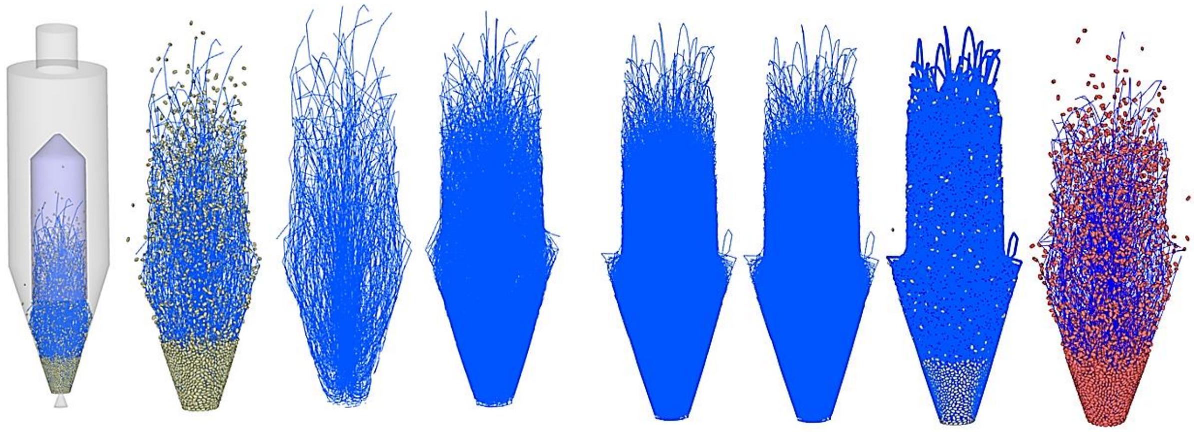

a) b)

Figure 7.36: Maximum Particle Trajectories within Selected Particle Stride

To overcome this limitation, a fountain confiner with the upper end closed is used to avoid air and solid leaving the device through its top section. Hence, the confiner forces the air to make a longer trajectory in which operation is possible at high values of the gas flow rate without direct loss of spouting gas in the bed and ensuring high solid circulation flow rates. Thus, it enhances the gas-solid contact, which significantly improves the efficiency of convective heat transfer in the contactor.

The variation in the particle temperature with different bed geometry of both the fountain confiner and the draft tube was simulated and the most efficient bed is selected as discussed above. In bed 2, particle temperature has reached a very high level over a certain duration of time than in the rest bed.

Higher particle temperature leads to a higher roasting rate. The temperature of air increases with time and the upper part of the bed exposes to a comparatively lower temperature than the lower part shown in Figure 7.38. a and b. Hence, with the increase of bed height, the average bed temperature will be low at the top of the bed however, the particles circulate over elevated temperature at the instant in a cyclic manner that creates dual hydrodynamics of conical spouted bed as indicated in Figure 7.37 a and b. A space plot of temperature distribution over the length of the bed is demonstrated.

The coffee bean temperature is considered to have a significant effect on the roasting rate which depends on fixed bed height (one kilogram of the coffee bean), the bed geometry with

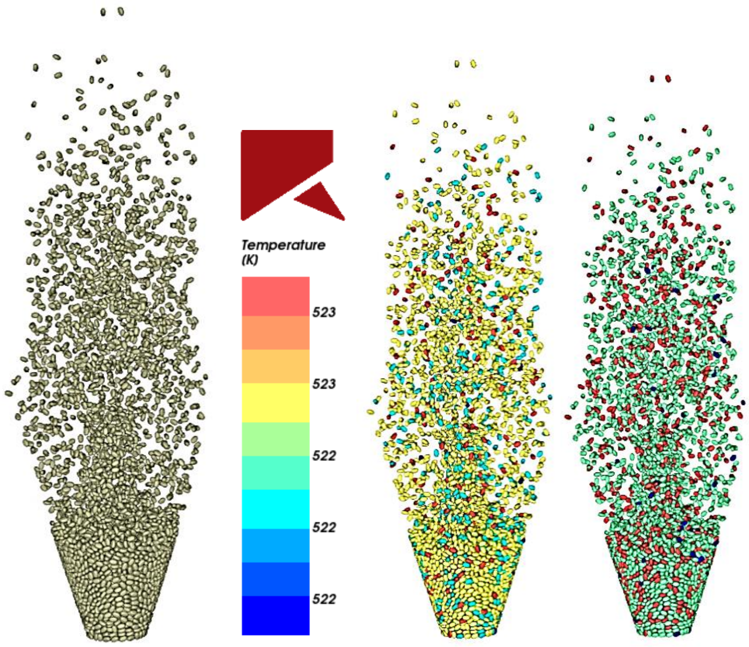

a)

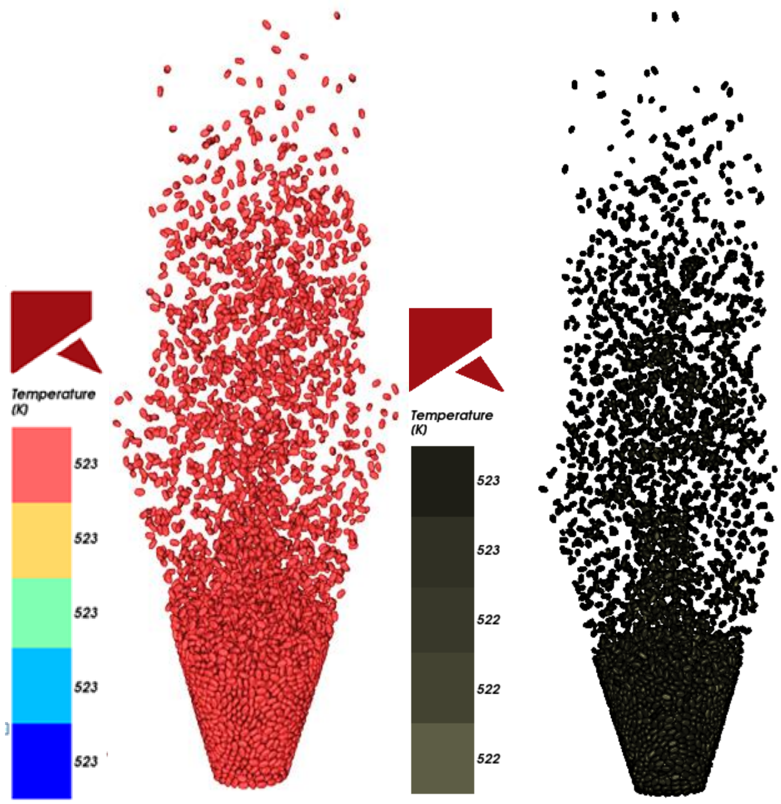

b)

Figure 7.37: The Contour of Temperature Distribution

a fountain confiner and an open-sided draft tube are highly influential for the bed temperature distribution, (Hemis et al., 2011). Likewise, for selected bed geometry the coffee bean temperate is gradual increases over time in which the trends of all curves were similar a good agreement of the real roasting time at which roasting temperature was achieved,

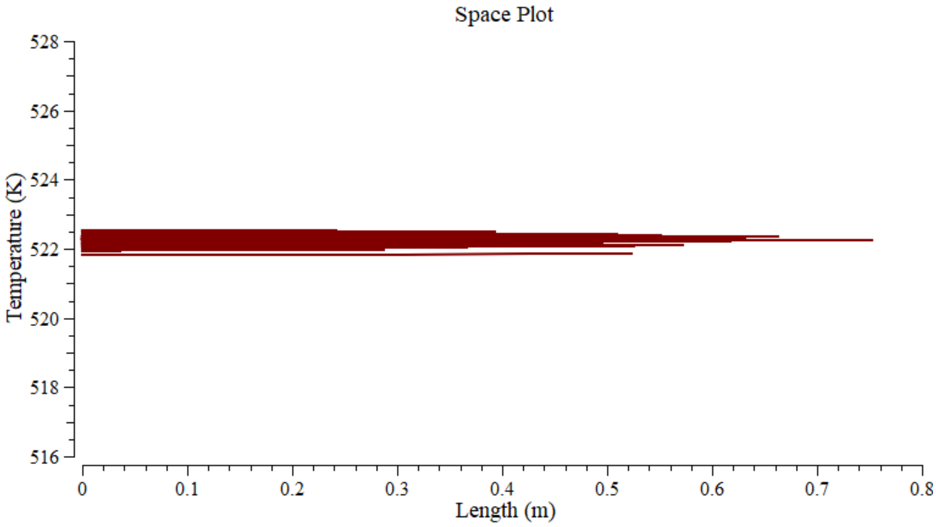

a)

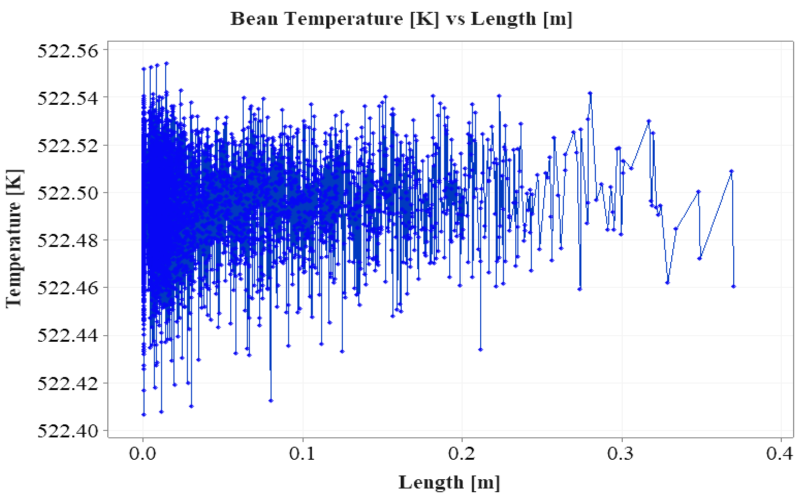

b)

Figure 7.38: Space Plot of Temperature Distribution Over a Length

which was approximately equal to 165s. Figures 7.39 a, b, and c indicate the coffee bean average, maximum and minimum, deviation, and variance of the temperature distribution curve.

7.7.7 The Average Bulk Density of Coffee Bean

The average bulk densities of coffee beans, which vary with roasting time, are shown in Figure 7.40. There is a significant decrease in bean density due to the increase in volume and other factors. The average density values, simulated for approximately 165 seconds of simulation time, agree with the bulk density of the 9-minute roast beans reported by Sivetz and Desrosier (1979) and by Clarke and Macrae (1987), respectively.

I. Turbulence Time of coffee beans Particles

Turbulence may be defined as the most general case of unsteady fluid motion allowed by the Navier-Stokes equations. It is irregular and disorderly, it causes rapid mixing of heat and momentum, it is rotational and three-dimensional, it occurs over a range of scales, and,

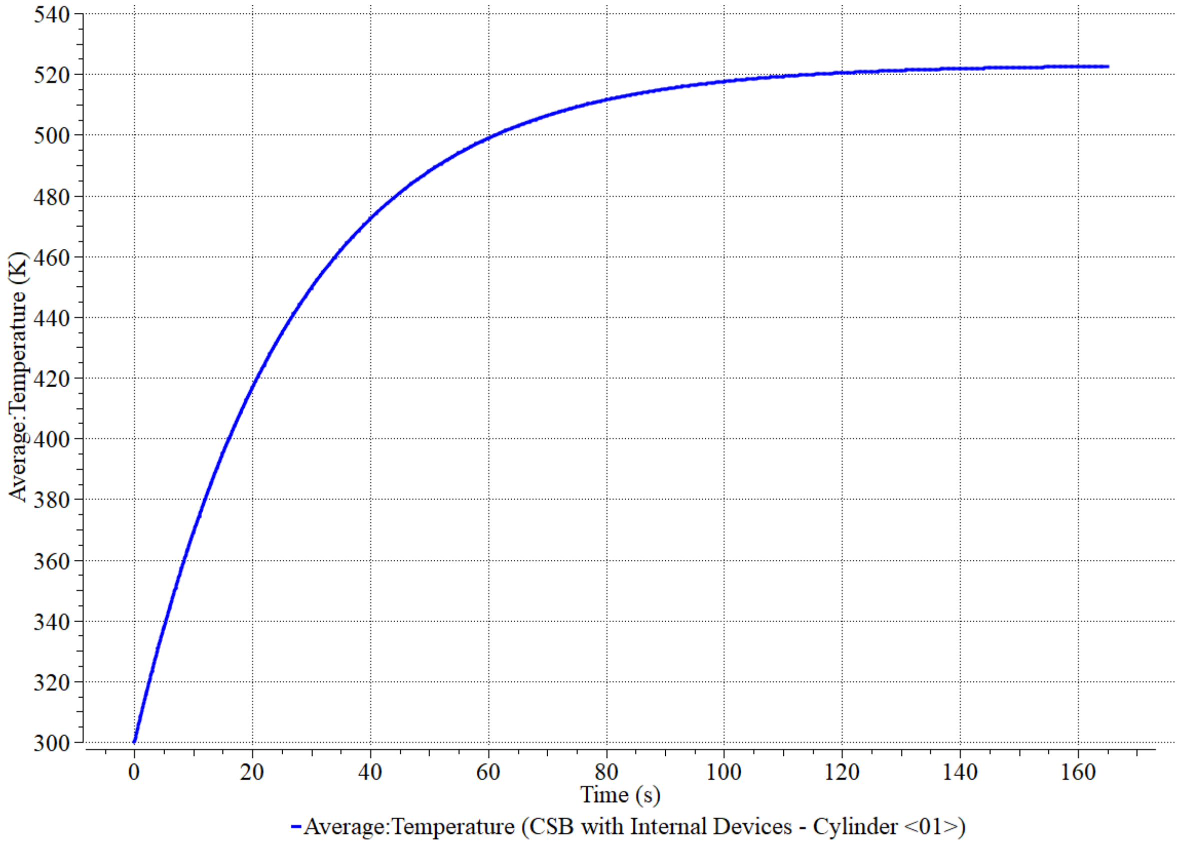

a)

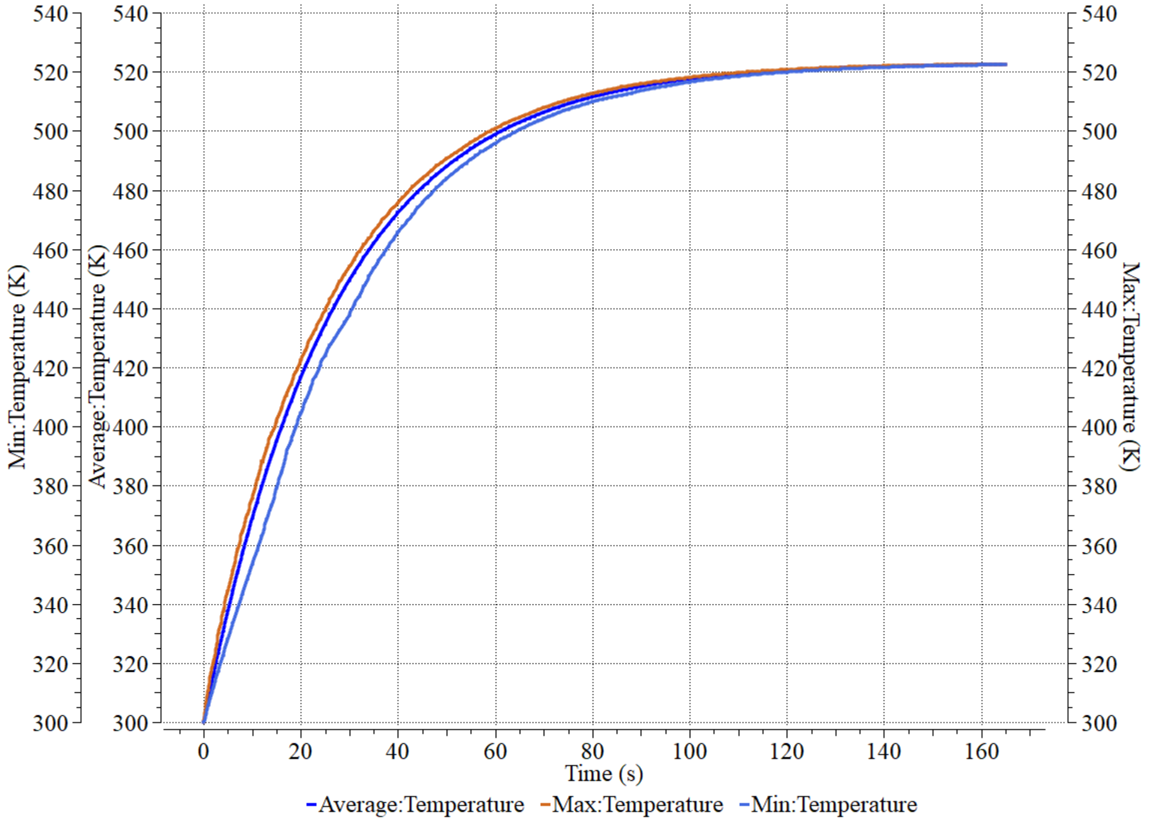

b)

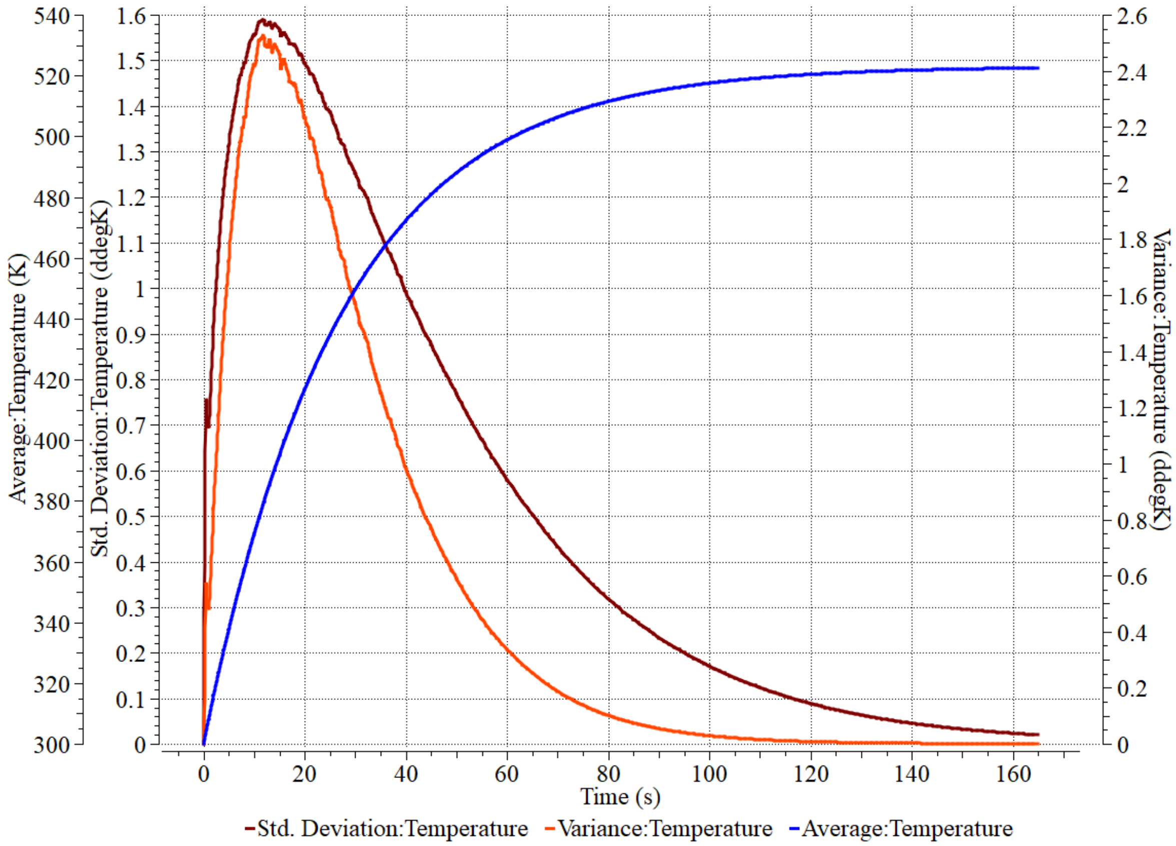

c)

Figure 7.39: Coffee Bean Temperature Distribution Over Time

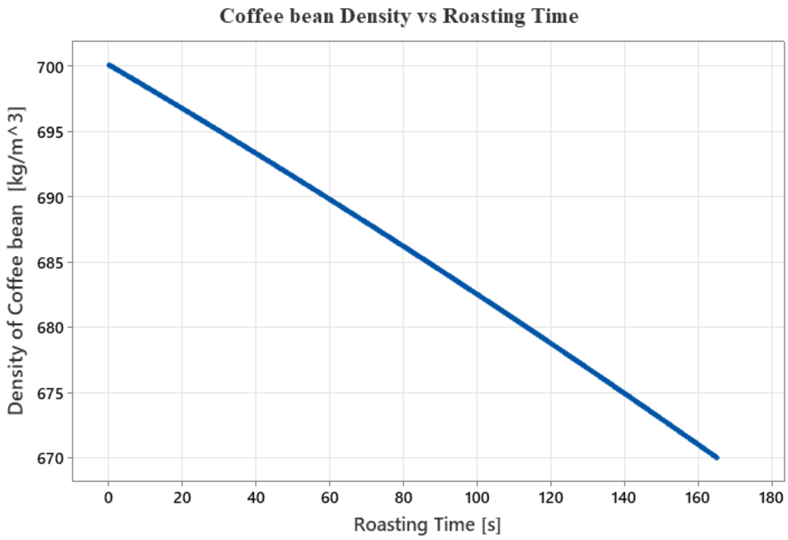

Figure 7.40 Bulk Density of Coffee Beans

it is dissipative. The turbulent effect of coffee beans in the domain of conical spouted bed contactor is displayed in the contour of Figure 7.41 a and the average magnitude is 0.05sec as illustrated in Figure 7.41 b.

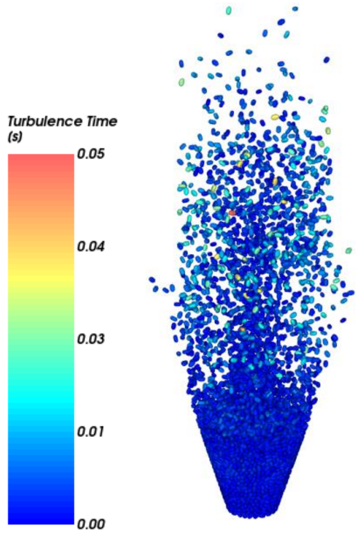

a)

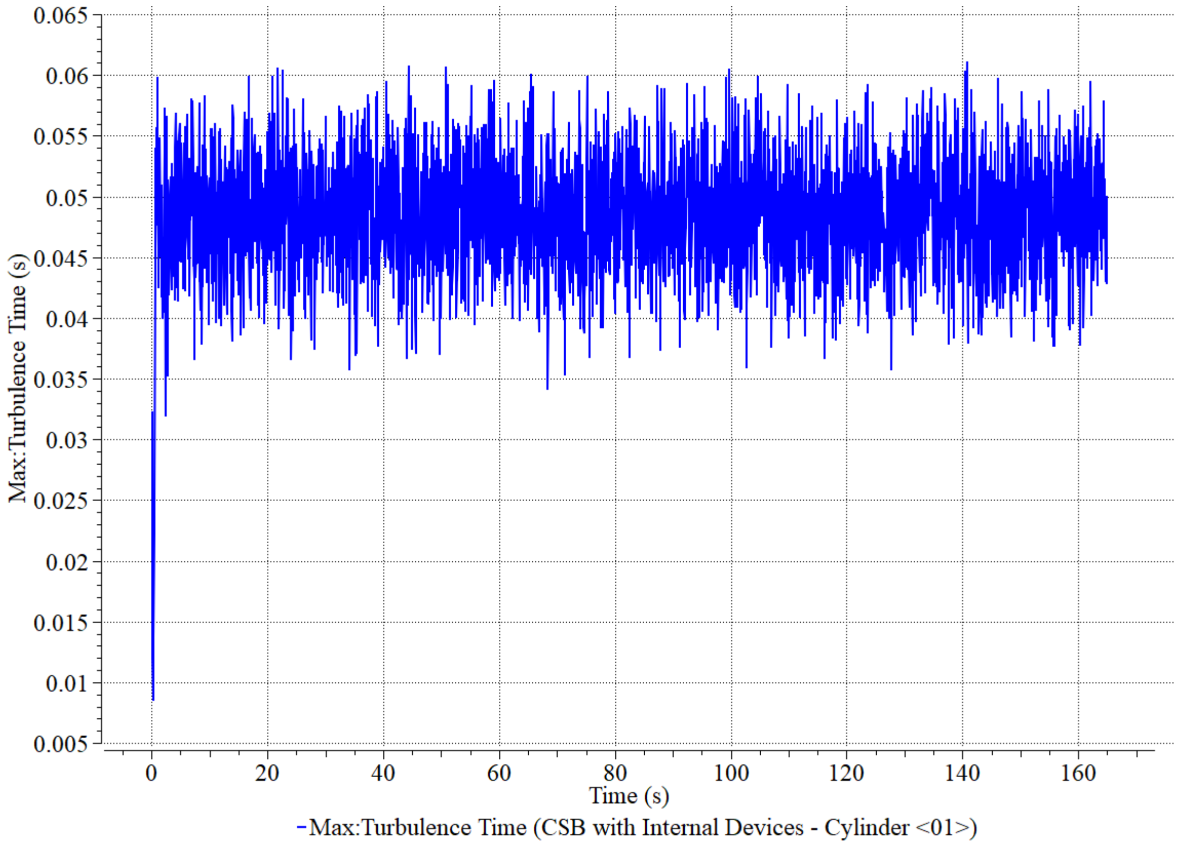

b)

Figure 7.41: Turbulence Time of Coffee Bean Particle

7.8 Particle Collision Statistics

The algorithm of operation of DEM programs assumes that particles are affected by two types of forces. One of them is mass forces (F_{body}), whose source is the mass of individual particles, included in the calculation model. The second type of force occurs on the surface of particles, at contact points, which develop as a result of inter-particle collisions. They are marked as surface forces ($F_{surface}$) which classified into normal and tangential forces. The normal forces determined based on the model of Walton and Braun linear spring hysteresis was used which describes an elastic collision with energy dissipation due to particle deformation. Whereas, the tangential forces that resulted from contact were determined using Coulomb's flexible model. In this case, the collision is treated completely elastically. Generally, collisions are central to any model that describes the dynamics of particulate materials. To allow users to gain insight into the statistical behavior of particle collisions, Rocky DEM can collect relevant collision data during a simulation. Then, this data can be processed and displayed in different ways for assisting in the analysis of the dynamic processes being simulated with Rocky. Dariusz et al., 2020.

Apart from, simulating particle thermo-hydrodynamics in a conical spouted bed with an internal device, the inter-particle collision among particles using a coupled CFD-DEM approach is also analyzed and discussed in detail.

7.8.1 Collision Frequency of coffee Bean Particles

The average collision frequency was recorded in different regions of the geometry of the coffee bean, during an output time step. It is the ratio of the total number of collisions registered at the given triangle that constructs 3D coffee beans geometry during the data collection time interval to the data collection time interval, which is the time lapse between two consecutive outputs. Figure 7.42.

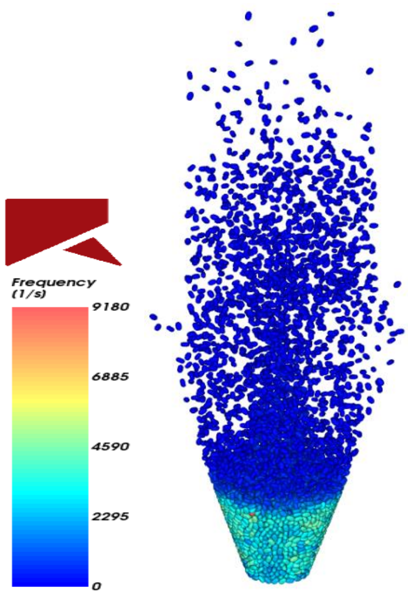

a)

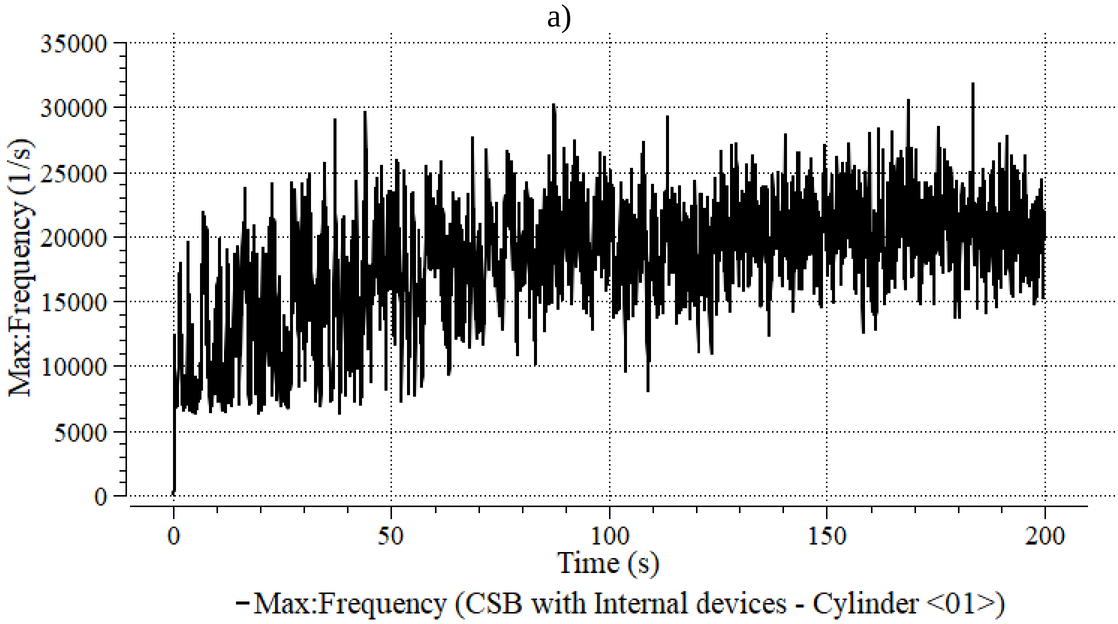

b)

Figure 7.42: The Contour of Frequency a) and Frequency Versus Time b)

1. Duration Kurtosis

Kurtosis is the value of the duration of the collisions recorded in different regions in geometry during an output time step. In another word, it is a measure of how tall and sharp the central peak of a statistical distribution is, in the simulation of coffee roasting and as given in Figure 7.43.

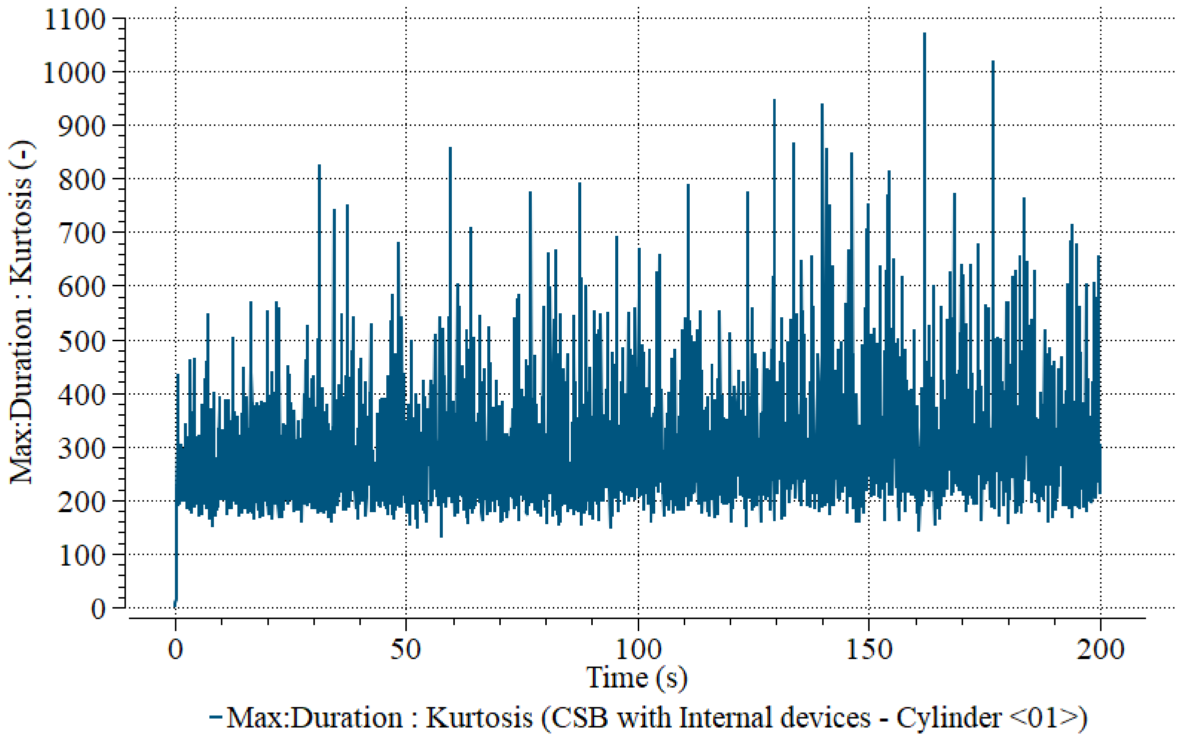

Figure 7.43: Coffee Beans Particle Contour of Kurtosis Duration

2. Duration Mean

The mean value of the duration of the collision's statistics recorded in different regions of the geometry, during an output time step, is exhibited in Figure 7.44.

7.8.2 Mean Normal Force

The average normal force acting between particles of coffee beans after time is 0.06 N, as manifested in Figure 7.45 a. In addition, as it is observed in the space plot of Figure 7.45b, the position where maximum inter particle normal force happens is the bottom end of the bed.

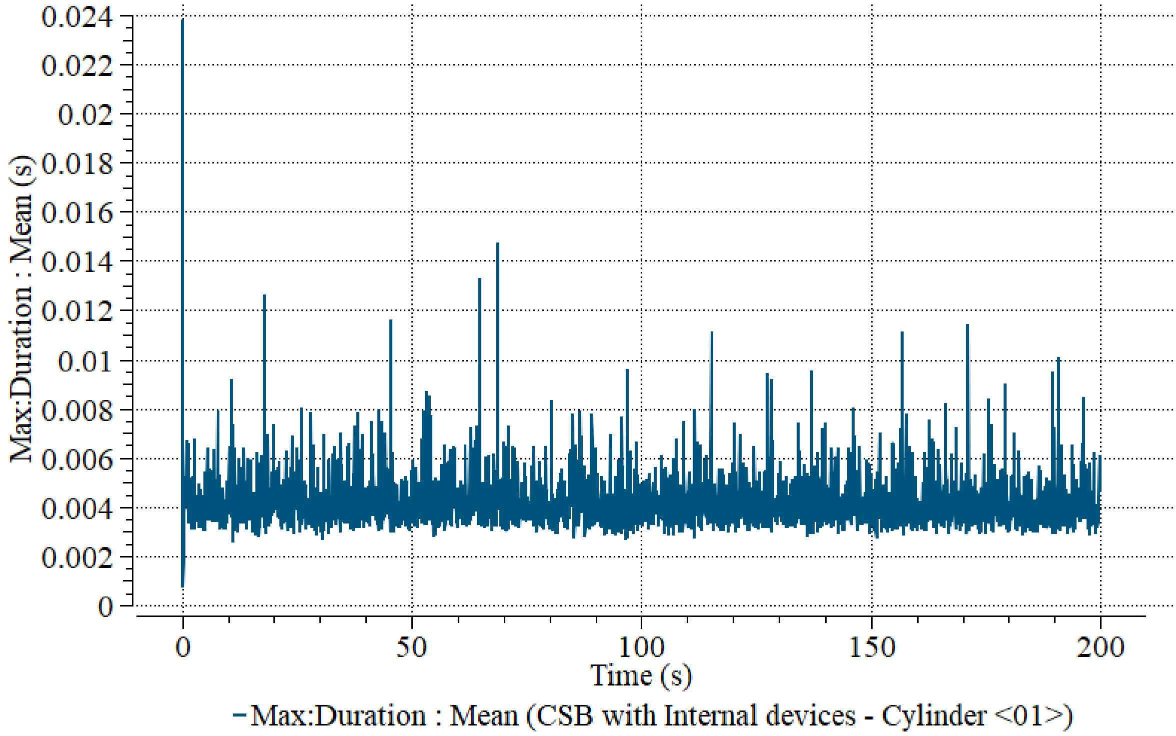

Figure 7.44: Mean Duration of Coffee Beans Particle

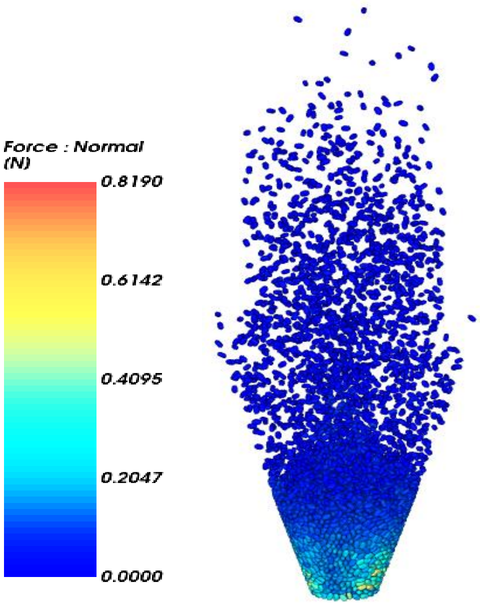

a)

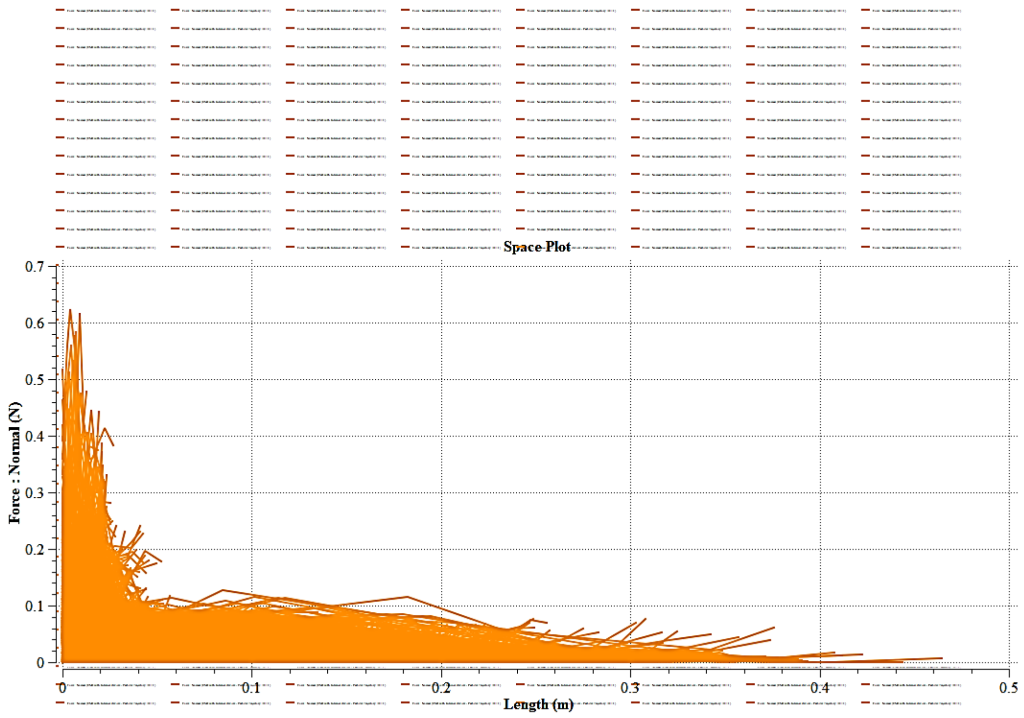

b)

Figure 7.45: Contour a) and Space Plot of Mean Normal Forces b)

7.8.3 Mean Tangential Force

The mean tangential forces acting on coffee bean particles were 1.4 mN as plotted in Figure 7.46 a. And also contour and space plot of tangential force are displayed in Figure 7.46 b.

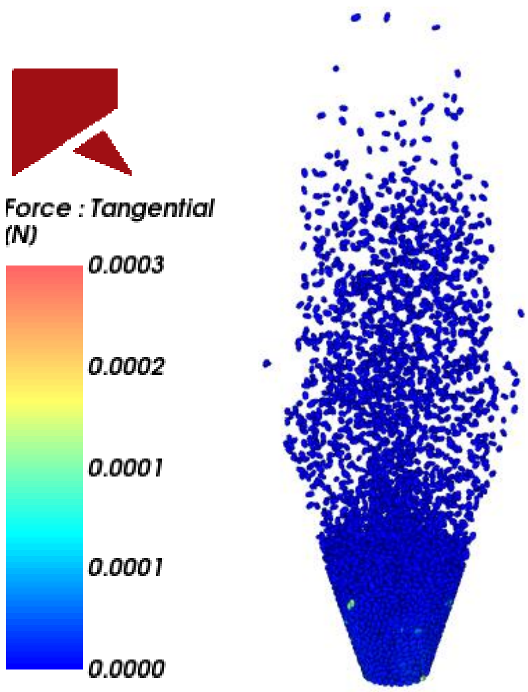

a)

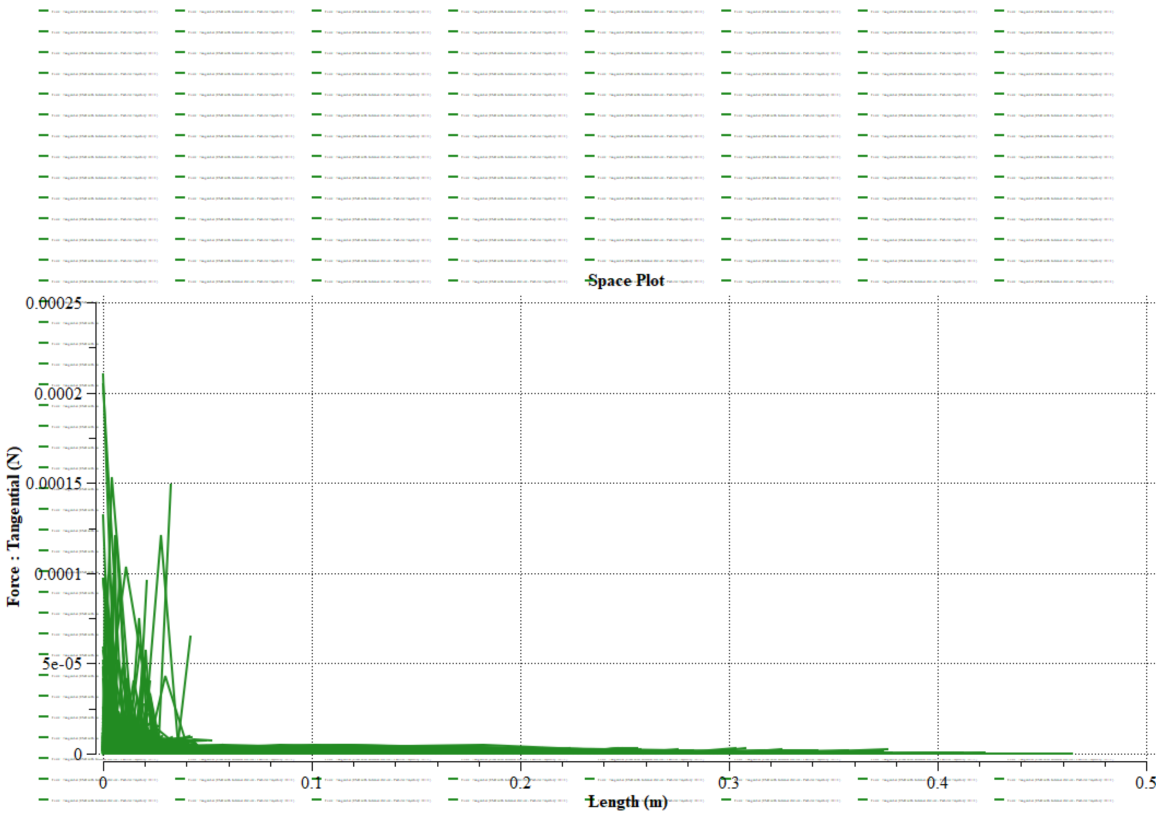

b)

Figure 7.46: Contour a) and Space Plot of Mean Tangential Forces b)

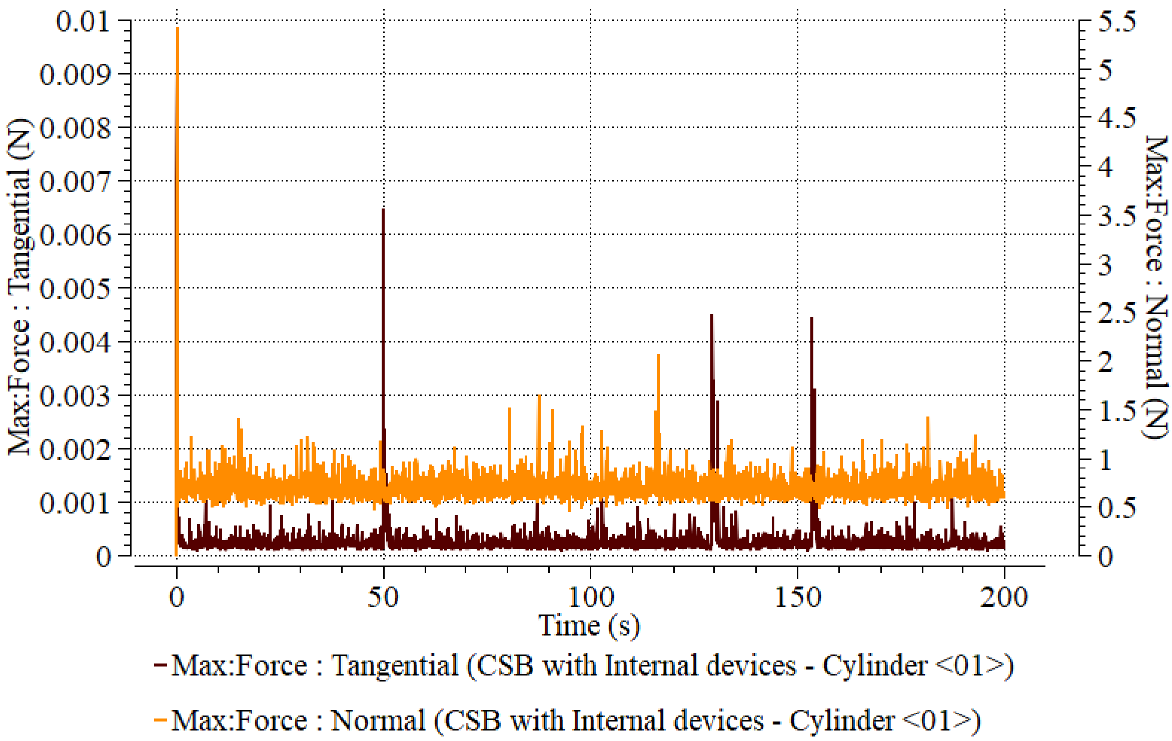

Figure 7.47: The Comparison Plot of Mean Tangential and Normal Forces

7.9 Experimental Results

The quality parameter like bean temperature is one of the most determinant variables in roasting which is the dependence of mass, hot airspeed, and roasting time. As indicated in Figure 7.48 a and c the light roasts are heated in a temperature range of 180-200℃ and are lighter in color, mostly light brown. This level of roast is used when the preservation of flavor and aroma of the coffee beans is needed. They are drier with no oil on their surface. This is due to the short time of about 4-5 minutes period they are roasted in the first run of this study.

a) b)

c) d)

Figure 7.48: a) Light b) Medium Roasted Coffee Bean

On the other hand, the medium roasts as shown in Figures 7.48 b and d are achieved by heating the coffee beans between 180 and 220 ℃ to retain the aroma and flavor of coffee beans up to an extent. They are roasted for about 5-7 minutes and become dry and lack oil on their surface.

7.9.1 Design of Experiment

Taguchi's which is one of the Designs of Experiment (DOE) applications are used to analyze the effect of multitudinous parameters and their comportment by performing a minimum number of experimentations and observing their effect on a specific behavior. It can conjointly determine the optimum condition for the experiment to give a better result. As stated by Taguchi it has three major phases and is planning, conducting, and analysis. The optimized parameters are determined by the Signal to Noise ratio (Krishnaiah & Shahabudeen, 2012). In this process, two parameters such as airspeed and mass of coffee beans were considered. In Taguchi's DOE concept, the preference for an orthogonal array depends on the total degrees of freedom of the process parameters. The experimental design of process parameters and numerical analysis is done by the Minitab 20 statistical software with two factors and three levels of the experiment.

A three-level two-factor (3^2) full factorial design was used as the experimental design (Table 7.3). The independent variables (factors or inputs) were airspeed and mass of coffee beans whereas roasting temperature and roasting time is the dependent variable.

7.9.2 Optimization of Roasting parameters

The main purpose of this work is to optimize the roasting parameters of an improved conical spouted bed coffee roaster using the Taguchi L9 orthogonal array method. Each experiment was conducted three times and values are averaged to avoid errors and airspeed was recorded from the experiment for further analysis.

Table 7.2: Roasting parameters and Checked at Levels

Roasting parameters	Level 1	Level 2	Level 3
A -Speed (m/s)	1.5	2	2.5
B-Mass coffee (kg)	0.125	0.25	0.5

Table 7.2 shows two input parameters checked at 3 levels. The larger the better criteria are suitable for bean temperature as it must be maximized. In the present study, Minitab software is used and Table 7.3 shows the actual measured responses during coffee roasting.

Table 7.3: Test Data Summary for Responses

Speed (m/s) A	Mass (kg) B	Bean Temperature (K)						Time (minutes)				
		T1	T2	T3	T4	T5	Av. T	t1	t2	t3	t4	t5
1.5	0.125	90.2	100.12	114.9	204.44	217.5	145.4	1.50	3.0	4.5	6.00	8.0
1.5	0.25	100.2	125.4	133	204	220	156.5	1.50	3.0	4.5	6.00	8.0
1.5	0.5	95.4	115.2	125.7	175	208	143.9	1.50	3.0	4.5	6.00	8.0
2	0.125	85.4	100.3	115.4	150.2	224.2	135.1	1.50	3.0	4.5	6.00	8.0
2	0.25	85	110	116	189	200	140	1.50	3.0	4.5	6.00	8.0
2	0.5	80.7	100.4	110	161.1	210	132.4	1.50	3.0	4.5	6.00	8.0
2.5	0.125	83.5	100.2	114.8	178.3	228	140.9	1.50	3.0	4.5	6.00	8.0
2.5	0.25	80	100	105	175	205	133	1.50	3.0	4.5	6.00	8.0
2.5	0.5	96	89	100	160	214	131.8	1.50	3.0	4.5	6.00	8.0

7.9.3 Analysis of S/N ratios

S/N ratio is defined as the signal to noise ratio which is the log functions of desired output and considers both the average and variation into account which can also be the amount of energy for the intended function divided by the amount of energy wasted. Win et al.,2005.

Table 7.4: Response table for Signal to Noise Ratios Smaller is Better

Level	Mass (A)	Speed(B)
1	42.95	43.43
2	43.10	42.66
3	42.67	42.62
Delta	0.43	0.82
Rank	2	1

From response Table 7.4 and the main effect plot for the signal to noise (S/N) ratios the speed has the greatest effect (as Delta = 0.82, Rank = 1). Whereas, the mass ranks second (Delta = 0.43, Rank = 2). The optimal parameter combination on larger is the better for roasting quality is A2B1 are the possible parameter combinations for increasing the quality of coffee beans. S/N ratio plots are plotted for the bean temperature variables. The optimal value is the one with the highest value of mean SNR. These plots have been shown in Figure

7.49. It has been found that 0.25kg of mass and 1.5m/s of speed, showed the maximum S/N ratio.

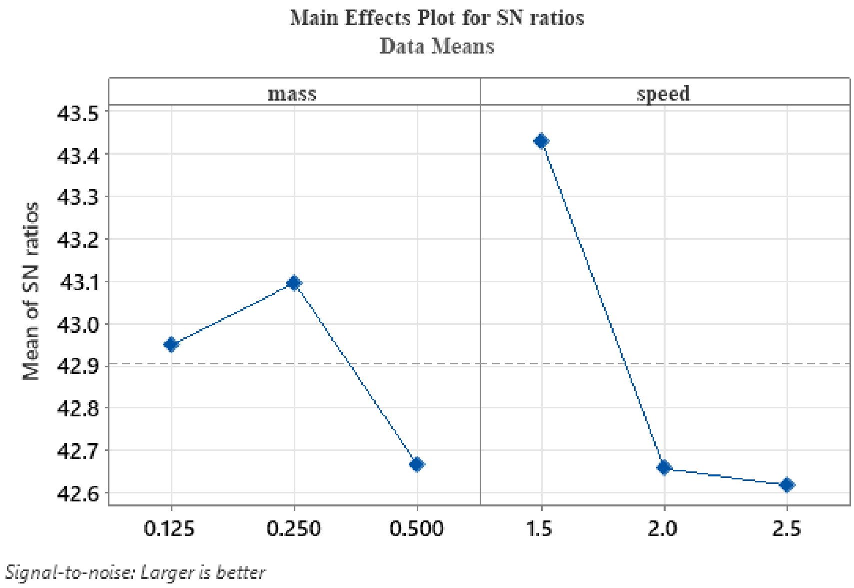

Figure 7. 49: Main Effects Plot for S/N ratios of Bean Temperatures

7.9.4 Response Table for Mean

Response table of mean is used to show which factors have the largest impact on the response and which level of the factor is related to higher or lower response characteristic values as given in Table 7.5.

Table 7.5: Table a Response Table for Mean Effects Plot for Larger is Better

Level	Mass (A)	Speed(B)
1	140.5	148.6
2	143.2	135.8
3	136.0	135.3
Delta	7.1	13.4
Rank	2	1

From the Table above the speed of hot air (A) has the highest value so it is ranked first and the mass of coffee (B) is ranked second. At these cutting parameters level (A2B1) selected for roasting coffee beans i.e., will be taken as a possible parameter combination for larger is better values. The control factor's main effect plot for means of roasting parameters value variations is shown in Figure 7.50.

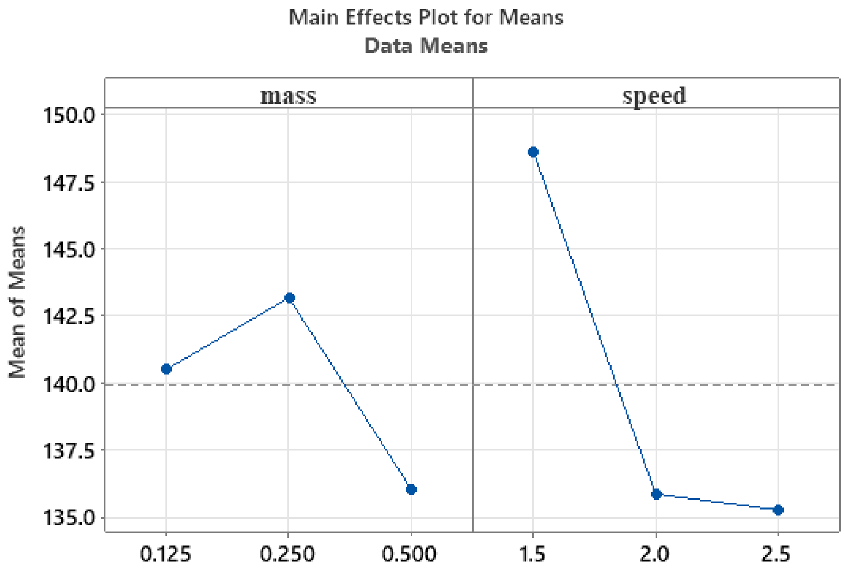

Figure 7.50: Main Effect of Plot for Mean

7.9.5 Analysis of Variance

ANOVA is the statistical technique used to find the influence of all control parameters. The P-value (probability of significance) is calculated from F-value and if it is less than 0.05 (for a 95% confidence level) then it can be concluded that the model is significant in the selected response. In the analysis of variance, the speed accounts for the largest percentage contributions of about 60.90%, while the mass has the next percentage contributions of about 36.45% on the performance of the roasting machine as indicated in Table 7.6.

Table 7.6: Analysis of Variance (ANOVA) for Roasting Parameters

Source	DF	SS	MSS	F-Value	P-Value	%Contribution	Significance (α=0.05)
Speed	2	1100.37	550.19	27.43	0.005	36.45%	Significant
Mass	2	1838.58	919.29	45.83	0.002	60.90%	Highly Significant
Error	4	80.24	20.06			2.66%	
Total	8	3019.20				100.00%	

7.9.6 Confirmation Test

The optimal process parameters obtained from the experimental result are verified by the predicted result. The optimum combination of parameters obtained from Table 7.6 was (A1B2) at 1.5 m/s airspeed and 0.250 kg mass.

Table 7.7: Optimum and Predicted Values Roasting Parameters

Response	Optimal parameter	Predicted value		Experimental value	
Bean Temperature	B2A1	Mean	SNR	Mean	SNR
		154.876	43.63	156.5	42.767

From Table 7.7 the result between the experimental value and the predicted value is very small. The values predicted by using the Taguchi approach are approximately near to the value which is experimentally obtained. This verifies that the experimental results of bean temperature are strongly correlated with the predicted results as also indicated in Figure 7.51.

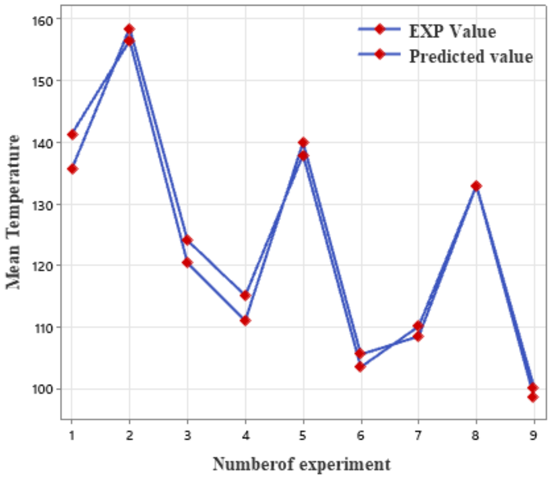

Figure 7.51: Experimental and The Predicted Value

7.10 Comparison between the Conventional and Modified CSBWD Model

7.10.1 Verifications and Validations

The results obtained from improved CSB coffee roasters guarantee, while verified by existing data available in the literature and obtained from conventional spouted bed coffee roasters as discussed in detail here below. On other hand, the values predicted by using the numerical method are approximately near to the values which are experimentally obtained which is valid. For instance, the experimental results of bean temperature are strongly correlated with the predicted results.

The variation in the particle temperature with conventional spouted bed and conical spouted bed with internal device for the air temperature of 250℃ is described in Figure 7.52. In the conical spouted bed, particle temperature has reached a very high level (more than 500 K), while in the conventional spouted bed, particle temperatures are found to be lower (around 470 K). Therefore, higher particle temperature leads to a faster roasting rate that assures modified spouted bed is the most efficient roasting device.

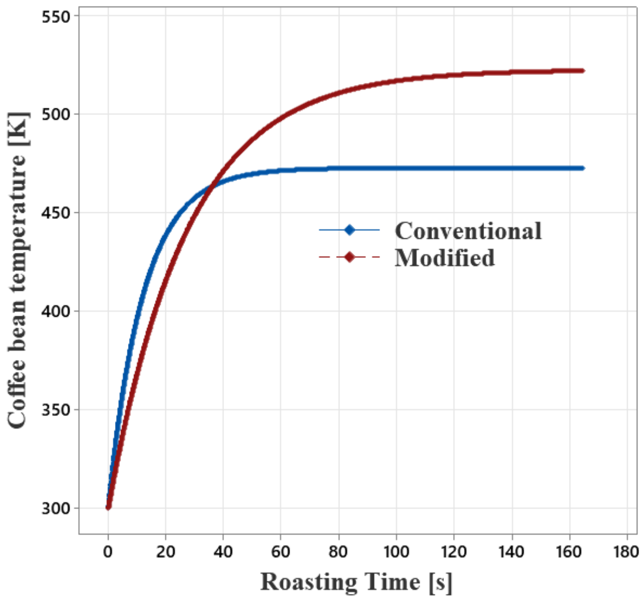

Figure 7.52: Particle temperature profile with conventional and modified SB at 250℃.

The instantaneous inlet air temperature results in an increase in the temperature distribution of the coffee bean particles through the spouted bed. The heat convection-conduction rate of heat transfer depends on flow variations around the coffee beans were calculated through the Nusselt number, Nu, a measure of convection heat transfer at the surface. Results of Nu were plotted against the Reynolds number, Re, which characterizes the airflow regime for both conventional and modified spouted beds, presented in Figure 7.53 a and b for conventional and modified spouted bed respectively.

Figure 7.55 shows the estimated heat transfer coefficients for coffee beans using a conventional spouted bed (existing) which was found to be 31 W/m^2℃. The values were in good agreement with the reported values Nagaraju *et al.,* (1997) reported a heat transfer coefficient ranging between 10 W/m^2K and 22 W/m^2K for roasting in a spouted bed roaster and air temperature range of 190 to 250℃ for similar food grains. Where Basile & Kikic (2009) found a value of 26.7 W/m^2K.

The Re number varied for describing heat transfer in presence of the coffee beans as observed in Figure 7.54 a. The plot indicates that heat transfer increases as the Re number increases for both conventional and modified spouted bed. However, the heat transfer coefficient for coffee beans using the conical spouted bed with the internal device is estimated to be about 77.5 W/m^2K which is valid according to values of roasted coffee beans with different heat transfer coefficient ranges between 14 W/m^2K and 75 W/m^2K (Eggers & Pietsch, 2001).

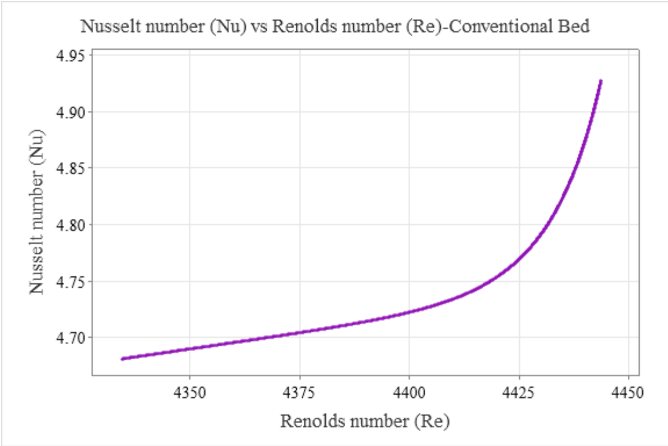

a)

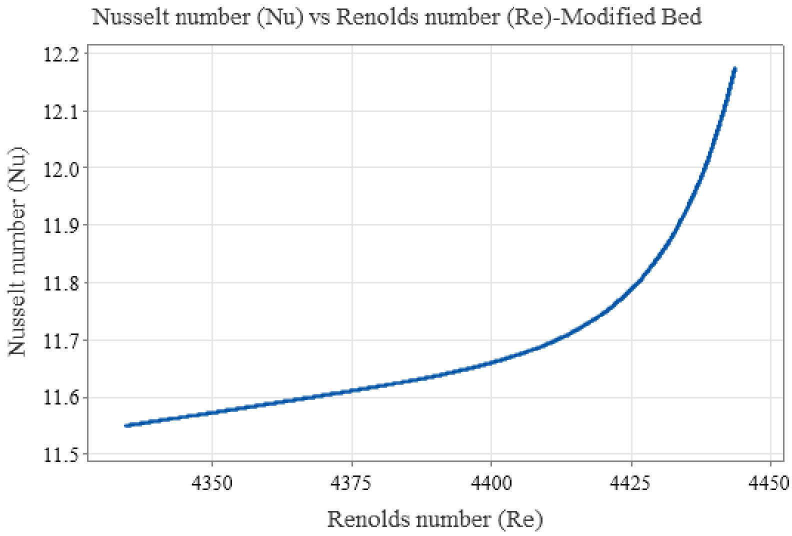

b)

Figure 7.53: Re vs Nu Number, for Conventional a) and Modified Spouted Bed b)

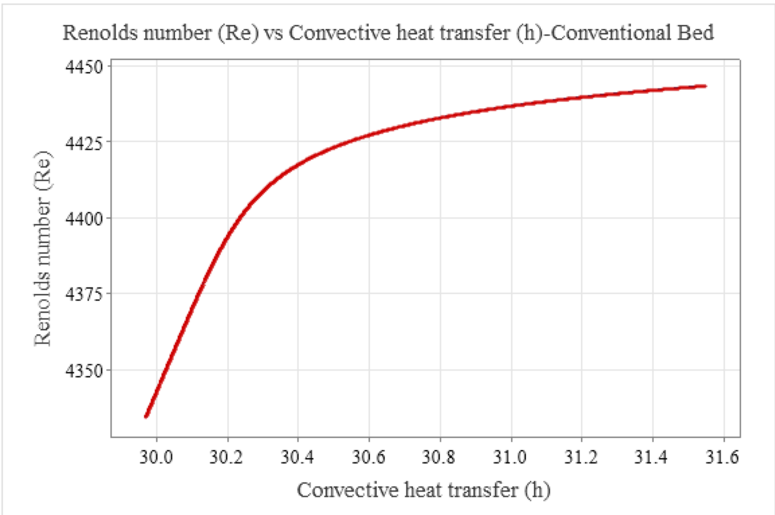

a)

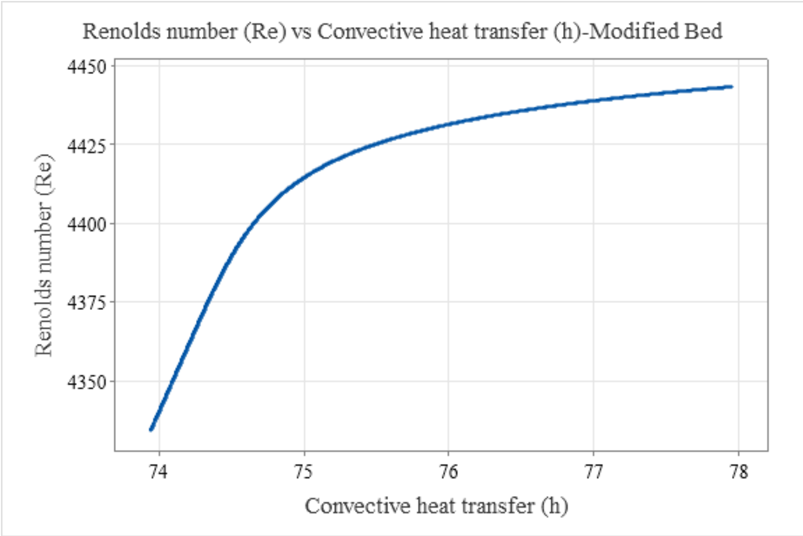

b)

Figure 7.54: CHT Versus Reynolds Number Conventional and Modified Bed

Figure 7.55 shows the variation of heat transfer coefficient with Reynolds number for both conventional and modified bed. From the graph, it is observed that the heat transfer coefficient gets increases to about 77.5 W/m2 -K with an increase in Reynolds number. The heat transfer rate is also dependent on the convective heat transfer coefficient so an increase in the Reynolds number results in higher heat transfer rates.

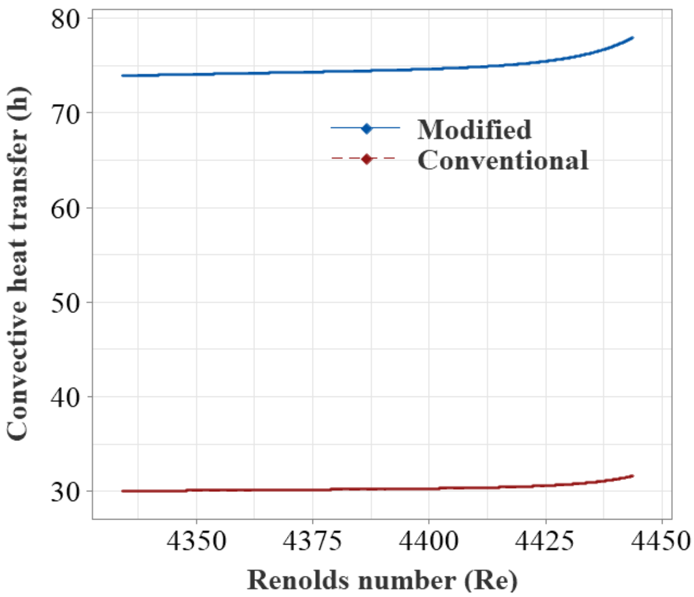

Figure 7.55: Effect of Variation of Reynolds Number on Convective Heat Transfer

The heat transfer coefficients for both conventional and conical spouted bed were determined numerically shown in Figure 7.55. The maximum heat transfer coefficients of 77.5 W/m^2K and 31W/m^2K are obtained at the conical spouted bed and conventional respectively. The values of heat transfer coefficients decrease rapidly for both the bed to a level of 74.5 W/m^2K and 29.5 W/m^2K respectively in 150 seconds as shown in Figure 7.56. These values further decrease as time elapsed.

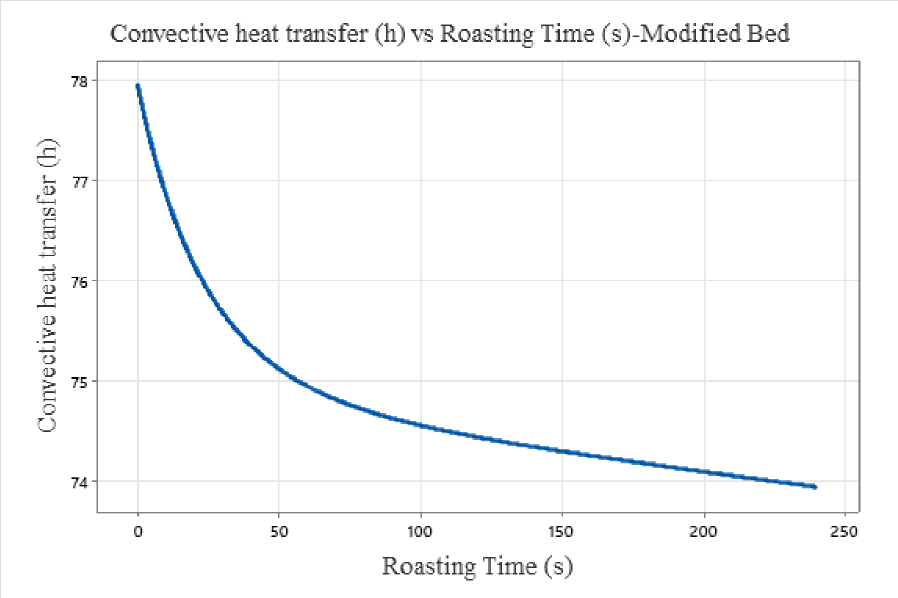

a)

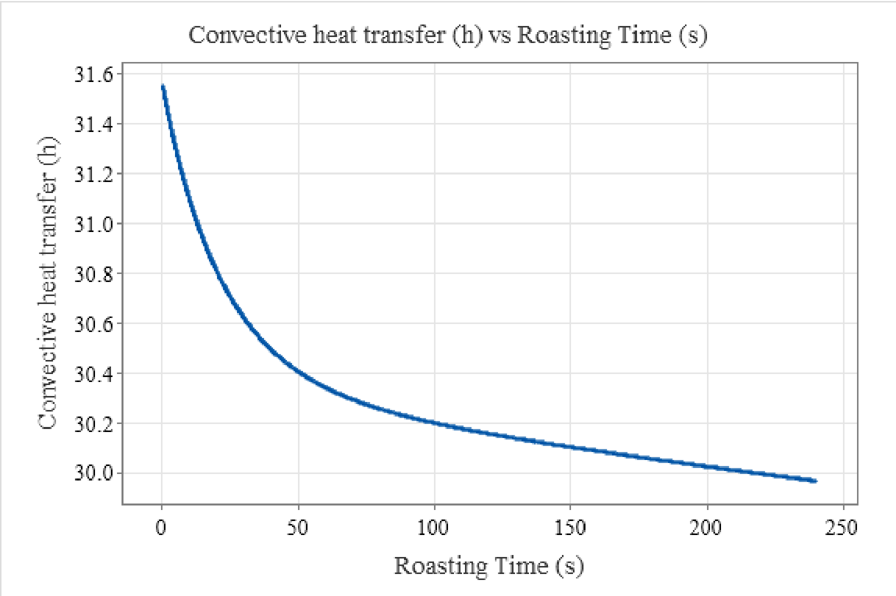

b)

Figure 7.56: Variation of Convective Heat Transfer Coefficient with Roasting Time

The other parameter for comparison between conventional and conical spouted bed with an internal device is the inter-particle collision among particles. In the first case Conventional spouted bed, the average Normal force acting among coffee bean particles after time was 41.7 mN, whereas in the case of the conical spouted bed with an internal device 60mN, which means that the average value of this force is about 30.5% lower in comparison with the conventional bed.

A similar character was obtained for the tangential forces acting among the particle. Figure 7.57 a and b show a comparison of graphs of mean forces (mean tangential and normal) acting on coffee bean particles. In this case, the average value after time for the conventional spouted bed was 2.42 mN; while for the conical bed, it was 1.4 mN, which is about 42% less than for the conventional bed.

The average power dissipated due to normal forces among particles of coffee bean is 1.48 mW in the case of conventional spouted bed, whereas it was about 1.5mW for conical bed which is about 1.3% less than for the conventional bed. Figure 7.58 shows the average power dissipated due to inter-particle collision.

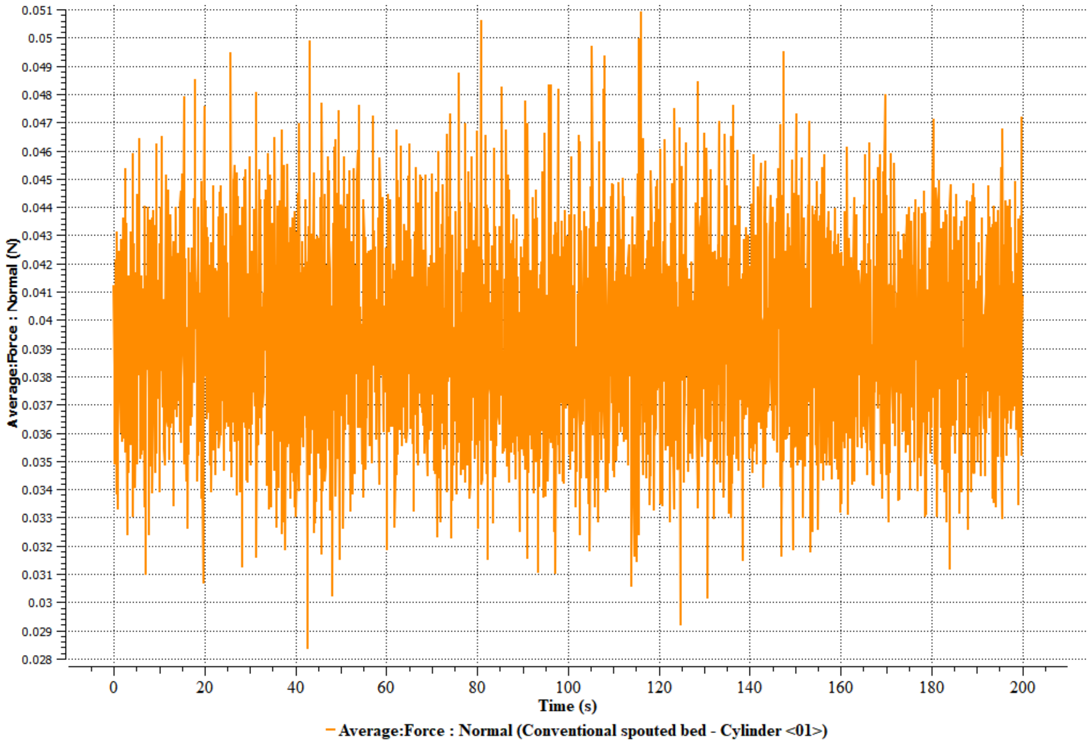

a)

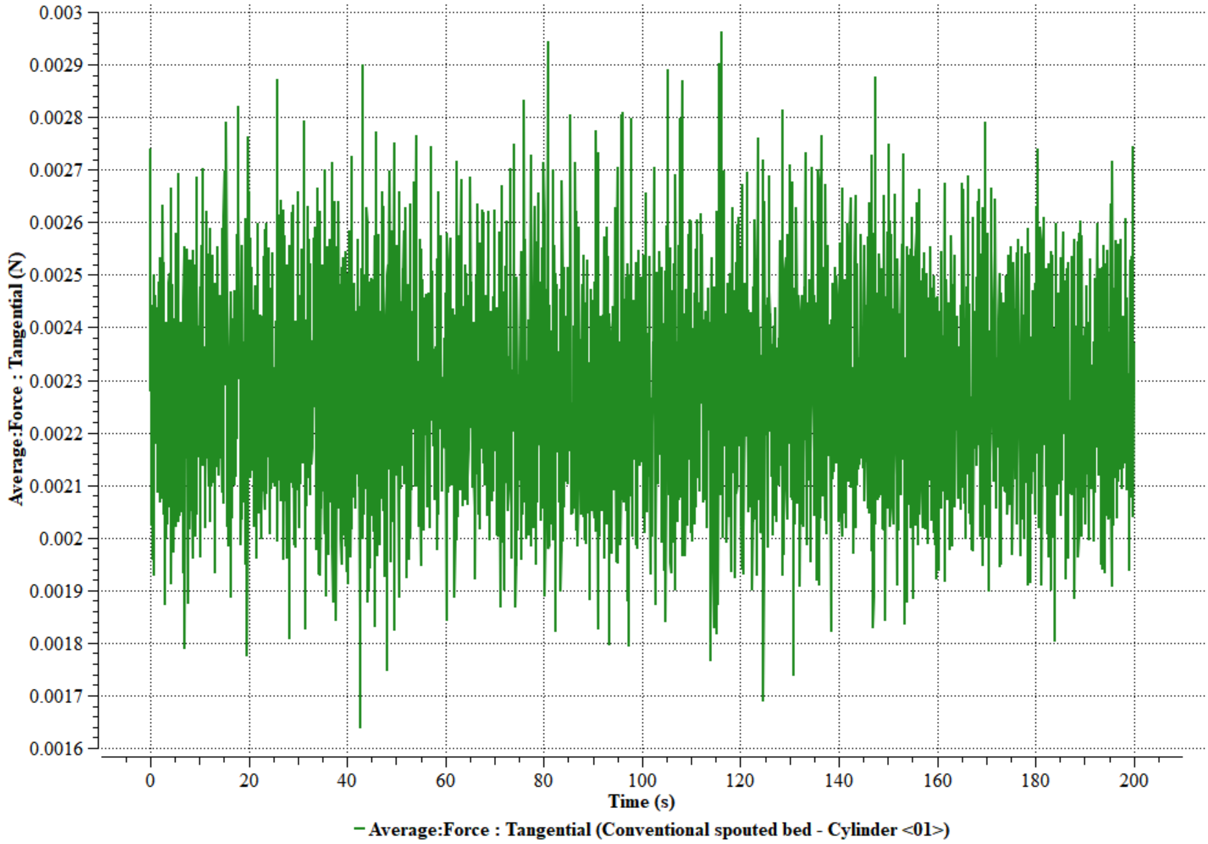

b)

Figure 7.57: Normal a) and Tangential Forces Acting among Coffee Bean Particles

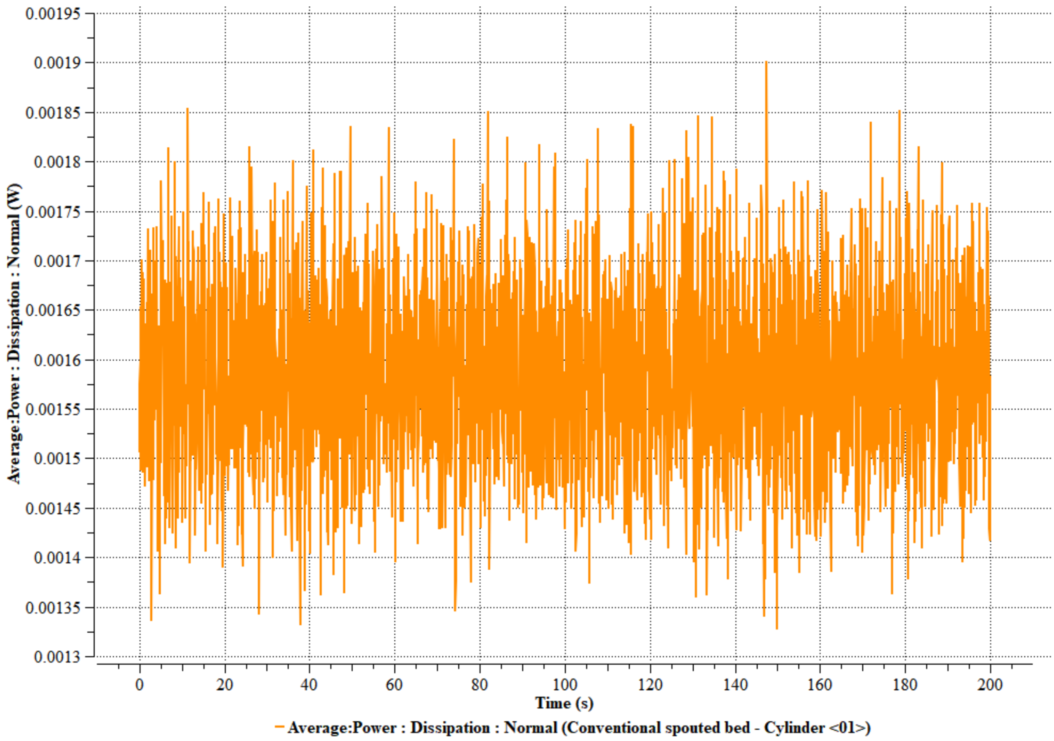

a)

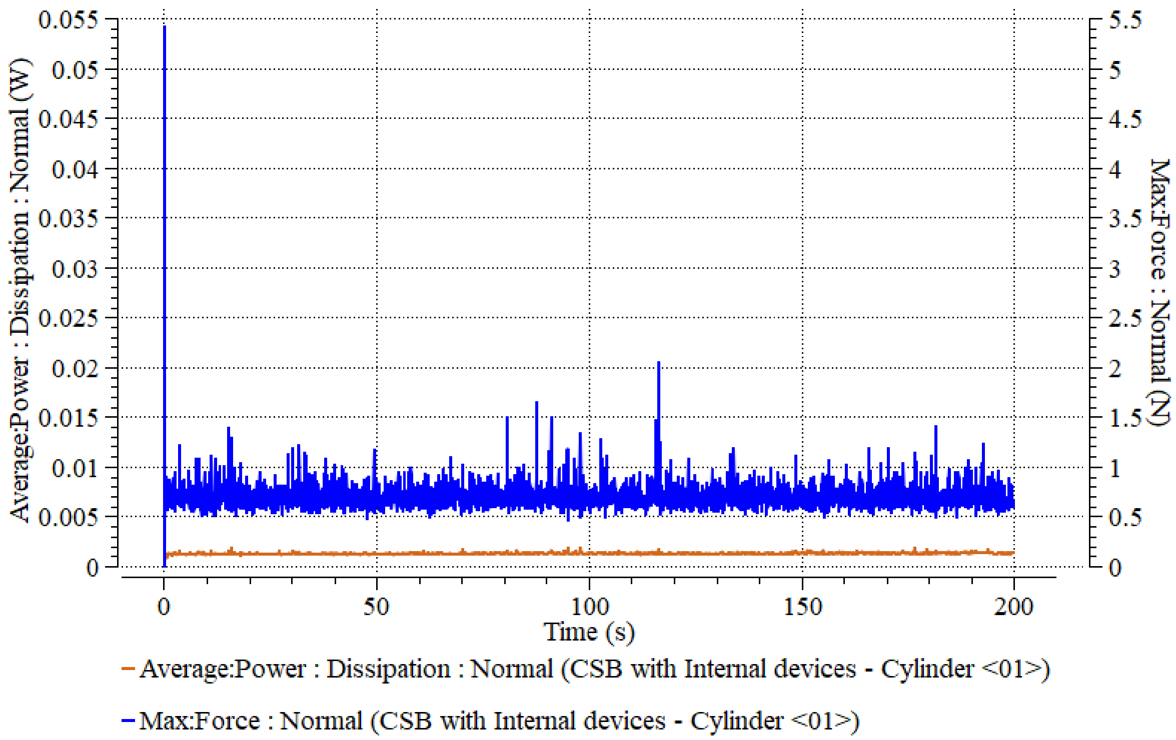

b)

Figure 7.58: Average Power Dissipation Due to Normal Force

CHAPTER EIGHT

CONCLUSIONS AND RECOMMENDATIONS

8.1 Conclusions

This thesis focuses on the numerical modeling of coffee bean roasting in a conventional spouted bed (The existing one) and conical spouted bed with the internal device (modified) based on the combined CFD-DEM Coupling approach. From the CFD-DEM analysis, it was found that the conventional spouted beds require higher flow rates and are a poor gas-particles contact due to the geometric factor of the roasting bed. Parametric studies are also conducted here to observe the effects of different operational conditions, grain properties, and bed geometries on the roasting of coffee beans. To improve the performance of the conventional spouted bed, a conical spouted bed with an internal device so-called fountain confiner, and the open-sided draft tube was designed and developed.

According to, CFD-Fluent with Rocky DEM Coupling, CFD Fluent the simulation program setting is done based on Ansys Fluent one-way Steady State coupled simulation. Hence, the ANSYS Fluent solver solves fluid flow, energy, and viscous data, in which both energy and viscous model are activated from the Fluent Models and in turn completely, solved and converge as possible as required, here in the fluent side. The following conclusions can be drawn from this study.

In the case of CFD Simulation result;

1) The inlet air velocity is one of the important factors in the roasting of coffee beans that could significantly develop buoyance force to overcome the weight of one kilogram (1kg) of coffee bean particles to create the spouting of the particle in the bed. This, velocity is called minimum spouting velocity. The minimum inlet hot air velocity that is sent to conventional spouted bed, passes through air inlet nozzle of 25mm diameter is about 20 m/s which are about 74m/s) as soon as leaving it. The roasting temperature of coffee beans for the dark degree of roasting is achieved at 250℃ of hot air temperature, within inlet air velocity carrying temperature.
2) Whereas, the minimum spouting velocity for a conical spouted bed with an internal device is 5m/s as it passes through an air inlet nozzle of about 12.5mm diameter is about 95m/s from CFD fluent simulation.

In Case of CFD-DEM Coupling Simulation Result;

1) Considering dynamics of particles during coffee bean roasting, the average magnitude of the absolute translational and rotational velocity vector is 1.34m/s and

175Rad/s respectively for conventional spouted bed, while it was found 0.58 m/s and 125 Rad/s for conical spouted bed with an internal device.

2) The instantaneous inlet air temperature results in an increase in the temperature distribution of the coffee bean particles through the spouted bed. The CFD-DEM simulation run was carried out for about 165seconds and the result of the simulation indicates that the coffee bean temperature T_b increases with the increment of air inlet temperature and time. Therefore, the variation in the particle temperature with conventional spouted bed and conical spouted bed with an internal device for the air temperature of 250℃ specifies that coffee beans increase to a very high level (more than "500K"), while in conventional spouted bed, particle temperatures are found to be lower (around "470K"). As the result, higher particle temperature leads to a faster roasting rate that assures modified spouted bed is the most efficient roasting device.
3) The convective heat transfer coefficient around coffee beans is the most important factor that enhances the heat transfer rate during coffee bean roasting using both conventional and modified spouted beds. The estimated heat transfer coefficients for coffee bean using a conventional spouted bed (existing) which was found to be 31 W/m^2K for an air temperature range of 250℃, while it increased to about 77.5 W/m^2K for conical spouted bed with an internal device.
4) The variation of heat transfer coefficient with Reynolds number for both conventional and modified beds indicates that the heat transfer coefficient is about 31W/m^2K for conventional, on the other hand, it gets increased to about 77.5 W/m2K for modified bed with an increase of Reynolds number. The heat transfer coefficient is also dependent on the Reynolds number so an increase in the Reynolds number results in higher heat transfer rates.
5) Considering the inter-particle collision among particles the average Normal force acting among coffee bean particles after time was 41.7 mN in a conventional spouted bed, whereas in the case of the conical spouted bed with an internal device is 60mN, which means that the average value of this force is about 30.5% greater in comparison with the conventional bed.
6) A similar character was obtained for the tangential forces acting among the particle in which, the average value after time for the conventional spouted bed was 2.42 mN; while for the conical bed; it was 1.4 mN, which is about 42% less than for the conventional bed.

7) The average power dissipated due to normal forces among particles of coffee bean is 1.48 mW in the case of conventional spouted bed, whereas it was about 1.5mW for conical bed which is about 1.3% less than for the conventional bed.

In Case of Experimental Result;

1) In the experimental investigation, optimum parameters for roasting performance have been determined using the Taguchi method. Nine (9) experimental runs have been performed based on the orthogonal array of three-level two factors (3^2) with full factorial design as the experimental design. The independent variables (factors or inputs) were airspeed and mass of coffee beans whereas roasting temperature and roasting time is the dependent variable.
2) In the analysis of variance, the speed accounts for the largest percentage contributions of about 60.90% which is the most significant factor, while the mass has the next percentage contributions of about 36.45% which is the next significant factor in the performance of the roasting machine.
3) Based on signal-to-noise ratio analysis and main effect plot for S/N the optimal parameter combination on larger is the better for roasting quality Hence, the optimum combination of parameters obtained at 1.5 m/s airspeeds and 0.250 kg mass.

8.2 Recommendations

According to a report by Global agricultural Information Network, our country Ethiopia exports about 4 million bags of coffee (240 metric tons), making it, the most important African coffee exporter and the tenth-largest exporter in the world. About 85% of Ethiopian coffee export is green coffee beans rather than processed coffee beans. Hence, Coffee processing technology should be developed, to the extent that a modern and automated coffee roasting machine is required for processed coffee export to involve in global market computation. Hence, the design and development of such a modern and automated coffee roasting machine require critical and bottomless scientific research.

The numerical simulation multiphase flow needs a high-performance computer, especially when using custom polyhedron particles of coffee beans modeled in CAD. This kind of problem is accomplished with ANSYS Fluent to work with Rocky in parallel using CPU and GPU and/or Multi-GPU capabilities, which leads to very fast DEM-CFD simulation results. Therefore, a high-performance computer with the best CPU and as well as GPU and Multi GPU should be *retrieved by ASTU for seeking of crafting the institution as the center of research.*

8.3 Recommendation for Future Work

The developed CFD-DEM model for roasting coffee beans has significant potential to study the thermo-hydrodynamics effect of particles in conical spouted bed as described in this thesis. This model gives detailed fluid and particle information, about roasting process parameters, but further investigation is necessary to apply this model for practical and a wide range of food processing products.

Further works are recommended in the following:

(1) This model is still limited to batch-wise systems which are not suitable to use on an industrial scale. To make it useful for large scale, this model needs to be scaled up and a proper conical spouted bed with an internal device needs to be designed for industry application. For scaling up of the roasting system, proper scaling method, parallel and GPU/Multi GPU computational techniques could be used.

(2) This model can provide detailed information about fluid flow and granular flow. However, the effects of some important parameters on roasting like the thermal expansion of coffee beans are not analyzed which needs further investigation.

(3) The CFD and DEM coupling approach is applied in this study, with the assumption of mono-sized particles of coffee beans for the seeking of computational cost. Depending on this limitation, the particle size distribution, and particle size concentration would be studied further as well.

(4) In Rocky DEM there is an adhesive/cohesive and liquid bridge model in which liquid or moisture in the particles and on the surface is studied through this model representation. In this study coffee bean particles, are assumed to be dry based due to the high computational time when this kind of model is activated. For this reason, further study on the moisture content of coffee beans is required using this model, with the help of parallel and GPU/multi-GPU computational techniques.

(5) To minimize the measurement errors, each test has been performed three times (3) under the same conditions, and the average values are reported. For this reason, the mass of coffee beans of about 0.125, 0.25, and 0.5 kg samples with their corresponding hot airspeed, were chosen for experimental runs by considering the current cost available on the market. Hence, it is strongly recommended to carry out an experimental test for one kilogram (1kg) of the coffee bean as future work.

REFERENCES

Meana, V. R. L., Kimkiman, N. S. P., & Dulay, A. C. (2019). Design, Fabrication, and Performance Evaluation of a Batch-Type Fluidized Bed Coffee Roaster for Small-Scale Coffee Growers. Mountain Journal of Science and Interdisciplinary Research (formerly Benguet State University Research Journal), 79(2), 90-97.

Nagaraju, V. D., Murthy, C. T., Ramalakshmi, K., & Rao, P. S. (1997). Studies on the roasting of coffee beans in a spouted bed. Journal of Food Engineering, 31(2), 263-270.

Nagaraju, V. D., & Bhattacharya, S. (2010). Roasting green coffee beans using spouted bed roaster: changes in physical characteristics. *Journal of food science and technology*, *47*(6), 674-677.

Nagaraju, V. D., Ramalakshmi, K., & Sridhar, B. S. (2016). Cryo assisted spouted bed roasting of coffee beans. Innovative Food Science & Emerging Technologies, *37*, 138-144.

Nagaraju, V. D., & Ramalakshmi, K. (2002). Roasting coffee beans in a spouted bed coffee roaster. Journal of Food Science and Technology, 39(5), 530-533.

Nagaraju, V. D., & Sridhar, B. S. (2014). Hydrodynamics And Heat Transfer Characteristics of Draft Tube Spouted Bed Roasting of Groundnuts (Arachis Hypogeae). International Journal of Scientific and Technology Research, 3 (7).

Robbins, P. T., & Fryer, P. J. (2003). The spouted-bed roasting of barley: development of a predictive model for moisture and temperature. *Journal of Food Engineering*, *59*(2-3), 199-208.

Estiati, I., Tellabide, M., Saldarriaga, J. F., Altzibar, H., & Olazar, M. (2019). Fine particle entrainment in fountain confined conical spouted beds. Powder Technology, 344, 278-285.

Xavier, T. P., Libardi, B. P., Lira, T. S., & Barrozo, M. A. (2016). Fluid dynamic analysis for pyrolysis of macadamia shell in a conical spouted bed. *Powder Technology*, *299*, 210-216.

Estiati, I., Tellabide, M., Pablos, A., Altzibar, H., Aguado, R., & Olazar, M. (2020). Design Factors in Fountain Confined Conical Spouted Beds. Chemical Engineering and Processing-Process Intensification, 155, 108062.

Sharma, M., Lousteau, M., & Schoegl, I. (2011). An Experimental Study of Small-Sized Conical Spouted Beds. In Conference Proceedings from the 2011 ASME Early Career Technical Conference, Atlanta, GA.

Epstein, N., & Grace, J. R. (Eds.) (2010). Spouted and spout-fluid beds: fundamentals and applications. Cambridge University Press.

Estiati, I., Tellabide, M., Pablos, A., Altzibar, H., Aguado, R., & Olazar, M. (2020). Design Factors in Fountain Confined Conical Spouted Beds. Chemical Engineering and Processing-Process Intensification, 155, 108062.

Yehuda, T.,&Kalman, H. (2020). Geldart classification for wet particles. *Powder Technology*, *362*, 288-300.

Chielle, D. P., Bertuol, D. A., Meili, L., Tanabe, E. H., & Dotto, G. L. (2016). Spouted bed drying of papaya seeds for oil production. LWT-Food Science and Technology, 65, 852-860.

Lopez, G., Cortazar, M., Alvarez, J., Amutio, M., Bilbao, J., & Olazar, M. (2017). Assessment of a conical spouted with an enhanced fountain bed for biomass gasification. *Fuel*, *203*, 825-831.

Tellabide, M., Estiati, I., Pablos, A., Altzibar, H., Aguado, R., & Olazar, M. (2020). The minimum spouting velocity of fine particles in fountain confined conical spouted beds. *Powder Technology*, *374*, 597-608.

Pablos, A., Aguado, R., Tellabide, M., Altzibar, H., Freire, F. B., Bilbao, J., & Olazar, M. (2018). A new fountain confinement device for fluidizing fine and ultrafine sands in conical spouted beds. *Powder Technology*, *328*, 38-46.

Bruchmuller, J., van Wachem, B. G. M., Gu, S., & Luo, K. H. (2010, January). Heat and mass transfer of drying particles in a fluidized bed. In International Heat Transfer Conference (Vol. 49392, pp. 289-295).

Bergman, T. L., Incropera, F. P., DeWitt, D. P., & Lavine, A. S. (2011). Fundamentals of heat and mass transfer. John Wiley & Sons.

Fox, R. W., McDonald, A. T., & Mitchell, J. W. (2020). Fox and McDonald's introduction to fluid mechanics. John Wiley & Sons.

Pritchard, P. J., & Mitchell, J. W. (2016). Fox and McDonald's introduction to fluid mechanics. John Wiley & Sons.

ANSYS (2013b). Fluent Theory Guide. ANSYS, Inc., Canonsburg, PA

ANSYS, I. (2013). ANSYS FLUENT theory guide: Release 16.2. ANSYS, Canonsburg, Pennsylvania.

Meana, V. R. L., Kimkiman, N. S. P., & Dulay, A. C. (2019). Design, Fabrication, and Performance Evaluation of a Batch-Type Fluidized Bed Coffee Roaster for Small-Scale Coffee Growers. Mountain Journal of Science and Interdisciplinary Research (formerly Benguet State University Research Journal), 79(2), 90-97.

Chiang, C. C., Wu, D. Y., & Kang, D. Y. (2017). Detailed simulation of fluid dynamics and heat transfer in coffee bean roaster. Journal of food process engineering, 40(2), e12398.

Sahin, S., Sumnu, G., & Tunaboyu, F. (2013). Usage of solar-assisted spouted bed drier in drying of a pea. Food and Bioproducts Processing, 91(3), 271-278.

Lu, Y., Zhang, M., Liu, H., Mujumdar, A. S., Sun, J., & Zheng, D. (2014). Optimization of potato cube drying in a microwave-assisted pulsed spouted bed. Drying Technology, 32(8), 960-968.

Arabiourrutia, M., Lopez, G., Elordi, G., Olazar, M., Aguado, R., & Bilbao, J. (2007). The product distribution was obtained in the pyrolysis of tires in a conical spouted bed reactor. *Chemical Engineering Science*, *62*(18-20), 5271-5275.

Sharma, M., Lousteau, M., & Schoegl, I. (2011). An Experimental Study of Small-Sized Conical Spouted Beds. In Conference Proceedings from the 2011 ASME Early Career Technical Conference, Atlanta, GA.

Saldarriaga, J. F., Atxutegi, A., Aguado, R., Altzibar, H., Bilbao, J., & Olazar, M. (2015). Influence of contactor geometry and draft tube configuration on the cycle time distribution in sawdust conical spouted beds. Chemical Engineering Research and Design, 102, 80-89.

Altzibar, H., Lopez, G., Bilbao, J., & Olazar, M. (2013). The minimum spouting velocity of conical spouted beds is equipped with draft tubes of different configurations. Industrial & Engineering Chemistry Research, 52(8), 2995-3006.

Gegenheimer, J. B. (2017). Development of Laboratory Scale Conical Spouted Bed Reactors.

Altzibar, H., Lopez, G., Bilbao, J., & Olazar, M. (2013). Minimum spouting velocity of conical spouted beds equipped with draft tubes of different configuration. *Industrial & Engineering Chemistry Research*, *52*(8), 2995-3006.

Epstein, N., & Grace, J. R. (Eds.). (2010). *Spouted and spout-fluid beds: fundamentals and applications*. Cambridge University Press.

Altzibar, H., Lopez, G., Bilbao, J., & Olazar, M. (2013). The minimum spouting velocity of conical spouted beds is equipped with draft tubes of different configurations. Industrial & Engineering Chemistry Research, 52(8), 2995-3006.

Tsvik, M. Z., Nabiev, M. N., Rizaev, N. U., Merenkov, K. V., & Vyzgo, V. S. (1966). A minimal rate of internal gushing during composite production of granulated fertilizers. *Uzb. Khim. Zh*, *10*(6), 3-6.

Bacelos, M. S., & Freire, J. T. (2008). Flow regimes in wet conical spouted beds using glass bead mixtures. Particuology, 6(2), 72-80.

Azmir, J., Hou, Q., & Yu, A. (2018). Discrete particle simulation of food grain drying in a fluidized bed. *Powder Technology*, *323*, 238-249.

Boac, J. M., Ambrose, R. P., Casada, M. E., Maghirang, R. G., & Maier, D. E. (2014). Applications of discrete element method in modeling of grain postharvest operations. *Food Engineering Reviews*, *6*(4), 128-149.

Hou, Q., Dianyu, E., Kuang, S., Li, Z., & Yu, A. B. (2017). DEM-based virtual experimental blast furnace: A quasi-steady-state model. *Powder Technology*, *314*, 557-566.

Jin, G., Zhang, M., Fang, Z., Cui, Z., & Song, C. (2014). Numerical study on spout elevation of a gas-particle spout fluidized bed in the microwave-vacuum dryer. *Journal of Food Engineering*, *143*, 8-16.

San Jose, M. J., & Alvarez, S. (2015). Bed Pressure Drop in a Draft-Tube Conical Spouted Bed for Thermal Treatment of Wastes. *Chemical Engineering & Technology*, *4*(38), 709-714.

Beltramo, C., Rovero, G., & Cavaglia, G. (2009). Hydrodynamic and thermal experimentation on square-based spouted beds for polymer upgrading and unit scale-up. *The Canadian Journal of Chemical Engineering*, *87*(3), 394-402.

Zhang, H., Liu, M., Li, T., Huang, Z., Sun, X., Bo, H., & Dong, Y. (2017). Experimental investigation on gas-solid hydrodynamics of coarse particles in a two-dimensional spouted bed. *Powder Technology*, *307*, 175-183.

Makibar, J., Fernandez-Akarregi, A. R., Díaz, L., Lopez, G., & Olazar, M. (2012). Pilot-scale conical spouted bed pyrolysis reactor: Draft tube selection and hydrodynamic performance. *Powder Technology*, *219*, 49-58.

Boukar, O., Belko, N., Chamarthi, S., Togola, A., Batieno, J., Owusu, E., & Fatokun, C. (2019). Cowpea (Vigna unguiculata): Genetics, genomics, and breeding. *Plant Breeding*, *138*(4), 415-424.

APPENDIXES

Appendix A

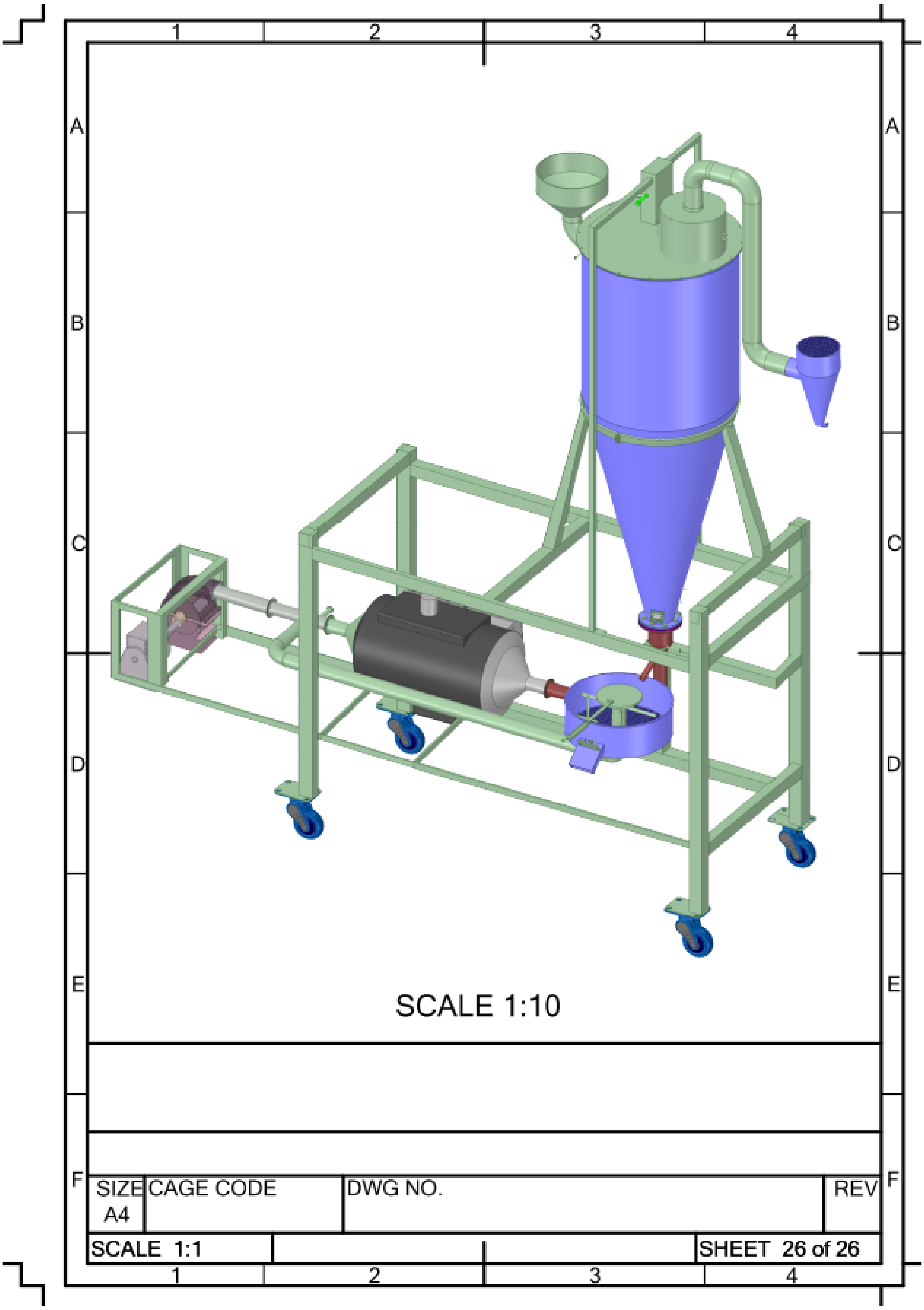

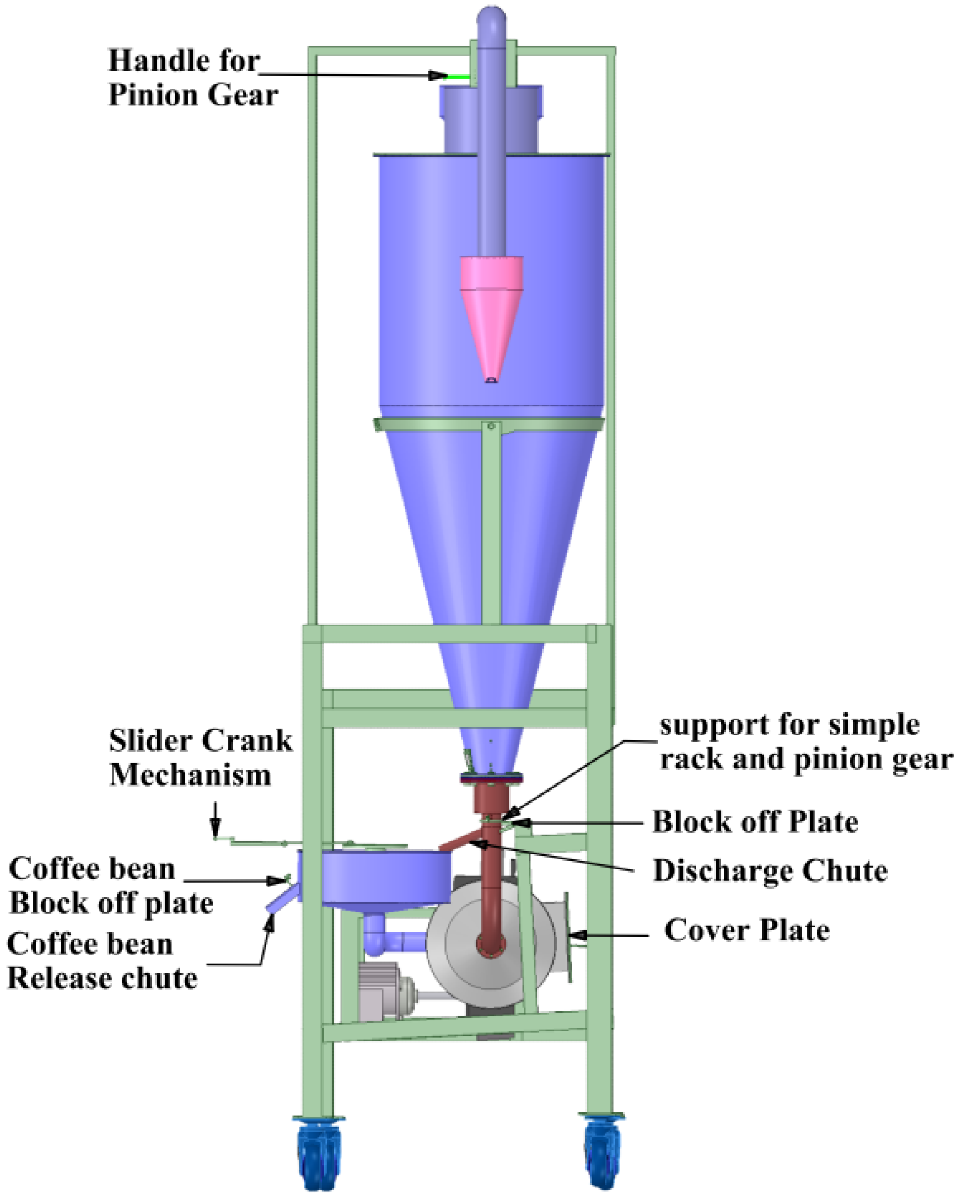
Handle for
Pinion Gear
Slider Crank
Mechanism
support for simple
rack and pinion gear
Block off Plate
Coffee bean
Block off plate
Discharge Chute
Coffee bean
Release chute
Cover Plate

SCALE 1:10

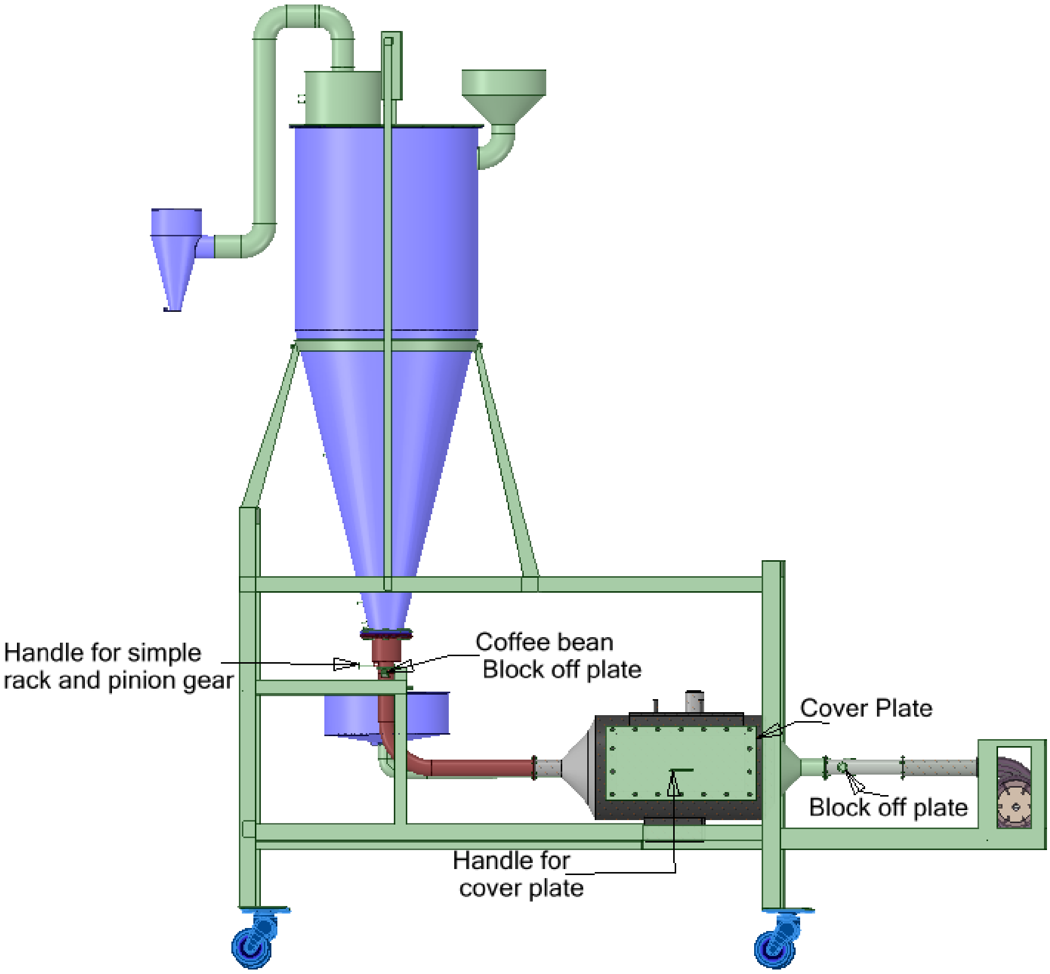
Handle for simple
rack and pinion gear
Coffee bean
Block off plate
Cover Plate
Block off plate
Handle for
cover plate

APPENDIX B

Table: Friction Loss per 100 Feet of Duct CFM

Duct Dia in	Friction Loss per 100 Feet of Duct CFM									
	100	200	300	400	500	600	700	800	900	1000
4	0.65	2.40	5.00	9.00						
6	0.10	0.30	0.70	1.20	1.80	2.60	3.50	4.50		
8	0.02	0.08	0.16	0.30	0.45	0.60	0.80	1.00	1.30	1.60
10		0.03	0.05	0.10	0.14	0.20	0.30	0.35	0.45	0.55
12		0.01	0.02	0.04	0.06	0.08	0.10	0.15	0.18	0.22
14			0.01	0.02	0.03	0.04	0.05	0.06	0.08	0.10
16				0.01	0.01	0.02	0.03	0.03	0.04	0.05

APPENDIX C

Table: Equivalent Resistance per Elbow in Feet of Straight Pipe

Equivalent Resistance per Elbow in Feet of Straight Pipe			
Duct Diameter (in)	**90° Elbows (ft)**	**Duct Diameter (in)**	**90° Elbows (ft)**
4	8	12	25
6	12	16	36
8	15	18	41
9	20	20	46
90° Elbows=0.67*90°	45° Elbows=0.50*90°	30° Elbows =0.33*90°	

APPENDIX D

Table: Temperature and Altitude Conversion Factors

Air Temp°F	Altitude in Feet Above Sea Level										
	0	500	1000	1500	2000	2500	3000	3500	4000	4500	5000
-50	0.77	0.79	0.80	0.81	0.83	0.85	0.86	0.88	0.89	0.91	0.92
-25	0.82	0.84	0.85	0.87	0.89	0.91	0.92	0.94	0.95	0.97	0.98
0	0.87	0.89	0.91	0.92	0.94	0.96	0.98	0.99	1.01	1.03	1.05
40	0.94	0.96	0.98	1.00	1.02	1.04	1.06	1.08	1.10	1.12	1.14
70	1.00	1.02	1.04	1.06	1.08	1.10	1.12	1.14	1.16	1.18	1.20
80	1.02	1.04	1.06	1.08	1.10	1.12	1.14	1.16	1.19	1.12	1.23
100	1.06	1.08	1.10	1.12	1.14	1.16	1.19	1.21	1.23	1.25	1.28

APPENDIX E

ROUND DUCT FRICTION CHART